Transcriptional upregulation as novel gene therapy strategy for neurological disorder

Yichen Qiu

Thesis submitted to University College London for the degree of Doctor of Philosophy

Department of Clinical and Experimental Epilepsy

UCL Queen Square Institute of Neurology

University College London

London, United Kingdom

Declaration

I, Yichen Qiu, confirm that the work presented in this thesis is my own. Where information has been derived from other sources, I confirm that this has been indicated in the thesis.

Abstract

Epilepsy remains one of the commonest serious neurological diseases. 30% of people with epilepsy are refractory to pharmacological treatment, and surgical resection of the focal brain area remains the best option. Gene therapy is currently the most promising candidate replacement for surgical treatment of pharmaco-resistant focal epilepsy. Gene therapy targets carried by adeno-associated virus (AAV) offer high-efficiency delivery without significant aversive effects. This project aims to test the possibility of using novel anti-epileptic gene therapy strategies with potential clinical translation. We carefully analysed the available gene therapy strategies and identified key issues that need to be addressed. Gene therapies that modulate neuronal excitability cannot discriminate between neurons involved in pathological circuits and the healthy 'bystanders'. We proposed a novel activity-dependent gene therapy strategy using inducible promoters to drive potassium channels overexpression in hyperactive neurons. We showed that this therapy successfully rescued pathological activities in epilepsy models. A second strategy we have investigated used CRISPR-activation (clustered regularly interspaced short palindromic repeats) system to transcriptionally modulate endogenous potassium channel expression at rescued epilepsy activities in animal epilepsy models. In conclusion, this thesis describes two novel gene therapy strategies that have great potential in treating neurological disorders.

Impact statement

Epilepsy is a global disease that affects up to 1% of the population. Effective treatments for epilepsy are limited and not applicable to all patients. Approximately 30% of patients with epilepsy continue to experience seizures despite optimal medication, a situation known as pharmacoresistant or refractory epilepsy. Novel and effective therapeutic options are urgently needed to address this problem. Gene therapy has emerged as a promising option to treat serious neurological disorders, including epilepsy. It has been shown to be effective as a permanent treatment when delivered directly to the seizure onset zone in preclinical models of focal epilepsy. It is arguably preferable to the only currently available treatment that offers a high chance of seizure freedom, which is resective surgery.

The main advantage of one of our proposed approaches, 'activity-dependent gene therapy', is significantly improved temporal and spatial specificity for the core pathology. By putting the expression of an anti-epileptic transgene under the control of an activity-dependent promoter, the excitability of cells involved in epileptic networks is automatically suppressed. Surrounding and intermingled circuits are unaffected and allowed to function normally. If seizures resolve, the therapy is automatically terminated. It does not require additional devices or drugs to achieve an anti-seizure effect, thus avoiding potential complications from device implantation or drug administration. Thus, the approach shows significant advantages over constitutive gene therapy, optogenetics or chemogenetics.

Furthermore, our activity-dependent gene therapy could potentially be used to treat a range of other neurological disorders where hyperexcitability may contribute to symptoms, such as Alzheimer's and Parkinson's diseases. Finally, by adjusting the strength of activity sensitivity and the effector transgene, it may be possible to change the potency of the therapy so it can be adjusted according to different needs.

This thesis also describes another approach based on manipulating endogenous gene expression using CRISPR activation. Upregulating transcription of a gene that has an anti-epileptic effect preserves its normal biogenesis. The technology could easily be switched to different endogenous genes by selecting other guide RNAs.

In conclusion, this thesis describes two novel gene therapy strategies that have great potential in treating neurological disorders.

Acknowledgement

First and foremost, I would like to thank my supervisors, Professor Dimitri Kullmann and Dr Gabriele Lignani, for their generous support, guidance, and opportunities for scientific developments. Thank you for all the advice and discussions throughout the PhD journey.

I would like to thank the MRC-DTP programme for offering this opportunity. The programme has provided help and guidance throughout, especially during the Covid pandemic.

I want to thank all past and current members of the Kullmann lab, Ligani lab, and DCEE with whom I had the pleasure to work with. In particular, I would like to thank Dr Nathanael O'Neill, Dr Amanda Almacellas Barbanoj, and Benito Maffei for helping me along the project and for data they produced as part of this thesis. It has been a privilege to work with so many wonderful people in the lab, and the moments we share will always be one of the best memories. I want to also thank Jenna, Amanda, Clara, Eleanora, Erica, Helen for the amazing friendship and support #womeninscience. I would like to thank Tom for the initial work, Albert for the help with cloning, Andy for taking me on an amazing journey when I first joined the lab and many cups of coffee, Bao-Luen for late night companionship, and Francisco for being the best master student one could wish for.

I would like to thank Professor Stephanie Schorge and Professor Trevor Smart for generously allowing me to perform experiments with appropriate licences.

And to Rai, my husband, for all the love and support throughout the years, this journey would not be possible without you by my side.

Last but not least, I am forever in debt to my loving mum and dad, my family and friend for the unconditioned love, care and support.

Abbreviations

4AP = 4-amino-pyridine

AAV = Adeno-associated virus

aCSF = artificial cerebrospinal fluid

ADAM22 = a disintegrin and metalloprotease domain-containing protein 22

AMPAR = α-amino-3-hydroxy-5-methyl-4-isoxazolepropionic acid receptor

Arc = cytoskeletal-associated protein

ATS = Andersen-Tawil syndrome

BDNF = Brain derived neurotrophic factor

BFNC = Benign familial neonatal convulsions

cAMP = cyclic adenosine monophosphate

CRE = calcium/cAMP response element

Cas = CRISPR associated protein

CBP = CREB binding protein

CHO = Chinese hamster ovary

CNS = central nervous system

copGFP = Copepod GFP

CREB = cAMP responsive element binding protein

CRISPR = clustered regularly interspaced short palindromic repeats

dsGFP = destabilized GFP

EA1 = episodic ataxia 1

EC = entorhinal cortex

EGTA = Ethylene glycol-bis(β-aminoethyl ether)-*N*,*N*,*N*′,*N*′-tetraacetic acid

ERG = early response genes

ESARE = enhanced SARE

GAD67 = Glutamate decarboxylase 67

GFP = green fluorescent protein

IEG = immediate early gene

ITR = inverted terminal repeat

KA = kainic acid

KOR = kappa opioid receptors

LGI1 = leucine-rich glioma inactivated protein

LRG = late response genes

MECF2 = Methyl-CpG-binding protein 2

MeCP2 = methyl CpG binding protein 2

MEF2 = myocyte enhancer factor

MODC = mouse ornithine decarboxylase

NIR = near-infrared

NMDAR = *N*-Methyl-D-aspartic acid receptor

NOR = Novel object recognition

NPAS4 = neuronal PAS domain protein 4

PDGF = *c-sis*–platelet-derived growth factor

PNS = peripheral nervous system

PTX = picrotoxin

PTZ = pentylenetetrazol

PV = parvalbumin

RAM = robust activity marking

SAM = Synergistic Activation Mediator

SARE = synaptic activity responsive element

SIE = PDGF-inducible factor element

SOM = somatostatin

SRE = serum response element

SRF = serum response factor

Sub = subiculum

TF = transcriptional factor

TLE = temporal lobe epilepsy

TSS = transcriptional start site

TTX = tetrodotoxin

VPR = virus protein R

VGCC = voltage-gated calcium channels

VIP = vasoactive intestinal peptide

Table of contents

Chapter 3. *In vivo* CRISPRa decreases seizures and rescues cognitive deficits in a rodent model of epilepsy

List of Figures and Tables

Chapter 1
Introduction

1.1. Epilepsy: Overview

1.1.1. Epidemiology of epilepsy

Epilepsy affects approximately 50 million people worldwide of all ages and races. It has been estimated that 75% of these are currently residents in developing countries with poor medical resources and limited access to adequate medical treatments (Meinardi *et al.*, 2001; Ngugi *et al.*, 2010; Beghi *et al.*, 2019) (Figure 1.1). In 2014, The ILAE (International League Against Epilepsy) updated the clinical definition of epilepsy from an earlier version published in 2005. New recommendations consider the disease to occur if any of the following conditions are met: '(a) At least two unprovoked seizures with longer than 24-hour interval; (b) one unprovoked seizure and a probability of further seizures similar to the general recurrence risk (at least 60%) after two unprovoked seizures, occurring over the next ten years; (c) diagnosis of an epilepsy syndrome' (Fisher *et al.*, 2014). This definition highlighted the difficulties of making an accurate diagnosis; in particular, seizures can be associated with a diverse range of diseases that do not necessarily manifest with any other symptoms. Furthermore, approximately 20-30% of patients referred with a suspected seizure have been found not to have epilepsy (Smith et al. 1999).

The estimated prevalence of epilepsy varies between studies and countries of interest. A recent meta-scale prevalence systemic study by Fiest *et al*, 2017 estimated an active prevalence of 6.38 per 1000 persons and a lifetime prevalence of 7.60 per 1000 persons (Fiest *et al.*, 2017). The life prevalence calculation includes remission cases who stopped experiencing seizures after appropriate treatment; hence the number is higher than active prevalence. For instance, in Norway and Ireland the crude

prevalence has been estimated at 11.7 and life prevalence at 10 per 1000 (Brodtkorb and Sjaastad, 2008; Linehan *et al.*, 2010). A recent meta-analysis estimated an incidence rate of approximately 61.44 per 100 persons/year (Fiest *et al.*, 2017).

Focal epilepsies with an unknown cause is the leading category for newly diagnosed epilepsy cases, with an incidence of 17.5 per 100,000 annually (Scheffer *et al.*, 2017). In the UK, it has been estimated that approximately 96,000 patients with epilepsy require continuous hospital care (Ngugi *et al.*, 2010). This highlights the size of the health burden to society, especially in countries with insufficient medical resources.

With adequate medical care and treatment, it is possible for approximately 80% of people with epilepsy to have prolonged seizure-free periods with appropriate care, and up to 50% can even remain seizure-free after treatment discontinuation (Beghi, 2020). The relapse risk after a first unprovoked seizure has been estimated at 36-37% after one year and 43-45% after two years (Beghi et al. 2015). Some studies suggest that the risk of recurrence is especially high with focal seizures (Beghi, 2020). There are also possible links between recurrence rate and a family history of epilepsy, suggesting a genetic contribution. Many factors could have an influence on recurrence risk, highlighting the difficulty of choosing effective treatments.

Among epilepsy patients, approximately one-third are considered to have 'refractory' or 'drug-resistant' or 'intractable' epilepsy (Kwan *et al.*, 2010). A patient is generally agreed to have refractory epilepsy when two or three appropriate medications (used as monotherapy or polytherapy), at appropriate doses, have failed to achieve prolonged seizure freedom (Schuele and Lüders, 2008; Stafstrom and Carmant, 2015). The failed treatment response could be due to multiple reasons, including factors related to the underlying seizure mechanisms, the resistance of the drug target, errors in diagnosis, and inappropriate drug choice (Schuele and Lüders, 2008).

Epilepsy is generally considered not life-threatening with low mortality rate. However, people with epilepsy have an increased risk of death, with

leading causes including SUDEP (sudden unexpected death in epilepsy), status epilepticus (SE), suicide and other unintended injuries(Thurman *et al.*, 2017). The mortality rate differs between low-mid income countries and high-income countries, and has been estimated as 1.6-3.0 and 19.8 per 1000 per year, respectively (Sander, 1993; Levira *et al.*, 2017). SUDEP has an annual incidence of 1.1-1.3 per 1000 persons with epilepsy (Beghi, 2020). Although the mortality rate of epilepsy is not as high as other more severe diseases, it is a common disorder that affects a large global population. The outcome could be improved with access to health facilities and effective treatments. In conclusion, epilepsy is a common disease in the global population, with a heavy burden on medical infrastructures and communities. It is complicated to diagnose, and treatment is suboptimal in a proportion of affected people, especially when resources are limited in developing countries.

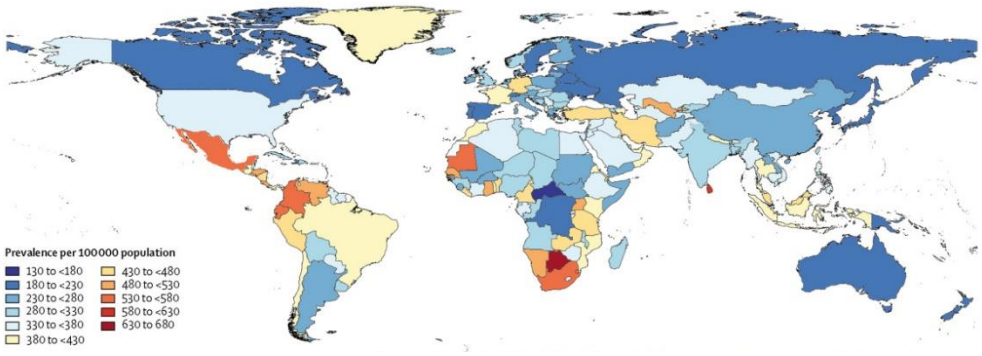

Figure 1.1 Estimate of global epilepsy prevalence in 2016. Image modified Beghi. et al, 2016 (Fig.1)

1.1.2. Clinical classifications of epilepsy

In 2017, ILAE updated its classifications for epilepsy based on a three-tier framework: 'seizure type', 'epilepsy type', and 'epileptic syndrome (aetiology)' (Scheffer *et al.*, 2017) (Figure 1.2). The framework outlines the initial identification of seizure types, followed by epilepsy types. The diagnosis of epilepsy syndromes should also be applied when

possible. Additional aspects to be included in the diagnosis are the underlying causes (e.g. aetiology) and associated comorbidities (Scheffer *et al.*, 2017). Together it forms the complete structure of epilepsy classification. In the next section, we will take a closer look at each of the components and how it affects epilepsy diagnosis.

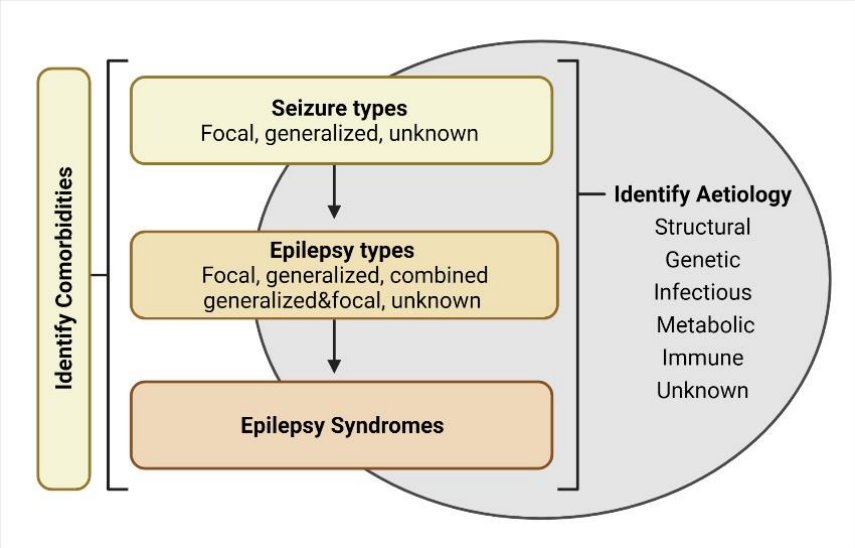

Figure 1.2 Framework for classification of epilepsies. The framework illustrates the initial diagnosis of seizures, followed by the diagnosis of epilepsy types and possible epilepsy syndrome if applied to the situation. The comorbidities and underlying aetiology are also considered. Images adapted from Devinsky, 2018 (Devinsky *et al.*, 2018) *Fig2.*

1.1.2.1. Seizure and epilepsy types

The first stage of classifying epilepsies is to understand seizure types. These can be roughly divided into focal onset, generalised onset and unknown onset. Focal onset seizures arise in a defined region of one hemisphere and can spread to both hemispheres (secondary generalisation) and evolve into a tonic-clonic seizure. Focal seizures can be categorised according to the clinical manifestations, which may be sensory or motor, or consist of other experiences such as déjà vu. Awareness may be impaired to various degrees during a focal seizure, although it is lost with secondary generalisation. Frequently observed motor manifestations include

myoclonic jerks and clonic and tonic muscle contractions. Tonic contractions refer to limb and axial stiffness, typically with co-contraction of flexors and extensors, while clonic movements are repetitive jerks. Non-motor manifestations of focal seizures include behavioural arrest, and sensory and other symptoms.

Primarily generalised seizures quasi-synchronously involve both hemispheres. They can be classified into motor and absence (non-motor) subgroups. A common type of generalised motor seizure is tonic-clonic convulsions, followed by a post-ictal period during which patients are unrousable. Patients can continue to experience exhaustion, muscle aches and headaches for a day or two. In infants, epileptic spasms can occur, manifesting as fixed head and neck positions with circumflexion of the upper limbs. An absence seizure typically manifests as brief mental and behavioural arrest, and patients rapidly return to normal afterwards. It is occasionally associated with subtle myoclonic jerks and characteristically exhibits runs of 3Hz spike and wave complexes on EEG (Meeren *et al.*, 2005). Other types of generalised seizures include myoclonic absence and eyelid myoclonia.

When stereotypical seizures occur in an individual patient, they define the 'epilepsy type', such as focal epilepsy, or primary generalized epilepsy (Scheffer *et al.*, 2017). In addition to the two well recognized category, a new category of 'combined generalised and focal epilepsy' was introduced to account for patients experiencing both focal and generalised seizures.

1.1.2.2. Epilepsy syndrome

In addition to seizure and epilepsy types, an additional layer of diagnosis is epilepsy syndrome. ILEA officially defined epilepsy syndrome as 'a characteristic cluster of clinical and EEG features, often supported by specific etiological findings'. The diagnosis largely depends on the seizure type, age, associated comorbidities

and results of investigations. Diagnosis of epilepsy syndromes involves comprehensive analysis of features that include seizure types, EEG traces and imaging analysis, and genetic background analysis. Some of the representative epilepsy syndromes include Dravet syndrome and absence epilepsy (Berg *et al.*, 2010; Stafstrom and Carmant, 2015; Scheffer *et al.*, 2017). Depending on the age of onset, it could be as early as the neonatal period (e.g. benign familial neonatal convulsions, BFNC, or early myoclonic encephalopathy), infancy (e.g. Dravet syndrome, benign infantile epilepsy, febrile seizures), childhood (e.g. childhood absence seizures), or adolescence (e.g. juvenile or progressive myoclonus epilepsies) (Berg *et al.*, 2010). Epileptic encephalopathy is a collective term describing epilepsy associated with the loss of certain cerebral functions (Berg *et al.*, 2010). Although many epilepsy syndromes with distinct comorbidity profiles characteristically manifest age-dependent onsets, this does not apply across the board, and it is often not possible to identify the syndrome unambiguously in an affected individual (Stafstrom and Carmant, 2015).

1.1.2.3. Aetiology

Aetiology refers to the underlying cause of epilepsy. It can be divided into structural, genetic, infectious, metabolic, immune and neurodegenerative (Balestrini *et al.*, 2021). The causes are diverse, and prognosis cannot be easily determined (Jain, Sharma and Tripathi, 2013). Furthermore, the cause of epilepsy remains unclear in many cases ('cryptogenic' epilepsy).

Structural abnormalities include tumours, hippocampal sclerosis, and glial scarring resulting from various injuries such as haemorrhage, infection, surgery and brain trauma (Blumcke *et al.*, 2017; Balestrini *et al.*, 2021). High-resolution imaging can provide evidence to support such a diagnosis. Tumours, for example, contribute to 10-15% of adult epilepsy diagnoses (van Breemen et

al. 2007). Other developmental cortical malformations, for example focal cortical dysplasia (FCD), also frequently result in intractable seizures (Guerrini and Dobyns, 2014).

Genetics of epilepsy is a rapidly expanding research area, greatly accelerated by advances in sequencing technology. Mutations in genes that encode subunits of ion channels or receptors are directly implicated in several inherited epilepsy syndromes (Kullmann and Hanna 2002; Kullmann 2002). Many genes have been identified in monogenic epilepsy syndromes, including *SCNA1*, *KCNQ2/3*, *SCNA1B*, *CHRNA4*, *CHRNB2* (Chang and Lowenstein, 2003). The genes implicated in epilepsy contribute to a variety of signalling cascades, including ion channels, synaptic support proteins, the mTOR (mammalian target of rapamycin) pathway and chromatin regulators (Kullmann, 2002; Ellis, Petrovski and Berkovic, 2020). The heritable epilepsy syndrome of benign familial neonatal convulsion is associated with genes encoding Kv7 potassium channels (Biervert *et al.*, 1998; Singh *et al.*, 1998). Autosomal dominant mutations in genes KCNQ2/3 lead to unprovoked seizures beginning in early infancy. The mutated channel shows reduced potassium ion conductivity, potentially contributing to prolonged neuronal depolarization and hyperexcitability (Biervert *et al.*, 1998),

Among ion channels, an infrequent cause of epilepsy relevant to this thesis is mutations in *KCNA1*, which encodes the voltage-gated potassium channel Kv1.1. Loss of function mutations cause episodic ataxia type 1, with some patients also experiencing seizures, although epileptic encephalopathy has also been reported (Zuberi *et al.*, 1999). Despite advances in genetics, the aetiology remains uncertain in many cases of early-onset epilepsy, and it is widely speculated that epilepsy is often polygenic. More recently, many mutations have been recognised as *de novo* events. Recent systemic genomic study revealed 11 novel genomic loci with significant

potential in epilepsy, further expanding the pool of potential antiepileptic drug targets (International *et al.*, 2018).

Severe seizures themselves, as can occur in response to toxins or infections such as herpes simplex encephalitis, can be followed by spontaneous seizures, i.e. epilepsy (Hussein and Shafran, 2000). Status epilepticus is defined as a situation where seizures fail to self-terminate or where a seizure follows closely after a previous episode without complete recovery from the first one (Lowenstein, Bleck and Macdonald, 1999). Convulsive status epilepticus is a perilous situation requiring immediate medical intervention if it lasts longer than five minutes (Lowenstein, Bleck and Macdonald, 1999). Following acute seizures, the probability of developing epilepsy depends on the type of infection and on the severity of the early seizures. Metabolic disturbances with or without underlying genetic conditions can also lead to epilepsy. Similarly, autoimmunity can also contribute to seizures and epilepsy. An increasing number of encephalitis disorders have been associated with autoantibodies (Geis *et al.*, 2019).

The last important aetiological category is neurodegenerative conditions. Although it is not officially recognized as a separate aetiology by the ILAE, some recent work indicates possible common factors involved in both epilepsy and dementia . Patients diagnosed with Alzheimer's disease or Parkinson's patients have an increased likelihood to develop epilepsy (Hesdorffer *et al.*, 1996). Elevated levels of pathological tau and amyloid species have been detected in hippocampal and neocortical regions of patients that underwent TLE resective surgery (Gourmaud *et al.*, 2020).

Overall, aetiology forms a crucial component of epilepsy diagnosis, and advances in neuroimaging and genomic sequencing have considerably altered our understanding of the causes of epilepsy.

1.1.3. Comorbidities

This term refers to conditions associated with epilepsy. Cognitive comorbidities are very commonly associated with epilepsy, occurring in 70-80% of people with long-standing epilepsy (Helmstaedter and Witt, 2017). Comorbidity is part of the epilepsy classification, as some neurobehavioral characteristics are often associated with specific epileptic syndromes and aetiologies of epilepsy (Scheffer *et al.*, 2017) (Figure 1.3).

The relationship between epilepsy and comorbidities is complicated. Seizures and cognitive or other comorbidities can be parallel manifestations of a common underlying pathology (for instance a brain injury leading both to seizures and to neurological deficits). As mentioned above, in dementia (e.g. Alzheimer's disease), infrequent seizures have been reported in up to 10-20% of patients (Sirven, 2015). Comorbidities and seizures may share some risk factors, such as genetics, or environmental, structural or physiological disorders (Gaitatzis, Sisodiya and Sander, 2012). Some studies proposed possible shared risk factors between cognitive decline and intractable seizures (Gourmaud *et al.*, 2020). In some cases, seizures occur prior to the main disease symptom manifestation, in which case there may be a 'two-way relationship'. This was suggested by some longitudinal studies on epilepsy and psychosis, tuberous sclerosis, autism, stroke, schizophrenia and dementia (Keezer, Sisodiya and Sander, 2016). However, there is no clear evidence yet to conclude bidirectional causality between epilepsy and those conditions (Keezer, Sisodiya and Sander, 2016).

Alternatively, there could also be a resultant mechanism where epilepsy causes seizures which then lead to the comorbidity, such as depression, suicidality, or anxiety. In this case, not only the recurrent seizures but possibly the treatment may lead to development of comorbidities. Progressive cognitive decline may accumulate with recurrent seizures. For example, childhood-onset epilepsy can be

accompanied with intellectual disability, memory deficits, hyperactivity, language regression and other conditions (Kim and Ko 2016). In addition, the comorbidity condition could also lead to seizures. For example, cerebrovascular disease leads to about 10% of epilepsy cases in a study from Iceland (Olafsson *et al.*, 2005).

In conclusion, there remain a multifactorial complicated relationship between comorbidities and epilepsy, and it is experimentally challenging to gather sufficient evidence for proving proposed relationship or causality.

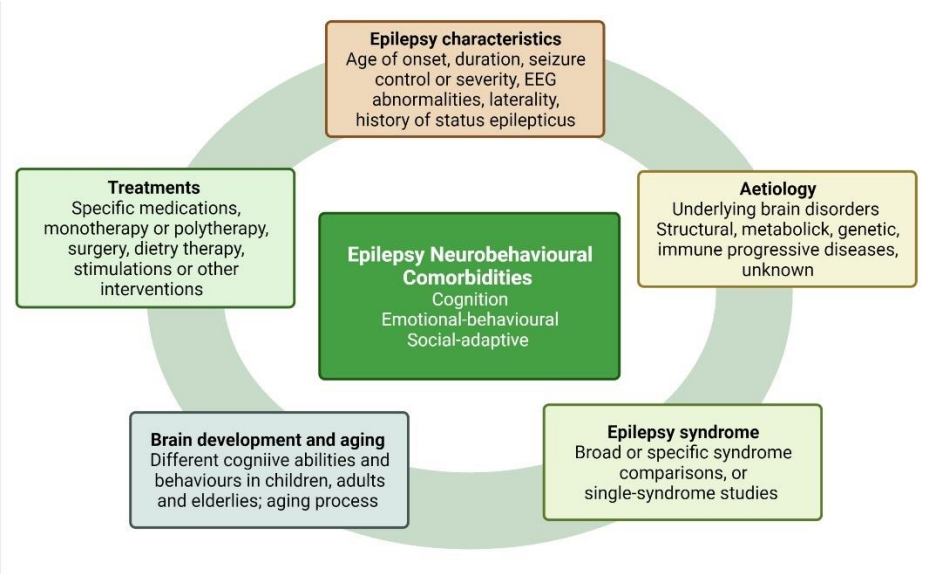

Figure 1.3 Epilepsy comorbidities: contributing factors. The five major contributing factors are shown on the outer circle. Image modified from Hermann, 2021(Hermann *et al.*, 2021) *Fig1.*

1.2. Temporal lobe epilepsy

Mesial temporal lobe epilepsy (TLE) is the commonest epileptic syndrome in adults (Sharma *et al.*, 2007). TLE is considered an acquired epilepsy, resulting from a precipitating event which includes trauma or injury to the brain, although in many cases this event is not known. The initial brain insult is typically followed by a seizure-free period known as the latent period before the first clinical seizure episode (epileptic phase). It is generally thought that during the latent phase, complicated

neurobiological processes make changes to the brain which lead to the transition into the epileptic phase.

TLE is characterized by seizures that arise from an epileptogenic focus localized to the hippocampal formation or associated structures in the temporal lobe (Engel. 1998). Pharmacoresistant TLE is the commonest type of epilepsy that is treated with surgery, and some cases require intracranial EEG is to delineate the epileptogenic zone. Characteristic interictal spike-wave discharges are an EEG signature of TLE (Engel. 2001).

1.2.1. Mechanisms of seizures

1.2.1.1. Limbic structure hypersynchronization in TLE

Seizures have for a long time been thought to consist of excessive and hyper-synchronous discharges of populations of neurons. Seizures can often be detected from EEG recordings, where they manifest as abnormal waveforms of high amplitudes. The seizure episode can be broken into three phases: initiation, propagation, and termination.

In focal epilepsies, seizure initiation occurs in the epileptogenic zone, often followed by propagation beyond the original seizure focus. In TLE, seizures typically originate from hippocampal and para-hippocampal structures, although it is often difficult to pinpoint an individual population of neurons or synapses as the 'detonator' (Engel J., 2001). The electrophysiological properties and anatomical structures of the hippocampal circuitry are thought to predispose to synchronization, not only in seizures but also in normal rhythms. For example, theta oscillations are implicated in learning and spatial navigation, while sharp-wave ripples (SWR) are observed during immobility and sleep (Avoli, 2010; Buzsáki, 2015). Scalp EEG, electrocorticograms and depth recordings pick up local field potentials generated by synaptic currents and action potentials

in a large population of neurons, coordinated under physiological and pathological conditions by fast excitatory and inhibitory signalling (Avoli, 2010). These signals span a range of frequencies, including theta, beta, gamma, and SWR). Synchronisation can occur at different levels, from neighbouring cells, local neural circuits, large networks to entire brain structures. Synchronisation can also last for different timescales, ranging from milliseconds to minutes. Excessive synchronization generates high-amplitude spikes which are biomarkers of the epileptogenic zone.

Spikes and seizures can be recapitulated in experimental models using various chemoconvulsants. The main type used are $GABA_A$ receptor blockers, including penicillin, bicuculine and picrotoxin; low Mg^{2+} to enhance glutamatergic transmission (generally used in vitro); or the potassium channel blocker 4-AP (4-aminopyridine) to enhance neuronal excitability. Paroxysmal depolarization shifts (PDS) of cortical pyramidal neurons are an intracellular correlate of the initial events accompanying seizures (Matsumoto and Marsan, 1964). Hippocampal CA3 regions are prone to generate similar large interictal discharges. The far reaching axonal connectivity of CA3 pyramidal cells, to other CA3 pyramidal neurons (ipsilaterally in primates and also contralaterally in rodents), to CA1 pyramidal cells, and to the septum, is thought to enable hypersynchronous firing patterns in the presence of inhibition blockers (Prince, 1978). Gap junctions have also been proposed to contribute to the fast spread of excitation, although it remains unclear to what extent synchronisation depends on them (Traub *et al.*, 2004).

1.2.1.2. Seizure Dynamics

As mentioned above, Seizures generally consist of three phases: onset, propagation and termination. The mechanism of ictal discharges varies between different types of seizures and epilepsy syndromes. Here is a brief general description of characteristic

features recognized in preclinical models. Ictal events (or ictal discharges, equivalent to the electrophysiological correlate of seizures) generally occur infrequently, separately by long 'inter-ictal' intervals. Evidence from animal models showed that the inter-ictal periods do not occur randomly (Williams *et al.*, 2009). Inter-ictal discharges may occur during these periods. There is some controversy around the significance of inter-ictal discharges. It has been proposed that they represent recruitment of the GABAergic inhibitory network, potentially acting to oppose increased glutamatergic activity (Zhang *et al.*, 2012; Blauwblomme, Jiruska and Huberfeld, 2014). Failure of this inhibition leads to the transition into ictal state. Conversely, it has been proposed that inter-ictal spikes are a pro-seizure phenomenon because it is associated with hypersynchrony. Although seizures are dominated by the activity of glutamatergic excitatory neurons, under certain conditions, GABAergic interneurons are readily recruited during interictal spikes (de Curtis and Avanzini, 2001; Avoli, 2010). Seizures themselves have a range of characteristic frequencies on the EEG, reaching approximately 100-120Hz. However, high-frequency oscillations (HFOs) or fast ripples with a 200-300 Hz frequency can also be detected, often just before seizure onset. Both inter-ictal spikes and HFOs are clinically helpful biomarkers of epileptogenic zones (Lignani, Baldelli and Marra, 2020). This intense GABAergic signalling during interictal discharges may represent an inhibitory brake, which, if it collapses, can lead to hypersynchronous activity of excitatory neurons that escapes to propagate and invade surrounding territories or even the whole brain.

The mechanisms by which GABAergic inhibition can collapse have attracted considerable attention(Cobb *et al.*, 1995; Bartos, Vida and Jonas, 2007). Among candidates mechanisms are the following: (i) interneurons become unable to release GABA, for instance because they are over-depolarized and repetitive action potential generation

fails, because of depletion of GABA-containing vesicles, or because of excessive presynaptic depression of GABA release; (ii) excessive activation of $GABA_A$ receptors on postsynaptic neurons overwhelms the ability of the chloride extrusion transporter KCC2, leading to a depolarization of the chloride reversal potential, in turn causing a failure of voltage inhibition or even a paradoxical excitatory effect of $GABA_A$ receptor activation; (iii) postsynaptic chloride accumulation secondary to $GABA_A$ receptor activation leads to KCC2-mediated efflux of potassium ions and extracellular potassium accumulation, which causes a depolarization of surrounding neurons (Köhling, 2002; Bartos, Vida and Jonas, 2007). These mechanisms are not mutually exclusive and evidence for all three has been reported by numerous laboratories (Liu et al. 2020).

Seizure onset can be accompanied by a spike that is indistinguishable from inter-ictal discharges, or by a slow voltage deflection, or by a high-frequency low amplitude signal in the electrocorticogram or EEG. When a large spikes is observed right at the beginning of the seizure, it is known as a sentinel spike (Figure 1.4). Focal seizures typically evolve into high-amplitude bursts (>5Hz). This may be accompanied by an increase in the affected bran territory. This propagating phase continues for the majority of the seizure duration with high-amplitude and high-frequency 'hypersynchronous' spikes (at 40s in Figure 1.4), known as the tonic phase of the seizure (Williams *et al.*, 2009).

This then progresses to distinct large spikes displaying multiple EEG spikes or rhythmic bursts, known as the clonic phase (Blauwblomme, Jiruska and Huberfeld, 2014). As the seizure starts to terminate, the EEG typically shows a reduction in amplitude relative to baseline, a so-called refractory period (de Curtis and Avoli, 2015). The post-ictal refractory period has numerous possible explanations, such as depletion of glutamate-containing synaptic vesicles, recovery of inhibitory synapses, ion shifts, or by the

inhibitory action of adenosine and other neuromodulators. The involvement of subcortical regions in this phenomenon remains incompletely understood (de Curtis and Avoli, 2015; de Curtis, Librizzi and Avanzini, 2015).

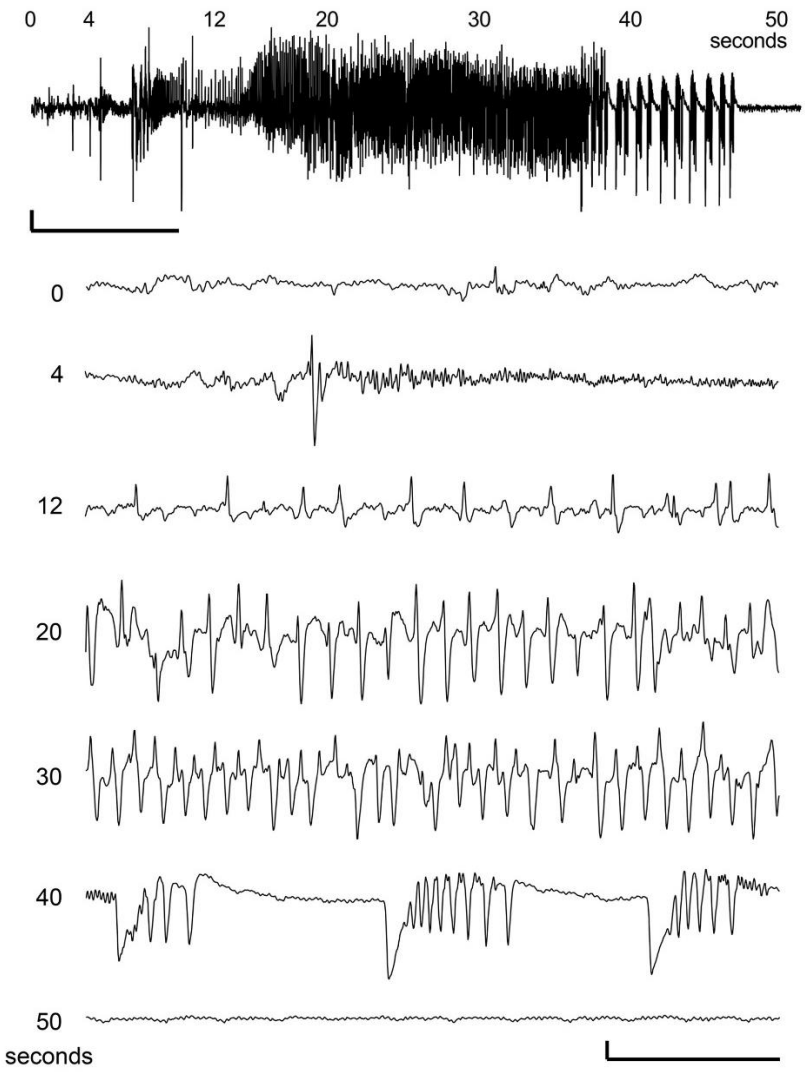

Figure 1.4. Representative seizure recorded from ipsilateral CA1 area with depth electrode from intra- amygdala kainic acid mouse model.(time window of zoomed in is 2s, scale bar 0.5s, 2mV). (Adapted from West, 2022(West *et al.*, 2021)*, Figure 1).*

1.2.2. Epileptogenesis and structural atrophy in TLE

As described in the beginning of this section, epileptogenesis refers to the process by which the brain transitions from a normal state to

one where spontaneous seizures arise (Pitkänen *et al.*, 2015). It has been extensively studied in the context of temporal lobe epilepsy, which can be induced by a variety of insults that elicit an initial period of status epilepticus. During the late period, the brain state may be profoundly abnormal, with changes in neuronal activity, morphology and connectivity, and neuronal death, gliosis and inflammation, before seizures emerge (Pitkänen *et al.*, 2015).

Biochemical and morphological abnormalities have also been extensively documented in the chronic epileptic state. Which of these are responsible for making the brain more susceptible to spontaneous seizures is debated. Changes occur in synaptic connections, neuronal firing properties, synaptic receptor membrane expression, and some inhibitory synapses (Avoli, 2010). Chronic epilepsy has fundamental differences from acute precipitated seizures: spontaneous seizures occur unpredictably, and are typically interspersed with interictal periods when the overt brain state is superficially unremarkable. This underlines a limitation of assuming that the epileptic state is simply equivalent to an excitation-inhibition imbalance (Staley, 2015). Accumulating evidence suggests that structural abnormalities continue to progress with every new spontaneous seizures (Pitkänen and Sutula, 2002; Lillis *et al.*, 2015).

Insights into the structural changes that occur in human temporal lobe epilepsy have mainly come from late-stage disease leading to surgery. In particular, hippocampal sclerosis is the most commonly reported lesion in 35.5% of cases in one series (Blumcke *et al.*, 2017). It remains debatable whether hippocampal sclerosis is the cause or the effect of recurrent seizures. Various degrees of specific neuron loss in typical regions, unusual synaptic reorganizations, axonal sprouting, and abnormal glial function, have been reported in tissue resected during epilepsy surgery (Thijs *et al.*, 2019). Pyramidal neurons in CA1, CA4 and CA3 are typically lost, accompanied by

heavy gliosis and scaring (Pitkänen and Sutula, 2002). CA2 pyramidal neurons are relatively resistant to cell death, as are granule cells. Granule cell neurogenesis has been described in rodents, but it is not clear if this process keeps up with neurodegeneration in the dentate gyrus (Devinsky *et al.*, 2018).

The interneurons in hippocampus carries important role in modulating neuronal circuits. Mossy fibre sprouting in the hippocampus has been extensively documented in both human patients and animal models. Normally mossy fibres, which are axons of granule cells, project from the dentate gyrus through the dentate hilus to stratum lucidum in CA3, forming glutamate releasing synaptic contacts with inhibitory interneurons, hilar mossy cells, as well as pyramidal cells in the CA3 region(Crawford and Connor 1973) (Figure 1.5). Thus, the mossy fibre collaterals sprout into the molecular layer of the dentate gyrus, and this has been observed in both animal models and in humans with temporal lobe epilepsy (Represa, Tremblay and Ben-Ari, 1987; Avoli, 2010; Navidhamidi, Ghasemi and Mehranfard, 2017). This process involves possible astrocyte scarring and death of CA3 pyramidal neurons triggered by the initial insult, with, possibly as a result of lost connectivity, aberrant mossy fibre sprouting as granule neurons attempt to form new postsynaptic connections. An association between mossy fibre sprouting and hippocampal sclerosis has been reported, but the specific mechanism remains unclear (Schmeiser *et al.*, 2017). Other studies also found that newly formed synapses are dominated by kainate receptors, while normal postsynaptic contacts predominantly express AMPA (α-amino-3-hydroxy-5-methyl-4-isoxazolepropionic acid) receptors instead(Botterill *et al.*, 2019). Because AMPA receptors have a crucial role in normal excitatory transmission and in synaptic plasticity(Abbott and Nelson, 2000), this change in receptor expression may contribute to epileptogenesis.

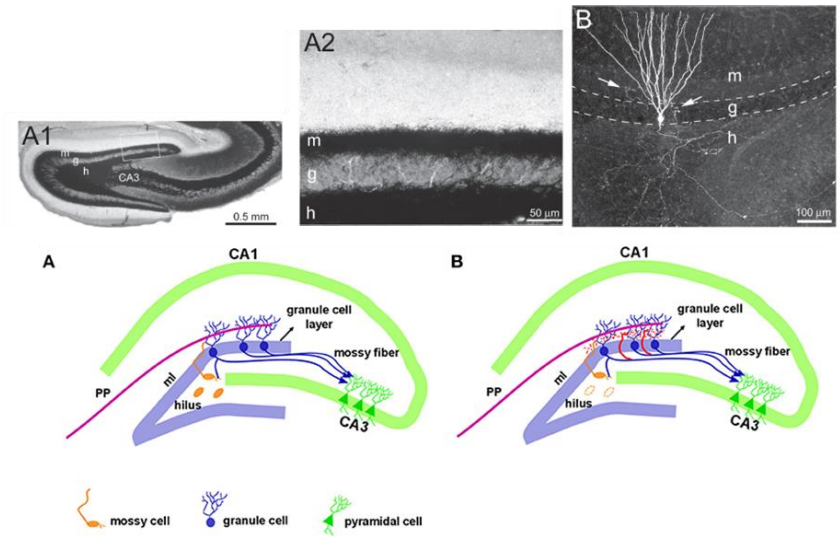

Figure 1.5. Mossy fibre sprouting in the dentate gyrus (DG). (Top) Images of mossy fibre sprouting (adapted from Figure 1, Buckmaster, 2012*); (Bottom) Schematic illustration of normal granule axon projecting to hilus (A) and mossy fibre sprouting with granule cell axons penetrating into n the molecular layer of the hippocampus in red (B). (Figure adapted from Figure 1,* Cavarsan *et al.*, 2018*).*

Despite the emphasis on mechanisms underlying the excitability of glutamatergic neurons, the role of interneurons must not be overlooked. Alterations in interneurons may be more subtle and changes more difficult to detect, not least because of their heterogeneity.

1.2.3. Homeostatic plasticity in epilepsy

Neural networks have an intrinsic machinery for stabilisation. Extrinsic changes in excitation are compensated by numerous mechanisms that return cells and/or circuits to a stable set point. This phenomenon is known as 'homeostatic plasticity'. In epilepsy, homeostatic mechanisms seem to fail to compensate for changes at a network level, allowing seizures to occur (Turrigiano, 1999; Lignani, Baldelli and Marra, 2020). Hypothetically, during epileptogenesis, the brain is repeatedly pushed outside its normal physiological range, exhausting the ability to compensate (Lignani, Baldelli and Marra, 2020).

Alternatively, the compensation at the cellular level is achieved at the expense of making the network unstable. In the pilocarpine rodent model of limbic epilepsy (see below), inhibitory neuronal changes have been reported to be compensated by increases in GABAergic synapses before the onset of spontaneous recurrent seizures (Jett, 2012).

1.3. Ion channels and receptors participating in seizures

1.3.1. Channelopathies

In contrast to the numerous mechanisms in temporal lobe epilepsy, where it is challenging to disentangle causative changes from epiphenomena, the mechanisms of epileptogenesis in some genetic disorders may be more tractable. As mentioned above, genetic mutations in ion channels or membrane receptors have provided especially compelling insights into pathophysiology. Malfunction of key ion channels, including sodium, potassium and calcium channels, or ligand-gated ion channels, leads to changes in intrinsic neuronal properties and ultimately affects the network and leads to epilepsy (D'adamo *et al.*, 2020). Changes in ion channel expression may also arise through transcriptional dysregulation, leading to abnormal firing properties.

This section will discuss some key ion channels and transporters in epilepsy mechanism.

1.3.2. Sodium channels

Voltage-gated sodium channels are fundamental to the initiation of action potentials in the brain. They were identified by Beneski & Catterall in 1980 with the use of scorpion toxins (Beneski and Catterall, 1980). In the mammalian genome, ten genes encode α subunits, with each subunit corresponding to a different subtype, except *SCN6A/SCN7A,* which both encode voltage-independent channels. Nav1.1, Nav1.2, Nav1.3, and Nav1.6 (encoded BY *SCN1A*, *SCN2A*,

SCN3A and *SCN8A,* respectively) are primarily expressed in the CNS. They are all sensitive to the selective, potent blocker tetrodotoxin (TTX) at nanomolar concentrations (Avoli, 2010). Other members of the Nav channel family have roles in the peripheral nervous system, skeletal muscle and heart (Catterall, 2012).

Changes in expression profiles of Nav1.1, Nav1.3, and Nav1.6, as well as β subunits, have been implicated to various levels in both experimental epilepsy models and in human studies (Avoli, 2010). Dominant mutations in Nav channel genes have also been involved in periodic paralysis, cardiac diseases, pain sensitivity disorders, and epilepsy. Nav1.1 is the primary action potential driver in interneurons in the CNS. Autosomal dominant or de novo loss of function mutations in *SCN1A*, encoding the Nav1.1 channel, lead to Dravet syndrome, also known as severe infant onset myoclonic epilepsy. Other disorders related to *SCN1A* mutations (generally with milder disruption of channel function) include benign neonatal convulsions, familial hemiplegic migraine type III, and generalised epilepsy with febrile seizures plus (Catterall, 2012). Studies using the mouse model of Dravet Syndrome have supported the hypothesis that loss of Nav1.1 channels impairs GABAergic interneuron excitability and possibly promotes disinhibition during development. Depending on genetic background, such mice have early-onset seizures and premature death (Catterall, Kalume and Oakley, 2010; Cheah *et al.*, 2012). Changes in Nav properties have also been implicated in epileptogenesis in rodent models of pilocarpine and kindling models of temporal lobe epilepsy (Avoli, 2010).

1.3.3. Potassium channels

The potassium channel is by far the most diverse ion channel family with over 80 genes in several subfamilies (Köhling and Wolfart, 2016). They can be roughly categorised into voltage-gated

potassium Kv channels, inwardly rectifying Kir channels, sodium-activated K_{Na} channels, and calcium-sensitive K_{Ca} channels.

1.3.3.1. Voltage-gated Kv channels

Voltage-gated potassium currents were historically first described by Hodgkin and Huxley in 1952 (Hodgkin and Huxley, 1952). Voltage-gated potassium channels control the waveform and propagation of action potentials. We will focus on two examples with a close link to epilepsy syndromes.

Kv1.1 channel is a voltage-gated fast activating delayed rectifier potassium channel. Its *Drosophila* homologue *Shaker* channel was the first identified voltage-gated potassium channel gene (Papazian *et al.*, 1987; Timpe *et al.*, 1988). The *KCNA1* gene encodes Kv1.1 on chromosome 12p13 in human (D'adamo *et al.*, 2020). The complete Kv1 channel is a tetramer composed of four α subunits; each has six transmembrane segments (S1-S6). The four domains bind together to form the pathway for potassium ions. The segments S5-S6 line the pore and contribute to the gate with the structural support of S1-S4, as revealed by the structure of the homologue Kv1.2 (Chen *et al.*, 2010; Kuang, Purhonen and Hebert, 2015). A highly conserved TVGY(F)G sequence functions as the selectivity filter capable of conducting potassium current at a rate close to the diffusion limit (Doyle *et al.*, 1998). The conductance of voltage-gated potassium channels is approximately 10,000 times higher than that of Nav channels; this kinetics is vital for modulating action potentials (Doyle *et al.*, 1998). Kv1.1 channels are rarely homotetrameric and are more frequently found forming a heterotetrametric complex with Kv1.2, Kv1.4 or Kv1.6 subunits (Ovsepian *et al.*, 2016).

Kv1.1 channels are primarily localised to the axon initial segment (AIS) and also at presynaptic terminals in the CNS (Wang *et al.*, 1994; Jenkins *et al.*, 2011). For instance, axon segments near mossy fibre

glutamatergic excitatory synapses are enriched with Kv1.1/1.4 and Kvβ subunits (Trimmer, 2015; Kim and Nimigean, 2016). Heterozygous dominant-negative mutations of the KCNA1 gene lead to episodic ataxia type 1 (EA1), a dominantly inherited disease (Zuberi *et al.*, 1999). The attacks of cerebellar ataxia in EA1 can be triggered by physical exertion, and patients experience muscle myokymia at other times (Graves *et al.*, 2014). Some patients also experience seizures (Van Dyke *et al.*, 1975; D'Adamo *et al.*, 1999; Zuberi *et al.*, 1999). Overexpressing deleterious mutated gene in CHO (Chinese hamster ovary) cell lines generated sustained potassium current known as 'delayed rectifier' (Smart *et al.*, 1998). Interestingly, heterozygous *Kcna1*$^{+/-}$ mice showed no spontaneous seizures or abnormal EEG activities. Only homozygous *Kcna1* null mice exhibited ictal discharges, spontaneous focal seizures, and an increase in mortality reminiscent of sudden unexpected death in epilepsy (SUDEP) (Smart *et al.*, 1998; Rho *et al.*, 1999). In contrast, a mutation associated with EA1 is embryonal-lethal in the homozygous state, most simply explained by a dominant negative effect of the mutation, affecting not just Kv1.1 but also other Kv1 subunits that normally co-assemble with it.

Current step injections of kcna1-/- homozygous knockout neurons showed reduced action potential threshold and firing propensity than wild type neurons (Brew, Hallows and Tempel, 2003) (Figure 1.6). A knock-in mouse with a point mutation altering a single amino acid in the Kv1.1 channel showed broadened presynaptic spikes and increased spike width (Begum *et al.*, 2016; Vivekananda *et al.*, 2017).

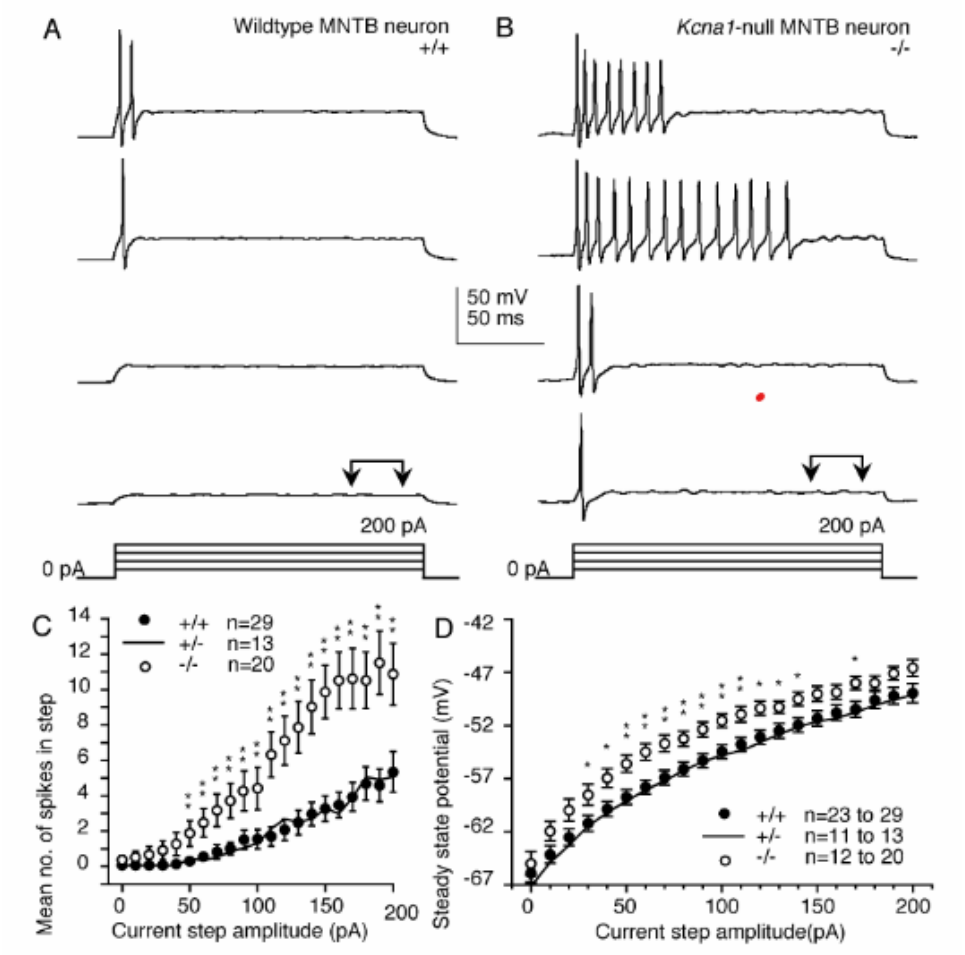

Figure 1.6.The current clamp (10pA steps, 0-200pA) of MNTB neurons with wt and kcna1-/- (homozygous knockout).(A,B) representative traces of wild type and kcna1-/- neurons; (C)(D) mean number of spikes and steady state potential. (adapted from Brew, Hallows and Tempel, 2003*).*

Kv1.1 channel expression has been reported to be affected by the secreted synaptic protein LGI1 (leucine-rich glioma-inactivated 1), altering neuronal excitability(Seagar *et al.*, 2017; Lugarà *et al.*, 2020). Mutations in genes encoding LGI1, and its receptor ADAM22 (disintegrin and metalloproteinase domain-containing protein 22), and binding partner MAGUKs (membrane-associated guanylate kinases), have also been shown to be related to epileptic seizures (Fukata, 2006). Recently, it was shown that the LGI1-ADAM22-complex could regulate the transsynaptic nanoarchitecture and interacts with PSD95 (postsynaptic density protein 95) in rodents (Fukata *et al.*, 2021). Defects in the interaction complex lead to

reduced synaptic transmission and seizures in mice and human (Fukata, 2006; Fukata *et al.*, 2021).

Another group of Kv channels fundamental for excitability is the Kv7 family. Kv7 channels are usually a tetramer made of Kv7.2 and Kv7.3 subunits, encoded by genes *KCNQ2* and *KCNQ3*, respectively (Leppert *et al.*, 1989). A small proportion of Kv7 channels is made of the Kv7.2 subunit only. Kv7 channels are responsible for the voltage-sensitive slowly activating M-current, which has a major role in determining the resting membrane potential (RMP) in neurons (Wang *et al.*, 1998; Hadley *et al.*, 2003). The slow potassium influx contributes to the afterhyperpolarisation of the membrane potential and prevents repetitive firing (Bean, 2007). The axonal scaffolding protein AnkG (Ankyrin-G) interacts with Kv7 subunits and guides their co-localisation with Nav channels at the AIS (Pan *et al.*, 2006; Trimmer, 2015). Interestingly, the Kv7 channel favours the distal axonal membrane, suggesting additional mechanisms may also participate in protein trafficking (Trimmer, 2015). In hippocampal CA1 neurons, Kv7 were shown to have an effect on burst firing, firing threshold and spontaneous firing (Brown and Passmore, 2009). Various defective mutations in *KCNQ2* or *KCNQ3* genes are associated with a rare autosomal dominant inheritable epilepsy syndrome called benign familial neonatal convulsions (BFNC) (Leppert *et al.*, 1989; Singh *et al.*, 1998, 2003). Affected newborns experience early-onset seizures weeks after birth which usually remit after a few weeks. A minority of patients continue to experience spontaneous seizures into adulthood (Singh *et al.*, 2003). The majority of identified mutations affect *KCNQ2*; fewer are found in *KCNQ3* (Brown and Passmore, 2009). The homozygous knock-in of mutated *Kcnq2/Kcnq3* genes leads to tonic-clonic seizures and changes in M-current kinetics in the hippocampus. Heterozygous mutations of *Kcnq2/Kcnq3* genes lead to a reduced threshold for

seizures (Singh *et al.*, 2008). The M-current enhancer drug Retigabine is effective in the treatment of epilepsy in animal models and in patients. It stabilises the open state of Kv7 channels and prolongs opening times (Brown and Passmore, 2009). Studies of other potential M-current enhancers are underway, for the treatment of epilepsy, chronic pain and migraine (Brown and Passmore, 2009).

1.3.3.2. Calcium and sodium activated potassium channels

This group of potassium channels has a versatile role in neurons. This group has less clear relationship with epilepsy. One study reported gain-of-function mutation in the negative regulator of BK ($K_{Ca1.1}$ channel) led to TLE (Köhling and Wolfart, 2016). BK channels are rather the more closely related to absence epilepsy, especially in human patients. A gain-of-function mutation in the α1 subunit mutation accounts for 50% of the affected patients (Yang *et al.*, 2010).

1.3.3.3. Inward rectifying Kir channel family

In addition to Kv channels, the non-voltage gated Kir family are an important modulator of potassium ion dynamics.

The Kir family contains seven subgroups (Kir1.x – Kir7.x), which can be either heteromeric or homomeric tetramers. Each subunit contains two transmembrane domains and a substantial intracellular domain (Hibino *et al.*, 2010). The name 'inward rectifier' describes the asymmetric pore opening and ion conductive properties of Kir channels (Hibino *et al.*, 2010). Because of the lack of voltage-sensor modules, Kir2.x channels are constitutively active. At RMP more negative than the potassium equilibrium potential (E_K, -90mV), the Kir channel conducts an inward potassium current. When the RMP is less negative than E_K, the Kir channel conductance is decreased and outward potassium currents are smaller than

predicted by extrapolating the current-voltage relationship measured at negative potentials (Hagiwara and Takahashi, 1974).

Kir channels are highly expressed in the CNS, peripheral nerves and other organs, including retina, heart, muscle, endothelial cells, kidney, and pancreas (De Boer *et al.*, 2010). Kir2.1 is expressed at highly levels in the brain (Trimmer, 2015), and it is more abundantly expressed by skeletal, cardiac and smooth muscle cells. Loss-of-function mutations in the *KCNJ2* gene encoding Kir2.1 cause Anderson-Tawil syndrome (ATS), a rare autosomal dominant disorder (Bendahhou *et al.*, 2003). In contrast, gain-of-function *KCNJ2* mutations cause a distinct disease called SQT3 (Short QT3) syndrome. The SQT3 syndrome manifests as cardiac arrhythmia and neurodevelopmental deficits (Ambrosini *et al.*, 2014). These pathologies highlighted the importance of the Kir2.1 channel in maintaining the function of different organs.

Overexpressing Kir2.1 in cortical pyramidal neurons led to reduced, but not completely abolished neuronal firing (Béïque *et al.*, 2011). Additionally, a 10mV hyperpolarising drift in resting membrane potential was reported in Kir2.1 overexpressing neurons, as a result of leaking potassium current thorough Kir2.1 channels (Béïque *et al.*, 2011) (Figure 1.7).

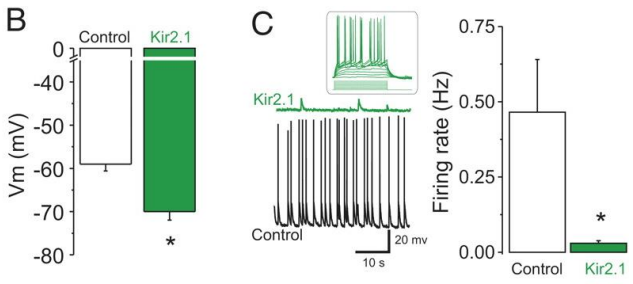

Figure 1.7. Overexpressing Kir2.1 in cortical pyramidal neurons. (B) Resting membrane potential (mV) measured from Control and Kir2.1 overexpressing neurons. (C) Current clamp of Kir2.1 overexpressing neurons showed largely diminished but not completely abolished firing activities (modified from Figure 1, Béïque *et al.*, 2011*).*

Another channel of this family is the astrocytic Kir4.1 channel, which has a more ambiguous role in epilepsy. Various mutations in this channel have been reported in multiple clinical cases, resulting in reduced seizure threshold or in one patient, temporal lobe epilepsy (Köhling and Wolfart, 2016). Loss of function mutation leads to a severe syndrome where epilepsy is accompanied with other deficits (Köhling and Wolfart, 2016).

1.4. Current treatments available for intractable epilepsy

Anti-seizure drugs (ASD) are the main and primary medical interventions in epilepsy. Approximately 60-70% of patients become seizure-free with successful treatment (Cascino and Sirven, 2011). Relief from seizure episodes results in significant improvements in quality of life. Further treatment goals are to mitigate comorbidities including intellectual disabilities, prevent a worsening of epilepsy, and reduce seizure-related mortality. There are a large number of ASDs available, which work through different mechanisms.

The mechanisms of action of the majority of ASDs fall into three rough categories: potentiation of GABAergic inhibition, modulation of voltage-gated ion channels or synaptic transmission, and attenuation of glutamatergic excitation (Black, 1897; Cascino and Sirven, 2011; Thijs *et al.*, 2019). Voltage-gated sodium channels constitute a significant target for ASDs that attenuate repetitive action potentials, such as phenytoin, carbamazepine, oxcarbazepine and lacosamide. Many drugs target more than one type of ion channel; for example, both sodium and calcium channels are targeted by lamotrigine. GABAergic inhibition potentiators such as benzodiazepines (e.g. diazepam, lorazepam) and phenobarbital, target $GABA_A$ receptors by altering their kinetics (Gibson and Patel, 2008). The choice of AEDs is influenced to some extent by epilepsy type, and in rare cases, inappropriate treatments can worsen the condition or elicit adverse effects (Cascino and Sirven, 2011). The priority concerns, safety, and risks should be

thoroughly evaluated in the treatment plan for individuals (Cascino and Sirven, 2011).

As discussed above, medical intervention with ASDs does not always result in seizure freedom. Approximately 30% of patients have pharmaco-resistant epilepsy (Kwan *et al.*, 2010). Drug-resistant epilepsy (DRE) is recognised when two or more appropriate AED plans (that is, with appropriate escalation of dose) have failed to prevent seizure episodes (Devinsky *et al.*, 2018). Failure to treat epilepsy satisfactorily is associated with increased risks of sudden unexpected death in epilepsy (SUDEP), as mentioned above, and poor quality of life. Despite the expanding range of newly approved ASDs, the proportion of drug-resistant epilepsy patients has not appreciably changed in 30 years (Devinsky *et al.*, 2018). This highlights the urgent need for effective alternative therapies.

In practice, the choice of alternative treatments once three or more ASDs have been tried includes resective surgery, electrical neuromodulation (vagal nerve or deep brain stimulation) or ketogenic diet. Surgical resection of the epileptogenic zone has a reasonable prospect of long-term seizure freedom in selected cases, especially in focal epilepsies such as temporal lobe epilepsy (Sperling *et al.*, 2008). However, epilepsy surgery is invasive and represents risks of haemorrhage, infection and death. Furthermore, it is not feasible in a substantial proportion of patients with pharmacoresistant epilepsy where the seizure focus is close to or overlaps with brain areas essential for language, memory, motor function or sensation.

Stimulation of the vagus nerve (VNS) has been claimed to result in >50% decrease in seizure frequencies in over half of patients who are implanted (Devinsky *et al.*, 2018). However, the results are not consistent, and clinical experience is generally disappointing, so the possibility of neurostimulation as a replacement for surgery remains questionable. Deep brain stimulation (DBS), typically targeting thalamic nuclei, has also been used in patients with pharmacoresistant epilepsy,

but this treatment too is invasive, with risks of electrode breakage and infection, and seizure freedom is often not achieved (Magloire and Lignani, 2021). Closed-loop stimulation in other regions of the brain as anti-seizure therapy has had variable results with regards of suppressing seizure generalization in pre-clinical models; thus the effectiveness of this approach requires further investigation (Magloire and Lignani, 2021). The potential reasons behind inconsistency in anti-seizure effects could include the choice of pre-clinical models, the target cell population, or stimulation frequency (Magloire and Lignani, 2021).

Restricted diets have been in practice for epilepsy treatment since the early 20th century, mainly for early-onset seizures in children. The ketogenic diet contains a high fat to carbohydrate ratio. With appropriate dietary management, over 50% of patients have been reported to experience a reduced seizure frequency in some series. Recent work has suggested that the type of fatty acids is key for effectiveness, with medium-chain fatty acids potentially more critical than the presence of ketones in the epileptic brain (Augustin *et al.*, 2018). A recent publication in Cell proposed that the gut microbiome may act on rebalancing GABA/glutamate ratio in suppression of seizures (Olson *et al.*, 2018). However, this diet is challenging to maintain in the long term and potentially leads to metabolic disturbance to other body parts.

In conclusion, currently available treatments are effective for many patients but all. Novel therapies for pharmacoresistant epilepsy with high efficacy and minimal invasiveness are thus urgently needed.

1.5. Gene therapy for epilepsy

1.5.1. Clinical development of gene therapy and historical perspectives

Gene therapy as a treatment for diseases caused by defective genes has a long history going back over 30 years. During 1970s-80s, the possibility of genetic modifications of human genes as a therapy was

widely recognized and discussed (Friedmann and Roblin, 1972; Miller, 1992; Bout, 1996).

The combination of well-understood molecular mechanisms of human genetic diseases, and the development of appropriate genetic editing tools have driven the initiative for human gene therapy clinical trials. The first human clinical trials of gene therapy was commenced in 1988 when there was great hope for 'curing' various diseases. However, with unsuccessful trials and some adverse events, It appeared that the science behind human gene therapy was not as well understood as people believed at the time.

Progress of gene therapy was slowed in the early 1990s, by the death of Jesse Gelsinger. The teenage boy suffered from a deficiency of ornithine transcarbamylase (OTC), which prevents the breakdown of ammonia in the body. The OTC transgene delivered with an adenovirus vector showed promising results in preclinical studies, leading to a phase I trial. Shortly after the viral infusion, Jesse had a severe adverse response and passed away two days later (Somia and Verma, 2000). This event raised alarm about the safety of viral vectors, relevance of preclinical work, pre-treatment screening, and other aspects of gene therapy.

It was not until 2000 that the potential of gene therapy for treating genetic diseases received strong support. Retroviral based *ex vivo* gene delivery of a replacement copy of γc-chain gene successfully rescued children with X-lined severe combined immunodeficiency (SCID) (Cavazzana-Calvo *et al.*, 2000). However, severe adverse events in treated patients was reported in 2003, which cast a shadow over the initial successful 'correction' (Hacein-Bey-Abina *et al.*, 2003). In 2008, five patients who received this gene therapy in France and the UK had developed leukaemia (Hacein-Bey-Abina *et al.*, 2008). Genetic work revealed that insertional mutagenesis had occurred near the LMO2 T cell oncogene (Hacein-Bey-Abina *et al.*, 2008). In-depth analysis revealed that the combination of immune

response and insertional mutagenesis probably led to a poor outcome. These cases all highlighted the need for improvements in delivery methods to minimise adverse reactions. This case in particular highlighted the important for long-term follow up observations in gene therapy, as the adverse events tend not to be immediately apparent after the treatment (FDA/CBER, 2020).

Among the breakthroughs that have made gene therapy much safer in the last 20 years is a switch from adenoviral to adeno-associated viral vectors (AAV). The immune response to adenovirus is reduced with the use of AAV (Büeler, 1999; Chirmule *et al.*, 1999; Chu *et al.*, 2003). Furthermore, AAV vectors have additional benefits of stable long-term expression of recombinant genes (Chu *et al.*, 2003). A detailed comparison between those two viral vectors will be discussed later in this chapter.

In 2003, Gendicine® became the first gene therapy approved by Chinese authorities for use in clinics (Pearson, Jia and Kandachi, 2004). This adenoviral vector was designed to express p53 as a treatment for head and neck squamous cell carcinoma, which accounts for 10% of cancer cases in China (Lang *et al.*, 2014). Since then, one other gene therapy product named Oncorine® was also approved for cancer treatment. As reviewed in 2020, there are currently 20 gene therapies in Phase I-III clinical trials in China (Wang, Wang and Cai, 2020). Both commercial and state funding have expressed great interest in bringing novel gene therapy treatments to the market and benefiting the population. Meanwhile, health and safety remained the primary concern and importance in any commercialisation of gene therapy products anywhere in the world.

Interest in gene therapy in the European and USA markets has also greatly accelerated. In 2013, EMA (European Medicines Agency) approved the use of Glybera®, which is an AAV1 delivering the lipoprotein lipase gene for treatment of the rare inherited disease

LPLD (lipoprotein lipase deficiency) (Bryant *et al.*, 2013). Another eight therapies have since joined the list until 2020. Adoption of gene therapies by insurers and government health systems has not been straightforward. Glybera® was withdrawn from the market in 2017 for its high price and commercial loss (Senior, 2017).

For neurological disorders, the first FDA approved gene therapy using systemic AAV9 infusion, Zolgensma, was approved in 2019 for use in human patients. It was also approved under EMA for use in EU and UK. This single-dose gene therapy portion is designed to treat spinal muscular atrophy (SMA) in infants (Novartis, 2019; European Medicine Agency, 2020). The intravenous infusion of the therapy provides the motor neurons with a functional copy of the *SMN1* gene to replace the mutated one, and restored the overall protein level for normal functionality (Novartis, 2019; European Medicine Agency, 2020). In 2021, this life-saving gene therapy treatment was approved for use in patients. Recent reports on Zolgensma however warn of the rare occurrence of a serious adverse effect, thrombotic microangiopathy (TMA), caused by the viral treatment in children (Yazaki *et al.*, 2022).

Other AAV based clinical trials are ongoing for Batten disease, Duchenne muscular dystrophy (DMD), X-linked myotubular myopathy (XLMTM), Parkinson's disease (PD), and Amyotrophic lateral sclerosis (ALS) (Baird, 2020). Among the ongoing clinical trials, some reported unexpected severe adverse cases and lasting consequences in participants. The reported toxicity cases include hepatotoxicity, kidney damage, TMA, and neuronal loss (e.g. DGN) (Kuzmin *et al.*, 2021).

Obtaining regulatory approval is the most difficult final step before commercialisation. However, there is also a high drop-out rate between Phase I and Phase II/III in clinical trials. Furthermore, current gene therapies approved in the EU and USA are for rare diseases, with limited target populations. For future success in gene

therapy commercialisation, improving efficiency and targeting larger populations may be a game-changer (Senior, 2017).

1.5.2. Gene therapy for neurological disorders

Gene therapy for CNS disorders presents raises some distinct challenges and advantages. For instance, because neurons are non-mitotic, insertional mutagenesis and dilution of episomes bearing the transgene may not occur. On the other hand, endogenous DNA repair mechanisms are not effective, limiting the potential of nuclease-based gene editing. Nevertheless, there are many potential approaches other than simply replacing defective genes (Table 1.1).

Gene therapy strategies	**Gene addition**	**Gene knockout/silencing**	**Gene edition**	**Ex vivo gene therapy**	**Non-integrating gene transfer**
Description	Addition of healthy gene copy to the target genomic loci to normalise overall protein expression	Knockout mutated gain-of-function gen copy from the genome; post-translational knockdown (e.g. small-interfering RNA)	Remove the mutated DNA sequence and replace with the 'correct' nucleotide sequence	Transduce the therapeutic gene in cultured cells which are from patients, and place the cells back into the patient	Delivery of functional transgene copy without genomic integration or genomic editing
Gene therapy examples for neurological disorders with ongoing-clinical trial	Parkinson's disease (AADC gene)	oculoparyngeal muscular dystrophy (PABPN1 gene); Huntington disease (mHTT gene)	Mucopolysaccharidosis (insert missing IDS gene); spinal muscular atrophy type 1 (SMA1 gene)	Metachromatic leukodystrophy (A/ARSA enzymes deficiency)	Mucopolysaccharidoses (h.SGSH gene*)

* human N-sulfoglucosamine sulfohydrolase (h.SGSH)

Table 1.1. Gene therapy strategies for neurological disorders (adapted from Kariyawasam, 2020 (TABLE 2); Deverman *et al.*, 2018; Hudry and Vandenberghe, 2019; Kariyawasam *et al.*, 2020).

1.5.2.1. Gene therapy design considerations

There are several important considerations when designing gene therapy strategies for neurological disorders. The following choices must be made (Blömer *et al.*, 1996; Simonato, 2014; Wykes and Lignani, 2018; Walker and Kullmann, 2019);

I. **Gene transfer type:** First, is the goal to 'correct' a faulty gene or to deliver a gene to alter a cellular process to compensate for the pathology?

II. **Germline or somatic**: It is also essential to consider the timing of gene therapy delivery. Somatic gene editing is so far the most common when discussing feasible gene therapy to correct DNA defects. While somatic gene therapy alters the DNA in selected cells to correct genetic defect, germline gene therapy will pass the correction onto future generations. The potential impact of germline gene editing is still unclear and remain unethical for human applications.

III. **Delivery route:** The delivery of gene therapy should be specific for the target cells and minimally invasive to the patient. Gene therapy for metabolic disorders often uses systemic delivery. However, to modulate the properties of specific populations of neurons, focal delivery may be sufficient to avoid affecting other unaffected circuits. The nuclear entry and transgene expression also partially depends on delivery choice; both viral and non-viral vectors are available.

IV. **Target gene/genes**: The possible target gene or genes depends on delivery capacity and expression efficiency. Alternatively, co-expressing the main target with its binding partner may improve overall effectiveness. For gene editing, the accessibility and chromosomal state of different genes are

variable; active genes are more accessible than quiescent ones.

V. **Specificity and selectivity**: The transgene expression should be exclusive to the target cells or regions.

VI. **Immunoreactivity:** Both humoral and cellular autoimmunity in the brain are increasingly recognised as important disease mechanisms. The introduction of vectors and surface-expressed foreign proteins potentially trigger an inflammatory response and cell death at and beyond the treated region.

VII. **Expression stability:** Persistent and stable gene expression is critical for successful therapy. Exosomes can persist indefinitely in non-dividing cells Genomic integrating strategies have advantages in achieving permanent correction because they do not depend on permanent expression of transgenes. Instead, transient expression of the editing machinery may be sufficient to induce changes to the host genome that either correct or compensate for the disorder.

1.5.2.2. Choice of delivery vectors

As mentioned in the previous section on the development and history of gene therapy, improvements in viral vectors had an important role in making gene therapy safer and suitable for human use. This section will make comparisons between viral vectors in gene therapy use, in the order of their discovery. A summary of available viral vectors are shown in Table 1.2.

1.5.2.2.1. Retrovirus

Retroviruses were the first reported viral vectors with the potential to deliver transgenes for therapeutic purposes. They are RNA viruses that contain reverse transcriptase, which creates a DNA from the viral RNA template. The major limitation of early retroviral vectors for use in CNS

was their inability to infect non-dividing cells. Furthermore, the transgene expression is not stable and often diminishes after a while.

1.5.2.2.2. Lentivirus

Lentivirus belongs to the retrovirus family. However, Lentivirus is capable of transducing post-mitotic non-dividing cells. It is therefore favoured in CNS delivery. With the careful and clever deletion of selected viral genes, lentiviral vectors can infect non-dividing host cells while not adversely impacting the host. Lentiviral construct typically includes WPRE (woodchuck post-transcriptional regulatory element) for enhanced transduction efficiency. The addition of central polypurine tract (cPPT) was considered beneficial for initiating double-stranded DNA synthesis (Somia and Verma, 2000). In addition, Lentivirus can package up to 9kb of transgene length, allowing the delivery of relatively large promoter-transgene combinations.

Viral vectors	*Adeno-associated virus*	*Adenovirus*	*Lentivirus*	*Simple retrovirus*	*Herpes virus*
Transgene capacity	*< 5kb*	*< 8kb*	*10kb*	*8kb*	*30-40kb*
Target cell types	*Mitotic and post-mitotic cells*	*Mitotic and post-mitotic cells*	*Mitotic and post-mitotic cells*	*Only mitotic*	*Mitotic and post-mitotic cells*
Host Genome integration	*Low*	*No*	*Yes*	*Yes*	*No*
Transgene expression stability	*Long-term*	*Short-term*	*Long-term*	*Long-term*	*Very long-term (life-time)*
Risk of host immunogenicity	*Medium/Low*	*Low*	*Low*	*Low*	*High*
Viral replicability in host cell	*Negligible*	*Possible but low risk*	*High*	*High*	*Possible but low risk*
Clinical translatability in neurological disorders	*Only factor approved by FDA so far for neurological disease clinical application; range of stereotypes available*	*Less favoured for clinical translation due to high immunotoxicity in human*	*Low penetrance of BBB in adults; unpredictable host genome integration (oncogenic risk)*	*Significant ontogenetic potential in human*	*Oncolytic potential; but effective in brain tumours*

Table 1.2. *Viral vectors for delivering gene therapy to CNS.*

Current lentiviral vectors achieve stable and persistent levels of transgene expression. The risk associated with insertional mutagenesis cannot be ignored. However, this can be limited by using an integrase-defective lentivirus (Lombardo *et al.*, 2007). As mentioned above, in non-dividing cells, the potential risk of genomic integration is, in any case, less concerning.

1.5.2.2.3. Herpes simplex virus (HSV)

HSV is a neurotropic DNA virus with a large genome (150kb) that contains around 70 genes. Modified HSV vectors can deliver multiple copies of the gene of interest or combinations of genes. HSV leads to transient expression peaking approximately two weeks after entry into the host cell, followed by host cell lysis. This property has been utilised as a lytic brain tumour treatment (Blömer *et al.*, 1996). Efforts to adapt HSV for gene therapy have concentrated on reducing the lytic potential of the virus. Engineered recombinant HSV vectors have been reported for stable and safe transgene (25kb) delivery in the CNS (Verlengia *et al.*, 2017). The potential risk is still associated with cross-contamination with a helper virus which could result in immune responses (Artusi *et al.*, 2018). Furthermore HSV vectors tend to spread trans-synaptically.

1.5.2.2.4. Adenovirus

Adenovirus contains a linear double-stranded DNA genome (36kb). The wild type adenovirus infection is pathogenic and recruits cytotoxic T lymphocytes. Gene transduction by modified adenoviral vectors has been reported in mitotic and non-mitotic cells, including the brain. However, despite the elimination of the replication mechanisms and oncogenic risk genes from the viral genome, a strong undesirable immune response occurs upon delivery to the brain (Akli *et al.*, 1993). Hitherto, optimised adenoviral vectors have not achieved an optimal balance between high transgene expression, low immune reactivity, and absent viral gene expression (Blömer *et al.*, 1996). Interest in using adenovirus as a therapeutic vector has thus

diminished over time both, because of these limitations and because of the introduction of better alternatives.

1.5.2.2.5. Adeno-associated virus (AAV)

AAV has a single-strand DNA genome which is approximately 4.7kb in length (Atchison, Casto and Hammon, 1965; Srivastava, Lusby and Berns, 1983). Its short genomic structure contains two inverted short repeats known as inverted terminal repeats (ITRs) unique to AAV. The two open reading frames (ORF) flanked by ITRs have genetic instructions for the *rep* and *cap* proteins involved in viral replication and structural integrity, respectively. The *cap* protein is the building block of the AAV viral capsid. In the absence of a helper virus, AAV only replicates under rare circumstances (Samulski, Chang and Shenk, 1989).

AAVs are increasingly regarded as promising gene therapy vectors. The early reports in the 1980s discussed the potentials of using AAV for gene delivery into cells (Samulski, Chang and Shenk, 1989). Since then, the application of AAV in gene therapy has undergone an enormous increase, with a handful approved for commercial. AAV has unique features which are favourable as a gene therapy carrier. First of all, AAV is generally considered non-harmful to humans, and an estimated 90% of the human population has already been exposed to AAV2. It suggests that AAV are likely not to cause dramatic immunoactivity upon entry into the human body (Erles, Sebökovà and Schlehofer, 1999). Second, AAV efficiently transduces both mitotic and non-mitotic cells with high efficiency (Kwon and Schaffer, 2008), and numerous reports have suggested successful infection of

muscle, lung, retina and brain(Kwon and Schaffer, 2008). Third, recombinant AAV (rAAV) with all the infectious components removed almost permanently remains as an exosome without any genomic integration(Kwon and Schaffer, 2008). Only under rare circumstances, rAAV can integrate into the human genome(High and Aubourg, 2012). It is particularly advantageous in comparison to Lentivirus, which randomly integrates into genomic loci upon nuclear entry. The particle size of the typical rAAV is about 20nm, which is five times smaller than Lentivirus, enabling better diffusion. However, despite the advantages, rAAV has limitations with smaller packaging size (4.5-4.7kb) and a low but not completely eliminated possibility of insertional mutagenesis.

In addition to wild type AAV2, thirteen serotypes of AAVs have been reported and counting. They have various degrees of transduction efficiency for different cell types, known as tropism. Some are capable of crossing the blood-brain barrier (BBB), while others can enter through a compromised BBB. For example, AAV2 and AAV9 show high transduction specificity for neurons with minimal toxicity (Howard *et al.*, 2008). Recently, AAV-PHP.S, AAV-PHP.B and AAV-PHP.eB have been generated by capsid engineering, and show high CNS transduction efficiency with intravenous systemic delivery (Chan *et al.*, 2017; Challis *et al.*, 2019). More recently, AAV.CAP-B10 was reported by the Gradinaru lab, with improved neuronal specific targeting. It showed more specific brain target and less liver delivery in both mouse and non-human primate with intravenous injection (Goertsen *et al.*, 2022). With continuous generation of new capsids more adapted for

appropriate gene therapy delivery, the precision and efficiency continues to improve.

1.5.2.2.6. Non-viral delivery routes

Non-viral particles benefit from minimal immune reactivity, lower cost and a more straightforward production pipeline. However, gene therapy delivered by direct DNA injection into cells has minimal efficiency and low transgene efficiency (Ingusci *et al.*, 2019). Enclosed particles have been developed to achieve improved stability and delivery efficiency and specificity, including cationic polymers and lipids, nanoparticles (Ingusci *et al.*, 2019). The combination of specialised nanoparticles and magnetic guided systems improved delivery specificity and efficiency to specific brain structures (Christiansen, Senko and Anikeeva, 2019).

1.5.2.3. Cell selectivity and specificity

The selectivity can be achieved in several levels. The capsid proteins themselves obtain selectivity against various cell types upon transduction. The surface topologies of AAV capsids determines its receptor binding upon entry, cell targeting, intracellular trafficking and antigenicity (Weitzman and Linden, 2011).

In addition to capsid proteins, the promoter driving transgene expression can also determine cell-type specificity of expression. Constitutive promoters are used for continuous expression of transgene upon delivery to the target cells. High transgene expression can be achieved by non-specific ubiquitous CMV (cytomegalovirus) promoter (Xia *et al.*, 2006). This viral derived promoter can be further modified by addition of enhancer module. Synthetic promoter CAG was produced by adding chicken beta-actin promoter and rabbit beta-Globin splice acceptor site to CMV

promoter for high expression and stable long-term activation (Jun-ichi *et al.*, 1989; Hitoshi, Ken-ichi and Jun-ichi, 1991). Furthermore, EF-1α (human elongation factor 1 alpha) promoter showed different protein expressions in selected mammalian cells (Qin *et al.*, 2010). For CNS delivery, more specific promoters can be used to drive expression in different cell types. The hSyn (human synapsin) promoter permits neuron-specific expression, while GFAP (glial fibrillary acidic protein) promoter (or its derivative gfaABC1D) is specific for astrocytes (Kügler, Kilic and Bähr, 2003; Lee *et al.*, 2008). In particular, the compact sequence of hSyn promoter (485bp) is a preferable choice for AAV packaging (Kügler, Kilic and Bähr, 2003).

Although hSyn is already specific for neurons, a high degree of functional and morphological heterogeneity is found among neuronal populations. For example, in the forebrain, CamKIIa (calcium/calmodulin-dependent protein kinase IIa) expression is almost exclusive to principal cells (Yizhar *et al.*, 2011). This has led to the use of the CamKIIa promoter to drive excitatory-cell predominant transgene expression in the cortex and hippocampus (Watakabe *et al.*, 2015). However, the CamKIIa expressing neurons are not always excitatory, for example, selected subtypes of CamKII-positive cortical neurons and striatal principal neurons resembles interneuron characteristics. This may present a potential problem with systemic delivery as the transgene could be expressed in other cell types.

Neuronal specific promoters were also reported for interneural population. Two studies identified neuron-specific distalless homeobox 5 and 6(*Dlx 5/6*) genes with GABAergic interneuron exclusive expression in forebrain (Lee *et al.*, 2014; Dimidschstein *et al.*, 2016). The synthetic mDlx (minimal Dlx) promoter sequence was extracted from regulatory enhancer regions of those genes (Dimidschstein *et al.*, 2016). More recently, another interneuron-

specific promoter (GAD65) derived from promoter sequences of the mouse *Gad2* gene was reported (Hoshino *et al.*, 2021). The GAD65 promoter showed preferential expression in PV interneurons in cerebral cortex (Hoshino *et al.*, 2021). However, it was not detected in Purkinje cells, which are the main GABAergic neuronal population in cerebellum (Hoshino *et al.*, 2021). Further investigation is required to understand the mechanisms underlying the promoter activity (Hoshino *et al.*, 2021). With the development of bioinformatic tools may help speed up the search for promoters with true cell-type specificity and no leaky expression in other cell types (Hrvatin *et al.*, 2019). For example, recent work from Allen Brain Institute utilized open chromatin analysis and found enhancer elements capable of activating gene expressions in different subtype of interneurons (Graybuck *et al.*, 2021; Mich *et al.*, 2021).

1.5.2.3.1. Inducible expression systems

Inducible expression systems provide temporal restriction of expression. The tyrosine site-specific recombinase (T-SSRs) induces cleavage, change, and re-ligation of DNA strands upon recognition of specific palindromic sequences, examples of T-SSRs including Cre (Causes recombination)-recombinases. The Cre recombinase was adapted from the mechanism that bacteriophage P1 recognised short 34*bp* loxP (locus of crossing (x) over of P1) sites and introduced a double stranded break which is then followed by DNA recomgination (Abremski, Hoess and Sternberg, 1983; Abremski and Hoess, 1984). With variable arrangements of loxP sites, several DNA modifications can be achieved with the Cre/loxP complex, including excision, inversion, translocation and sequence exchange (Meinke *et al.*, 2016). A further engineered cre-dependent system, Cre-ER (estrogen receptor) combines cre recombinase protein with a mutated ligand binding domain of

human ER (Santoro and Schultz, 2002). The enzymatic activities of the fusion protein is only turned on in the presence of drug tamoxifen, limiting the sequence modification to a specified time window (Metzger *et al.*, 1995). For *in vivo* application, this is useful for creating an inducible knock-out transgenic line when the early gene knock-out is harmful (Metzger and Chambon, 2001). This could, in principle, also be used in gene therapy to add temporal control onto transgene expression; although the use of recombination technology in potential clinical aspects raises substantial safety concerns, including inhibition of neural progenitor cells, and tamoxifen itself interferes with hormonal signalling (Lee *et al.*, 2020).

Another system which is also dependent on drug activation or inactivation is the tetracycline-based system (Gossen and Bujard, 1992; Gossen *et al.*, 1995). This reversible system induces or blocks downstream transgene expressions with the application of tetracycline or its derivatives for switchable gene expressions. The synthetic drug-inducible gene expression system has two modes, TetON and TetOFF, by switching between two drug-responder molecules, rtTA or Tta, respectively (Loew *et al.*, 2010) (Figure 1.8). This system was discovered from *Escherichia coli*, it contains the Tet repressor protein (TetR), and the tet operator (tetO) element for regulating Tn10 tetracycline resistance operon (Berens and Hillen, 2003). The TetR dimer interacts with tetracycline and undergoes conformational change that prevents it from binding to tetO on DNA. The promoters P_A and P_R are then relieved from TetR blockage, inducing protein production (Gossen *et al.*, 1995).

This was soon adapted for mammalian systems, by which the rTA (tetracycline-controlled activator) was produced by adding transcriptional activator domains VP16 and AD (transcriptional activator), as well as combining tetO sequence with a minimal CMV derived promoter (Gossen and Bujard, 1992). This system was

given the name Tet-OFF which works in opposite way, permitting downstream gene expression in the absence of tetracycline. However, the TetOFF configuration is not beneficial for long-term gene expression with continuous drug administration. An alternative tetracycline response system, TetON was engineered to induce gene expression only in the presence of the presence of the doxycycline, a tetracycline derivative (Gossen *et al.*, 1995; T. Das, Tenenbaum and Berkhout, 2016). The protein rtTA was optimized thorough a series of random mutagenesis for more stable binding to DNA in the absence of drug. The latest generation of TetON system has minimal level of background activity and more sensitive to doxycycline (Das, Tenenbaum and Berkhout, 2016).

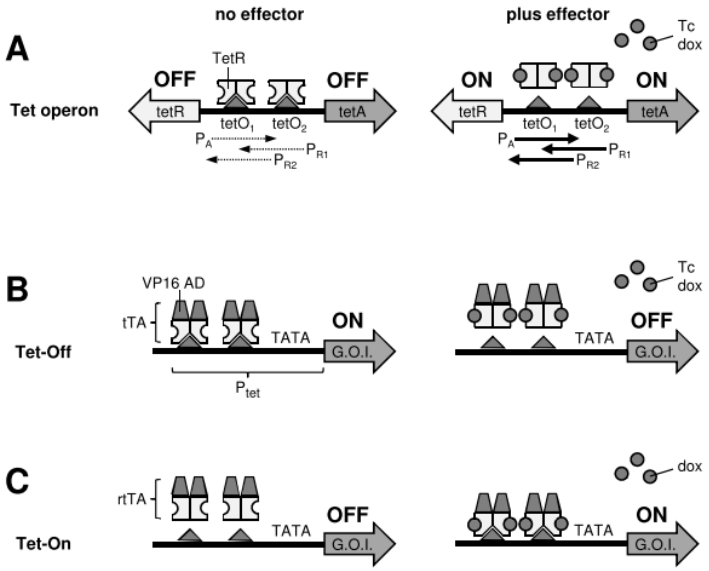

Figure 1.8. Illustration tetracycline-inducible expression system. (A) *TetOperon from E.Coli, modified mammalian gene expression modulator of (B) Tet-OFF and (C) Tet-ON. From* Das, Tenenbaum and Berkhout, 2016).

This is a particularly powerful tool for transient activation or inactivation of transgenes in a tightly controlled time window (Loew *et al.*, 2010).

For example, when therapeutic transgene expression needs to be expressed shortly. The TetON and TetOFF distinguish themselves

from the irreversible cre-dependent system, allowing more versatile applications and controlled gene expression or inhibition without permanent sequence modification. Additionally, as tetracycline and doxycycline are both common antibiotics, its administration to human system also lead to fewer safety concerns.

1.5.2.4. Development and overview of gene editing technologies

1.5.2.4.1. ZFNs and TALENs

Both Zinc-finger nucleases (ZFNs) and transcription activator-like effector nucleases (TALENs) are classical genomic editors. ZFNs contain two FokI domains that wrap around the double-stranded DNA and cut one strand each, creating a double-stranded break (DSB). The ZFNs recognise approximately 5-7bp spacer sequences flanking the cleavage site. TALENs take advantage of naturally occurring protein domains; each is specific for a single base pair. By arranging those domains in any order, it is possible to target any sequences in the gene. The combination of TALE repeats and Folk nucleases generated TALENs for stringent and flexible genome editing. However, both ZFNs and TALENs require extensive protein re-engineering and re-synthesis for every new target. It also limits the number of actual targets they can and able to efficient edit.

1.5.2.4.2. CRISPR

CRISPR (Clustered regularly interspaced short palindromic repeats) genetic editing technology has taken gene therapy into a new era, with the incredible ease to use and to edit target genes. This chapter will discuss the details of this technology, as it is the fundamental technique used in *Chapter 3*.

1.5.2.4.2.1. Discovery and application to human genome

The CRISPR system was discovered a decade before its mechanism was elucidated. In 2012, it was shown that *Streptococcus thermophilus* bacteria can integrate pieces of infecting phage genome into its genome as a new spacer (Barrangou *et al.*, 2007). A specialised enzyme Cas9 explicitly recognised the spacer sequence and has DNA nuclease properties. Further investigation revealed how short CRISPR RNAs (crRNAs) guide the binding of complementary sequences. The additional finding of a critical role of the spacer, known as PAM (protospacer-adjacent motifs), in the CRSPPR machinery ultimately led to the development of CRISPR-gene editing tools. Doudna and Charpentier reported how the CRISPR system could be applied, and identified the essential components (Jinek *et al.*, 2012). This discovery sparked a new research field. Less than one year later, three research groups simultaneously published modified CRISPR gene-editing tools for human genome editing (Cong *et al.*, 2013; Jinek *et al.*, 2013; Mali *et al.*, 2013).

The CRISPR-Cas9 gene-editing system contains a short guide RNA, typically under a U6 promoter, a gRNA scaffold for secondary structure, and a human codon optimised Cas9 protein. Cas9 recognises the 'NGG'-containing PAM consensus sequence and binds to the short guide RNA sequence inside the nucleus (NGG represents any nucleic acid followed by two guanines).

It searches for a complementary sequence in the genome and performs a double-stranded break (DSB) at this site. This may trigger homologous repair (HR) or non-homologous end-joining (NHEJ) DNA repair mechanisms, which can be used to knock in and edit the genomic sequence. In dividing cells where DNA homology template is available, HR is

preferentially triggered for precise DNA sequence repairment, for example in embryonic stem cells (ESCs). NHEJ is the preferred DNA repair mechanism activated in non-dividing cells (Heidenreich and Zhang, 2016).

Due to the limitation of NHEJ, genomic engineering with CRISPR to introduce edits other than deletions in post-mitotic cells presented significant difficulties. The highly error prone NHEJ unavoidably introduces random bases (indels) near the DSB repair site, which then leads to gene knockout or gene deletion (Heidenreich and Zhang, 2016). A novel strategy published by Suzuki et al, 2016 shed light on genomic modifications other than deletion. It is known as HITI (homology-independent targeted integration), which was capable to introduce a functional transgene in a site-specific manner. In essence, the donor DNA contains the transgene which is flanked by two short sequence containing the complementary sgRNA sequence and cleavage sites (Suzuki *et al.*, 2016). They are arranged in a way that when the donor is inserted corrected ,the cleavage sites are then disrupted and eliminated (Suzuki *et al.*, 2016). This robust gene editing strategy provided new possibilities for gene knock-in with NHEJ, however, current technique had less than 5% successful insertion (Suzuki and Izpisua Belmonte, 2018). Further mechanistic studies are required to help improve efficiency for therapeutic benefits.

In addition to changes to the DNA or RNA sequence, defective Cas9 (dCas) derived CRISPR-activation (CRISPRa) and CRISPR-inhibition (CRISPRi) systems are potent transcriptional modulators for increased or decreased protein expression respectively, without genomic editing (Qi *et al.*, 2013; Gilbert *et al.*, 2014). The 'defective Cas9' protein was generated by introducing two mutations in the RuvC1

and HNH cleavage domains (D10A, H841A) (Qi *et al.*, 2013). The removal of enzymatic function from Cas9 protein was independent from sgRNA-Cas9 interaction with DNA sequence (Gilbert *et al.*, 2013; Qi *et al.*, 2013). By fusing dCas9 protein with a high efficiency transcriptional activator or repressor, the dCas9-fusion protein retained highly specific DNA binding properties. Strategically designed sgRNA guided the fusion protein to the appropriate site in proximate promoter of target gene, allowing attached transcriptional regulator to bind to the promoter site and induce or suppress gene transcription (Qi *et al.*, 2013; Gilbert *et al.*, 2014). Therefore the dCas9-sgRNA system can be repurposed as transcriptional modulators for various gene targets. The epigenetic modulation of target genes greatly broadened the scope of CRISPR application . This technique will be explained in more details below for its convenient application in post-mitotic cell populations.

In addition to the spCas9 from *Streptococcus thermophilus,* alternative Cas9 proteins have been discovered. The Staphylococcus aureus Cas9 (saCas9) has similar core enzymatic properties to spCas9 but is smaller in size, therefore more amenable to AAV delivery (Kleinstiver *et al.*, 2015; Ran *et al.*, 2015). Additionally, saCas9 recognized different PAM sequence, therefore potentially unlocking the previously unusable genomic loci for genetic editing (Kleinstiver *et al.*, 2015; Ran *et al.*, 2015).

Furthermore, new types of Cas proteins continued to be discovered, e.g. Cas12 (Cpf1) is a compact and efficient enzyme that makes ssDNA staggered cuts (Zetsche *et al.*, 2015). More recently, a CRISPR-Cas13 RNA targeting system was reported, with was shown to have high fidelity and efficiency in RNA known down (Abudayyeh *et al.*, 2016;

Gootenberg *et al.*, 2017). Further interrogations into the potential off-target.

In all the available Cas9 type gene manipulation systems, off-targets remain an unresolved problem. Due to the limited sgRNA size, the possibility of off-target recognition is present. Another potential obstacle for clinical translation with CRISPR is the immune response to this non-mammalian protein (Crudele and Chamberlain, 2018). Nevertheless, CRISPR gene editing has become the most popular gene-editing tool. Over 20,000 publications using CRISPR have already appeared.

1.5.2.4.2.2. Application of CRISPR to CNS

As neural cells are post-mitotic non-dividing cells, their DNA repair mechanism has poor precision and unavoidably incorporates random base pairs upon DNA end-re-joining of the NHEJ. The Zhang lab published a CRISPR based gene editing study in rodent brains, which targeted MeCP2 genomic loci and knocked out over 70% of the protein expression in neurons (Swiech *et al.*, 2015). Additionally, they have also demonstrated the possibility of multiplex gene editing platform using CRISPR sgRNA sequences arranged in tandem (Swiech *et al.*, 2015). Although the multiple gene silencing effectiveness was not uniform, leading to less effective readout. However, the study provided promising evidence that CRISPR can be applicable for neurological disorders. An example of therapeutic strategies was genetic ablation in neurons was the leptin receptor (LEPR) dysregulation which led to severe obesity. The CRISPR-mediated specific knockout of the LEPR gene in AGRP (Agouti-related peptide) expressing neurons led to disease phenotype and offered possibilities for rescue (Xu *et*

al., 2018). A different study of using CRISPR in neurological disorder focused on early onset Alzheimer's disease. The study attempted to knockout mutated copy of amyloid precursor proteins (APP). Although *in vivo* effectiveness was limited by low neuronal transduction rate, it nevertheless demonstrated new gene therapy strategies for treating neurodegenerative disease using CRISPR.

Due to the challenging nature of genomic editing with CRISPR in brains, CRISPR transcriptional modulator becomes a promising alternative for CNS diseases (Colasante *et al.*, 2019; Savell *et al.*, 2019). In 2019, Colasante et al published a novel gene therapy strategy for Dravet syndrome by targeting the *SCN1A* gene (Colasante *et al.*, 2019). The heterozygous dominant mutation led to haploinsufficiency in *SCN1A* gene expression. The study applied CRISPR activation (CRISRPa) to target the promoter of scn1a gene in a mouse model of Dravet Syndrome, upregulating both alleles to restore the functional protein level, using neonatal AAV9 intracerebroventricular delivery. It also ameliorate febrile seizures, features of the Dravet Syndrome phenotype, in the same mouse model (Colasante *et al.*, 2019).

1.5.3. Preclinical epilepsy models used to evaluate gene therapy

Pre-clinical validation is a crucial step to understand the effectiveness and efficacy of any gene therapy strategy. Some well-characterised *in vivo* models recapitulate the morphological, electrophysiological and pathological features of human TLE or other epileptic syndromes. Understanding the mechanisms of different preclinical model is therefore important for making the most appropriate choice of epilepsy models.

1.5.3.1. Genetic models

Since the advances in genetic techniques, a growing range of transgenic lines has become available for research and aligned with corresponding pathologies in human patients. Rodents manifest seizures and comorbidities that often reflect symptoms in humans. So far, we have seen many gene mutations that can be modelled in animal models with seizures. However, it is also to note that comorbidities observed with human patients do not always manifest in the same way in rodents or other animals. The animal traits are more difficult to evaluate and they may be manifested in drastically different ways.

1.5.3.2. Kindling models

Kindling refers to the phenomenon whereby repeated electrical or chemical stimulation applied to susceptible regions of the brain lead to a gradual lowering of the threshold to elicit epileptiform discharges. In some cases, it ultimately leads to spontaneous epileptic activities. Repetitive electrical stimulations in certain brain structures, such as the amygdala, lead to the recruitment of pathological discharges that propagate through widespread circuits (Goddard, 1983).

Chemical kindling mainly refers to the use of pentylenetetrazol (PTZ). PTZ is a non-competitive GABA receptor antagonist which binds to a t-butylbicyclophosphorothionate (TBPS) site outside the GABA binding region. PTZ is utilised in both acute and chronic models with different protocols. A single subcutaneous injection at a suprathreshold dose (60-100mg/kg) immediately leads to myoclonic seizures and tonic extensions in mice. Repeated injections of sub-threshold PTZ (20-40mg/kg) can be used for kindling, eventually leading to spontaneous seizures (De Deyn *et al.*, 1992). The PTZ model has been used extensively to test anti-seizure or anti-epileptic drugs or test for protective treatments. The overall

threshold dosage, latency to clonus onset, and duration of clonus are all indicative of treatment effects.

1.5.3.3. Chemoconvulsant models for TLE

1.5.3.3.1. Kainic acid (KA)

Kainic acid is an agonist of ionotropic glutamatergic kainite receptors. It was isolated from red algae in 1950s (Murakami, Takemoto and Shimizu, 1953). Originally used as medicine for parasites, it was later found that KA was a powerful chemoconvulsant in rats when injected directly into the cortex. Since then, KA has been used extensively to reveal pathological, electrochemical and mechanistic properties of seizures and to induce an experimental model for TLE (Ben-Ari, 1985). Systemic KA administration induces immediate excessive firing in limbic structures, leading to status epilepticus. This is followed by a latent period before spontaneous recurrent seizures start. This process closely mimics observations in human TLE following episodes of status epilepticus caused, for instance, by toxins or infections. Other features, including hippocampal sclerosis, mossy fibre sprouting, dentate gyrus dispersion, are all present in KA models (Ben-Ari, 1985, 2010).

Kainate receptors are abundant in the hippocampus and to various levels in other brain structures, including the amygdala, entorhinal cortex (EC), cerebellum, and basal ganglia. Several kainate receptor subunits exist (GluK1-5). The complete receptor is tetrameric. GluK4 and GluK5 subunits have an especially high affinity to KA (Lévesque and Avoli, 2013). KA also acts as a non-desensitising agonist of AMPA receptors, which are structurally related glutamatergic ionotropic receptors.

1.5.3.3.1.1. Intracranial administration

The first study using intraventricular administration of KA into the brain to induce excitation was carried out more than 30 years ago (Victor Nadler, 1981). Later studies with KA delivery to limbic structures (amygdala or hippocampus) consistently led to hippocampal neurodegeneration and convulsive seizures in rodents (Ben-Ari *et al.*, 1978; Bouilleret *et al.*, 1999). Unilateral local administration of KA can avoid global damage observed with systemic delivery.

Intra-hippocampal and intra-amygdala models have similar mechanisms, behavioural manifestations and neuropathological characteristics. KA injection (0.3 µg in mice, 2µg in rats) induces convulsive status epilepticus (SE) within 60 minutes. The latent period varies between individual mice. The SE is scorable by the Racine scale from stage 1 to stage 5, from non-convulsive behaviours to falling over and wild jumping (Phelan *et al.*, 2015). In practice, animals are typically treated with diazepam or lorazepam with appropriate delay after KA to reduce mortality (Welzel *et al.*, 2020). In a side-by-side comparison of two models in mice, a lower mortality rate was observed during and in subsequent days after SE with intra- intrahippocampal than amygdala injection (Welzel *et al.*, 2020).

Epileptogenesis occurs after the initial insult, leading to recurrent spontaneous seizures 2-4 weeks post-injection (Welzel *et al.*, 2020). The intra-amygdala model generates more frequent generalised seizures and fewer focal seizures. Ipsilateral hippocampal damage in CA1-CA3, hilus, and dental gyrus is present in both models (Welzel *et al.*, 2020). Studies have shown that CA3

pyramidal cells are more vulnerable than CA1 to SE induced damage (Ben-Ari, 2010; Lévesque and Avoli, 2013). Intra-amygdala KA injection leads to neuronal death in ipsilateral BLA (basolateral amygdala) in addition to the hippocampus (Welzel *et al.*, 2020). Such damage occurs immediately after the SE and is similar to observations in TLE in humans. During the chronic phase, both models develop a secondary seizure focus in the contralateral side that accompanies accelerating generalised seizure initiation and propagation, a phenomenon which has been observed in patients too (Williamson *et al.*, 2009).

Both models are adequately suited to study mechanisms of TLE: they generate high frequency spontaneous recurrent seizures for therapy studies, and they both generate cognitive deficits amenable to behavioural assessments.

1.5.3.3.1.2. Systemic administration

Systemically delivered KA is a less invasive procedure than intracranial injections without the need to gain access to the brain; however, the experimenter has less control of how much KA has entered the brain. KA can be delivered via intraperitoneal (i.p.) or subcutaneous (s.c.) routes. Blood-brain barrier disruption has been observed during SE. It has moreover been reported that albumin entry into the brain promotes hyperexcitability and seizure severity (Noé *et al.*, 2016). Early studies showed that a single dosage of 6-15mg/kg in rats was sufficient to induce SE but with a high mortality rate (Lévesque and Avoli, 2013). An improved model of repeated low dosage KA (5mg/kg) produced the same

result but with a lower mortality rate (Tse *et al.*, 2014). Global lesions and neurodegeneration were observed with systemic KA in bilateral hippocampal CA1-CA3 pyramidal cell layers as well as parvalbumin (PV) interneurons.

1.5.3.3.2. Pilocarpine

Pilocarpine is a potent cholinergic receptor agonist which is also used for epilepsy animal models. This process also targets limbic structures, similar to kainic acid. Firstly described by *Turski et al*, 1983: a single dose of pilocarpine (300-400mg) in rat introduced limbic seizures (Turski *et al.*, 1983; Mello *et al.*, 1993).

When delivered systemically or intracranially, pilocarpine induces progressively intense and prolonged status epilepticus that lasts 24 hours without drug intervention (Scorza *et al.*, 2009). Similar to KA, recurrent seizures are precipitated from the initial SE event caused by pilocarpine injection (Scorza *et al.*, 2009). Cell loss and mossy fibre sprouting were both present in the chronic phase of the mode, recapitulating key pathological features of TLE (Christine J Müller *et al.*, 2009; Christine J. Müller *et al.*, 2009).

1.5.3.4. Other animal models

Other experimental models have been used to study epilepsy mechanisms and test therapies. Tetanus toxin (TeNT), for example, cleaves synaptobrevin and prevents GABA and glycine exocytosis (Schiavo *et al.*, 1992). Injections of low doses of TeNT into the hippocampus or neocortex lead to recurrent seizures in rodents for several weeks (Nilsen, Walker and Cock, 2005). It is noted that although TeNT can induce spontaneous seizures, the injected site does not display structural changes or tissue damages, therefore, the reduction in seizure frequency as a result of applied therapy may

be limited to demonstrating an anti-seizure effect (Mainardi *et al.*, 2012).

Recently, a new optogenetic kindling model of neocortical epilepsy model was reported (Cela *et al.*, 2019). Repetitive pyramidal cell activation led to seizure activity without neural loss or inflammation as observed in conventional kindling models (Cela *et al.*, 2019).

1.5.4. Gene therapy for genetic epilepsy

Monogenic epilepsies resulting from defined mutations are, in principle, amenable to gene therapy to correct or mitigate the molecular defect. Epileptic encephalopathies with more complicated aetiologies (for instance, polygenic or with unknown causes) are, in contrast, difficult to treat with experimental gene therapies due to the lack of clear target. The options for single gene disorders include direct correction of the genomic mutation or modifications of transcriptional or translational machinery to modulate protein expression. For mutations that lead to protein truncations or loss of function, gene replacement is an obvious option, although may be limited by the size of the transgene that can be packaged in a viral vector (Deverman *et al.*, 2018). For point mutations, the genomic sequence could potentially be corrected. However, the safety concerns and limited efficiency of methods to achieve this with CRISPR or other technologies are major obstacles. Post-transcriptional modulation of gene expression can potentially be achieved by targeting mRNA with antisense oligonucleotides, or with trans-acting RNA or other long-non-coding RNA approaches. Several strategies for post-transcriptional modulation to rescue autosomal dominant *SCN1A* mutations that lead to Dravet Syndrome have been published, including antisense targeting a 'poison exon', which leads to mRNA degradation if spliced in. This achieves an increase in gene expression from the unaffected wild type allele to overcome haploinsufficiency (Han *et al.*, 2020). For applications of

those strategies in clinic, there are still many steps to go before they can be deemed safe and effective in human.

1.5.5. Gene therapy for acquired epilepsy

When designing appropriate gene therapy for refractory epilepsy, we must consider (1) Specificity to the epileptic network or the region from which seizures initiate; (2) Specificity for the mechanism of epilepsy and cause of the disease; (3) Absence of interference with physiological processes in the brain to minimise side effects. As discussed in previous sections, the epileptic state goes beyond a simple inhibition-excitation imbalance, which implies that simply increasing or decreasing the level of receptors and ion channels may not always yield an optimal therapeutic outcome. In the next section, we will discuss some examples of gene therapy ideas that have been explored in the literature.

1.5.5.1. Neuropeptides and neuromodulators

1.5.5.1.1. Neuropeptide Y and Y2 receptor

NPY (nuropeptide Y) is a small peptide (36a.a.) abundantly expressed in the CNS and peripheral nervous system. NPY binds to G-protein coupled receptors (GPCRs) in the brain. Among them, NPY has a high binding affinity for Y1, Y2 and Y5 receptor subtypes (Noè *et al.*, 2008). Its interaction with Y2 receptors leads to inhibition of voltage gated calcium channels which then reduces presynaptic glutamate release in rat CA1 (Qian, Colmers and Saggau, 1997). The anti-epileptic potential of NPY overexpression is prompted by two observations: epileptogenesis and seizures modify the expressions of NPY and its receptors; and NPY modulates neuronal excitability (Noè *et al.*, 2008). The level of NPY expression is increased in the hippocampus of TLE patients, coupled with higher Y2 receptor expression (Furtinger *et al.*, 2001). AAV mediated delivery of the

NPY gene in the hippocampus showed a potent effect on seizure prevention in rodent kainic acid and PTZ models (Noè *et al.*, 2008; Avoli, 2010; Noe *et al.*, 2010). Considerable evidence demonstrates the anticonvulsant effect of NPY and receptor overexpression (Woldbye *et al.*, 1997). Later, more work was done on combinatorial AAV therapy with both NPY with Y2 receptors, and showed reduced seizure severity in a rodent kindling model (Woldbye *et al.*, 2010). In 2016, a company (CombiGene AB) initiated a clinical development programme to overexpress NPY with Y2 with an AAV (CG01) (Woldbye *et al.*, 2010). The most recent preclinical study reported decreased seizure duration in male rats treated with CG01, suggesting that CG01 could be a safe and stable gene therapy for TLE (Szczygieł *et al.*, 2020).

1.5.5.1.2. Galanin

Galanin is another neuropeptide that have been studied for its anti-epileptic potential as a therapeutic transgene. This 29-30 amino acid long neuropeptide coexists with several neurotransmitters in excitatory and inhibitory neurons. Its receptors are also GPCRs, namely GalR1-GalR3 (Mazarati *et al.*, 1998). Increase in galanin release was observed with high frequency activity in several disease models (Mazarati *et al.*, 1998). Activation of galanin receptors effectively reduced seizure activity in the pilocarpine model, suggesting a gene therapy potential (Mazarati *et al.*, 1998). Galanin overexpression via rAAV local delivery in the hippocampus reduced seizure frequency in kainic acid intrahippocampal rodent models(Lin *et al.*, 2003). AAV-delivered galanin in piriform cortex increased resistance to kainic acid-induced limbic seizures in rats (Webling *et al.*, 2016) It also protected rats from developing seizures in an electrical kindling model (McCown, 2006). However, it was reported to be

ineffective when applied to human tissue *ex vivo* (Ledri *et al.*, 2015).

1.5.5.1.3. Adenosine

Adenosine is a ubiquitous modulator. The level of adenosine and A1 receptors was elevated after traumatic injury in hippocampal slices. Multiple dysregulated adenosine pathways were found in epileptogenesis and chronic seizures. Dynamic regulation of adenosine is disrupted; restoring the ambient adenosine seems to be a potential gene therapy for traumatic injury related seizures (Boison, 2006).

1.5.5.1.4. Somatostatin

Somatostatin (SST) is a neuropeptide highly expressed by interneurons. In epileptic seizures, an increase in SST expression was observed after hippocampal kindling(Tallent and Qiu, 2008). Overexpressing SST has inhibitory effects in vitro and in vivo animal models, providing promising evidence that SST could be a transgene for epilepsy gene therapy (Tallent and Qiu, 2008). Some concerns associated with endogenous neuropeptide overexpression as gene therapy include both disruption of the endogenous system and receptor desensitization (Tallent and Qiu, 2008).

1.5.5.1.5. Dynorphin

Dynorphin is an endogenously expressed opioid neuropeptide, which binds to the kappa opioid receptor (KOR). This Gi-coupled receptor triggers a downstream MAPK signalling pathway (Houser *et al.*, 1990). In TLE human samples, a decrease in dynorphin expression was observed while the KORs level was maintained (De Lanerolle *et al.*, 1997). It was shown by multiple studies that KOR activation by endogenous ligands can act as a

protective agent against anticonvulsants (Loacker *et al.*, 2007). An AAV delivering release of a precursor of dynorphin in response to intense activity achieved acute seizure suppression and cognitive behaviour rescue in mice (Agostinho *et al.*, 2019; Christian-Hinman, 2021).

1.5.5.1.6. GDNF (glial-cell lined-derived neurotrophic factor)

The GDNF family of ligands are released from neurons and they bind to GFRα1-4 receptors to activate tyrosine kinases and activate downstream signalling pathway. In kainic acid rodent models, an increase in GDNF level was observed in various regions of hippocampus (Schmidt-Kastner *et al.*, 1994; Mikuni *et al.*, 1999). In a pilocarpine induced seizure model, an increase in GDNF was also present in striatum and cortex (Schmidt-Kastner *et al.*, 1994). These observations suggested a possible link between GDNF and an increase in seizure-induced excitation. GDNF delivered by rAAV improved the survival rate post-SE, was neuroprotective, and had anti-epileptic effects in the mouse kainic acid model (Kanter-Schlifke *et al.*, 2007). Recent encapsulated cell technology delivered GDNF directly into hippocampus showed long-term and stable release of GDNF reduced seizures (Paolone *et al.*, 2019).

1.5.5.1.7. Clinical application of neuropeptides as anti-convulsant agents

Neuropeptides are attractive because they act at very low concentrations via specific interactions with target receptors to modulate networks. However, neuropeptides as virally delivered transgenes also face several challenges to clinical translation, including the difficulty to restrict their action to specific neuronal targets in the treated region. Because neuropeptides potentially interact with multiple receptors or have roles in multiple

signalling pathways, potential side effects should be thoroughly investigated to avoid undesirable outcomes. Nevertheless, coupled with advanced delivery, neuropeptides could be effective anticonvulsants to treat intractable epilepsy.

1.5.5.2. Endogenous channels and receptors

Glutamatergic transmission is central to neuronal excitation. Therefore, glutamate receptors seem to be suitable therapeutic targets. In pilocarpine-induced status epilepticus, membrane accumulation of NMDARs seems to play a role in excessive excitation (Naylor *et al.*, 2013). Ion channels are potential endogenous targets. For example, Kv1.1 channel has two essential roles in action potential modulation: setting the shape of the action potential and modulating synaptic release .

Kv1.1 channel overexpression delivered to excitatory neurons with a Lentiviral vector increased the current threshold for firing and reduced the action potential frequency-current relationship when measured in *ex vivo* acute brain slices (Wykes *et al.*, 2012). When lentiviral vector overexpressing Kv1.1 was injected in TeNT treated motor cortex, it prevented spontaneous seizure occurrence in the model (Wykes *et al.*, 2012). This earlier work provided convincing evidence that overexpressing Kv1.1 predominantly in the excitatory neuronal population was sufficient to suppress spontaneous seizures.

To further evaluate the strategy and improved the design of the therapy, an engineered codon-optimised version of KCNA1 gene was introduced by Snowball, Chabrol & Wykes*, et al,* 2019. The delivery vector was switched to a non-integrating lentivirus with more clinical application in mind. This study also showed that AAV delivered CamKII-KCNA1 therapy reduced seizure frequency in a rat model of TLE (Snowball *et al.*, 2019). Kv1.1 channel overexpression

is thus effective in seizure attenuation in multiple models of epilepsy.

Furthermore, a different strategy was proposed to upregulate endogenous mouse *Kcna1* gene in a mouse TLE model. In this study, CRISPRa was used to upregulate endogenous Kv1.1 channel expression in excitatory neurons. This epigenetic modulator successfully increased Kv1.1 expression *in vivo* and reduced frequency of spontaneous seizures in an established mouse TLE model (Colasante *et al.*, 2020).

This series of studies demonstrated consistent anti-seizure and anti-epileptic effects of Kv1.1 channel overexpression.

1.5.5.3. Exogenous and engineered candidates

1.5.5.3.1. Optogenetics

The first opsin used to control behaviour was validated in *Drosophila*. Among versatile opsins, the light-activated ion channel Channelrhodopsin (ChR2) was derived from an algal protein. The expression of ChR2 in neurons was sufficient to control their firing properties (Boyden *et al.*, 2005). Inhibitory light-responsive ion transporters were derived from proteins expressed by archaea: NpHR (Natronomonas pharaonis halorhodopsin, inward chloride pump) and Archaerhodopsin (AR family) outward proton pump) (Zhang, Aravanis and Adamantidis, 2007). A modified ChR2 with anion conducting properties has recently been developed for direct photo-stimulated chloride influx and neuronal inhibition (Berndt *et al.*, 2014; Wietek *et al.*, 2014).

Optogenetic control of neuronal excitability attracted attention from researchers. The Kokaia group reported that overexpressing NpHR in excitatory neurons of hippocampal organotypic slices reduced epileptiform activity (Tønnesen *et al.*, 2009). After the demonstration in cultured hippocampus, Soltesz's group showed

that optogenetic modulation of various cells reduced epileptiform activities in temporal lobe epilepsy model with kainic acid (Armstrong *et al.*, 2013; Krook-Magnuson *et al.*, 2013). In 2012, Wykes *et al.* demonstrated similar inhibitory effects *in vivo* in a rodent focal cortical epilepsy model (Wykes *et al.*, 2012). In another study optogenetic suppression of thalamocortical activity restricted the spread of epileptiform activity and enhanced GABA mediated inhibition for seizure attenuation (Paz *et al.*, 2013; Paz and Huguenard, 2014). The optogenetic strategy in various animal models of epilepsy demonstrated its therapeutic potential for application in human, with carefully selected target cell population, choice of opsin and fine turning of the stimulation strength (Paz and Huguenard, 2014).

However, clinical translation of optogenetic techniques still requires further validation and technical improvements (Vandekerckhove *et al.*, 2021). The insertion of an optic fibre is invasive and increases the chance of infection. Temperature increases around the illuminated region should be avoided. In addition, as opsins are not native to the human body, there is a risk of immunoreactivity. The efficiency of ChR2 on neuronal excitability control needs to be further evaluated. Closed-loop optogenetics has been developed to avoid manual control of the light delivery, making an automatic seizure attenuation device feasible (Armstrong *et al.*, 2013; Mickle *et al.*, 2019).

1.5.5.3.2. DREADDs

Designer Receptor Exclusively Activated by Designer Drugs (DREADDs) were introduced by Bryan Roth's laboratory in 2005 (Roth, 2016). This group of engineered receptors originated from muscarinic acetylcholine (ACh) receptors with binding sites mutated to make them insensitive to ACh but activated by the inert molecule clozapine-N-oxide (CNO). The 3rd generation

DREADDs include $hM3D_q$(excitatory, Gq-based) and $hM4D_i$ (inhibitory, Gi-based) receptors for potent neural excitability modulation. In 2014, Katzel et al. reported that overexpressing inhibitory $hM4D_i$ coupled with systemic administration of CNO had a reversible anti-seizure effect (Kätzel *et al.*, 2014). The AAV5 expressing $hM4D_i$ under a CaMKII promoter protected rats from severe acute evoked seizures and showed a reduction in seizure frequency in a chronic tetanus toxin model (Kätzel *et al.*, 2014). In the absence of CNO, the $hM4D_i$ receptor is not active. An important re-evaluation of DREADD technology was made in 2017, revealing that CNO itself cannot cross the BBB. It is reverse-metabolized to clozapine for brain access (Gomez *et al.*, 2017). The conversion rate is relatively low; a high dosage of CNO was required for DREADD activation *in vivo*. Clozapine is itself a DREADD agonist, and is a commercially available antipsychotic medicine, raising the prospect of using it as an alternative re-purposed activator. However, it has a poor side effect profile, calling for alternative ligands to activate DREADD more safely. Both perlapine and compound 21 are alternative muscarinic DREADD ligands but their safety profiles are not known. In 2019, Weston *et al.* characterized olanzapine, another antipsychotic drug in clinical use, as a potent agonist of $hM4D_i$ receptors, with validation in rodent behavioural experiments (Weston *et al.*, 2019). The search for more suitable ligands for clinical use will continue, and hopefully, in the future, a better system with no side effects will be produced.

1.5.5.3.3. GluCl

One limitation of DREADDs is poor temporal control of receptor activation; it may takes an hour or more for the intracranial drug concentration to reach adequate levels, and there may also be a lag for chemicals to be metabolised entirely out of the system. A

self-regulatory chemogenetic approach may overcome these problems. The glutamate-gated chloride channel GluCl is expressed by many invertebrates including *C. Elegans* (Cully *et al.*, 1994). The anti-helminthic drug ivermectin activates this channel (Walker and Kullmann, 2019). In the mammalian brain, glutamate is the main fast neurotransmitter at excitatory synapses. In physiological conditions, the extrasynaptic spread of glutamate is tightly restricted by glutamate transporters. In the epileptic brain, however, the extrasynaptic glutamate concentration is increased, in part because excessive synchronous glutamate release overwhelms transporters (During and Spencer, 1993; Stephens *et al.*, 2014; Lieb *et al.*, 2018). A GluCl derivative with increased glutamate sensitivity was engineered to detect this phenomenon as an indicator of epileptic activity and, in response, open the chloride channel (Lieb *et al.*, 2018). The chloride conductance shunts excitatory currents, attenuating further action potential generation (Lieb *et al.*, 2018). It is, therefore, autoregulatory without the need for pharmacological induction. Viral delivery of GluCl showed anti-seizure effects in two different focal cortical rodent models, and I contributed to this project by showing that it had no effect on locomotor function (Lieb *et al.*, 2018).

However, clinical application of GluCl faces the same issue as CRISPR with regard to potential immunity against exogenous proteins. Whether it triggers neuronal inflammation calls for further investigation.

1.6. Summary

This chapter provided a general overview of epilepsy, highlighting the largely unmet need for effective non-invasive therapies to treat refractory epilepsy. Gene therapies are more advantageous than conventional resective surgery for its minimal disruptions to brain

anatomy while eliminating the recurrent seizures, potentially returning the patients to normal lifestyle. Among the published strategies in the literature, we highlighted a few which either hold great clinical promise or are already on the path to clinical translation.

This chapter also highlighted the ground-breaking gene editing technology CRISPR and how it could be a powerful tool in treating neurological disorders, including those that do not result from a genetic aetiology. The application of CRISPR technology in epilepsy will be further investigated and discussed in details in Chapter 3.

This chapter have also identified and discussed the limitations of gene therapy strategies for epilepsy. Chapter 4 of this thesis will discuss a novel therapy which could address some of the limitations and improve its efficacy.

In this thesis, we will introduce and discuss two new gene therapy strategies for refractory epilepsy, aiming to address different limitations of current gene therapy strategies for acquired epilepsy.

Chapter 2

Materials and Methods

2.1. Plasmid design and constructions

2.1.1. c-FosP-dsGFP/c-FosP-dsGFP-*KCNA1* $^{co/1400v}$

The *KCNA1* $^{co/1400v}$ sequence was gifted by Dr Snowball(Snowball *et al.*, 2019). The vector pCCL-c-FosP-dsGFP was made by cloning the c-Fos promoter (c-FosP) sequence from Fos-tTa(Reijmers *et al.*, 2007) (Addgene #34856) and replacing the PCK promoter in PGKP-dsGFP. The pCCL-c-FosP-dsGFP-T2A-*KCNA1*$^{co/1400v}$ plasmid was produced by subcloning dsGFP-T2A-*KCNA1*$^{co/1400v}$ into the c-FosP-dsGFP plasmid digested with BamHI and SalI. The pX552-c-FosP-dsGFP and pX552-dsGFP-*KCNA1* constructs were produced with restriction enzyme digestion and religation into empty pX552 construct backbones.

2.1.2. c-FosP- dsGFP -*KCNJ2*

The dsGFP-T2A-*KCNJ2* fragment was synthesized by GeneArt customized DNA synthesis service (ThermoFisher) and was used to replace the dsGFP-T2A-*KCNA1* in the previous construct (1.1.1) via restriction enzyme digestions and ligation.

2.1.3. miniArc-dsGFP/miniArc-dsGFP-*KCNA1*$^{co/1400v}$/miniArc-dsGFP-*KCNJ2*

The miniArc (mArc) promoter was extracted from a pAAV-ESARE-miniArc-ERT2-Cre-ERT2 construct that had been previously produced as a gift with primers for the addition of a MluI digestion site at the 5' end. This was followed by restriction enzyme digestion of pX552-c-FosP-dsGFP with MluI and EcoRI to generate a backbone vector without a promoter sequence. Subsequent ligation replaced the promoter with the new miniArc promoter

sequence. The same enzyme digestion and ligation protocol was used to generate miniArc-dsGFP *KCNA1*$^{co/1400v}$ and miniArc-dsGFP-*KCNJ2* plasmids for viral packages.

2.1.4. ESARE-dsGFP/ESARE-dsGFP-*KCNA1*$^{co/1400v}$/ESARE-dsGFP-*KCNJ2*

The steps for creating ESARE constructs were identical to what was described in 1.1.3; however, the ESARE promoter has a different 5' initiation site and, therefore, a new forward primer was designed to extract and add the MluI restriction site to the extracted ESARE promoter fragment.

2.1.5. Egr1-dsGFP-*KCNA1* $^{co/1400v}$/Egr1-dsGFP-*KCNJ2*

The Egr1 promoter sequence (516bp) was extracted from the mouse EGR-11 promoter components of EGR-1 TurboGFP construct (Addgene)(Varma and Voldman, 2015). The promoter sequence was aligned 100% identical to the 5' UTR of the mouse EGR-1 gene. This mouse EGR-1 promoter, flanked by MluI and EcoRI restriction enzyme sites, was synthesized by GeneArt (ThermoFisher). It was then purified with restriction enzymes MluI and EcoRI digestions and ligated into vector backbones that lack the promoter: pX552- dsGFP-*KCNA1* $^{co/1400v}$ and pX552 -dsGFP-*KCNJ2* as promoters.

2.1.6. N_{RAM}-dsGFP-*KCNA1* $^{co/1400v}$/ N_{RAM}--dsGFP-*KCNJ2*

The N_{RAM} enhancer sequence was described by Sun *et al 2020* (Sun *et al.*, 2020). The enhancer repeats were followed by the human promoter sequence (hc-FosP) extracted from *Sorensen*, et al. 2016 (Sørensen *et al.*, 2016). The DNA fragment was synthesized by GeneArt (ThermoFisher) with customised request.

2.1.7. c-FosP-Ctrl-dCas9A and c-Fos-KCNA1-dCas9A

2.1.7.1. U6-sgRNA19-c-Fos-rtTA-T2A-EGFP/ U6-sgLacZ-c-Fos-rtTA-T2A-EGFP

The pLenti-U6-sgRNA19-c-Fos construct was produced by insertion of the c-Fc-Fos promoter sequence from pCCL-c-Fos-dsGFP-T2A-KCNA1$^{co/1400v}$ into a XhoI and AgeI restriction enzyme digested pLenti-U6-sgRNA19 backbone (gift from Vania Broccoli lab). The rtTA-EGFP construct was custom made by GeneScript containing BanHI and AgeI restriction sites, and was sub-cloned into pCCL-U6-sg19-c-Fos construct to produce pLenti-U6-sgRNA19-c-Fos-rtTA-T2A-EGFP. A control construct with sgLacZ was produced by extracting sgLacZ from pLenti-U6-sgLacZ-Hpgk-rtTA (gift from Vania Broccoli lab) with PCR, using primers sgLacZ_F and sgLac_R. It was cloned into pCCL-U6-sgRNA19-c-Fos with restriction enzyme PpuMI and XhoI digestion to produce pCCL-U6-sgLacZ-c-Fos-rtTA-T2A-EGFP. The U6-sgRNA19-c-Fos-rtTA-T2A-EGFP and U6-sgLacZ-c-Fos-rtTA-T2A-EGFP fragment was then extracted with PCR using MluI_F and SalI_R primers. An empty AAV backbone was produced by restriction enzyme MluI and SalI digestion of pAAV-U6-sgRNA19-hSyn-rtTA (gift from Vania Broccoli lab). And the U6-sgRNA-c-Fos-rtTA-T2A-EGFP and U6-sgLacZ-c-Fos-rtTA-T2A-EGFP were ligated with the digested backbone to produce pAAV-U6-sgRNA19-c-Fos-rtTA-T2A-EGFP and pAAV-U6-sgLacZ-c-Fos-rtTA-T2A-EGFP.

2.1.7.2. pAAV-TetON-dCas9-VP64

The pAAV CamKII-tdTomato-T2A-rtTA-U6-sgRNA19, control construct pAAV CamKII-tdTomato-T2A-rtTA-U6-sgLacZ, and pAAV-TetON-dCas9-VP64 plasmids were gifted by Vania Broccoli lab (Colasante *et al.*, 2019, 2020). All the primers used in the steps above are listed in full in Table 2.1

Experiment	Primer Name	Sequence
C-Fos promoter extraction from Addgene template	BamHI_F	ACAGCGGATCCAGCGCTGTGAATGGATGG
	EcoR1_R	ACAGCGGAATTCTCTTCGCTATTACGCCAGGC
C-Fos promoter extraction	c-Fos_F	ACAGCTCGAGTTCGCTATTACGCCAGGC
	c-Fos_R	ACAGACCGGTATCTTCATGGCGGGCATG
mArc promoter extraction	MluI_Arcmin	CAC*acgcgt*CGCGCAGCAGAGCAC
	EcoRI_Arcmin	CACA*gaattc*TCTGCTAGCCTGGTCGTCGGTG
ESARE extraction	MluI_esare	GGCCGCacgcgtAGC
sgLacZ extraction	sgLacZ_F	ACAGGATCCATCGTTTCAGACCCACCTCC
	sgLacZ_R	ACACTCGAGACCCCGTGGGAaATCGATG
U6-sgRNA-c-Fos-rtTA-T2A-EGFP extraction	MluI_F	ACAACGCGTTTAACGAGGGCCTATTTCCC
	SalI_R	ACAGGTCGACCATACGGGAAGCAATAGC

Table 2.1. List of primers used in all primers used in the project.

2.1.8. Polymerase change reaction (PCR)

Reactions were performed with PfuUltra II Hotstart PCR master mix 2x (Agilent Technologies). The PCR samples were prepared with 25µl PCR master mix, 1ul of each primer (forward and backward, 10µM), 1ul of DNA template (100ng/µl) and distilled water to a total volume of 50µl. Samples were placed in the thermocycler with the following programme (modified from PCR master mix manual) (Table 2.2). The reaction mixture was purified with a QIAquick PCR purification Kit (Qiagen, #28104).

Segment	**Number of cycles**	**Temperature**	**Duration**
1. Pre-denaturation	1	95°C	2 minutes
2. Denaturation	30	95°C	30 seconds
Annealing		Primer (T_m-5°C)	30 seconds
Elongation		72°C	1 minute (< 1kb) 1min/kb (>1kb)
3. Final elongation	1	72°C	10 minutes

Table 2.2. PCR protocol in details.

2.1.9. Restriction Enzyme Digestion

Restriction enzyme digestion of primers and DNA plasmids were performed according to standard protocols of the supplier New England Biolabs (NEB). High-fidelity® versions were used whenever

possible to enhance yield. Digested products were purified with a QIAquick PCR purification Kit (Qiagen, #28104).

2.1.10. Gel electrophoresis and DNA extraction

Digested DNA may require gel electrophoresis to separate out undesirable fragments of the wrong size. The mixtures were loaded and separated on 1% agarose gel containing GelRed™ nucleic acid stain (Biotium) for DNA visualization. The band of desirable size was then extracted from the gel and purified with Wizard® SV gel and PCR clean-up system (Promega).

2.1.11. DNA ligation

Ligation reactions were performed with T4 ligase (NEB, #M0202S) and standard buffer from the supplier. In general, the total reaction is 20 µl, with 1 µl T4 ligase, 2 µl 10x T4 ligase reaction buffer, 100 ng backbone DNA and the appropriate amount of insert, and distilled water. The amount of insert that we used was determined by the size ratio of insert and backbone plasmids, ranging from 1:10 to 1:2. The thermocycler maintained the sample temperature at 16°C for 18-20 hours.

2.1.12. Bacterial Transformation

Ligated DNA plasmids were transformed into One Shot® Stbl3™ chemically competent Escherichia as per manufacturers' instructions (Thermo Fisher Scientific (TFS), #C737303). The transformants were grown on imMedia™ ampicillin Agar plates (TFS, #Q60120) at 37°C for 16-18 hours. When colonies appeaed, they were picked and grown in imMedia™ ampicillin media liquid (TFS, #Q60020) for 20 hours at 37°C and shaking at 200-250rpm.

2.1.13. DNA extraction, purification and sequencing

Bacterial cells were collected, and plasmid DNA was extracted using GenElute™ plasmid miniprep kit (Sigma-Aldrich, #PLN350-1KT). For larger volume, plasmid DNA was extracted with EndoFree plasmid maxiprep kit (Qiagen, #12362). All the plasmids made were sequenced in part, or in full, with the Overnight Service™ (Source Bioscience) before subsequent use.

2.2. Viral vector synthesis

2.2.1. In-house lentivirus synthesis

Lentivirus of pCCL-c-Fos-dsGFP and pCCL-c-Fos-dsGFP-*KCNA1* were synthesized in-house with the help of T. Turner and Dr J. Carpenter. Human embryonic kidney (HEK) 293T cells were cultured with DMEM Glutamax™ +pyruvate (Gibco, TFS, #10569010) supplemented with 10% HI-FBS ((Heat-inactivated, US origin, TFS, #16140071) and 1% Penicillin Streptomycin (100x; Invitrogen). Cultures were maintained at 37°C with humidified 5% CO_2 environment. HEK 293T cells were passaged every 3-4 days with a maximum passage number of no more than 20. For lentiviral synthesis, HEK 293T cells were seeded in T500 triple-layer flask per manufacturer's instructions to reach 70 - 80% confluency. Cells were transfected with second-generation lentiviral packaging, envelope and transfer plasmids at 2:1:2.25 ratio (Tiscornia, Singer and Verma, 2006). The cell medium containing viral particles was harvested 48 hours after transfection. It was clarified with centrifugation at 1000rpm for 3 minutes at 4°C, followed by passing it through 0.45 µm filter and stored at 4°C to avoid yield loss. The viral particles were collected by centrifugation at 20,000rpm for 2 hours (Beckman Ultracentrifuge). The clear medium was discarded, and the virus pellet was re-suspended with 200µl PBS (TFS) after a 6-hour incubation at 4°C. Lentiviral

suspensions were aliquoted and snap-frozen in liquid nitrogen or dry ice and immediately stored at in a -80°C freezer.

2.2.2. In-house AAV synthesis

The in-house AAV synthesis was carried out with help from I. Zalivina, using a protocol adapted from (Grieger, Choi and Samulski, 2006). In essence, a half prep of AAV required 600µg helper plasmid, 200µg cap-rep plasmid of AAV9 serotype and 200µg construct plasmid. The helper plasmid and AAV9 cap-rep plasmids were both gifts from L. Ussingkaer (Schwartz *et al.*, 2007). HEK-293T cells culture was the same as in the lentiviral preparation; cells were plated on 20x 150 cm^2 Petri Dishes (Thermo Scientific™ Nunc™ Cell Culture/Petri Dishes). Cultures were maintained at 37°C with humidified 5% CO_2 environment and checked daily for confluency. Once the cells reached 80% confluency, they were transfected with helper plasmid, cap-rep plasmid and constructs at 3:1:1 ratio together with transfection reagent PEI MAX (PEI MAX Transfection Grade Linear Polyethylenimine Hydrochloride (MW 40,000)) at a ratio of approximately 2PEI:1DNA (Negrini *et al.*, 2020). The cells were added with Opti-MEM (Opti-MEM I Reduced Serum Media). Typical viral production time was 96-120 hours after transfection with AAV9. Afterwards, cells containing viral particles were harvested with specialized flasks and lysed (Schagen *et al.*, 2000). The cell lysate went through freeze and thaw cycles followed by Benzonase treatment (Benzonase® Nuclease) to destroy non-viral DNA and RNA (Schagen *et al.*, 2000). The viral particles were further purified by iodixanol gradient, which concentrates the viral particles into a dense, thin layer inside the centrifuge tube (Zolotukhin *et al.*, 1999). The viral particles were then carefully withdrawn using a 19-gauge needle from the distinguished layer (Zolotukhin *et al.*, 1999). The viruses were further concentrated to

120-250 µl for titre suitable in experiments. The final yield of AAV viral suspension was also dependent on the size of the construct plasmid, therefore variability was present between different constructs (Grieger and Samulski, 2005). The titres of in-house AAV were calculated with an AAV pro® titration kit (Takara). For in-house AAV productions, all viruses used in experiments had titre estimates of at least 10^{13} vg/ml, sufficient for *in vitro* and *in vivo* applications (Aschauer, Kreuz and Rumpel, 2013).

2.2.3. Commercial AAV vector synthesis

AAV9 c-FosP-Ctrl-dCas9A and AAV9c-FosP-KCNA1-dCas9A viruses and parts of the AAV9 c-FosP-dsGFP/c-FosP-KCNA1 were produced by a commercial supplier (Vector Builder) with quoted titres of > 10^{12} GC/ml (or vg/ml).

2.3. Primary neuronal cultures

2.3.1. Primary Neuronal Cultures

Primary cortical neurons were prepared from postnatal 0-1 (P0-2) WT CBL6 mice pups. After dissection, cortices were washed with ice-cold HBSS based buffer (HBSS and 5mM HEPES, 1M, pH7.4; Sigma-Aldrich (SA) and Invitrogen) and treated with trypsin (25-30mg trypsin; 10mg ml-1 DNase, 137mM NaCl; 5mM KCL; 7mM Na2HPO4; 25mM HEPES). The tissues were then dissociated with dissociation buffer (12mM MgSO4, 10mg ml-1 DNAse in HBSS buffer). And the cell suspension was pelleted by centrifugation, resuspended, and counted with a haemocytometer and an inverted microscope. The cell suspension was then diluted with Neurobasal A complete medium (Neurobasal A, Invitrogen, # 10888022) supplemented with B27 (Invitrogen, #17504044), Glutamax (Invitrogen, #35050038), and 1/1000 Penicillin-Streptomycin (5,000 U/ml, TFS, #15070063). With the exceptions of Western Blot and MEA experiments, neurons were plated with

a density of 120,000 – 150,000 cells/well on poly-lysine (10mg/ml, in borate buffer) treated coverslips (13mm, VWR, #631-0148) in 24-well cell culture plates. The neurons were maintained at 37 degree with humidified 5% CO_2 environment, and 50% of the media was changed each week until the time of the experiment.

2.3.2. Lentiviral transduction on primary cultures

Lentiviral transduction of cortical neurons was performed on DIV1. neurons were transduced with 1:100 – 1:300 dilution of lentivirus after removal of 50% of conditioned medium. Neurons were incubated with the virus for at least 24 hours and then all of the virus-containing media was removed. Neuronal media was replaced with 50% reserved conditioned medium and 50% of fresh medium.

2.3.3. AAV transduction on primary cultures

AAV transduction of cortical cultures was performed between DIV6-8 (Howard *et al.*, 2008). Cells were transduced by directly adding the viral suspension with MOI (multiplicity of infection) > 5000 into the neuronal culture media. The cells were monitored for 24 hours post-transduction for signs of neuronal toxicity. If no cytotoxicity was observed, the AAV was left in the media. If some toxicity was apparent, a 50% media change was performed to reduce the number of viral particles.

2.4. Electrophysiology

2.4.1. *In vitro* electrophysiology whole-cell current-clamp recording

For current-clamp recordings of culture neurons, the internal solution contained (in mM): 126 K-gluconate, 4 NaCl, 1 MgSO4, 0.02 CaCl2, 0.1 BAPTA, 15 Glucose, 5 HEPES, 3 ATP-Na2, 0.1 GTP-Na, pH 7.3. The extracellular (bath) solution contained (in

mM):, 140 NaCl, 4 KCl, 2 $CaCl_2$, 1 $MgCl_2$, 10 HEPES, , 10 glucose, pH 7.3. D-(−)-2-amino-5-phosphonopentanoic acid (D-AP5; 50 µM), 6-cyano-7-nitroquinoxaline-2, 3-dione (CNQX; 10 µM) and picrotoxin (PTX; 30 µM) were added to block synaptic transmission. Cultured cortical neurons grown on coverslips were used for electrophysiological recordings. At 1DIV neurons were transduced with either lentivirus c-FosP-dsGFP or c-FosP-*KCNA1* as described in 1.3.2 of this chapter. The electrophysiology experiments were performed at 18-20DIV. Prior to patch recordings, 50% of the medium was removed and cells were incubated with 100µM PTX and 30µM 4-AP for 30 minutes. The cells were then treated by exchanging the reserved 50% medium containing 1 µM tetrodotoxin (TTX) for 2 hours. The coverslips were washed at least two times in extracellular solution to wash out TTX just before starting the experiment. The coverslips were visualised with Olympus

The pipette was pulled from thin wall capillary (1.5OD, 1.17ID) (Harvard Apparatus) with a two-step vertical puller. Action potentials were counted only if the voltage crossed 0 mV. All the recordings were carried out from neurons held at -70mV at room temperature with continuous perfusion of the extracellular solution. Electrophysiological recordings were made with a Multiclamp 700A (Axon Instruments, Molecular Devices) amplifier. The amplifier was used in combination with Power3 1401 (CED) and Signal 6.0 software (Cambridge Electronic Design, Ltd). The data was filtered at 10 kHz and digitized at 50 kHz. The acceptable resistance was no more than 18MΩ. The current step protocol contains 10pA current steps from -20pA to 250pA, with 500ms per step.

2.4.2. MEA (multielectrode array)

2.4.2.1. Preparation and recordings

All the 6-well-MEA chambers with 60 electrodes were purchased from MultiChannel Systems (60-6wellMEA200/30iR-Ti). The chambers were sterilized with UV and washed with 70% Ethanol before use. The bottoms of wells were coated with Bovine Serum (TFS, #261700430) or HI-Fetal Bovine Serum (TFS) for 2-24 hours, washed with sterile dH_20, air-dried and then coated with a fresh solution of Poly-L-lysine (1mg/ml in borate buffer, Sigma-Aldrich P2636) and laminin (laminin from engelbreth-holm-swarm murine, #L2020-1MG, and PBS (Phosphate-Buffered Saline, pH = 7.4, TFS, #10010023) with a ratio of 4:1:55 (Hales, Rolston and Potter, 2010). The cortical neurons were plated directly onto the electrodes with a high density of 90,000 – 100,000 cells/well. The neurons were transduced with AAV on DIV6-8 with MOI > 9000. For the recording, MEA chambers were placed on the MEA recording setup, which was grounded, fixed on an air-supported platform and enclosed in a Faraday cage, in order to minimise electrical noise. The recordings were carried out for 5 or 10 minutes period in cultured medium (Colombi *et al.*, 2013).

The recording chamber was maintained at 37°C with a 1-channel temperature controller (Multichannel systems, #TC01). For experiments that required repeated repeat recordings from the same chamber, the top was tightly covered with a sterile piece of Parafilm.

2.4.2.2. Data acquisition and analysis for MEA

Raw data were collected using 'MC_Rack' (V 4.6.2, MultiChannel Systems). The sampling frequency was 25,000Hz and the recording time was 5-10 minutes per

session. Data processing and analysis were performed with MatLab based software, 'SpyCode', which was a generous gift from Dr. Ilaria Colombi in Michela Chiappalone's Lab (Istituto Italiano di Tecnologia) (Bologna *et al.*, 2010; Colombi *et al.*, 2013). The data analysis pipeline followed steps of data conversion, data filtering, baseline thresholding, spike detection and burst detection. The data filtering used cut-off frequency at 300Hz (Quian Quiroga and Panzeri, 2009). The threshold for noise of the signals was set as 10x of the standard deviation. Channels with high-level of noise were manually annotated, if the data were not valid for analysis, they were removed from the dataset. Burst detection was computed as described in Pasquale, et al, 2010 (Selinger *et al.*, 2007; Pasquale, Martinoia and Chiappalone, 2010). The algorithm outputs include spike frequency (spike/second), burst frequency (burst/min), burst duration, inter-burst intervals, and number of spikes per burst.

2.4.3. *Ex vivo* electrophysiology whole-cell current-clamp recordings

Acute brain slices were prepared in a similar manner to that described by Booker *et al*, 2014 (Booker, Song and Vida, 2014). Mice were lightly anaesthetized with isoflurane and then administered with a lethal dose of pentobarbital intraperitoneally (0.3 - 0.4 mL). Once a deep plane of anesthesia was achieved, as indicated by the reduction in the breathing rate and complete absence of reflexes, the mouse was transcardially perfused with cold (2-4 °C), carbogenated (95 % O2/5 % CO2) sucrose-ACSF, containing (in mM): 87 NaCl, 2.5 KCl, 25 $NaHCO_3$, 1.25 NaH_2PO_4, 25 glucose, 75 sucrose, 7 $MgCl_2$, 0.5 $CaCl_2$. The brain was then excised from the skull and allowed to uniformly cool for 1 minute in a beaker containing a semi-frozen 'slush' of sucrose-ACSF

undergoing constant carbogenation. The brain was placed on filter paper (Whatman) in a perti-dish and surrounded by sucrose-ACSF and blocked with a single-edged razor blade: the cerebellum and the rostral third of the frontal cortices were removed, and the brain was hemisected along the sagittal fissure. The right hemisphere was placed on its medial surface and the dorsal surface of the cortex was removed at an angle that best preserves the integrity of the CA1 hippocampal subregion i.e. the so-called 'magic cut' (blade tangential to the dorsal surface and 10° acute to the sagittal plane) (Bischofberger *et al.*, 2006). The right hemisphere was mounted on the freshly cut dorsal surface to a vibratome stage (Leica VT1200S, Leica Microsystems) that was coated with a shallow strip of cyanoacrylate glue. The stage was then placed into the slicing chamber, submerged in sucrose-ACSF, and oriented so that the lateral extent of the brain faced the vibratome blade (Personna). 400 µm brain slices were prepared at a horizontal oscillation amplitude of 1.2 mm and a slow forward velocity of 0.05 $mm.s^{-1}$. Cut slices were transferred individually using a disposable wide mouth Pasteur pipette into a submerged brain slice holding chamber that contained carbogenated sucrose ACSF maintained at 33°C. After 30 minutes the holding chamber was removed from the water bath and stored at room temperature until needed.

Individual slices were transferred to a submerged recording chamber that was continually perfused with room temperature, carbogenated ACSF containing (in mM): 125 NaCl, 2.5 KCl, 25 $NaHCO_3$, 1.25 NaH_2PO_4, 25 glucose, 1 $MgCl_2$, 2 $CaCl_2$). The ACSF flow rate was 6-8 $mL.min^{-1}$ and slices were held in place with a 'harp' fabricated from an O-shaped platinum wire strung with parallel nylon threads. CA1 pyramidal neurons were visualized using an upright microscope (Scientifica slice scope) equipped with infrared differential interference contrast illumination and a water

immersion objective (Olympus XLUMPLFLN water-immersion objective, 1.00 NA). Fluorescently labelled neurons were identified under epifluorescence using a metal-halide lamp epifluorescence illumination system (X-cite 120Q) and GFP filter sets (Chroma), and a CMOS camera (Hamamatsu C11440-36U ORCA-spark).

Whole-cell patch-clamp recordings from GFP-positive CA1 pyramidal neurons were performed using thin-walled borosilicate glass pipettes (1.5 mm OD, 1.17 mm ID; Harvard Apparatus). Pipettes had a tip resistance of 2-3 MΩ when filled with a K-gluconate based internal solution: (in mM) 142 K-gluconate, 4 KCl, 0.5 EGTA, 10 HEPES, 2 $MgCl_2$, 2 Na_2ATP, 0.3 Na_2GTP, 1 Na_2Phosphocreatine, pH = 7.25;285-295 mOsm.

Electrophysiological recordings were made with a Multiclamp 700B (Molecular Devices) amplifier, filtered online at 10 kHz with the built-in 4-pole Bessel Filter, and digitized at 62.5 kHz (BNC-2090A, National Instruments) using WinWCP software (courtesy of John Dempster, University of Strathclyde, Glasgow, UK). Bridge balance and parasitic pipette capacitance neutralization were applied. A calculated +14 mV liquid junction potential was left uncorrected. Neuronal excitability was assessed from the input-output relationship of the neuron. Action potentials were elicited using a family of square-wave depolarizing current steps (25 pA steps, 500 ms; 0 – 525 pA) from a holding potential of -60 mV. If no action potentials were observed with this protocol, 50 pA steps (500 ms; 0 – 1 nA) were applied from a holding potential of -60 mV to try and obtain the action potential current threshold. The number of action potentials during each 500 ms step was obtained using the threshold event detection function in Clampfit (Molecular Devices).

2.5. Animal Care and Welfare

All animal work was conducted in accordance with the Animals (Scientific Procedures) 1986 Act and approved by the local ethics committee. All procedures mentioned in this project was carried out in accordance with appropriate project and personal licences. Male and female wild-type (WT), C57BL6 mice (Envigo, Charles River Laboratory, or UCL breeding facility; 15-30g, 2-3 months). They were housed with free access to food and water in 12 h light/dark cycles, in an enriched environment and whenever possible in groups of 2-3. Animals were acclimatized for at least 7 days before any procedures or behaviour assessments. The experimenter was blinded for all of the performed experiments and procedures.

2.6. *In vivo* surgical procedures

2.6.1. Chronic kainic-acid amygdala model and CRISPRa-kcna1 treatments in mice

2.6.1.1.1. Intra-amygdala chronic epilepsy model in mice:

Male and female wild-type C57BL/6J mice (3 months old, supplied by Charles & River or Envigo) were placed in a stereotaxic frame (David Kopf. Instruments) under isoflurane anaesthesia. They were injected with kainic acid (0.3µg, 10mg/ml, Tocris) in the right amygdala (AP: 0.94, ML: +2.85, DV: 3.75) using a microinjection pump (WPI Ltd.). The injection volume was 200nl at 200 nl/min using a Hamilton Syringe (900 series, 5 µl, 33 gauge flat-end needle, EssLab Ltd.), under isoflurane anaesthesia (typical surgery time 10-15 min). The mice were placed in a 32°C recovery chamber until they awakened and then returned to the home cage for observation. The mice were closely monitored during status epilepticus (SE), and scored according

to 5 stages on the Racine scale. SE typically commenced as soon as 10 minutes after full recovery from the isoflurane anaesthesia. The status epilepticus was terminated with intraperitoneal injection of diazepam (10mg/kg) no more than 40 minutes post- kainic acid injection. Only the animals that exhibited seizure episodes above stage 4 were carried into the subsequent studies.

2.6.1.1.2. Transmitter implantation for EcoG recordings: An electrocardiogram (ECoG) transmitter (single channel, 256 Hz, A3028C-CC, Open Source Instruments, Inc.) was subcutaneously implanted and the recording electrode was placed above the viral injection site (AP: -2/3 of bregma/lambda distance, ML: 3 mm). The ground/reference electrode was placed on the contralateral hemisphere, approximately above the motor cortex. The mice were then returned to the home cage for recovery and were single-housed for the remainder of the study. The transmitters were switched on magnetically at least 48 hours after transmitter implantation surgery to avoid residual isoflurane effects.

2.6.1.1.3. Virus injection into ventral hippocampus: In the same surgery as 2.6.1.1.2, a total volume 1.5 µl of AAV CamKII-sg19-rtTA-tdTomato and TetON-dCas9-VP64 were mixed with a ratio of 1:1 and injected at 100 nl/min via Hamilton 5 µl syringe. The injection volume was equally split between three coordinates along the dorsal-ventral axis in the right ventral

hippocampus (AP: -2/3 of bregma/lambda, ML: 3 mm, DV:3.5/3/2.5 mm) The needle was left untouched for 5 minutes after each injection to prevent backflow. After virus injection, a transmitter was implanted of the same site as described in 2.6.1.1.2.

2.6.1.1.4. Doxycycline diet: After baseline was recorded, normal animal food was switched to ad libitum doxycycline pellet (TD.120769-BLUE 625 mg/kg). Then the mice continued to be recorded for the following 2 weeks. The researcher who acquired and analysed the data was blinded to the virus that was injected.

2.6.2. Acute-pilocarpine model and CRISPRa-kcna1 treatment in mice:

2.6.2.1. Transmitter implantation in primary visual cortex: Male wild-type C57BL/6J mice (3 months old) were used with the same transmitter model as described in 2.6.1.1.2. The recording electrode was placed above the right primary visual (V1) cortex (AP: -2.8, ML: 2.4). A cannula (Bilaney Consultants Ltd.) was implanted in the same location as the recording electrode and used for sequential pilocarpine injection.

2.6.2.2. Virus injection into visual cortex: The viral preparation as described in 2.6.1.1.3 was injected into layer 2/3 -5 of the V1 cortex at the same site as the recording electrode, as described above (DV: 0.7/0.5/0.3 mm). Transmitters were implanted after the viruses were injected.

2.6.2.3. Acute seizure induction by intra-cranial pilocarpine: Animals were allowed to recover from transmitter implantation surgery for two weeks before induction of acute seizures by pilocarpine (3.5M in saline)(Magloire *et al.*, 2019) Pilocarpine was injected 0.5 mm below the cannula (DV = -1.0) with a Hamilton 5 µl syringe. The injection volume was incremented on consecutive days (180 nl, 300 nl and 500 nl) until spike-wave discharges (SWD) was observed on EcoG; this was recorded as the threshold dose. If mice experienced a seizure before all three doses were completed, the sequence of injections was stopped and the last injection volume was noted as the threshold dose. If seizures failed to terminate spontaneously, the animal was excluded from the study. To assess the viral treatment, the animals were placed on a doxycycline diet for 7 days. Then the threshold dose of pilocarpine for each animal was repeated to induce a single seizure while ECoG data was collected for the ictal activities.

2.6.2.4. EcoG monitoring was used to assess seizure severity for one hour after each pilocarpine injection. The researcher who acquired and analysed the data was blinded to the virus that was injected.

2.6.3. Acute pilocarpine seizure induction with c-FosP-dsGFP and CamKII-EGFP in mice:

1.5ul AAV c-FosP-dsGFP or AAV CamKII-EGFP(Snowball *et al.*, 2019) was injected into layer 2/3 -5 of the V1 cortex in different mice (DV: 0.7/0.5/0.3). A cannula for guided substrate injection were implanted at the same coordinate after the viruses were

injected. Mice were returned to home cage for post-surgery recovery for two weeks before induction of acute seizures by pilocarpine (3.5M in saline) (Magloire *et al.*, 2019). Pilocarpine was injected 0.5 mm below the cannula (DV = -1.0) with a Hamilton 5 µl syringe for volume of 300 nl. The mice were observed for 2 hours post-pilocarpine inject for evaluating seizure severity. The brain were then extracted and fixed with PFA for immunohistochemistry.

2.6.4. Acute-pentylenetetrazol (PTZ) model and c-Fos-*KCNA1* treatment in mice:

Male and female mice wild-type C57BL/6J mice (3 months old, supplied by Charles & River or Envigo) were placed in a stereotaxic frame and injected with 1.5 µl AAV of c-Fos-GFP/c-Fos-*KCNA1* into bilateral ventral hippocampi (AP: 3 mm, ML: 2/3 bregma-lambda, DV = 3.5/3/2.5 mm) with 500 nl at each depth. The needle remained in position for 5 minutes after each injection. The mice were marked and returned to the home cage for recovery. Two weeks after the virus injection, mice were subjected to PTZ seizure induction. A single dose of PTZ (Sigma-Aldrich) dissolved in saline was administered intraperitoneally at 54-57mg/kg. The mice were observed closely for the first 30 minutes and their behaviours were scored every 5 minutes according to Racine scale(Van Erum, Van Dam and De Deyn, 2019). The latency to seizure onset was timed and recorded. The mice were further monitored for 2 hours until they completely returned to normal and then they were returned to the home cages. The PTZ-seizure induction was repeated, with the same dose and observation period, at two time-points: 24 hours and 14 days after the initial PTZ

administration. The researcher who performed the experiments were blinded to the virus injected.

2.6.5. Chronic-intra amygdala kainic acid model in mice and c-FosP-*KCNA1* treatment in mice:

2.6.5.1. Intra-amygdala kainic acid model in mice: as described in 2.6.1.1.1 of this chapter. Mice remained group housed for at least one-week post-kainic acid administration for recovery and separated once they developed recurrent seizures.

2.6.5.2. Transmitter implantation: The same transmitter model and type described in 1. 6.1.1.2 of this chapter was implanted two weeks post-kainic acid injection; the recording electrode was placed above the right ventral hippocampus (AP: -2/3 of bregma/lambda, ML: +3 mm). At the same coordinate, a cannula was implanted for guided injection later. An identical cannula was placed above the left ventral hippocampus. The ground electrode of the transmitter was placed in the posterior region of the left hemisphere. The mice were then returned to home cage and kept single housed for the remainder of this study.

2.6.5.3. Virus injection via pre-implanted cannulas:

1.5µl AAV c-FosP-dsGFP, c-FosP-*KCNA1* or c-FosP-*KCNJ2* was injected bilaterally via cannulas into the ventral hippocampus (DV = 3.5/3/2.5 mm, cannula length = 7.05) under isoflurane anaesthesia. The mice were returned to home cages for recovery. Two weeks later, transmitters were turned back on, along with cameras if available, for

post-virus video recordings. The animals were sacrificed after the experiments for brain collections.

2.6.6. EcoG (Electrocorticography) recordings

2.6.6.1. Recording and hardware set-up

Detailed methods of Ecog recording and analysis can be found in 'Method and Materials' section of Colasante & Qiu, et al 2020(Colasante *et al.*, 2020). In brief, The ECoG was acquired wirelessly using hardware and software from Open Source Instruments, Inc (https://www.opensourceinstruments.com/SCT/).

The ECoG was sampled at a frequency of 256Hz, band-pass filtered between 1 and 160Hz, and recorded continuously for the duration of the experiments up to 4 weeks. The signals were collected via wireless subcutaneous transmitters and received by octal data receiver (A3027) before sent thorough to a desktop where it is recorded and saved by a LWDAQ Driver (A2071E). The animals were housed independently in a Faraday enclosure for minimising environmental electrical noises.

2.6.6.2. Video recordings

When video recordings were taken, they were recorded with IP cameras from Microseven. The camera clock was synchronised to Windows time serve to the same as the ECoG recordings. **Software specification:** LAWQ (Long-Wire Data Acquisition) software was designed by Open Source Instruments, Inc. (http://www.bndhep.net/Software/).

2.6.6.3. Event detection and analysis (PyEcog)

Spontaneous seizures were detected from chronic recordings using a semi-automated supervised learning approach. An annotated library containing examples of epileptiform activity was

built using seizures identified from previous studies. Recordings were chunked into 5 second blocks that were labelled as either "ictal" or "interictal" depending on whether epileptiform patterns were present, respectively. The library of labelled features were extracted into classifiers unique for each of different animal seizure model. When new unlabelled ECoG recording data was analysed, the classifiers were applied first to make predictions on the 5-second chunks of the unlabelled data. Each of the classifier derived prediction was evaluated to obtain marginal probability of being a seizure state with forward-backward algorithm. Following the smoothed prediction generation, each of the positive entry was manually annotated by an researcher blinded to the treatments given for false-positives. The start and end locations of each seizure were also manually adjusted if appropriate (Colasante *et al.*, 2020).

Additional parameters including frequency spectrum, coastline, kurtosis and day/night comparisons were extracted from the pyecog software and analysed further. The scripts for the pyecog software used throughout this project are available in full on: https://github.com/jcornford/pyecog.

2.7. Behaviour assessments

2.7.1. Contextual Fear Conditioning (CFC)

The contextual fear conditioning protocol was performed under T. Smart's PPL (P4114FCF5). The fear conditioning was carried out using the NIR Video Fear Conditioning package by Med Associate. Inc. A glass chamber with metal grid is placed inside a sound proof chamber. The NIR (near-infrared) light were equipped for recording with infra-red camera. The electric shock is delivered via the metal grid with the glass chamber and sound proof chamber closed.

Mice were randomised into two groups, each injected bilaterally with either c-FosP-dsGFP or c-FosP-*KCNA1*. Mice were returnedto their home cage for at least 3 weeks before the start of the CFC test. Mice were handled as normal for 7 days before the experiment. On the day of the experiment, mice were kept in a separate room and were only introduced to the behaviour room where the CFC apparatus was located when they were due to take the test.

The CFC experiment consisted of three phases. On day one, the mice received non-harmful electrical foot shocks. The electrical current (0.6 mA) was delivered by the metal grid under manual control. The electric current strength was tested before each trial to ensure it did not cause harm to the mice. The mice were placed in the chamber for 2 minutes of habituation, then three foot shocks were delivered for 2s each, with intervals of 60 seconds. The mice were kept in a dark environment and their behaviour was recorded with the NIR camera. The mice were then returned to the home cage. 24 hours after the foot shock, mice were returned to the same chamber with the same conditions, for assessment of fear recall. The mice were placed in the chamber for five minutes. No foot shock or any stimuli was delivered. After 1 hour, the chamber was modified to replace the grid floor with a hard plastic board, and the walls were covered with paper. We also placed a filter paper in the chamber with a drop of almond essential oil. This created a new context designed to be different from the previous one. The mice were placed in the 'new' context for five minutes. The freezing behaviour of the mice was counted manually by an experimenter blinded to the treatment given.

2.7.2. Object Location Test (OLT) and novel object recognition (NOT)

All behavioural assessments were carried out between 8am – 4pm during the light cycle. Mice were handled and acclimatised for 1-2 weeks prior to the experiment. The behaviour room was set with evenly distributed dimmed red lights and appropriate sound isolation. Four non-transparent arenas (50cm50cmx50cm), consisting of open-top boxes with white walls and bottom, were arranged together, and each arena was occupied by one mouse. The arenas were cleaned thoroughly with 70% Ethanol before each new session. The mice were acclimatized to the behaviour room for 10 minutes on the day before the test, but not to the arena (Leger *et al.*, 2013). The objects used include tomato cans, 50ml tube filled with water. A colourful wooden toy block was used for the novel object recognition test.

In the experiment set-up where both object location test and novel recognition test took place, they were carried on two consecutive days with at least 24 hours apart.

In the object location test, two identical tomato cans or 50ml falcon tubes were placed at two opposite corners along the diagonal direction, at least 10cm away from the wall. The mice were bought into the room with 5-10 minutes of habituation and placed in the centre of the arena facing away from the objects. The mice were allowed to explore the arena for 8 minutes, and then returned to their home cage. They were returned to the behaviour room 6 hours later, with one of the objects moved to a new corner. The same recording was repeated and they were allowed to explore for a total of 8 minutes.

In the novel object recognition test, one of the objects was exchanged for a wooden toy block in the second phase of the recording. The rest of the protocol remained the same.

Videos were captured with Raspberry Pi4 cameras (XL-RB-AluP4+07FAN) and VideoArchiver software (M. Weston). The exploration was visually assessed by a researcher blinded to the treatments.

2.7.3. Open field assessments

The open field assessments were carried out in the same arena as the OLT with the same room settings with same arena setting and light conditions as described in 1.7.2 of this chapter. Mice had no prior exposure to the behaviour room or to the apparatus before the start of the experiment.

The mice were habituated in a quiet room different from home cage location for 30 minutes before being introduced into the behaviour room. To start the experiment, mice were gently placed in the centre of the arena. The habituation sessions were 30 minutes with the experimenter not present in the same room. The behaviours were recorded with an overhead Raspberry Pi4 camera (XL-RB-AluP4+07FAN) and VideoArchiver software (M. Weston).

The animal tracking and data analysis were carried out semi-automatically using a script written in Bonsai (Open Ephys, https://open-ephys.org/bonsai) (Lopes *et al.*, 2015). In brief, the outline of the animal was extracted and its body central point was calculated. The software generated a location for the centre of the mice as a (x.y) coordinate every 30 frames of the recording. The tracked locations were then used to analyse parameters including thigmotaxis, travel distance, and velocity using an in-house Python script.

2.7.4. Spontaneous T-maze alternations

Mice were returned to the same behaviour room 24 hours after the Open field assignment for T-maze alternations. The apparatus was specially made with transparent Pyrex materials. The walls of

the apparatus were no less than 20cm height, with a full length and width of 50cm. Each of the arms were 25cm long, and the running track was 50 cm long.

The protocol for T-maze alternation was adapted from Deacon & Rawlins, 2006(Deacon and Rawlins, 2006). The mice were habituated to the room for 5-10 minutes before the experiment start. They were then placed in the start area at the bottom of the 'T-shaped' maze, facing away from the track. The mice were handled gently using a plastic tube which they were habituated to during the handling sessions prior to the experiment. The animal would initiate running down towards the arms and chose one to enter, a central partition was placed at the end of the track to differentiate two directional choices. A positive entry was confirmed once the whole body of the mouse has entered the arm. The guillotine door was lowered to form an entrapped space for mice to stay for 30 seconds. The mice were then transported back to the start area, then the mice were allowed to run down the track again with all doors open. Their second positive arm entry was recorded as either same or different from the first entry. The mouse was immediately returned to the start area with no relay time to start the second trial. For each mice, ten continuous trials were performed.

In any of the trials, if the mice failed to leave the start area after 90s, they were taken out of the maze for a short break of 10 minutes and tried again. If the mice repeatedly failed to run, they were temporarily suspended from the test, and another trial was conducted on the next day. If the animal still failed to initiate directional movements, they were eliminated from the dataset.

2.7.5. Olfactory Discrimination

Mice from open field exploratory assessment were subjected to the olfactory discrimination test with at least 48hour interval. The

olfactory stimuli were prepared by diluting essential oils of peppermint, almond and raspberry in water (1:20)(Mihalick *et al.*, 2000). The solutions were prepared and we briefly dipped clean cotton swaps in the solution. The mice were habituated for 30 minutes in an empty IVC cage without bedding. It contained a dry cotton swap inserted prior to the start of the test. This was to remove any novelty confounder represented by the cotton swap tip. After that, they were introduced to the scented cotton swaps, inserted to the same height as the mouse head. The order of the scent was water, peppermint and almond , with three repeats of each scent. Each repeat lasted for two minutes, and mice were free to explore. The exploration of scented cotton swap tip was taken on-site by an experimenter blinded to the treatment given. After post-virus tests were completed with water, peppermint and almond, a new day of test was introduced to replace almond with raspberry for assessing learning abilities.

2.8. Immunohistochemistry and imaging

2.8.1. Endogenous fluorescence imaging

Primary cortical neuronal cultures plated on treated coverslips were used for this experiment. On DIV6, the cultures were randomised and transduced with c-Fos-dsGFP or cFosP-*KCNA1* with MOI >= 1:5000. The virus were added to the media and incubated for at least 22 hours. After that, the medium was replaced with 50% fresh NBA. On DIV15, cells were either treated with 30µM picrotoxin (PTX, dissolved in DMSO). The control coverslips were collected before addition of PTX. At 6, 24 and 48 hours of PTX incubation, coverslips were collected. The coverslips were washed twice in PBS, and immediately incubated in 4% paraformaldehyde (PFA) (dissolved in PBS) for at least 30 minutes. The PFA was removed and coverslips were washed for further three times with PBS. The coverslips emerged in PBS-0.01% sodium

azide were temporarily stored at 4^{o}C in fridge until further application. The coverslips were kept in the dark after the collection step to avoid photobleaching of endogenous fluorescence.

For imaging, the coverslips were mounted onto microscopic glass (VWR) with soft-mounting medium dissolved with DAPI (0.1%, Sigma). The coverslips were stored at 4^{o}C overnight on a flat platform before imaging for solidification.

2.8.2. Immunohistochemistry

2.8.2.1. c-Fos immunohistochemistry in primary neuronal cultures

Primary cortical neurons in cultures were treated with 30µM PTX or equal volumes of water as control on DIV18-21. At 2, 6, 24, and 48 hours post-drug treatment, neurons were fixed with 4% PFA at room temperature for 30 minutes. The coverslips were then washed with PBS, followed by membrane permeabilization and non-specific binding block in PBS-T-BSA buffer (PBS plus 0.1% - 0.3% Triton, 1-3% BSA and 10% goat serum for 30 minutes. The blocking solution was replaced with PBS-T buffer supplemented with polyclonal rabbit cfos antibody (1:500, Synaptic systems, #226003) with gentle rocking at 4°C overnight. The cells were washed with PBS-T to remove residual primary antibody, followed by incubation with secondary antibody Alexa 568® (goat-anti rabbit, 1:1000, Life technologies) for 1 hour. Depending on the availability, cells were then briefly incubated in Hoeschst solution (1:10000 diluted in PBS) for 30 minutes for nuclear staining or mounted directly onto glass slides with Vectorshield (Vector Laboratories #H-1200), or directly mounted with Fluoroshield (#ab104129, Abcam) supplemented with DAPI (#D9452, Sigma).

2.8.2.2. Immunohistochemistry in PFA-fixed rodent brain sections:

This experiment was primarily carried out by Benito Maffei who has kindly allowed me to include the data in this thesis. The PFA-fixed mouse brains were sliced to 50-70µm thick coronal slices (VT1000 S, Leica). Approximately 6-8 adjacent slices were chosen to cover the transgene expression from dorsal to ventral hippocampal region. The slices were permeabilised at room temperature using blocking buffer with 0.3% Triton X-100 (Sigma) diluted in 1xPBS, supplemented with with 0.3% Bovine Seum Albuim (BSA), 5% goat serum, at room temperature for 1-2 hours. The primary antibodies: mouse anti-GAD67 (Merk, 1:500) or rabbit anti-parvalbumin (Merk, 1:500), and chicken anti-copGFP (Origene, 1:500), were incubated overnight at $4^{o}C$ with constant gentle rocketing. The slices were washed with PBS three times and incubated in secondary antibody-conjugated with fluorophore as a dilution of 1:1000 (donkey anti-rabbit Alexa 568 or anti-mouse Alex568, or goat anti-chicken A488 when appropriate) for 2 hours at room temperature. The slices were washed with PBS thrice and mounted onto microscopic slides (VWR) using Dako mounting medium containing DAPI (Abcam).

2.8.3. Image acquisition and analysis

2.8.3.1. Image acquisition

Confocal images were acquired with Zeiss Axio Scope A1 polarized light microscope and/or inverted LSM 710 confocal laser scanning microscope (ZEN 2009).

2.8.3.2. Particle or cell counting *in vitro*

This was conducted using ImageJ(Fiji) analyse module of 'Analyse particle'. All the images were acquired with identical laser settings and digital gain values. The images were thresholder automatically, followed by 'binary' and 'watershed' steps to separate partially overlapping cells (https://imagej.net/imaging/watershed).

This was followed by 'analyse particle' step, which counts the number of particles in the processed binary image (https://imagej.net/imaging/particle-analysis). This was processed separately for DAPI and dsGFP channels and the dsGFP count was normalised to DAPI.

2.8.3.3. Particle or cell counting *in vitro*: The images were analysed using Fiji/ImageJ accompanied with manual verification.

2.8.3.4. Fluorescence intensity analysis

Fluorescent imaging was analysed using 'measure' module in ImageJ (Fiji). This calculates the fluorescent signal intensity in the image. The intensity of dsGFP signals were extracted.

2.9. Statistical analysis

The statistical analysis performed is shown in detail in figure legends. The graphs show mean with ± standard error mean (SEM) unless specifically stated. Student's *t-test* (parametric) or Mann-Whitney test (non-parametric) tests were used as appropriate to compare two groups. Fisher's exact test was used for event occurrence frequency comparisons. One-sample t-test was used to compared normalised values to 1. One-way or two-way ANOVA followed by Bonferroni multiple comparisons test were used when appropriate to compare repeated measures. Three-way ANOVA was applied to make comparisons between groups with three variables.

Statistical analysis was carried out using Prism (GraphPad Software, Inc., CA, USA) and SPSS (IBM SPSS statistics, NY, USA).

Chapter 3

In vivo CRISPRa decreases seizures and rescues cognitive deficits in a rodent model of epilepsy

Abstract

The work described in this chapter was published as: *Colasante, G.*, Qiu, Y.*, Massimino, L., Di Berardino, C., Cornford, J. H., Snowball, A., et al. (2020). In vivo CRISPRa decreases seizures and rescues cognitive deficits in a rodent model of epilepsy. Brain 143, 891–905.*

In this study, we pioneered the use of CRISPR to treat temporal lobe epilepsy. We upregulated the expression of an endogenous voltage-gated potassium channel, Kv1.1, encoded by *Kcna1*, using a modified CRISPR approach, CRISPR activation (CRISPRa). This genetic tool is based on using a nuclease-defective Cas9 protein (dCas9) in combination with a synthetic guide RNA (sgRNA) to recruit transcriptional enhancers to modulate the expression of endogenous genes (Maeder *et al.*, 2013; Perez-Pinera *et al.*, 2013). As discussed in introduction, CRISPRa increases endogenous gene transcription by specifically targeting promoter region and tethering transcriptional activators to enhance endogenous protein expression level. This does not involve direct editing of genomic sequences (Maeder *et al.*, 2013; Perez-Pinera *et al.*, 2013). In comparison to putative therapeutics, the advantages of modulating endogenous gene expression preserved the post-transcriptional and -translational modifications which are essential for full functions of the therapeutic proteins.

First, we tested several sgRNAs in cell lines and primary hippocampal cultures expressing dCas9 fused to the transcriptional activator VP160 (dCas9-VP160) to

identify the optimal sgRNA with the highest degree of *Kcna1*/Kv1.1 upregulation (Lau *et al.*, 2019).

Then we verified that the CRISPRa-mediated *Kcna1* upregulation led to a decrease in neuronal excitability in primary cultures and *ex vivo* in CA1 pyramidal cells, without off-target effects on other genes. Then, using continuous video-ECoG telemetry, we showed that stereotaxic AAV9-mediated delivery of dCas9-VP64 (fused to another transcriptional activator) together with the sgRNA in the hippocampus decreased spontaneous seizures in a model of chronic focal epilepsy induced by intra-amygdala kainic acid injection. Finally, we showed that this approach was able to rescue both cognitive and transcriptomic alterations.

In conclusion, CRISPRa can modulate endogenous gene expression and reduce neuronal excitability. A additional advantage of this approach is that it is that it can upregulate any potential genes regardless of its size, as discussed previously, size of transgene can be a limiting factor for efficient viral delivery.

In this project, my contribution was to perform the *in vivo* experiments. I assessed the efficacy of this new tool to decrease seizures and to rescue the behavioural phenotype, and I collected tissues for transcriptomic analysis. A summary of the main findings of the project is shown below in Figure 3.1, and the published manuscript is attached in Appendix.I.

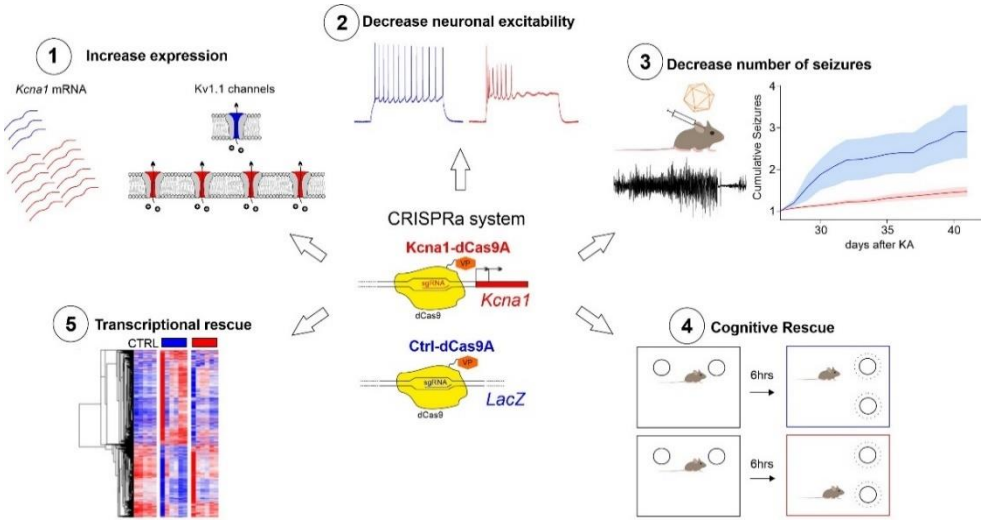

Figure 3.1. *Graphical abstract. (modified fron Colasante & Qiu, 2020*(Colasante *et al.*, 2020). *Blue represents Ctrl-dCas9 and red represents kcna1-dCas9 treatment. (1) Cartoon showing expression of endogenous Kcna1 gene leads to increase in membrane-bound Kv1.1 channel expressions. (2) Examples of reduced excitability in dynamic clamp experiments. (3) Kcna1-CRISPRa showed reduced seizure propensity in mice intra-amygdala kainic acid chronic mise model. (4) Cognitive and spatial memory rescue was observed with Kcna1-CRISPRa treated mice. (5) Transcriptomic changes with Kcna1-CRISPRa led to a network with more similarities to non-epileptic brains.*

3.5. Kcna1-CRISPRa reduced seizure frequency in the chronic mice epilepsy model

In essence, a dual-viral system was designed for modulation of the endogenous *Kcna1* gene using the CRISPRa tool. The treatment successfully increased Kv1.1 channel expression in excitatory neurons in the ventral hippocampus, reducing neural excitability and seizure frequency in a chronic model of limbic epilepsy.

Chronic temporal lobe epilepsy was induced by intra-amygdala kainic acid (IAK) injection in 3-4 month old C57BL/6J mice. The unilateral injection of high-dose kainic acid into amygdala produced spontaneous seizures similar to drug-resistant epilepsy after a latent period. It also mimics some morphological traits and behaviour deficits to TLE (Lévesque and Avoli, 2013; Conte et al., 2020).

Mice experienced an initial episode of status epilepticus, and later developed infrequent spontaneous seizures. After one week, mice were treated with either AAV9 *Kcna1*-CRISPRa or Ctrl-CRISPRa (a control AAV9

where the sgRNA was designed to recognise *Lacz*, a non-mammalian gene) in the ipsilateral ventral hippocampus. As demonstrated in Figure 3.2(a), due to the package limitation of AAV, we designed a dual viral system. One of the viruses contained the CamKII promoter for excitatory neuronal expression, followed by the fluorescent marker tdTomato. This plasmid also contains the U6 promoter, scaffold protein sequence and sgRNA sequence for genomic sequence recognition. The dCas9-VP64 construct was incorporated in the second AAV. The dual viral system incorporated a TetON inducible expression system to ensure that only in the presence of both viruses and drug doxycycline, the *Kcna1*-CRISPRa will be turned on. The TetON was divided between two viruses, the promoter TetON was attached with dCas9-VP64 while the response protein rtTA was attached to the sgRNA construct and fluorescent marker (Figure 3.2a). In the absence of doxycycline, rtTA blocked expression of dCas9-VP64 in transduced cells. Therefore, with AAV injections, the virus expression remained off for the first two weeks when ECoG were taken from epileptic mice. After that, we provided the mice with doxycycline, a tetracycline analogue, to turn on the virus expression, allowing the CRISPRa to interact with the endogenous gene expression machinery. Due to the small packaging capacity of a single AAV virus, the components of this system were packaged separately into two AAV viruses. The CRISPRa system will only take an effect when the AAVs co-transduced the same cell. The two viruses were always delivered in a 1:1 ratio in the subsequent experiments for optimised therapeutic effects (Colasante *et al.*, 2020). The virus was injected one week after the kainic acid induced status epilepticus, into ventral hippocampal region. At the same time, the mice were implanted with wireless transmitters with battery power enough for 4 weeks' continued ECoG monitoring. The electrodes were placed on the surface of the cortical region directly above the injection site, near the visual cortex. This placement was to ensure we captured generalized seizures in those mice.

Mice were monitored and recorded with EcoG for two weeks after the transmitter implantation as baseline recording. During this period, no

effector dCas9-VP64 protein was produced. Then doxycycline was administrated in the food to activate the CRISPR machinery. The doxycycline activated the TetON promoter and in turn the dCas9-VP64 protein, which was guided with a specific sgRNA to the *Kcna1* promoter region to increase its activity. The post-virus recording was of equal duration, 2 weeks, as the baseline. In the ECoG recordings, we observed that the frequency of seizures was significantly reduced, only in animals treated with AAV9 *Kcna1*-CRISPRa ($p = 0.008$, 2-way ANOVA, Bonferroni multiple comparisons).

Furthermore cumulative seizure analysis demonstrated a clear decrease in total seizures over time in animals transduced with AA9 *Kcna1*-dCasA compared to control ($p < 0.0001$, 2-way ANOVA,). Immunofluorescence imaging of post-treatment mice showed strong expression of a TdTomato reporter in the dentate gyrus (DG) and hilus, as well as CA1-CA2 of the ventral hippocampus (Figure 3.2B). (As the DG immunofluorescence reached the maximum detectable level, CA1-CA2 expression is not readily apparent from the image.) In this study, we did not gather evidence on co-localization as fluorescent marker was attached to one virus only. So it could be possible that not all neurons were transduced with both viruses.

In summary, AAV9 *Kcna1*-CRISPRa, increasing endogenous Kv1.1 channels, effectively reduced seizure propensity in a mouse model of TLE.

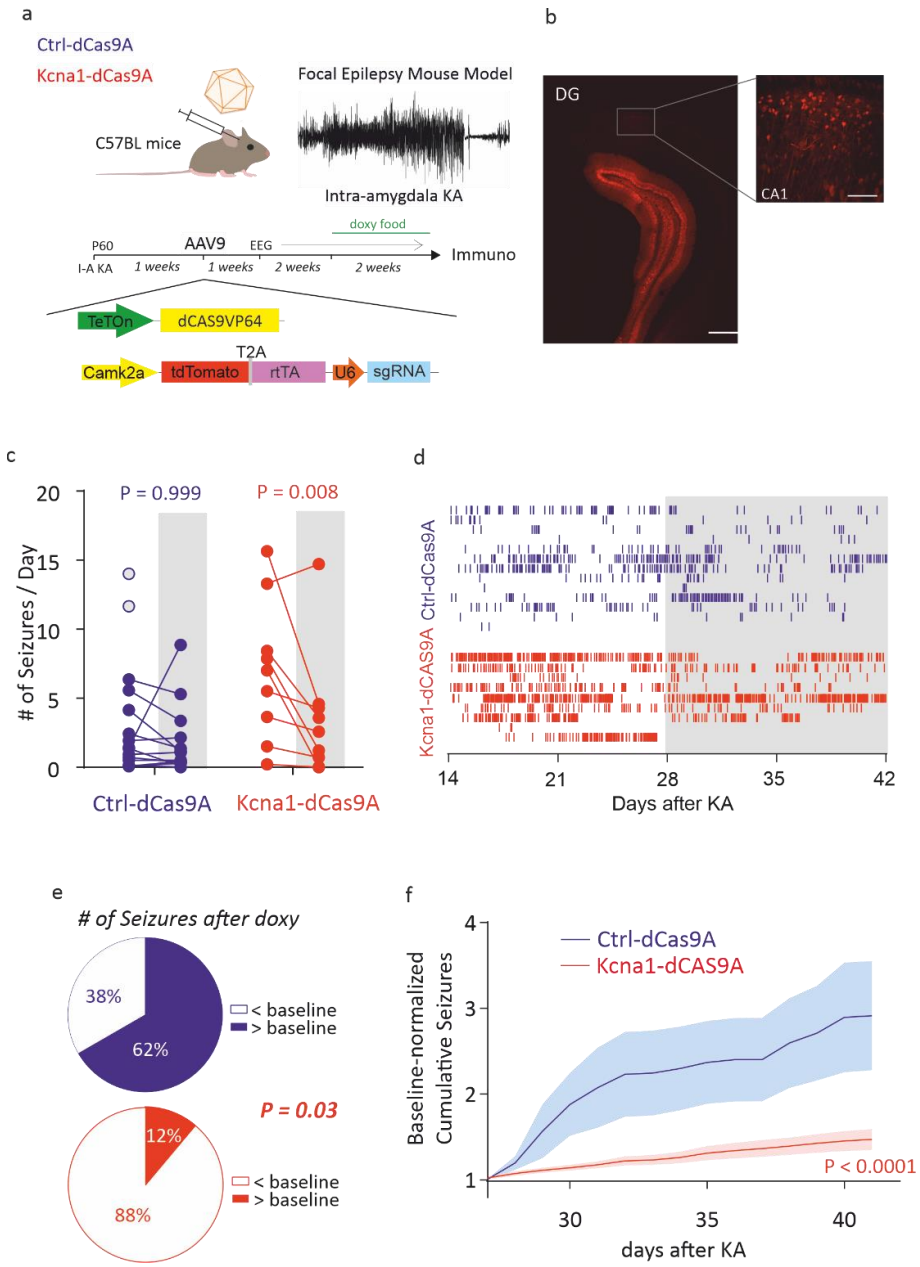

Figure 3.2. Intra-amygdala kainic acid chronic epilepsy model treated with Ctrl-CRISPRa and Kcna1-CRISPRa. (a) Schematic representation of the CRISPRa approach used in vivo to treat intra-amygdala kainic acid focal chronic epilepsy model. Mice were injected with AAVs 1 week after kainic acid induction of status epilepticus. Baseline ECoG recordings started the following week and continued for 2 weeks. The EEG recording continued for further 2 weeks with mice feeding on the doxycycline diet. (b) Representative immunofluorescence images of TdTomato after 2-week virus activation. Scale bars: DG = 500µm, CA1 50µm. (c) Seizure frequency per day was plotted for Ctrl-CRISPRa (n=13) and Kcna1-CRISPRa (n=9) treated mice before and after the therapy was switched on with doxycycline (2-way ANOVA, Bonferroni multiple comparisons test). The two mice that died after the baseline (open symbols) were excluded from the statistical analysis. (d) Raster plot showing all seizure occurrences before and after starting the doxycycline administration (transparent background = before; grey background = after) (2-way ANOVA, Bonferroni multiple comparisons test.) (e) Pie chart showing changes in seizure numbers after virus activation by doxycycline in comparison to baseline (Fisher's exact test). (f) Weighted cumulative seizure numbers after the virus activation by doxycycline. The values are normalized to baseline in mice transduced with Ctrl-CRISPRa or Kcna1-CRISPRa (2-way ANOVA). (Figure modified from Colasante *et al.*, 2020).

3.6. Effect of *Kcna1*-CRISPRa on acute evoked seizures

We also tested our therapy in an alternative acute epileptic model in another brain region to investigate whether this treatment can be applied to different seizure/epilepsy models.

Pilocarpine is a cholinergic receptor agonist which can be delivered intracranially to induce acute focal seizures (Magloire *et al.*, 2019). When injected in the primary visual cortex, it induces convulsive status epilepticus which self-terminates within 60 minutes (Magloire *et al.*, 2019). We therefore firstly injected Ctrl-CRISPRa or *Kcna1*-CRISPRa into layer 2/3 of visual cortex with two weeks recovery time. The mice were kept off doxycycline to suppress dCas9 expression during this period. The mice were injected with 180µl, 300µl and 500µl pilocarpine (3.5M) on three subsequent days(Magloire *et al.*, 2019). The different doses were used because, depending on the precise placement of the cannula and gliosis around it, there is some variability in the degree to which the chemoconvulsant penetrates the brain. The dosage that generated convulsive seizures was defined as the threshold dose for each mouse.

Mice were returned to the home-cage for one week and fed doxycycline to switch on the CRISPR-activation therapy, before being subjected to a further injection of pilocarpine at the previously defined threshold dose. We then compared the ECoG epileptiform activity in response to the same dose of pilocarpine before and after CRISPR-activation treatment.

The viral expression was visualised with the fluorescent marker TdTomato as shown in Figure 3.3(B). Layer 2/3 pyramidal neurons expressed the CRISPRa therapy, while some damage can be observed where the cannula guide was implanted. In this model, we observed no significant difference between the *Kcna1*-CRISPRa and Ctrl-CRISPRa treated animals in either the duration or severity of pilocarpine-evoked seizures. The power spectrum showed a trend towards a reduction with *Kcna1*-CRISPRa but this did not reach the pre-defined significance threshold of p=0.05 (Figure 3.3(D)).

Previous data on lentiviral or AAV-mediated overexpression of KCNA1 or a codon-optimized variant with a point mutation to mimic post-

transcriptional editing has shown antiepileptic effects when co-injected with tetanus toxin, or when delivered after tetanus toxin, or in a TLE model, but it has not been tested in a similar acute chemoconvulsant model (Wykes *et al.*, 2012; Snowball *et al.*, 2019). Unfortunately, in the acute pilocarpine model, we did not observe significant reduction in seizure severity after the treatment. It may suggest the Kcna1-CRISPRa acts more likely thorough long-term modulation of the network properties. The acute seizure showed a possible trend, but not significant improvements in seizure duration or severity.

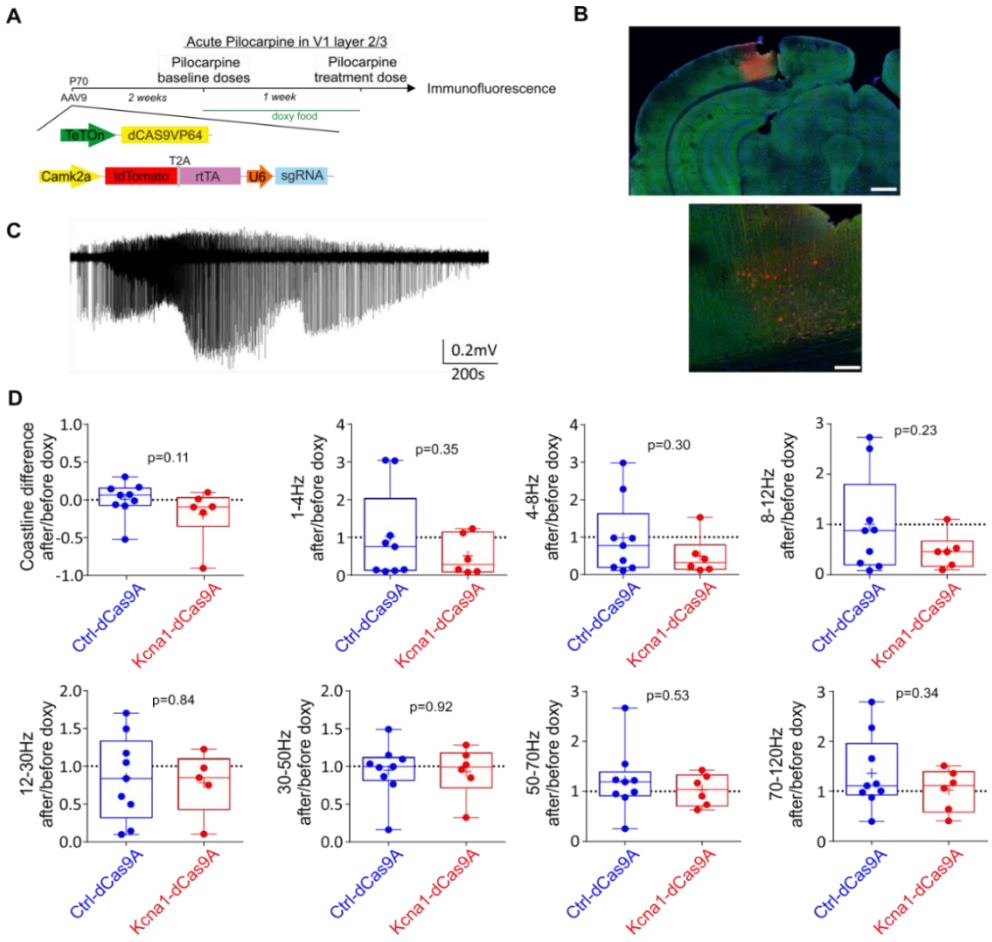

Figure 3.3 Acute pilocarpine injection in V1 cortex treated with AAV. (A) Graphical experimental design (see Material and methods). (B) Representative coronal image from a Ctrl-CRISPRa injected mouse at the site of injection, with transduced neurons in red, MAP2 in green and DAPI in blue. Scale bar top: 0.5mm; bottom: 0.1mm. (C) Representative acute seizure induced by pilocarpine. (D) Seizure parameters after and before doxycycline administration. Coastline (top left) measured either before or after doxycycline was normalized by a period before pilocarpine injection, and is shown as the difference (after-before doxycycline). The rest of the panels indicating power spectrum bands were shown as the ratio before and after the doxycycline. Student's t test. (Taken from Colasante, Qiu et a.,l 2020 Supplementary Figure S8).

3.7. *Kcna1*-CRISPRa improved spatial memory in chronically epileptic mice

Over 50% of people with epilepsy present at least one additional comorbidity (Thijs *et al.*, 2019). One of those is cognitive impairment, which includes memory deficits. It has previously been shown in the kainic acid model that chronically epileptic animals are prone to spatial memory deficits, which are detectable by the object location test (OLT) (Pearson, Schutz and Patel, 2014). This test depends on the mouse's natural instinct for exploring objects in novel locations, and it is sensitive to hippocampal damages and dysfunctions (Zeidler *et al.*, 2018).

Another similar test known as novel object recognition (NOR) has also been applied in parallel to assess perirhinal cortex guided recognition memory, which is compromised in some animal models of epilepsy (Pearson, Schutz and Patel, 2014). We applied these tests in the present study, Each of the tests consists of two phases: familiarisation and test. During the familiarisation phase, animals were allowed to explore two identical objects inside the arena for 8 minutes, allowing them to habituate to their location, surface texture, shape and colour. After 6 hours, animals were returned to the same arena with one of the object changed. In the OLT one object was moved to a new location, and in NOR one object was replaced with another object with different shape and colour. In the test phase, mice were allowed to explore the arena for 8 minutes.

The exploration was recorded and analysed by an experimenter blinded to the treatments. The exploration times were scored as when mice came into close proximity to the objects, interacting with them. The difference between the time spent exploring the new object or location, and time spent exploring the unchanged object or location, was calculated as a proportion of total time in the tests. This value is known as the discrimination index (DI) which gives an indication of the ability to recognise the change. Therefore, a DI > 0 suggests that mice spent longer exploring the new object or location. DI = 0 implies an impairment of spatial or recognition memory. A DI < 0, showing that the mice spent a

longer time exploring the familiar object or location, may reflect anxiety and/or implies a failure of memory encoding or retrieval.

Saline-injected mice all showed non-negative DI values for the OLT, indicating the ability to discriminate between old and new locations. This phenomenon was also apparent after both treatments (control and *Kcna1*-CRISPRa), showing no effect of our therapy on spatial memory acquisition and recall (Figure 3.4 (C)). On the other hand, kainic acid injected epileptic group showed mostly negative DI values before treatment, suggesting disrupted spatial recognition pathways and/or increased anxiety, in agreement with the literatures (Pearson, Schutz and Patel, 2014).

Interestingly, with *Kcna1*-CRISPRa activation in the ventral hippocampus, all the mice regained spatial recognition of the new object, with a significant increase in exploration of the new location over the old location. This rescue was not observed with mice treated with Ctrl-CRISPRa (Figure 3.4 (C)) .

In NOR experiments, all mice group showed a positive DI values, including kainic acid epileptic cohort mice (Figure 3.4(D)). Epileptic mice showed a non-significant trend towards lower DI values. Absence of significant impairment in epileptic mice may be explained by the involvement of extrahippocampal structures such as prefrontal cortex in novelty recognition and memory, in contrast to spatial memory formation which is very sensitive to hippocampal dysfunction. Neither *Kcna1*-CRISPRa nor Ctrl-CRIPRa had a significant effect on NOR.

In summary, these results show that *Kcna1*-CRISPRa therapy rescued spatial memory function in a model of TLE.

3.8. Summary

In conclusion, this dual-viral CRISPRa strategy of endogenous upregulating kcna1 gene significantly reduced seizure frequency in kainic acid TLE model, as well as improving spatial recognition memory. The effect of the therapy on acute pilocarpine-induced seizures was not clear.

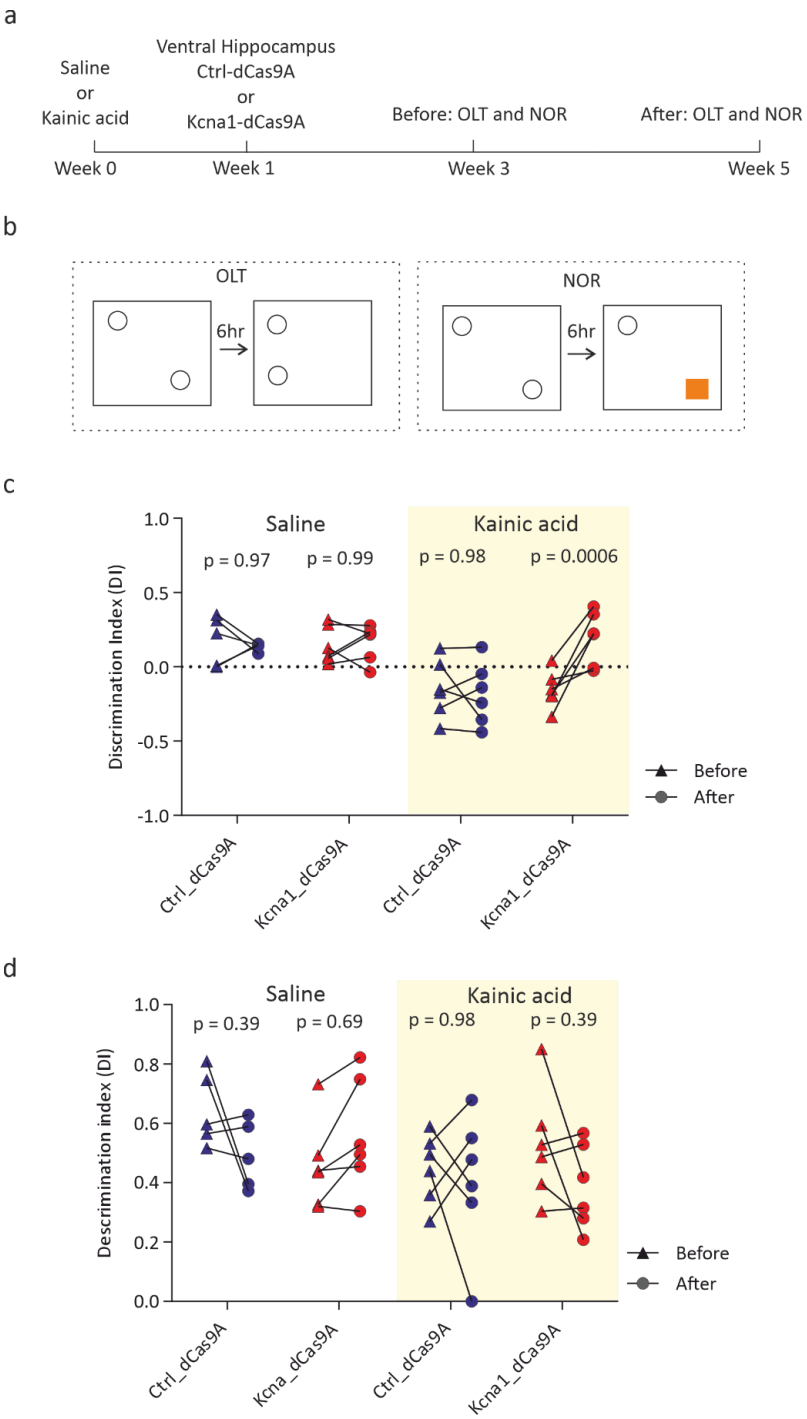

Figure 3.4 Behaviour assessments of OLT and NOR.(a)Experimental plan. Saline/Kainic acid mice were allowed to recovery from status epilepticus for one week before virus injections. Before tests were carried out 2 weeks after the virus, followed by continuous doxycycline diet and post-treatment tests. (b) Experimental setup with the OLT and NOR. Mice from the same cage were allowed to explore the arena with objects. (c) OLT results before and after doxycycline diet in saline and kainic acid treated mice groups. (2-way ANOVA). (d) NOR OLT results before and after doxycycline diet in saline and kainic acid treated mice groups. (2-way ANOVA). Figure modified from Colasante, Qiu et al 2020 Supplementary Figure S9)

Chapter 4.

Activity-dependent gene therapy for refractory epilepsy

The work described in this chapter was published as: *Qiu Y, O'Neill N, Maffei B, et al. On-demand cell-autonomous gene therapy for brain circuit disorders. Science (80-). 2022;378(6619):523-532.*

This chapter describes a novel gene therapy strategy for treating temporal lobe epilepsy induced by increased neuronal activity in seizures. The approach proposed here overcomes the limitation that gene therapy typically targets all neurons in the treated region, with only capsid tropism and conventional promoter activity determining which cells are modified. Instead, we aim to specifically target those neurons that are recruited to pathological levels of activity during seizures. The gene therapy can be targeted to overactive neurons involved in the epileptic network without significantly affecting neighbouring or intermingled neurons that fire normally. The work described here aimed to determine whether this strategy could be used to treat epilepsy.

4.1. Introduction

A hallmark of epileptic seizures is that a subset of neurons exhibits abnormal firing patterns. Although activity in seizure foci is dynamic and the mechanisms of neuronal recruitment are incompletely understood, we hypothesise that overactive neurons are responsible for triggering seizures or mediating their propagation.

4.1.1. Limitations with current strategies

Current gene therapy strategies are based on a view of seizure as a monolithic hypersynchronous event and are therefore aimed to

restore the excitation/inhibition balance by permanently modifying circuit excitability (Penfield and Jasper, 1954). Most efforts have been devoted to decreasing excitation or increasing inhibition to return the brain to a more stable status. These changes can be achieved by modifying neuronal properties or by expressing exogenous genes in target cells. Cell-type specific promoters are also applied to limit transgene expression to specific cell types, excitatory or inhibitory. For example, the *CamKII* promoter biases expression to excitatory neurons in the cortex, while *mDlx* or the GAD65 promoter preferentially drives expression in inhibitory neurons (Nathanson *et al.*, 2009; Tye *et al.*, 2011; Dimidschstein *et al.*, 2016; Hoshino *et al.*, 2021). However, these approaches lead to transgene expression in cells in and around the treated brain region with no discrimination between neurons actively participating on abnormal network states and neurons that are not directly involved (Kullmann *et al.*, 2014). More advanced designs with chemogenetics or optogenetics rely on the combination of exogenous gene expression and chemical or light activation to improve the temporal precision of the therapeutic effects (Walker *et al.*, 2013; Kätzel *et al.*, 2014; Wykes *et al.*, 2016). These strategies, however, are still limited by the global modification of targeted neurons when switched on. The requirements for device implantation and drug administration represent additional risks of surgical complications or drug adverse effects in clinical practice (Wykes *et al.*, 2016; Walker and Kullmann, 2019). Although optogenetics and chemogenetics allow specificity in time, they do not address the limitations of widespread effects on neurons that may not be primarily part of the epileptic network.

Therefore, simply targeting neuronal sub-types without evaluating circuit dynamics is a suboptimal approach to achieving an anti-seizure effect. We, therefore, designed a novel gene therapy to overcome the limitations of available treatments.

4.1.2. Selectively target neurons with novel gene therapy design

The solution proposed here is to target transgene expression selectively to neurons that participate in seizure initiation and/or propagation, identified as such on the basis that they fire excessively. Some studies have suggested that seizures recruit heterogeneous populations of neurons with varying changes in spike rates (Truccolo *et al.*, 2011). More recent studies have argued that neurons involved in seizure initiation are recruited in a stereotypical manner, albeit with varying time delays (Neumann *et al.*, 2017; Wenzel, Jordan P Hamm, *et al.*, 2017; Wenzel *et al.*, 2019). Despite continued uncertainty regarding seizure initiation mechanism, we propose that targeting overactive neurons should be an effective therapy. By restricting antiepileptic transgenes only to neurons which have fired excessively, we are able to distinguish between pathological and healthy cells in and around epileptic foci, and effectively stop them from triggering further seizure attacks. This activity-dependent induction of gene therapy can be achieved using activity-dependent promoters which naturally exist in the genome. A highly conserved family of genes known as immediately early genes (IEGs) are rapidly turned on in response to increases in activity (Sheng and Greenberg, 1990; Greer and Greenberg, 2008). They are primarily downstream responders of calcium signalling pathways. The promoter regions of IEGs are enriched with domains that are recognised by proteins which are phosphorylated in response to elevations in intracellular calcium as well as other signalling cascade, which allow their rapid activation (Sheng and Greenberg, 1990; Greer and Greenberg, 2008).

Therefore, taking the promoter sequences of those IEGs, we are able to design a novel strategy: the transcription of the therapeutic transgene increases with neuronal activity. The main advantage of using activity-dependent promoters over conventional constitutively active promoters is that it could improve both the

spatial and the temporal specificity of expression of an anti-epileptic effector protein. We hypothesized that the therapy will be selectively activated in neurons which are hyperactive, and with the appropriate effector transgene their excitability can be reduced, thereby preventing seizure initiation or propagation. Healthy intermingled or surrounding neurons in the same brain region are not affected by the treatment. This prevents healthy neurons from being over-silenced.

Furthermore, activity-dependent gene therapy follows activity in the treated neurons, and should turn itself on and off in an autoregulatory fashion. If neurons are becoming overactive, the treatment will detect this change and modulate their excitability, potentially even before overt seizures are detected. Conversely, if pathological activity disappears, the treatment should switch itself off, meaning that there is no residual alteration of neuronal function, although because the activity-dependent promoter and transgene are still present, the treatment could switch on again at a later time.

4.1.3. Activity-dependent immediate early genes (IEGs) in CNS

Activity-dependent molecular signalling was first described by Greenberg & Ziff in 1984 with regard of the *c-fos* proto-oncogene (Greenberg and Ziff, 1984). The paper described *c-fos* as a growth-factor responding nucleic protein that controls the re-entry of G0 phase cells into the cell cycle (Greenberg and Ziff, 1984). A rapid increase in *c-fos* transcription was observed within a few minutes of the addition of growth hormone and rapidly turned over after 30 minutes (Greenberg and Ziff, 1984; Sheng and Greenberg, 1990). In post-mitotic cells like neurons, IEGs continue to perform crucial roles in regulating cellular responses to changes in external perturbations thorough a variety of mechanisms. Stimuli received by various membrane proteins and sensors are translated into

either immediate electrophysiological processes or secondary messenger signalling pathways. Such responses may go beyond individual neurons and spread onto neighbour cells, neural circuits, networks, or distant structures (Herdegen and Leah, 1998).

The main mechanism that controls the downstream activation of IEGs is the calcium signalling pathway. It was shown that *c-fos* gene transcription activation was blocked by calcium chelation with EGTA (ethylene glycol-bis(β-aminoethyl ether)-*N*, *N*, *N'*, *N'*-tetraacetic acid) (Bading, Ginty and Greenberg, 1993; Herrera and Robertson, 1996). In addition to c-Fos, additional genes considered to be in the family of IEGs include *bdnf (brain-derived neurotrophic factor), arc/arg3.1(activity-regulated cytoskeleton-associated protein),* egr1/2/3 (early response genes 1,2 and 3), *npas4* (neuronal PAS domain protein 4), and more (Greenberg, Thompson and Sheng, 1992; Kornhauser *et al.*, 2002; Greer and Greenberg, 2008). The promoter regions of IEGs are highly conserved across species for their critical role in development. Homozygous deletion of the *c-fos (c-Fos)* gene in mice leads to multiple defects and increased mortality at birth (Johnson, Spiegelman and Papaioannou, 1992).

4.1.3.1. Mechanism of calcium dependent IEGs activation

4.1.3.1.1. Calcium dependent signalling pathway

Sensory inputs, synaptic signals or growth factors trigger calcium entry from extracellular space, often through L-type voltage-gated calcium channels (L-VGCCs), secondary to depolarization of the postsynaptic membrane (Greenberg, Ziff and Greene, 1986; Sheng and Greenberg, 1990; Sheng, Thompson and Greenberg, 1991; Ghosh and Greenberg, 1995). A complete summary of cellular signalling pathway for IEG activation is summarised in Figure 4.1.

Cytoplasmic calcium release from intracellular stores also occurs secondary to calcium influx via L-VGCCs. In addition, the

excitatory neurotransmitter glutamate acting via NMDARs (N-methyl-d-aspartate receptors), and AMPARs (α-amino-3-hydroxy-5-methyl-4-isoxazole propionic acid receptors) contribute to postsynaptic calcium influx (Ghosh and Greenberg, 1995). In early development, in particular, NMDARs account for a large fraction of calcium influx triggered by synaptic activity (West *et al.*, 2001). Calcium ions act as a secondary messenger in the cytoplasm and trigger several signalling cascades, including the MAPK (Ras-mitogen-associated protein kinase), calcium/calmodulin-dependent protein kinases (CaMKs), and calcineurin-mediated signalling pathways (Sheng, Thompson and Greenberg, 1991; Bito, Deisseroth and Tsien, 1996; Hardingham *et al.*, 1997). L-VGCCs seem to be a more important driver for IEG activation than glutamate receptors, even though they are not activated prominently by synaptic activity(Murphy, Worley and Baraban, 1991). This may be due to the strong calcium conductance of L-VGCCs and their dendritic and somatic location, as observed in hippocampal pyramidal neurons (Westenbroek, Ahlijanian and Catterall, 1990; Schuman, Dynes and Steward, 2006).

Nucleic and cytoplasmic calcium signals drive different but overlapping signalling pathways in neurons (Hardingham *et al.*, 1997). Cytoplasmic calcium ions primarily interact with CaMKs (CaMKII and CamKIV), calcineurin, and Ras (rat sarcoma virus)-GTPase (Johnson *et al.*, 1997). Each of these proteins interacts with downstream signalling cascades. The RAS/MAPK (mitogen-activated protein kinase) pathway recruits ERKs (extracellular signal-regulated kinases) and RSKs (ribosomal protein S6 kinases), and other kinases. Downstream targets also include transcriptional factors (TFs). Calcium ions that enter the nucleus can also directly interact with CaMKs. They phosphorylate the transcriptional factor CREB (cyclic adenosine monophosphate

(cAMP) response element-binding protein) at multiple sites, leading to IEG activation (Sheng, Thompson and Greenberg, 1991; West *et al.*, 2001; Kornhauser *et al.*, 2002). Phosphorylation of CREB at ser142 in particular has been shown to play an essential role in circadian clock functions (Gau *et al.*, 2002).

4.1.3.1.2. Transcriptional activation of IEG promoters

The level of IEG expression remains very low under basal conditions, but increases very rapidly when stimuli are detected by the calcium sensors (Morgan *et al.*, 1987; Herrera and Robertson, 1996). This fast response is partially enabled by a pre-assembled transcriptional complex at the transcriptional start site (TSS), the 'TATA' box, of the IEG genes. This partially constructed complex is stalled at the TSS until the activation signal triggers transcription initiation (Saha *et al.*, 2011). This process enables the characteristic rapid changes in expression levels of IEGs (Saha *et al.*, 2011). The proximate promoter regions close to the TSS governs the activity-dependent behaviour of IEG expression downstream of synaptic activities and membrane depolarization. They contain a variety of binding sites for inducible regulatory TFs. These TFs include serum response factor (SRF), *c-sis*–platelet-derived growth factor (PDGF)-inducible factor element (SIE), CREB and myocyte enhancer factor (MEF2) (Yap and Greenberg, 2018). CREB, for example, has a classic leucine zipper domain for protein dimerization and DNA binding (Ahn *et al.*, 1998). The DNA recognition sequence specificity is embedded in the polypeptide sequence and the three dimensional structure of the heterodimer that enables them to form DNA-protein interactions only at specific sites in the genome (Habener,

1990). The heterodimer composed of two different proteins together forms the basic interface to bind with nucleic acids.

The recognisable consensus sequences include SRE (serum response element), CRE (CaMP response element) or CaRE (calcium response element), and SIE. The DNA sequences are conserved across mammals, including rodents and human. The calcium response element (CaRE) consensus sequence was the first cis-regulatory component discovered. It interacts with phosphorylated CREB downstream of calcium dependent pathway (Sheng and Greenberg, 1990). Interestingly, this is not the only activity-control mechanism that triggers c-Fos expression, additional sites are found in c-Fos promoter region that guards its activity-dependent expression. SRE (serum response element) was discovered further upstream from the c-Fos gene locus (Treisman, 1985; Flavell and Greenberg, 2008). Experiments showed that this site attracts multiple DNA binding proteins, including SRF and Elk-1 (Flavell and Greenberg, 2008). Additional enhancer sites are also present further upstream from the IEG gene loci, but those sites are the core components for inducible transcriptional control (Joo *et al.*, 2015).

The fully assembled transcriptional initiation machinery starts the transcription process leading to expression of the IEG product . The expressed protein becomes detectable only 15 minutes after a strong stimuli, such as seizure in rodent brains (Sheng and Greenberg, 1990; Smeyne *et al.*, 1992; Johnson *et al.*, 1997).

4.1.3.1.3. Roles and functions of IEG protein products

The protein product of IEGs can act as TFs and form transcriptional regulators for regulating wide range of targets. For example, Fos protein combines with a member of the jun family to create AP-1 (activator protein 1) transcriptional

factors (Chiu *et al.*, 1988; Sheng and Greenberg, 1990; He and Ping, 2009). Homodimer formed of Fos family members cannot form stable chemical bonds with DNA sequence (Patel, Curran and Kerppola, 1994). AP-1 complex interaction favours the conserved site TRE (TPA-response element), which can be found upstream of several IEGs (Eferl and Wagner, 2003). The function of the AP-1 complex can be modulated according to its composition: the c-Fos/junB combination forms a transcriptional activator; however, c-Fos/c-Jun combinations, under some scenarios, can act as transcriptional suppressors (Chiu, Angel and Karin, 1989). Different isoforms of the same transcriptional factors can also be produced by alternative splicing or post-translational modifications, resulting in biphasic regulation of the same downstream targets (Foulkes and Sassone-Corsi, 1992).

Interestingly, the same inducible TFs can also act as repressors to suspend gene expression. Transcriptional repressors receive less attention than activators. NFκB family and plasticity-related MEF2 and MeCP2 are all repressors related to activity-level (Benito and Barco, 2015). These transcriptional regulators form either repressive or active complexes in the absence or presence of calcium to achieve calcium-dependent transcription control (Greer and Greenberg, 2008).

4.1.3.1.4. The early and late IEGs and their different roles

Yap & Greenberg, 2018, proposed that the IEGs family can be divided into two groups, early response genes (ERGs) and later response genes (LRGs), according to their temporal and spatial profiles of activation (Yap and Greenberg, 2018). The calcium-MAPK pathway only activates ERGs as a first wave of gene expression, and their protein products then act as TFs and activate the second wave of LRGs (Yap and Greenberg, 2018).

The activation of LRGs involve more complicated epigenetic control (cis/trans-distal regulators) for fine-tuning of expression levels. And their proteins usually are not TFs and will exit nucleus (Hrvatin *et al.*, 2017). They are more directly involved as effectors to modulate cellular pathways or as secreted signals that act on neighbouring cells. Both *Arc* and *BDNF* have functional roles in synaptic plasticity. The *Arc* protein is required for both long-term potentiation (LTP) and long-term depression (LTD) (Steward *et al.*, 1998; Korb and Finkbeiner, 2011). In addition, newly synthesized *Arc* mRNA selectively accumulates in active dendritic locations of granule cells upon high-frequency activation of the perforant pathway to the dentate gyrus (DG) (Steward *et al.*, 1998). The ERG product NPAS4 acts as a TF to interact with the *bdnf* promoter region and induce its activation within 30 minutes after the initial stimulation event (Greer and Greenberg, 2008). When secreted, *BDNF* interacts with TrkB (tropomyosin-related kinase receptor B) and activates downstream pathways that cause Narp to be released, which can modulate synaptic plasticity (Mariga *et al.*, 2015).

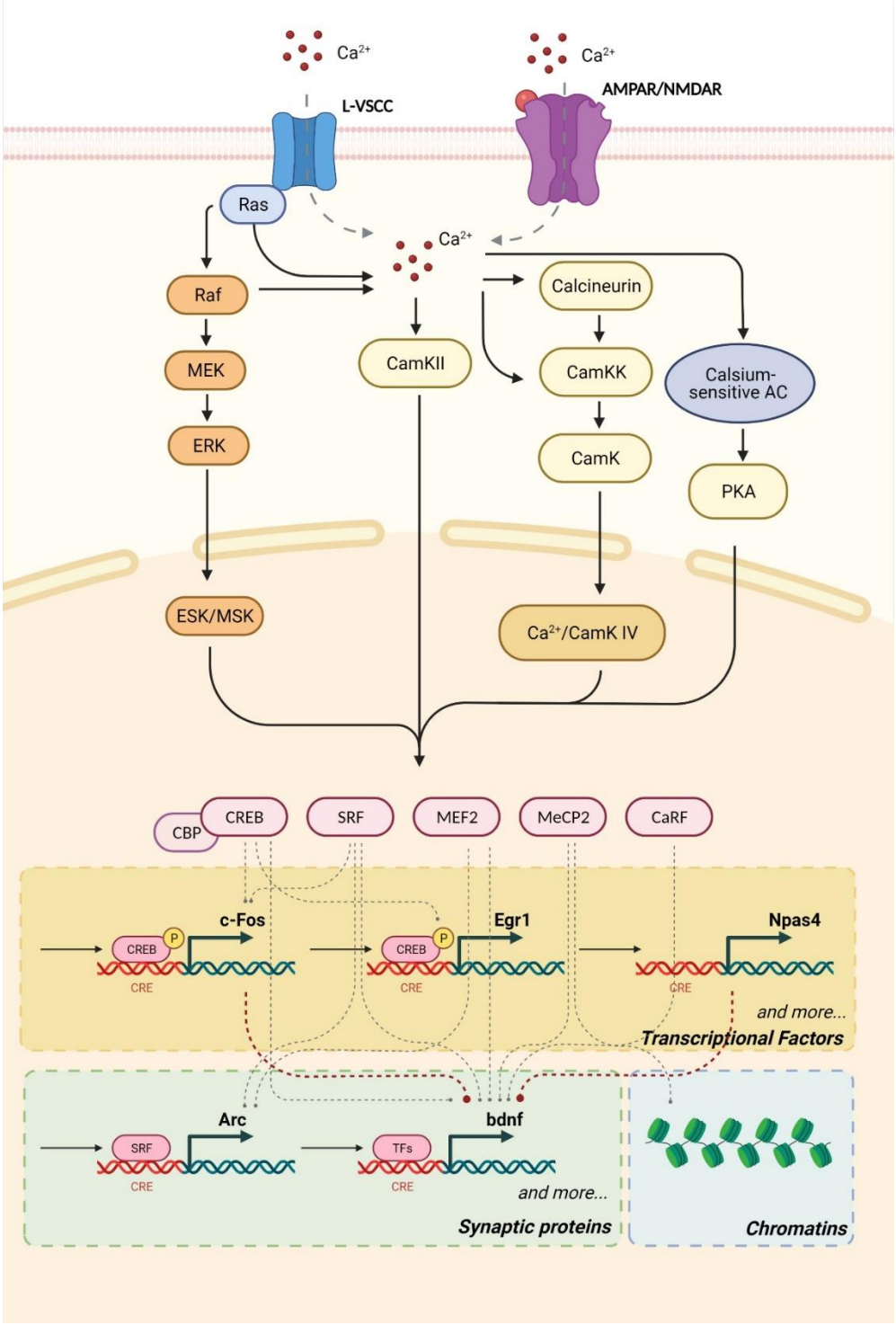

Figure 4.1. Activity-dependent signalling pathway in CNS (modified from Fig3, Flavell and Greenberg, 2008*; Fig1,* Greer and Greenberg, 2008*; and Fig6,* Yap and Greenberg, 2018*). AC (adenylate cyclase); PKA (protein kinase A); calcium-/calmodulin-dependent kinase II and IV (CamKII, CamKIV); CaRF (calcium response factor); ESK/MSK (ERK/mitogen-dependent kinase).*

4.1.3.2. The roles of IEGs in physiological activities and neurological disorders

Detrimental genetic mutations in proteins participating in calcium-dependent pathways and transcription of IEGs can lead to severe diseases. Some examples include mutations in L-type VGCCs in Timothy syndrome, mutations in CBP (CREB binding partner) in Rubinstein-Taybi syndrome and mutations in MeCP2 in Rett Syndrome (Ebert and Greenberg, 2013; Ip, Mellios and Sur, 2018; Yap and Greenberg, 2018).

Abnormal stimuli patterns can also lead to changes in the signalling pathway upstream of IEGs. For example, persistent hyperexcitability of the network may activate IEGs unexpectedly, leading to abnormal downstream gene expression and changes in cellular profiles. This phenomenon of abnormal excitability is shown in schizophrenia, autism, Alzheimer's disease and epilepsy (Flavell and Greenberg, 2008; Greer and Greenberg, 2008; Yap and Greenberg, 2018). Epileptic seizures, in particular, would be expected to be very strong drivers of IEG expression, and the downstream consequences for the homeostatic regulation of circuit excitability remain incompletely understood (Lignani, Baldelli and Marra, 2020) (Figure 4.2).

Several important IEGs will be discussed in more detail below with regard to their roles in physiological and pathological conditions, with a focus on hyperexcitability.

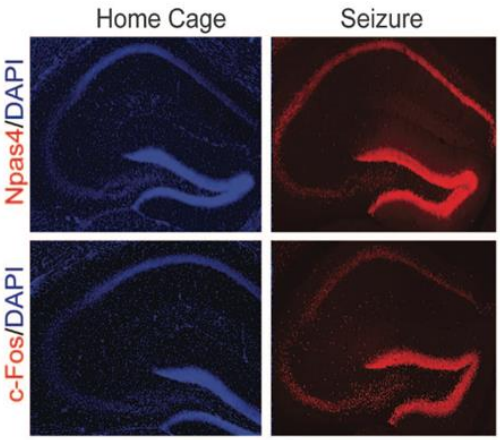

Figure 4.2. Rapid activation of IEGs (c-Fos and NPAS4) after seizure.
Strong positive expression of NPAS4 after induction of seizures across hippocampus; no such expression is present in home cage (adapted from Ramamoorthi, 2011).

4.1.3.2.1. c-Fos

c-Fos was one of the first IEGs whose expression was demonstrated to increase with high levels of activity (Curran and Teich, 1982). A connection between IEGs and memory has long been speculated, however, the molecular mechanism was not fully dissected (Guzowski *et al.*, 1999). With progress in tools which enable labelling of active neurons *in vivo,* several groups have established some mechanistic links between IEGs and memory. In 2012 a Liu *et al* demonstrated that the c-Fos promoter was sufficient to identify and label cells activated during a window of memory formation In the contextual fear conditioning test (CFC) (Liu *et al.*, 2012). In the memory recall phase of CFC, re-activating the targeted neurons alone was sufficient to elicit a memory of the conditioning context in a different and neutral environment not associated with fear memory formation (Liu *et al.*, 2012). This study demonstrated the direct involvement of c-Fos in associative memory mechanism. Follow-up studies by the Tonegawa group further dissected the mechanisms of memory 'engram' formation. Manipulation of engram cells using c-Fos promoter

driven cell activation or silencing tools were sufficient to alter the memory consolidation network and change the memory readouts from CFC (Ramirez *et al.*, 2013, 2015; Tonegawa *et al.*, 2015). During memory recall, c-Fos positive engram cells were identified in various regions across the brain beyond hippocampal circuits (Roy *et al.*, 2022).

The degree of c-Fos activation differs in health and disease status. In control mice, it was found that c-Fos expression was relatively sparse in pyramidal cells in CA1 and CA3, as well as in the hilus and stratum oriens, possibly reflecting its role in normal learning and memory (Peng and Houser, 2005). On the other hand, c-Fos expression is strongly activated after seizures and in the epileptic brain (James I. Morgan *et al.*, 1987; Herdegen and Leah, 1998; Nehlig, 1998). c-Fos expression has been shown in the hippocampal DG, 30 minutes post-PTZ (pentylenetetrazol) induced seizures, and these levels peaked after approximately 1-2 hours (Morgan *et al.*, 1987; Nehlig, 1998). A comparable c-Fos expression profile was reported in pilocarpine and kainic acid models (Vol *et al.*, 1973; Peng and Houser, 2005). In the pilocarpine model of acute seizures, it was reported that initial c-Fos expression occurs in DG cells, followed by hippocampal CA1-CA3 (Peng and Houser, 2005). c-Fos expression returned to baseline 18-24 hours after seizures (Peng and Houser, 2005). In chronic epileptic brains, spontaneous seizures induced DG granule cell c-Fos expression 15 minutes post-seizure, followed by similar increases in hippocampal CA1, CA3, subiculum, and entorhinal cortex (Peng and Houser, 2005).

Multiple studies have consistently reported that c-Fos expression was more readily and rapidly detected in granule cells than other neurons (Herrera and Robertson, 1996; Zhang *et al.*, 2002; Peng and Houser, 2005). One may speculate that the activation propagated from the granule cells, followed by strong activation of interneurons participating in feedback inhibition of the same granule cells (Peng and Houser, 2005). In addition, it was shown that when two seizures that were introduced with 24 hour interval, there was strong activation of c-Fos expression at the merging side of granule cell layer and hilus, indicating prominent involvement of interneurons (Peng and Houser, 2005). This suggests that there is a complicated relationship between neuronal activities and c-Fos activation.

Furthermore, c-Fos was also found to modulate glutamate-induced excitotoxicity by interacting with the kainic acid receptor GluR6 and BDNF, reducing neuronal death during kainic acid-induced acute status (Zhang *et al.*, 2002).

In conclusion, c-Fos is a key player in activity-dependent mechanism and it modulates both excitability and neurotoxicity in response to changes in activity inputs.

4.1.3.2.2. *Arc*

Arc (also known as *Arg3.1*) is a cytoskeleton-interacting protein which has been studied extensively for its central role in synaptic plasticity (Link *et al.*, 1995; Lyford *et al.*, 1995). *Arc* expression in the brain is almost exclusive to glutamatergic neurons in the

hippocampus and neocortex (Guzowski *et al.*, 2005). There is little to no expression in other neuronal populations. Arc protein has been isolated in postsynaptic membranes, bound to NMDARs, with none detected in presynaptic terminals or axons (Shepherd and Bear, 2011). Upon repeated high-frequency stimulation, newly synthesized *Arc* mRNA is transported to active dendrites for rapid local protein synthesis (Steward *et al.*, 1998). This leads to *Arc* mRNA accumulation in dendritic compartments and enhanced local protein synthesis (Steward *et al.*, 1998). The Arc protein then binds with the endocytic proteins dynamin and endophilin to regulate AMPA receptors (Chowdhury *et al.*, 2006). Increases in Arc expression lead to enhanced endocytosis and less membrane abundance of AMPA receptors at active synapses (Bramham and Wells, 2007).

Arc has also been implicated in changes in network stability during epileptogenesis. In the latent period of the intrahippocampal kainic acid model, *Arc* expression was reported to be only detectable in dispersed dentate gyrus granule cells, which are located near the kainic acid injection site (Janz *et al.*, 2018). It was speculated that Arc contributes to the formation of new synaptic contacts to restore dentate gyrus circuit function. However, excessive synapses in turn, further destabilize the network (Janz *et al.*, 2018).

4.1.3.2.3. Egr family

The early growth response (EGR) family was simultaneously discovered from multiple cell lines by various groups in late 1990s (Duclot and Kabbaj, 2017).

Hence, Egr gene has been given several alternatives names over time, including *zif268*, in earlier publications (Yamada *et al.*, 1999). The expression of this IEG can be induced by various stimuli, including growth factors, neuronal activity and hormones (Tsai *et al.*, 2000). Egr1 is particularly interesting because it is involved in synaptic plasticity, neurotransmitter release, receptor expression, miRNA regulation, and actin cytoskeleton (Duclot and Kabbaj, 2017). Its malfunction is implicated in addiction, anxiety and several other neuropsychiatric disorders (Duclot and Kabbaj, 2017).

Egr1 has a similar initial activation profile as c-Fos, i.e. via the calcium-sensitive MAPK pathway (Saffen *et al.*, 1988; Kaczmarek, Zangenehpour and Chaudhuri, 1999). Egr1 activates a different but overlapping set of downstream targets to c-Fos, most of which are involved in growth and plasticity (Kaczmarek, Zangenehpour and Chaudhuri, 1999; Yamada *et al.*, 1999). Interestingly, Egr1 is constitutively expressed during normal brain activity in the hippocampus and other structures (Gallo *et al.*, 2018).

Egr1 has also been studied in epileptic brains. Egr1, along with other Egr members (Egr2, Egr3), was found to be overexpressed after ictal events in the seizure initiation region (López-López *et al.*, 2017). Egr1 expression increased rapidly after electrically induced seizures, peaking around 2hrs, followed by a decrease back to basal levels. In contract, Egr3 expression showed a much slower activation and persistently high expression up to 10 hours after the seizure (O'Donovan *et al.*, 1999).

In the PTZ model of acute seizures, Egr1 expression significantly increased in CA1, CA3, DG and entorhinal cortex (Szyndler *et al.*, 2013). One recent study using an Egr1-CreER transgenic mouse showed that granule cells, hilus mossy cells, and pyramidal layers of CA1-CA3 expressed Egr-1 after a PTZ-induced acute seizure (Longueville *et al.*, 2021). No Egr-1 expression was detected in microglia or inhibitory interneurons, although astrocytes were sparsely labelled (Longueville *et al.*, 2021). In a different model of PTZ-evoked seizures, similar structures were labelled; however, very few Egr-1 positive neurons were found in CA2 (Szyndler *et al.*, 2013).

In human TLE patients, Egr1 expression was observed at epileptic foci, together with c-Fos and Egr2 (Rakhade *et al.*, 2007). Interestingly, their expression levels correlated with the frequency of interictal spikes (Rakhade *et al.*, 2007). In particular, the correlation patterns of Egr1 highly resemble that of c-Fos, suggesting a similar activation pathway (Rakhade *et al.*, 2007). The mRNA of Egr1 increased transiently after the epileptic attack, which may lead to prolonged sustained changes of downstream targets. One of those targets is Cav3.2, a subunit of T-type voltage-gated calcium channel, which is believed to be pro-epileptogenic (Van Loo *et al.*, 2019). In addition, an increase in Egr1 level was detected in human hippocampal tissue resected at epilepsy surgery (Van Loo *et al.*, 2019). These findings raised the possibility that Egr1 may be involved in epileptogenesis pathways with unknown functions. In conclusion, Egr1 is another

good indicator of epileptic activity, and has a similar expression profile as c-Fos.

4.1.3.2.4. Npas4

Npas4 is a member of the bHLH PAS (basic helix–loop–helix-PER-ARNT-SIM) family and is primarily expressed in neurons (Flood *et al.*, 2004; Ooe *et al.*, 2004). Npas4 expression has been detected downstream of membrane depolarization and/or calcium entry into the nucleus (Ramamoorthi *et al.*, 2011). A rapid increase in the Npas4 protein level was observed 90 minutes post-stimulation. Several upstream receptors, including NMDA, AMPA and kainate receptors, can regulate Npas4 expression (Ramamoorthi *et al.*, 2011). This neuron-specific transcriptional factor has been reported to be involved in GABAergic inhibitory synapse development. The level of Npas4 has also been shown to affect the number of inhibitory synapses on excitatory neurons, possibly by a fast attenuation of BDNF promoter transcription in an activity-dependent manner (Lin *et al.*, 2008). This suggests that Npas4 plays an important role in the maintenance of the excitation /inhibition balance.

Similar to c-Fos, Npas4 has been implicated in CFC fear memory mechanism. mRNA expression of Npas4 was detectable 5 minutes after foot-shock stimulation, and the level decreased after 1 hour (Ramamoorthi *et al.*, 2011). Importantly, a strong Npas4 expression in CA3 and a large increase in protein expression in all hippocampal structures was reported post-seizure (Ramamoorthi *et al.*, 2011). The expression of Npas4 was weaker in CA1. In response to stronger stimulation

by systemic kainic acid-induced seizures, nearly all excitatory neurons in the pyramidal layer of CA1, and a minor portion of inhibitory neurons, expressed Npas4 (Bloodgood *et al.*, 2013). Another study reported that Npas4 may act as homeostatic regulator during epileptogenesis by controlling Homer1a expression and its binding partner AMPAR GluA1 subunit(Shan *et al.*, 2018). Indeed, in some studies the temporal onset of Npas4 expression appears to be more rapid than that of c-Fos activation. Furthermore, Npas4 has been shown to induce distinct cohorts of genes to modulate synapse formation (Spiegel *et al.*, 2014). Within a single fear memory engram, c-Fos and Npas4 drove differential reactivation patterns of in fear recall of similar context (Sun *et al.*, 2020). While the c-Fos dependent ensembles respond to excitatory inputs from medial entorhinal cortex, the Npas4-governed ensemble primarily were modulated by upstream inhibitory inputs from CCK+ (cholecystokinin-expressing) interneurons (Sun *et al.*, 2020).

4.1.3.3. Cell specific and development specific expression of IEGs

IEGs trigger cell-specific activity-dependent transcriptomic changes, for example, in excitatory or inhibitory neurons, by suppressing or activating different genes (Yap and Greenberg, 2018). A study showed that in three interneuron subpopulations, SST-, vasoactive intestinal peptide (VIP)-, and parvalbumin (PV)-positive interneurons, IEGs expression patterns were similar immediately after stimulation but diverged profoundly with time (Spiegel *et al.*, 2014; Mardinly *et al.*, 2016). Furthermore, in excitatory neurons, BDNF was

secreted to recruit inhibitory inputs onto its soma, while in VIP-interneurons, AP-1 preferentially activates IGF1 secreted protein to recruit inhibitory inputs (Mardinly *et al.*, 2016).

Activity-dependent neuronal development was first described in developing visual cortex where stimulation is crucial for sculping neural connectivity in the postnatal brain (Hubel and Wiesel, 1970). An appropriate balance of activity levels is required at every stage of CNS development, from axonal growth, dendritic arborization, synapse formation, to axonal elimination (Thompson *et al.*, 2017). In rats, cats and monkeys, increases in c-Fos and Egr1 expression coincide with the critical period of eye-opening in developing visual cortex (Kaczmarek and Chaudhuri, 1997; Kaczmarek, Zangenehpour and Chaudhuri, 1999). In contrast, the basal expression of those genes in the adult visual cortex is relatively low (Kaczmarek and Chaudhuri, 1997). A recent study demonstrated that activity signals propagate via the JAK2 pathway to modulate axonal survival in postnatal mouse brains (Yasuda *et al.*, 2021). Dynamic interactions occur at synapses, which ultimately determines their fate depending on the signals that they receive (Yap and Greenberg, 2018). This process occurs at a critical period in development. Abnormalities can lead to an altered excitation-inhibition balance in the adult brain and may increase the risks of neurological disorders, including schizophrenia, autism, seizures and cognitive disabilities (Yap and Greenberg, 2018).

4.1.3.4. IEG expressions and homeostatic plasticity

Homeostatic mechanisms generate stable activity patterns while allowing dynamic storage of information such as memory (Turrigiano, 2012). This involves both individual neural synapse regulations and regulations that occur on a more 'global' level.

In addition, short-term and long-term changes are different (Turrigiano, 2012). The activity-dependent properties of IEGs place them in a perfect role for synaptic plasticity and behaviour adaptations, such as memory and learning (Korb and Finkbeiner, 2011).

4.1.4. Use of IEG based novel strategies to access and manipulate active neurons

The activity dependent expression of IEGs can be used to faithfully report neuronal activity changes. Novel molecular systems have been designed based on the promoters of various IEGs to label active cells (Kovács, 1998). Transgenic mouse models were created to investigate the global expression of IEGs after stimulation, e.g. c-Fos-GFP, c-Fos-LacZ, and Egr1-Cre (Smeyne *et al.*, 1992; Kasof *et al.*, 1995; Robertson *et al.*, 1995; Kim *et al.*, 2016; Wang *et al.*, 2021). These models provide enormous information on the patterns of activity that follow stimuli such as seizures or behavioural tasks (Smeyne *et al.*, 1992). Importantly, using the promoters of IEGs to drive reporter genes can potentially provide not only spatial information regarding activity, but also insights into temporal profiles (Schilling *et al.*, 1991; Smeyne *et al.*, 1992; Kawashima, Okuno and Bito, 2014). Transgenic mice expressing LacZ driven by the c-Fos promoter, for instance, have been used to map early neuronal activation after seizures and other stimuli (Schilling *et al.*, 1991; Smeyne *et al.*, 1992). However, this only revealed a snap-shot of the activity profile, and was not able to show changes in expression over time. New techniques of live imaging combined with IEG promoters have enabled the activity of neurons to be monitored in real-time and correlated with behaviours (Kim *et al.*, 2016). The promoter of *arc* has been used in live cortical two-photon imaging at cellular resolution in order to study visual cortex orientation specificity (Wang *et al.*, 2006). In addition to delivery and

detection techniques, various attempts have been made to increase the efficiency/sensitivity of IEG promoters in response to changes in activity (Kawashima, Okuno and Bito, 2014).

In addition to promoters of IEGs that are well characterized in seizures and epilepsy, we also investigated synthetic promoters reported in literature with activity-dependent properties. Synthetic/engineered promoters have also been developed based on bioinformatic analysis of IEG promoter regions. SARE (synaptic activity–responsive element), conserved between mouse and human, was discovered upstream (>1000bp) of the *Arc* gene, and showed strong regulatory properties in response to increased activity (Kawashima *et al.*, 2009). SARE is 100bp in length, and contains activity-dependent CREB, MEF2 and SRF binding sites (Kawashima *et al.*, 2009). By organizing the SARE sequence in tandem, a new synthetic promoter, E-SARE (enhanced-SARE), was developed. E-SARE showed >800 fold higher reporter expression in the presence of stimulation than the c-Fos promoter (Kawashima *et al.*, 2009, 2013; Inoue *et al.*, 2010). Furthermore, by carefully re-arranging activity-dependent domains, a synthetic RAM (robust activity marking) enhancer was also recently developed (Sørensen *et al.*, 2016). By combing the NRE (Npas4 response element) and AP-1 sites together, RAM exhibited high induction efficiency following stimuli, with the advantage of low baseline/background expression. This enhancer was also coupled with the minimal promoter region of either c-Fos or Npas4 to develop the cell-specific promoters, P_{RAM} and N_{RAM} respectively. They were used recently side-by-side to reveal distinct neuronal ensembles in memory consolidation (Sun *et al.*, 2020). It was shown that c-Fos expressing neurons received enhanced excitatory inputs for memory generalization; In contrast, Npas4 expressing neurons were dominantly influenced by local inhibition for memory discrimination (Sun *et al.*, 2020).

In addition to IEG promoter and reporter combination for passive neuronal labelling, it is also possible to attach functional effector gene downstream of IEG promoter to manipulate the excitability of neurons with critical functions in memory formation and consolidation (Ramirez *et al.*, 2013). Fear memory conditioning, in particular, has been to study memory assessments (Fendt and Fanselow, 1999; Strekalova *et al.*, 2003). In a series of experiments published by the Tonegawa lab, IEG promoters were used to manipulate memory formation and consolidation in rodents (Tonegawa *et al.*, 2015; Kitamura *et al.*, 2017; Tonegawa, Morrissey and Kitamura, 2018; Josselyn and Tonegawa, 2020). Memory formation and memory consolidation are considered separate processes which occur in sequence. One study used AAVs with the c-Fos promoter driving the expression of ChR2 (channelrhodopsin-2) in a Tet(tetracycline)-OFF design. Neurons activated during memory acquisition were thus tagged, with c-Fos promoter activation leading to ChR2 expression, and then subsequently re-activated optogenetically, in a test of context-specific memory recall (Liu *et al.*, 2012). Activation of c-Fos-promoter tagged neurons was sufficient to alter behaviour (Ramirez *et al.*, 2013; Tonegawa *et al.*, 2015). IEG promoter activation can thus be exploited to manipulate neuronal excitability.

4.2. Hypothesis and Project Objectives

4.2.1. Hypothesized mechanism

We hypothesized that, by placing antiepileptic effector genes under IEG promoters should reduce neuronal excitability in closed loop, and thereby treat epilepsy. We also hypothesise that the activity-dependent gene therapy approach will be self-regulated: once the epileptic network is restored to baseline, and seizures or epileptiform activity fade, the tool is switched off, although can be subsequently reactivated if needed.

The schematic illustration (Fig. 4.3) shows how a network can transition into a hyperexcitable and hyper-synchronized state in epilepsy. With treatment, its excitability is reduced below seizure threshold. Constitutive promoters decrease the excitability not only of seizure-generating neurons but also of bystander neurons not involved in the epileptic process. In contrast, activity-dependent gene therapy can potentially restore a physiological status by selecting for pathologically hyperactive neurons.

Based on literature findings and understanding of IEG promoters, we proposed a hypothesized mechanism of how activity-dependent gene therapy will work in targeted neurons. To recapitulate the logic of the anti-epileptic strategy, epileptiform activity and/or seizures will first trigger rapid activation of the IEG promoter, which drives the expression of the effector gene that leads to an increase in membrane expression of effector protein. The effector protein expression reduces neuronal excitability and synaptic release, potentially reducing circuit excitability and seizures. With decreased activity, the IEG promoter activity switches off, and protein overexpression ceases. The inserted effector protein will remain in membrane to keep neuronal excitability low. The overexpression of effector gene will gradually fade, but if further seizures occur the therapy will be switched on again. However, if there are no further seizures, effector protein expression will return to baseline,

restoring neurons to a physiological ground state. The grey error indicated transition between different network status(Figure 4.4).

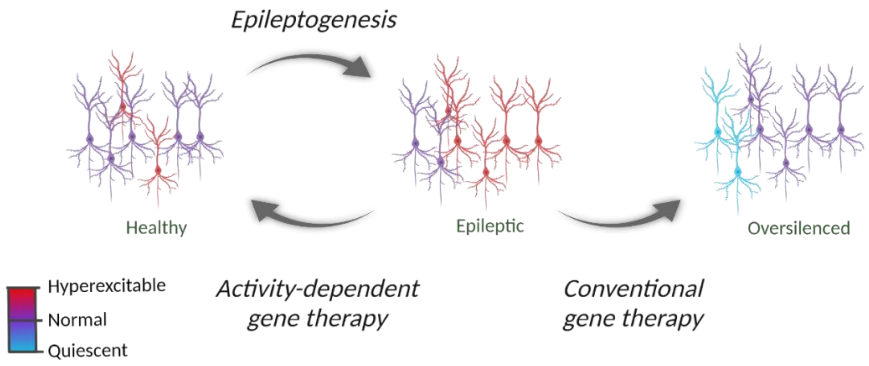

Figure 4.3. Illustration of physiological, epileptic and suppressed networks. The expected transitions between them by process of epileptogenesis, global suppression with conventional gene therapy and activity-dependent gene therapy. Heatmap: red (hyperexcitable), purple (normal), and blue (quiescent).

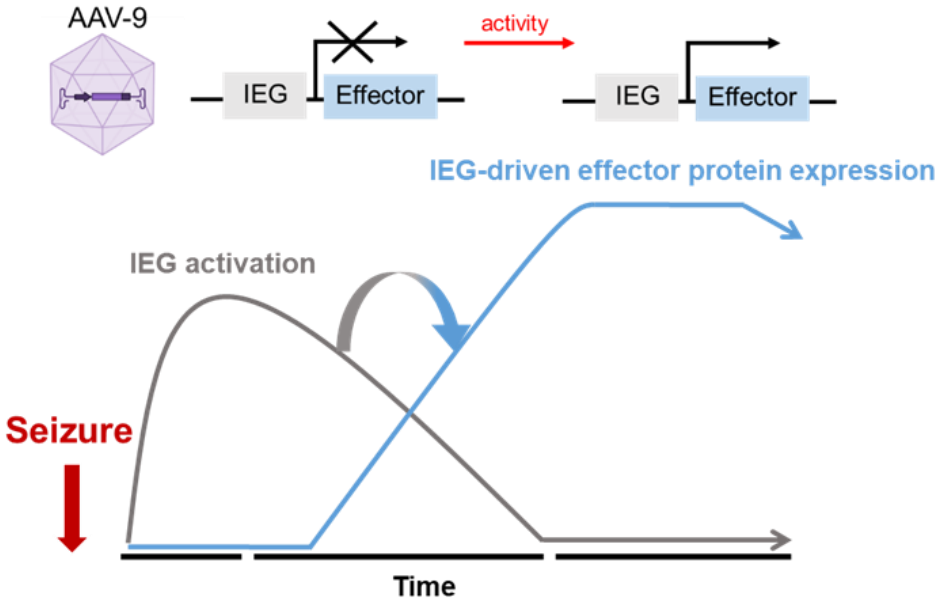

Figure 4.4 schematic representation of hypothesized mechanism of IEG promoter-effector activity-dependent gene therapy. The black line indicates the timeline from when the seizure activity was detected. The grey line represents the activation curve of IEG promoters, which is only transient. The blue line illustrated the proposed changes in protein levels of effector. The elevated membrane expression was represented by the plateau.

4.2.2. Project aims

This project aims to investigate the effectiveness and efficacy of using IEGs promoters to drive activity-dependent gene therapy for TLE.

For proof of principle, we chose the promoter of c-Fos (c-FosP), as it is well studied with a clear expression profile (Kovács, 1998). For the effector gene, we focused initially on *KCNA1* (Kv1.1 channel), based on its previously demonstrated anti-seizure effects when expressed continuously (Wykes *et al.*, 2012; Wykes and Lignani, 2018; Snowball *et al.*, 2019). We asked if this promoter-transgene pair is effective in seizure prevention, whether it has adverse effects, and how it may be translated into clinical practice. We first asked whether transient c-FosP activation is sufficient to drive an increase in expression of Kv1.1. We then asked whether cFosP-*KCNA1* treatment can be switched on and off according to the presence and absence of cellular or network activity fluctuations, respectively. Furthermore, we wanted to investigate anti-seizure effects of c-FosP-KCNA1 treatment in a chronic temporal lobe epilepsy model.

In addition, we also consider other IEGs promoters, including natural promoters extracted from genome sequence and synthetic promoter sequences which also have activity-dependent characteristics. For effector protein, we also investigate whether an alternative potassium channel, Kir2.1, will exert similar effects on hyperexcitable neurons.

In summary, this project aims to investigate whether activity-dependent gene therapy is an effective therapy in seizure prevention with minimal adverse effects.

4.3. The construct design for 'IEG promoter-Effector'

4.3.1. Backbone and shared components in all 'IEG promoter-Effector' vectors

For all plasmids used in this project, the expressed constructs were inserted in a AAV backbone plasmid (pX552) (Swiech *et al.*, 2015). In all the constructs, the IEG promoter sequence was bridged by a chimeric intron for enhanced splicing and eukaryotic cellular expression. The fluorescent marker gene was inserted after the chimeric intron to visualize the transient promoter activation. We chose a green fluorescent marker with shorter half-life of 2 hours (Li *et al.*, 1998). This destabilized GFP was synthesized by fusing a short domain of mouse ornithine decarboxylase (MODC) to the C-terminal of EGFP (enhanced GFP) coding sequence (Li *et al.*, 1998). This transient reporter is better suited to report transcriptional regulations, and fast turnover help reduced toxicity when stably expressed in cells (Li *et al.*, 1998). The effector gene is downstream of the dsGFP gene, separated by a self-cleaving short T2A linker for expression of both genes under the same promoter (Kim *et al.*, 2011). The effector gene was inserted after T2A peptide in frame with the dsGFP gene. Thses components are illustrated in Figure 4.5.

4.3.2. IEG promoters: natural and synthetic candidates

4.3.2.1. c-Fos promoter

As proof of principle, we started characterizing the therapy with c-Fos promoter (c-FosP) (Greenberg and Ziff, 1984). A fraction of 583bp upstream of the mouse c-Fos gene was extracted as c-Fos promoter (Berkowitz, Riabowol and Gilman, 1989; Robertson *et al.*, 1995). This chosen c-Fos promoter contains the necessary binding motifs for activity induced TFs, which include SRE (-261bp), SIE (-299bp), and CRE (-25bp) sites (He and Ping, 2009; Chung, 2015) (Figure 4.5). This fraction also

contains two TF-II sites (-267bp, -296bp) for enhanced promoter activation (Kim *et al.*, 1998). The TF-II sites overlapped partially with SRE and SIE sequences. Additionally, it includes a TRE site at -252bp for rapid AP-1 binding upon c-Fos activation (Chiu *et al.*, 1988).

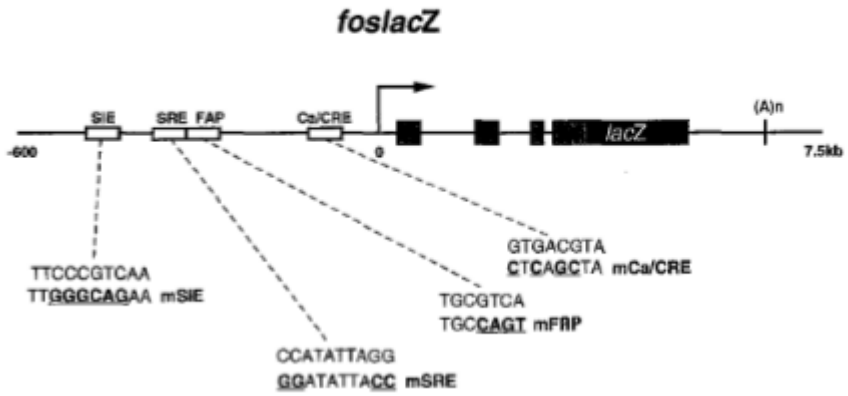

Figure 4.5. Illustration of the Calcium and growth serum response sites on cFos promoter region (Image modified from Robertson *et al.*, 1995*)*

4.3.2.2. Arc promoter

The Arc promoter stretches a long length on the genome (>1kb), which is more complicated than c-Fos (Inoue *et al.*, 2010). The regulatory elements extends more than 10kbp upstream into the genome. Therefore, instead of taking entire length of the promoter sequence, we found a minimal-Arc promoter which contains mainly the TATA box for transcription initiation (Inoue *et al.*, 2010). This minimal promoter is 421bp long, with weaker activity-dependent response in the presence of 4-AP and bicuculline(BIC) (Kawashima *et al.*, 2009).

4.3.2.3. E-ARE-miniArc (ESARE) promoter

In 2009, Kawashima. *et al* identified a potent element located approximately 7kb upstream of Arc TSS site, which are termed SARE (synaptic activity-responsive element). The unique 100bp

showed activity-dependent behaviours, containing binding sites for CREB, MEF2 and SRF transcriptional factors (Kawashima *et al.*, 2009). When SARE was used in combination with mini-Arc promoter, it was sufficient to recapitulate activity-dependent activation similar to endogenous *arc* gene (Kawashima *et al.*, 2009). The SARE is conserved in mouse and human, which means has comparable activity profile across the species. In 2013, the group reported an enhanced version of the synthetic promoter by arranging five enhancer motif SARE in tendon (Kawashima *et al.*, 2013). This new synthetic promoter (975bp), termed E-SARE (enhanced SARE) generated the most potent increase in reporter gene than other existing activity-dependent promoters. It enabled up to 800-fold increase of reporter in luciferase assay and it is highly sensitive to spontaneous activities (Kawashima *et al.*, 2013) (Figure 4.6).

This promoter was included for its exponential increase in activation and we asked the question whether high increase in protein expression of effector will generate stronger silencing effects on neurons.

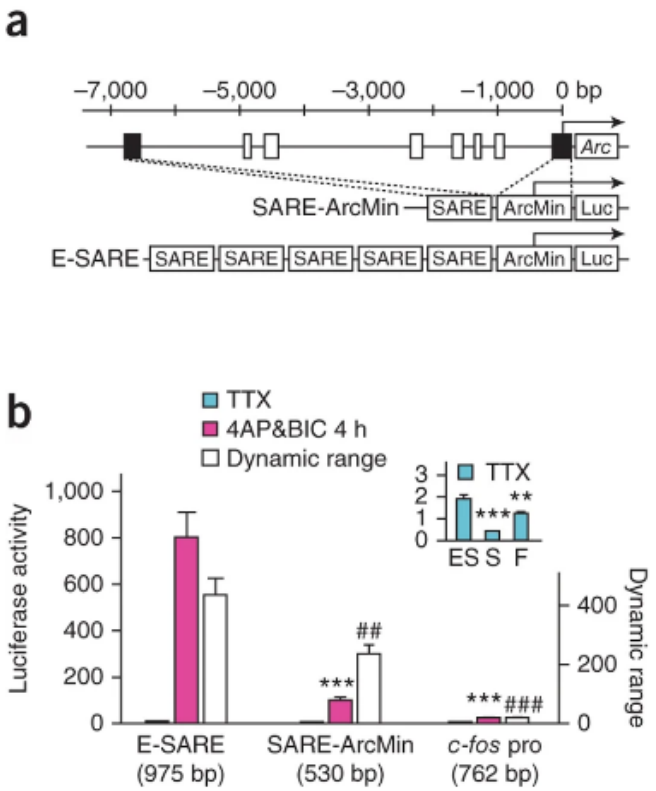

Figure 4.6. E-SARE promoter.(a) Illustration of the E-SARE construct with SARE components arranged in tandem. (b) The dynamic range of E-SARE, SARE-ArcMin and c-fos promoters measured by luciferase assay. (Image modified from Figure 1, , Kawashima *et al.*, 2013*)*

4.3.2.4. EGR1 promoter

The mouse promoter sequence of *egr1* gene was extracted from the Uniport database and previous publications (Tsai-Morris, Cao and Sukhatme, 1988; Varma and Voldman, 2015). Due to size limitation, we had to select a short sequence of 516bp, which contains multiple copies of SEF (SRE) sites, CRE sites and the core TATA box for transcriptional initiation (Tsai-Morris, Cao and Sukhatme, 1988; Tsai *et al.*, 2000; Varma and Voldman, 2015). We hypothesized that it may work similar to c-Fos but maybe in differential spatial resolutions or different regions of the brain.

4.3.2.5. N_{RAM} (Npas4) promoter

Npas4 attracted the interest of making synthetic promoter enhancers for activity-dependent labelling of active neurons. Sørensen. *et al*, 2016 identified conserved short motifs from c-FosP activity detection were identified with bioinformatics search, and used to build an enhancer package of RAM (robust activity marking) (Sørensen *et al.*, 2016). Similar type of conserved motif was also identified from Npas4, which was named NRE (Npa4 response element) to be the core binding site of the Npas4 promoter. This short 'TCGTG' sequence was inserted into a central midline element (CME) to form a transcription favourable secondary structure (Sørensen *et al.*, 2016; Sun *et al.*, 2020) (Figure 4.7). This N_{RAM} (Npas4 RAM) motif was organized into repeats followed by a minimal human c-Fos promoter to form a complete functional promoter(Sun *et al.*, 2020). This promoter was relatively new and less well characterized. In Sun. *et al*, 2020 where the function of N_{RAM} was tested, it showed differential activation pattern during memory process than c-FosP based RAM (Sun *et al.*, 2020) (Figure 4.7).

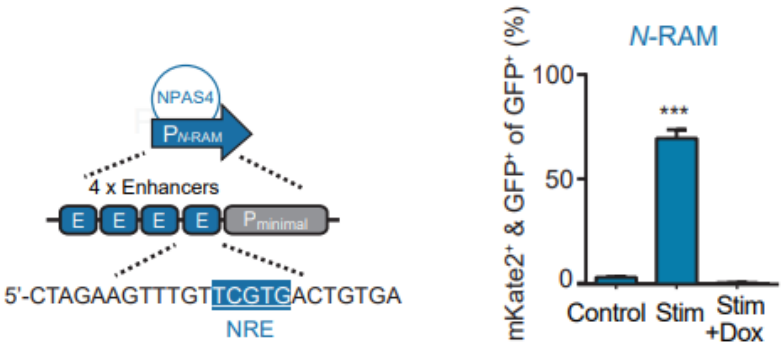

Figure 4.7. Illustration of N_{RAM} construct design. It contains four enhancer sequences arranged with a minimal c-fos promoter sequence. The expression profile of N-RAM after stimulation (Image modified from Figure S1, Sun *et al.*, 2020*).*

4.3.3. Effector genes: two different potassium channels

4.3.3.1. KCNA1 (Kv1.1 channel)

The main protein structure of Kv1.1 channel is encoded by the gene *KCNA1* (1488bp) whose length is suitable for AAV vector expression. The effector Kv1.1 channel was chosen as previous studies by our group showed prominent anti-seizure and anti-epileptic effects achieved by overexpressing the Kv1.1 channel encoded by *KCNA1* either under the control of the forebrain principal neuron specific *CAMKII* promoter or when the endogenous *Kcna1* gene is increased by CRISPR activation (Snowball *et al.*, 2019; Colasante *et al.*, 2020). We decided to use a human amino acid sequence for the purpose of clinical translation, but the nucleotide sequence was codon-optimized and contains a single amino acid mutation from isoleucine (I) to valine (V) at position 400 (Hoopengardner *et al.*, 2003; Decher *et al.*, 2010). This mutation mimics the effect of post-transcriptional editing of *KCNA1* by ADAR (Adenosine Deaminases Acting on RNA). Kv1.1^{I400V} channels have a 20-fold acceleration of recovery from inactivation with negative membrane potentials (Bhalla *et al.*, 2004; D'Adamo *et al.*, 2013). I400V edited Kv1.1 channels also have a reduced pharmacological sensitivity to the potassium channel blockers TEA (Tetraethylammonium) and 4AP (Decher *et al.*, 2010; Streit *et al.*, 2011). We refer to *KCNA1*co/I400V as *KCNA1* for simplicity in the following sections.

4.3.3.2. KCNJ2 (Kir2.1 channel)

In addition to Kv1.1 channel, we also would like to investigate another potassium channel with different cellular localization and kinetic properties downstream of IEG promoter. We performed a search of the literature for potential targets and decided to use the inward rectifying Kir2.1 potassium channel

(Kubo *et al.*, 2005). Kir2.1 is encoded by the *KCNJ2* gene (1284bp), which is located in chromosome 17q23 in the human genome (Kubo *et al.*, 1993; Leonoudakis *et al.*, 2004). Inward rectification describes a depolarisation-dependent decline in K^+ conductance at voltages more positive than the potassium reversal potential (e.g. for equal but opposite driving forces for K^+, the channel conducts larger inward currents than outward currents) (Hibino *et al.*, 2010).

4.3.4. Summary

The c-FosP-dsGFP, c-FosP-dsGFP-*KCNA1* and c-FosP-dsGFP-*KCNJ2* formed the basic framework for the other novel activity-dependent gene therapy vectors. These vectors were generated by replacing the c-FosP promoter with other IEG/synthetic activity-dependent promoters, but with no additional changes to downstream dsGFP and *KCNA1* or *KCNJ2* genes. The full overview of plasmids tested is illustrated in Figure 4.8.

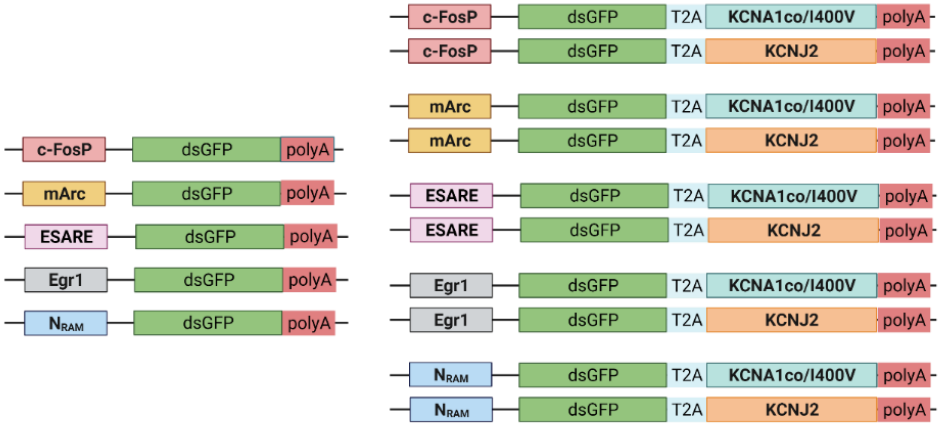

Figure 4.8. Illustration of IEG-Effector plasmids used in this project. The c-FosP, mArc, ESARE, Egr1 and N_{RAM}-dsGFP (left) are controls and the rest are either attached with an effector gene of KCNA1 or KCNJ2 (right). The same promoter is shown in the same colour.

4.4. c-FosP is activated by increasing network excitation *in vitro*

4.4.1. The endogenous c-Fos activation is an indicator of neuronal activity

To begin with, we wanted to verify the activity-dependent expressions of the c-Fos in an in vitro hyperactivity model. Mouse cortical primary neuronal cultures were treated with $GABA_A$ receptor blocker picrotoxin (PTX, 30 µM) and the potassium channel blocker 4-aminopyridine (4-AP, 100 µM) to increase overall neuronal activity. The level of c-Fos protein was measured with immunofluorescence at 2, 6, 24 and 48 hours of 4-AP/PTX incubation. We used saline-treated cultures as control, and then sampled at the same timepoints for comparison. The percentage of c-Fos positive cells was counted and expressed as a percentage of DAPI positive cells (Figure 4.9).

The results showed rapid elevation with number of c-Fos expressing cells after 2 hours of PTX/4ap treatments. This was then followed by slight drop in percentage at 6, 24hrs, however, the c-Fos level remained significantly higher than that of controls collected side-by-side ($p < 0.01$, $p < 0.01$, and $p = 0.02$, 2-way ANOVA, Bonferroni multiple-comparison test, respectively). By 48 hours after the initial drug application, the overall c-Fos level was close to baseline. This could have resulted from homeostatic compensation of the network. cFos in untreated cultures were relatively stable for the first three timepoints, but at 48 hours, showed an unexpected decrease, which could have resulted from poor image quality or neuronal loss due to culture ageing.

In summary, endogenous c-Fos expression increased sharply in response to a chemical stimulus to increase neuronal network activity *in vitro*.

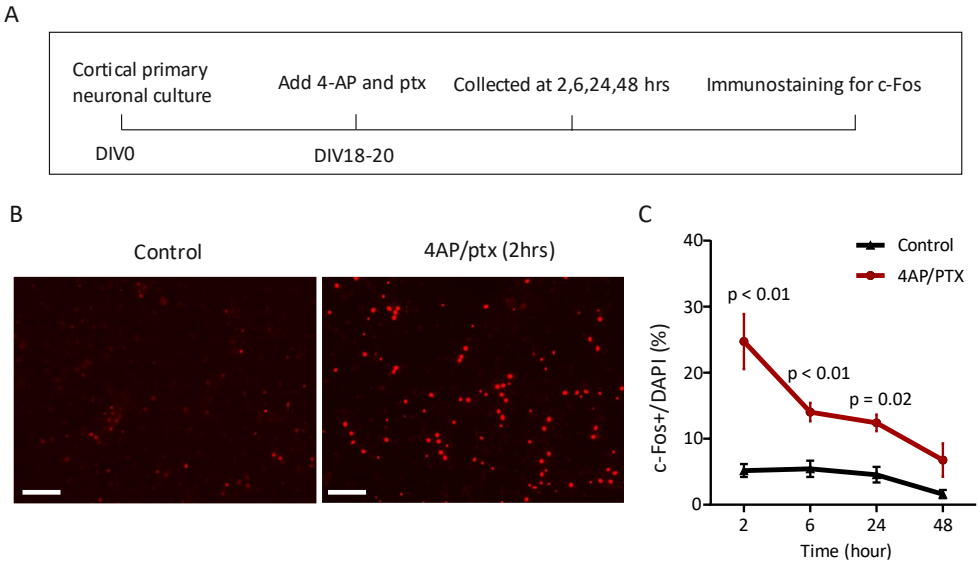

Figure 4.9. In vitro characterization of activity-dependent c-Fos (a) Example images of c-Fos staining (Red) of control and 2 hours post 4ap/ptx (scale bar = 100 µm). (b) Quantitative analysis of percentage of c-Fos positive neurons compared to DAPI positive cells at 2, 6, 24 and 48hours after the PTX/4AP treatments (n = 3, 9, 7, and 2 coverslips). Control groups refers to untreated cultures with saline (n = 5, 5, 6, and 3 coverslips). All statistics were 2-way ANOVA, Bonferroni multiple-comparison test.

4.4.2. Reporter expression from c-FosP-dsGFP reflected neuronal excitability

Having verified that endogenous cFos protein is upregulated in vitro following PTX/4-AP treatment, we wanted to understand whether c-FosP activation has comparable sensitivity to increased neuronal activity, and how well it can be detected by the fluorescent marker dsGFP. We synthesized AAV9 expressing a c-FosP-dsGFP construct, and transduced primary cortical neuronal cultures on DIV6.

At DIV15 30µM PTX was added to block GABAergic inhibition, leading to a global increase in network excitability. The neurons were subsequently assessed for dsGFP expression at 6, 24, and 48 hours. In parallel we monitored dsGFP expression in control cultures treated with PBS. For each coverslip, three ROIs (regions of interest) were taken at random and the average value of three ROIs was used for the data analysis. Representative images from control, 6hr, 24hr and 48 hr cultures are shown in Figure 4.10. At 24 hours after PTX treatment, there was a significant (1.6-fold) increase in fluorescence intensity, compared to baseline (Kruskal-Wallis test, p =

0.024). This suggests that an overall higher level of fluorescent marker was detectable with increased network activity. The fluorescence was also raised at 6 hours, although not significantly, and returned close to baseline 48 hours after PTX treatment, possibly as a result of homeostatic compensation(Pozzi *et al.*, 2013; Pecoraro-Bisogni *et al.*, 2018; Lignani, Baldelli and Marra, 2020).

Moreover, we analysed the proportion of cells (identified by DAPI staining) that were dsGFP-positive. We applied same criteria using particle count function in ImageJ for consistent analysis across coverslips. Consistent with the results from assessment of overall dsGFP fluorescence, there was a significant increase in the percentage of dsGFP positive cells both at 6 hours, with an increase from 5% in baseline to 22% ($p < 0.001$, Kruskal-Wallis test) and at 24hours, with 14% positive ($p = 0.008$). The percentage positive decreased by 48 hours to 10%, close to baseline.

The fluorescence analysis thus confirms that dsGFP under the control of c-FosP, delivered with an AAV, followed changes in network excitability.

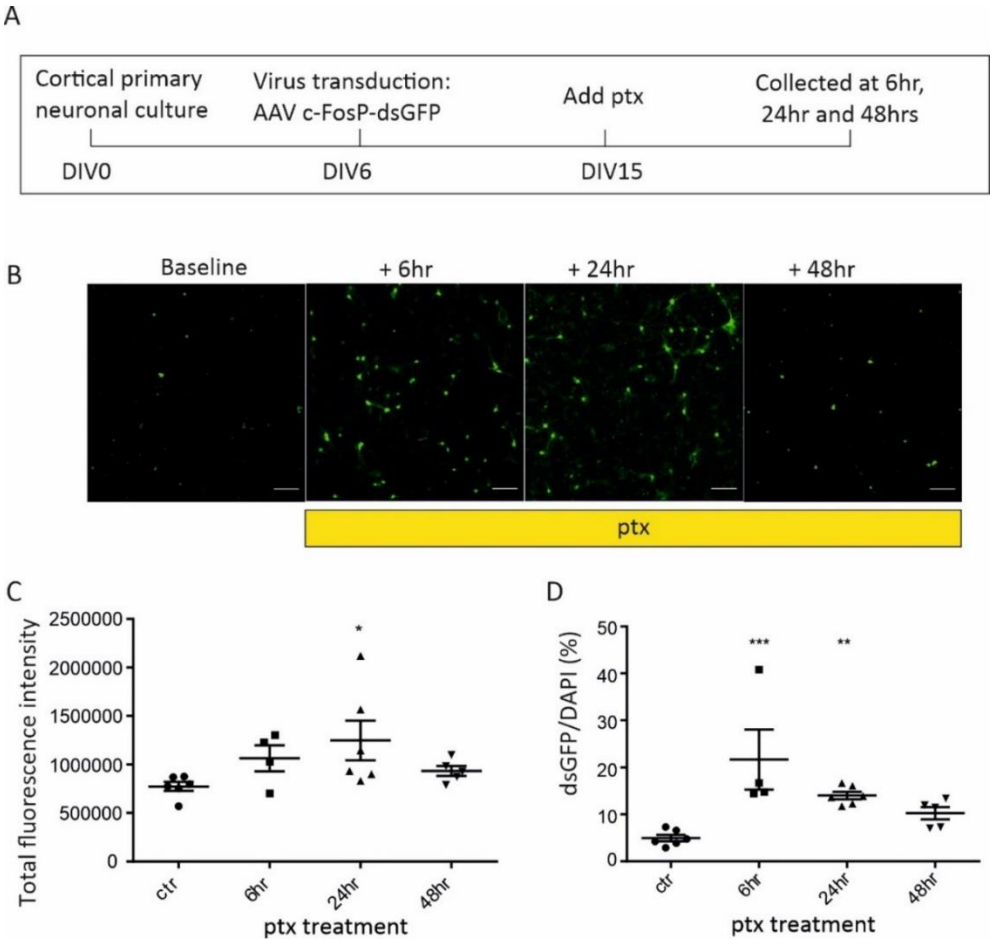

Figure 4.10. Immunofluorescence analysis of AAV c-FosP-dsGFP in primary cultures (n = 6 ctr, n = 4 at 6hr, n = 6 at 24hr, n = 4 at 48hrs, n represents coverslips). (A) Schematic illustration of experiment. (B) Example images of dsGFP fluorescence images taken before ptx treatments, at 6, 24 and 48 hours of the ptx incubation (scale bar = 100µm). (C) Total fluorescence intensity calculated from ImageJ. (D) Fluorescence-positive cells as proportion of DAPI stained nuclei numbers.

4.5. c-FosP-*KCNA1* expression decreases neuronal excitability

4.5.1. c-FosP-*KCNA1* reduced neuronal excitability

We next asked if c-FosP-*KCNA1* is able to alter neuronal firing properties. We used primary neuronal cultures from wild type mice, and transduced them with lentivirus carrying c-FosP-dsGFP or c-FosP-*KCNA1* vectors. Lentivirus was used in this experiment for high-efficiency transduction. It was also simpler to produce in-house at the time of the experiments. Because the fluorescence image analysis described above showed that baseline activity in neuronal cultures is able to drive some c-FosP activation, we designed a protocol that aimed to suppress neuronal firing. We therefore initially treated the neurons with 30µM picrotoxin for 30 minutes to activate c-FosP activity, followed by complete exchange with medium containing 1µM TTX (tetrodotoxin) and further incubation for 2 hours. This pre-treatment prevented activation of c-FosP outside the time window of PTX treatment. Because the TTX incubation lasted for 2 hours, all dsGFP expressed before the start of the protocol would be expected to have decayed prior to the acute experiments (Figure 4.11). We then washed out TTX thoroughly, and moved the coverslip to an upright microscope for current clamp recordings. This protocol ensured that all the fluorescent neurons we patched were activated during the 30 minute PTX incubation.

We selected dsGFP-positive neurons and held the RMP at -60mV. We then applied square current steps of 25pA up to 500pA, and measured the maximum number of action potentials (APs), comparing c-FosP-dsGFP with c-FosP-*KCNA1* transduced neurons. The results showed that c-FosP-dsGFP fired a maximum of 5.2 APs, while c-FosP-*KCNA1* fired significantly fewer APs: 1.67 ($p = 0.0087$, Mann-Whitney test) (Figure 4.11). This implies that neuronal excitability was robustly decreased by c-FosP-*KCNA1* expression.

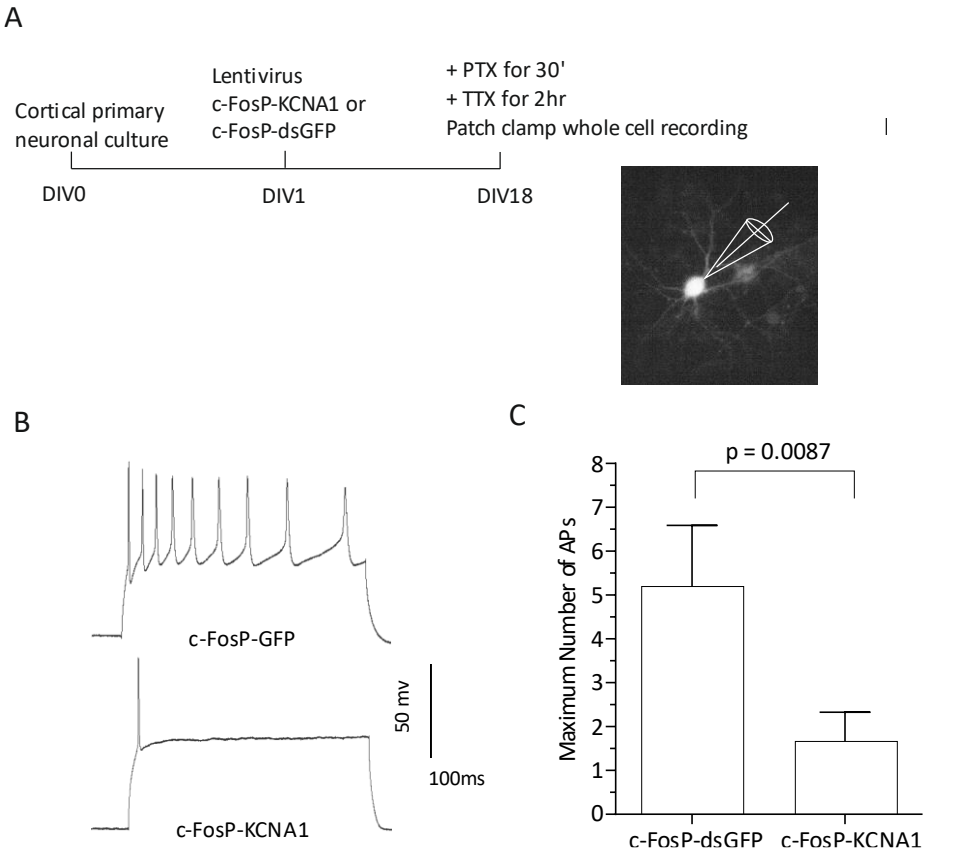

Figure 4.11 Patch clamp of cultured neurons transduced with either lentivirus c-FosP-dsGFP (n=5) or c-FosP-KCNA1 (n=6).(A) Illustration of a fluorescent positive neurons patched (B) Example traces of action potentials of principle neurons transduced with cfosP-dsGFP and cfosP-KCNA1. (C) Histogram of maximum number of action potentials fired.

4.5.2. Multi-electrode array (MEA) recordings from neuronal cultures *in vitro*

In the previous section, we showed that c-FosP-*KCNA1* led to a potent reduction in neuronal firing. We next asked if it was sufficient to reduce network activity with MEA recordings of high-density primary neuronal cultures (Ito *et al.*, 2010; Negri, Menon and Young-Pearse, 2020). Cultured high density neurons were capable of continuously generating global synchronous events which allowed long-term network activity levels (Wagenaar *et al.*, 2005). The neuronal cultures continued to generate epileptiform activity detectable late in maturation (Furshpan and Potter, 1989). This provided a perfect platform to test the effect of treatments on the same network before and after.

Each well of the MEA plate has an array of electrodes , enabling the recording of extracellular field potentials from a large population of neurons simultaneously (Buzsáki, Anastassiou and Koch, 2012) (Figure 4.12(A)). We chose to use a 6-well MEA layout from Multichannel Systems inc. (3x3 electrodes per well). Each well could be treated with different drugs or viruses (Figure 4.12(A)). Cortical neurons were grown on the chips. With time the neurites are evenly distributed and cover most of the recordable area, and somas are densely packed across the electrodes array (Figure 4.12(A)). The high connectivity facilitates the generation of synchronous spikes (Ito *et al.*, 2010). Such spikes are a prominent feature of cortical neurons, both *in vitro* and *in vivo* (Kenet *et al.*, 2003; Eytan and Marom, 2006). P0 cortical neurons were plated at a density of 90,000 – 100,000 cells per well, sufficient for synchronous spike recordings (Ito *et al.*, 2010).

MEA recordings provided a readout of network activity, and allowed the same neuronal population to be sampled repeatedly. We could therefore monitor the evolution of activity over time to assess the

effects of gene therapy (Eytan and Marom, 2006; Spira and Hai, 2013).

4.5.2.1. c-FosP-*KCNA1* expression in developing cortical neuronal cultures reduced network spiking frequency

Cortical neurons directly plated on MEAs were transduced with either AAV9 c-FosP-dsGFP or c-FosP-*KCNA1* between 6 and 8 DIV. Two weeks after the transduction (18-20DIV), spontaneous activity was recorded (Chiappalone *et al.*, 2006; Harrill *et al.*, 2015).

Representative traces from AAV9 c-FosP-*KCNA1* and AAV9 c-FosP-dsGFP transduced cultures are shown in Figure 4.12(B). Quantitative analysis of spike frequency showed that AAV9 c-FosP-*KCNA1* significantly reduced network excitability ($p = 0.02$, unpaired Student's t-test). A 58% decrease in spike frequency was seen, compared to AAV9 c-FosP-dsGFP treatment. This is consistent with spontaneous network activity during in vitro maturation activating the c-Fos promoter to drive *KCNA1* overexpression, resulting in an overall less active mature network.

We also observed that cortical cultures showed stereotypic patterns of spiking occurring in bursts(Cotterill *et al.*, 2016). We analysed the burst patterns of the recordings and applied stringent selection criteria to eliminate cultures with uneven firing patterns across the electrodes. Data were included only if at least 50% of the electrodes had burst patterns. The recording was dissected into 100 ms window and burst event was recognised when there are at least at least ten spikes per window(Bologna *et al.*, 2010). We found a significant reduction in burst frequency (burst/min) in cultures transduced with AAV9 c-FosP-*KCNA1* compared to AAV9 c-FosP-dsGFP ($p = 0.014$, unpaired Student's t-test) (Figure 4.12(D)). The number

of spikes per burst was also reduced in cultures transduced with AAV9 c-FosP-*KCNA1* compared to AAV9 c-FosP-dsGFP ($p = 0.035$, unpaired Student's t-test) (Figure 4.12(E)). This result suggests that c-FosP-*KCNA1* not only reduces the propensity for bursting but also causes bursts to contain fewer spikes. Although there was a small reduction in burst duration, this did not reach significance (Figure 4.12(E)). We also measured the time between bursts as inter-burst interval (IBI) (Figure 4.12(G)). This parameter increased moderately with c-FosP-*KCNA1* treatment, but not with the c-Fos-dsGFP ($p = 0.06$, unpaired Student's t-test).

These results, taken together, show that c-FosP-*KCNA1* reduces bursting activity, most simply explained as a result of Kv1.1 overexpression in c-Fos positive overactive neurons.

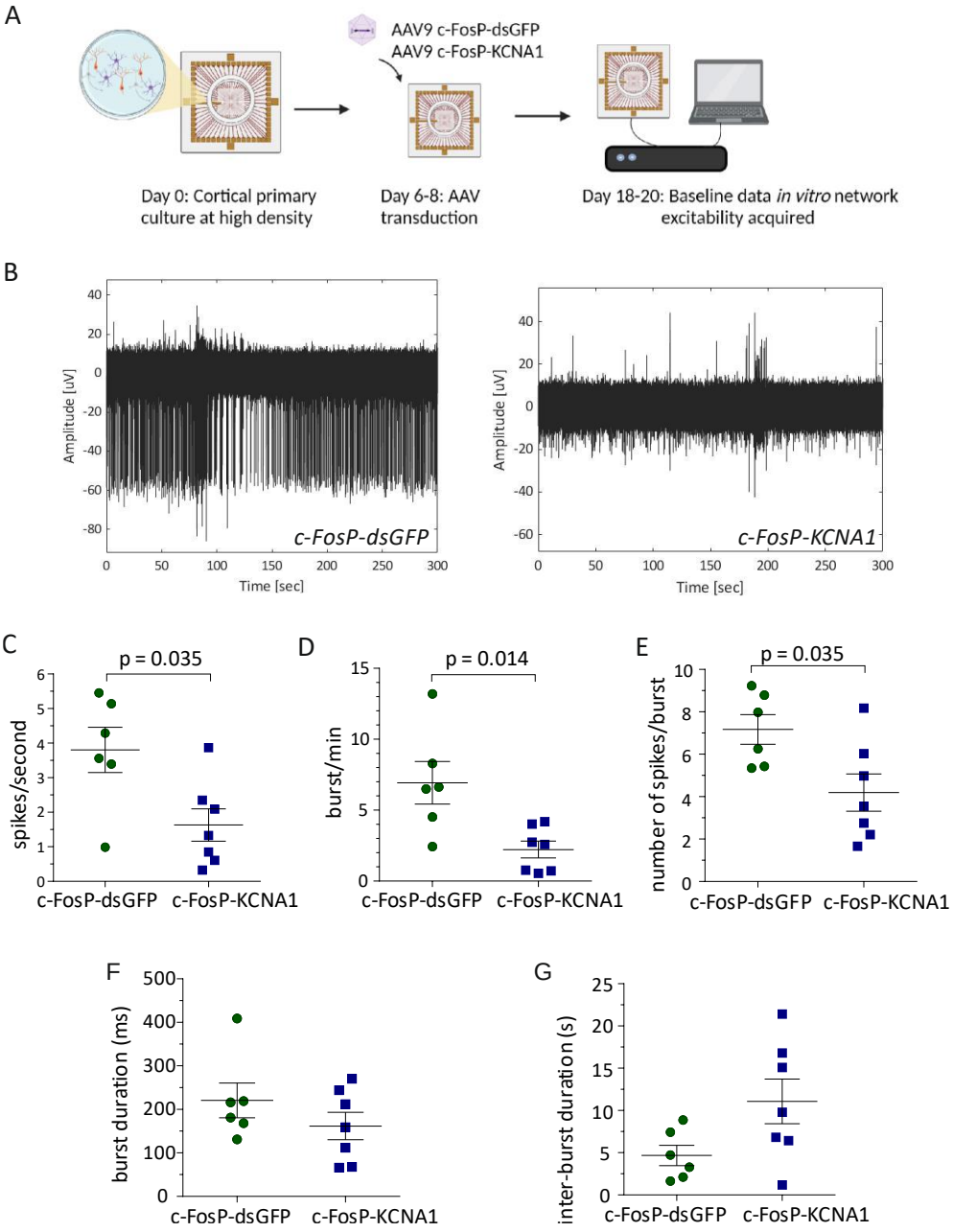

Figure 4.12 In vitro hyperexcitability model cortical neuronal network activities with c-FosP-dsGFP (n=6) or c-FosP-KCNA1 (n=7). (A) Experiment design is outlined on top. Cortical neurons were plated on the surface of MEA wells at a density of 90,000 – 100,000 cells/well. (B) Example of MEA recording of c-FosP-dsGFP and c-FosP-KCNA1 treated cultures. (C-G) Quantitative analysis of network excitability. Parameters including mean firing frequency (spikes/sec), mean burst frequency (burst/min), burst duration and the number of spikes per burst, burst intervals were analysed. (Mann-Whitney test).

4.5.2.2. Network disinhibition evokes an increase in spikes and burst events

In the previous section, we measured epileptiform activity from high-density primary cultures grown on MEAs. We wanted to investigate the effect of an acute increase in network excitability in cultures treated with either AAV9 c-FosP-dsGFP or AAV9 c-FosP-*KCNA1*. After obtaining a baseline measurement of activity, cultures were exposed to 100µM PTX, and then network activity was recorded again at 2, 6, 24 and 48 hours post-treatment (Figure 4.13). The time points were assigned based on our previous immunostaining results to correlate the changes in network activity level with the c-FosP activation profile.

Network disinhibition with PTX led to a rapid increase in activity in both AAV9 c-Fos-dsGFP and AAV9 c-Fos-*KCNA1* treated wells. At 2 hours, the spike frequency increased 1.7- and 1.4-fold from baseline in c-FosP-dsGFP and c-FosP-*KCNA1* treated cultures, respectively. The activity further increased at 6 hours post-PTX treatment. At 24 hours, the c-FosP-dsGFP group showed a >4.2-fold increase in activity relative to baseline, while the c-FosP-*KCNA1* excitability increase was blunted. The overall activity continued to decrease for the next 24 hours, and undershot the baseline by 48 hours (Figure 4.13(B)).

The burst frequency followed a similar trend, in that they experienced an initial increase for 2-6 hours, which then faded (Bateup *et al.*, 2013). The activity already started to decline at 24 hours. This temporal activity profile had a slightly different timecourse than previous c-Fos immunohistochemistry and dsGFP imaging results, which both showed a continued increase in network activity for at least 24 hours after drugs(Figure 4.13(C)). This could be explained by either the addition of the potassium blocker 4-AP in the previous experiments, which is

expected to further stimulate the network, or a temporal lag between network activity and protein expression. At 48 hours, both spike frequency and burst frequency were reduced below the baseline level. Among the parameters analysed, only burst duration changes were significantly different between AAV9 c-FosP-dsGFP and AAV9 c-FosP-*KCNA1* viruses (p=0.006, 2-way ANOVA followed by Bonferroni multiple comparison tests) (Figure 4.13(D)).

As the AAV9 c-FosP-dsGFP treated cultures experienced longer bursts as time passed, the AAV9 c-FosP-*KCNA1* treated cultures experienced only minor fluctuations in burst duration in the first 6 hours, followed by a dramatic decrease afterwards. This highlights the possibility that activity-dependent *KCNA1* overexpression reduced the propensity for repetitive firing. It is possible that further increases in network activity triggered more Kv1.1 channel expression.

In summary, disinhibition evoked increases in network excitability in both AAV9 c-FosP-dsGFP and AAV9 c-FosP-*KCNA1* expressing neurons. Both groups showed a wave of excitability increase followed by an apparent homeostatic compensation. In particular, AAV9 c-FosP-*KCNA1* treated cultures showed a significant decrease in burst duration with a prolonged increase in network activity.

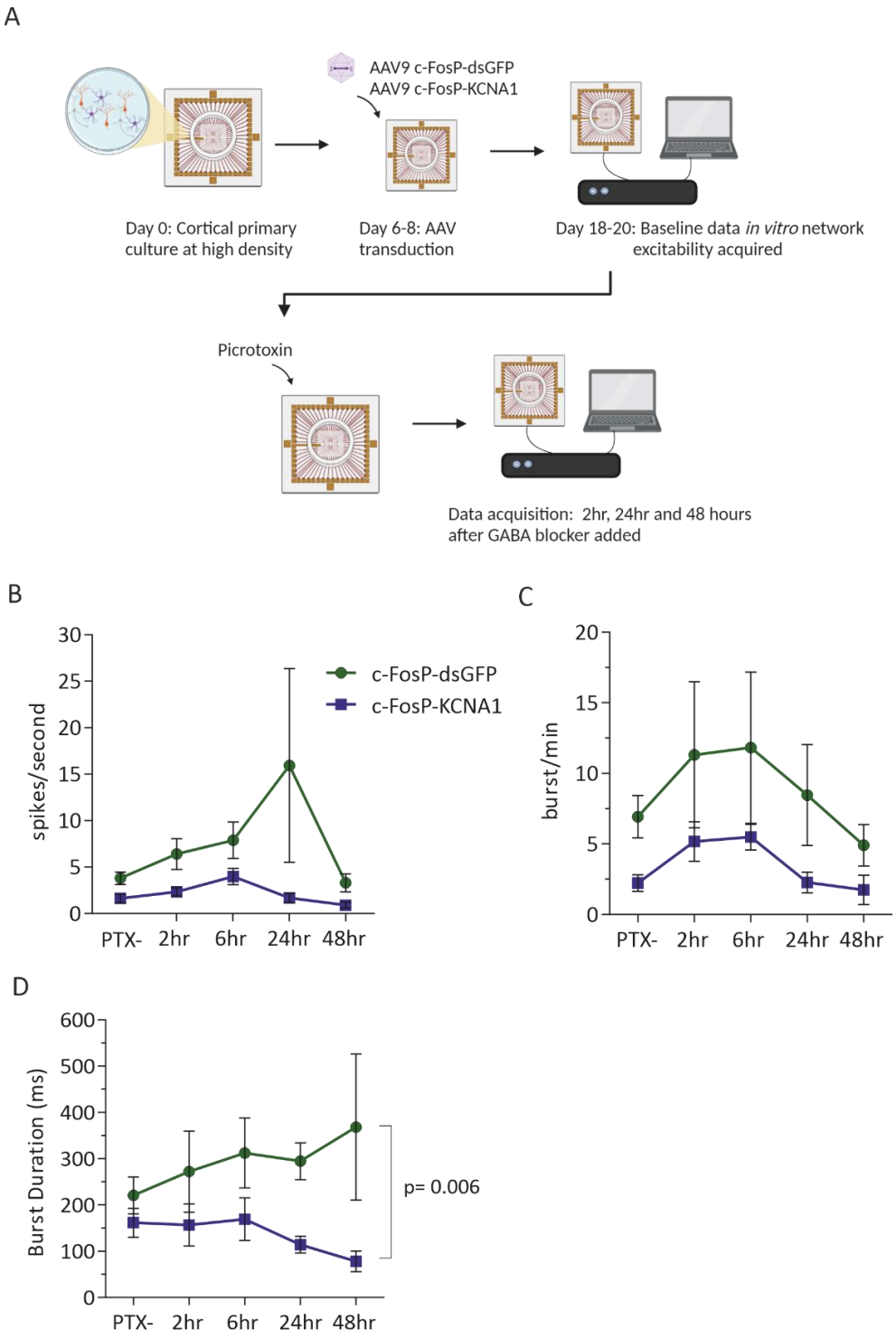

Figure 4.13 Network activity profile post-picrotoxin (PTX) treatment. (A) Experiment plan. Recordings were taken before PTX (30µM) treatment and subsequently at various time-points (2hr, 6hr, 24hr and 48hr) after PTX application. (B-D) Measurements of spike frequency, burst frequency and burst durations plotted against timepoints. The burst duration of the two groups was significantly different over the time course (p=0.0077, 2-Way ANOVA followed by Bonferroni multiple comparison test).

4.5.2.3. Controlled activation of c-FosP-CRISPRa-*KCNA1* expression reduced network hyperexcitability induced by a pro-convulsant

In the previous two experiments performed on MEAs, we observed significant differences between spontaneous activity in c-FosP-dsGFP and c-FosP-*KCNA1* treated cultures prior to the addition of PTX This suggests that spontaneous bursting during culture maturation may have activated c-FosP. To allow c-FosP-dsGFP and c-FosP-KCNA1 neurons to be compared from the same baseline we designed new viruses and experiments.

Based on previous work we published using CRISPRa to upregulate endogenous *Kcna1* gene expression (Chapter 3) (Colasante *et al.*, 2020), we designed a new dual-AAV strategy based on *Colasante & Qiu, 2020*. The expression constructs are illustrated in Figure 4.14. This CRISPRa based design incorporated a drug-inducible TetON system, so that the dCas9 protein is only expressed in the presence of doxycycline. In the absence of the drug, the TRE (tetracycline response element) alone is unable to induce downstream gene expression (Zhou *et al.*, 2006; Loew *et al.*, 2010). In the presence of doxycycline, rtTA (reverse tetracycline-controlled trans-activator), a protein created by fusing rTetR and VP16 together(Loew *et al.*, 2010), binds to TRE and induces downstream expression of dCas9 and VP64 on the second AAV (Gilbert *et al.*, 2014; Colasante *et al.*, 2020). The expression of rtTA was placed under the control of the activity-dependent c-Fos promoter. Therefore, only in the presence of doxycycline and with c-FosP activation, does c-FosP-CRISPRa-*Kcna1* upregulate endogenous *Kcna1* expression. In the control AAV, sg19 (which recognises a promoter region of *Kcna1*) was replaced with sgLacZ, which does not match any genomic site in mice, and therefore will not lead to a change in endogenous gene expression (Colasante *et al.*, 2020).

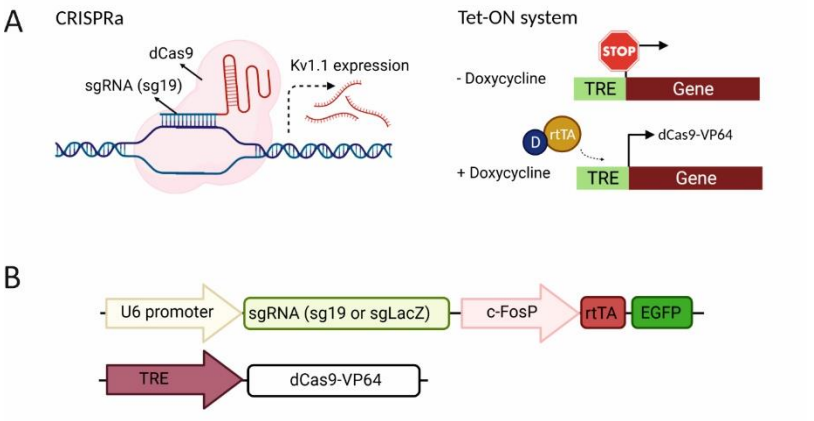

Figure 4.14 Illustrations of c-FosP-ctrl-CRISPRa and c-FosP-kcna1-CRISPRa constructs and mechanisms of endogenous gene overexpression. (A) Illustration of CRISPR-activation system. dCas9 protein and sgRNA form a complex which bound to DNA and initiates gene expression to produce Kv1.1 subunits. (B) Illustration of TetON system. (C) Illustration of expression constructs for c-FosP-kcna1-dCas9a and c-FosP-Ctrl-dCas9a. It represents a dual-AAV system with components distributed across two AAV9s.

The experiment timeline is shown in Figure 4.15(A). Primary cortical cultures were transduced with both sgRNA-c-FosP-rtTA-EGFP and TRE-dsCas9-VP64 at a ratio of 1:1 at 6-7DIV. The dual virus system will be referred to as c-FosP-ctrl-CRISPRa and c-FosP-kcna1-CRISPRa for simplicity.

We recorded baseline activity at 14DIV in the absence of doxycycline (Chiappalone *et al.*, 2006). At this stage in development, dissociated neurons exhibited stable and sustained burst pattens, owing to the formation of synaptic connections (Chiappalone *et al.*, 2006). At 14DIV, the cortical cultures showed persistent spontaneous spikes and some burst events, with no significant differences between the two viral treated groups. We then incubated the cultures in doxycycline for four days to switch on the TetON system for dCas9 expression in a cFosP-dependent manner. Spontaneous activity in both groups of transduced cultures continued to increase with maturation.

MEA cultures were treated with 100µM PTX to disinhibit the network at 18DIV. At 2, 6, 24 and 48 hours after PTX treatment, spontaneous activity was recorded from each well. Recordings taken at various timepoints were analysed for spiking and burst events, and normalised to the pre-doxy recording. c-FosP-ctrl-CRISPRa cultures continued to experienced increase in spike frequencies for 24 hours after PTX treatments, up to 3.5 folds of basal firings. With c-FosP-kcna1-CRISPRa viruses, the cultures showed minor fluctuations in spontaneous firings with loss of GABAergic inhibition (Figure 4.15B). In particular, significant changes in spike frequency were observed at 6 and 24 hours post-PTX ($p = 0.05$ (6h), $p = 0.04$ (24hr), 2-way ANOVA, Bonferroni multiple comparison test). The bursts were shown to increase for the first 6 hours, followed by reduction at 24 and 48 hours with both virus treatments. The c-FosP-ctrl-CRISPRa virus treated cultures changed bursts dramatically from 3.2 to 7.1 over the first 6 hours of picrotoxin, the c-FosP-kcna1-CRISPRa increased less, from 2.1 to 4.0 (Figure 4.15C). At 48 hours, the burst rate were returned to pre-PTX values with both virus treatments.

Furthermore, those were endogenous gene manipulations, which the changes in protein level were restrained by transcriptional and translational controls, and therefore the protein changes were speculated to be lower than exogenous overexpression.

This experiment with controlled KCNA1 overexpression in mature dissociated cortical cultures showed that transient activation of c-Fos inducible Kv1.1 channel overexpression were sufficient to increase network resistance to hyperexcitability.

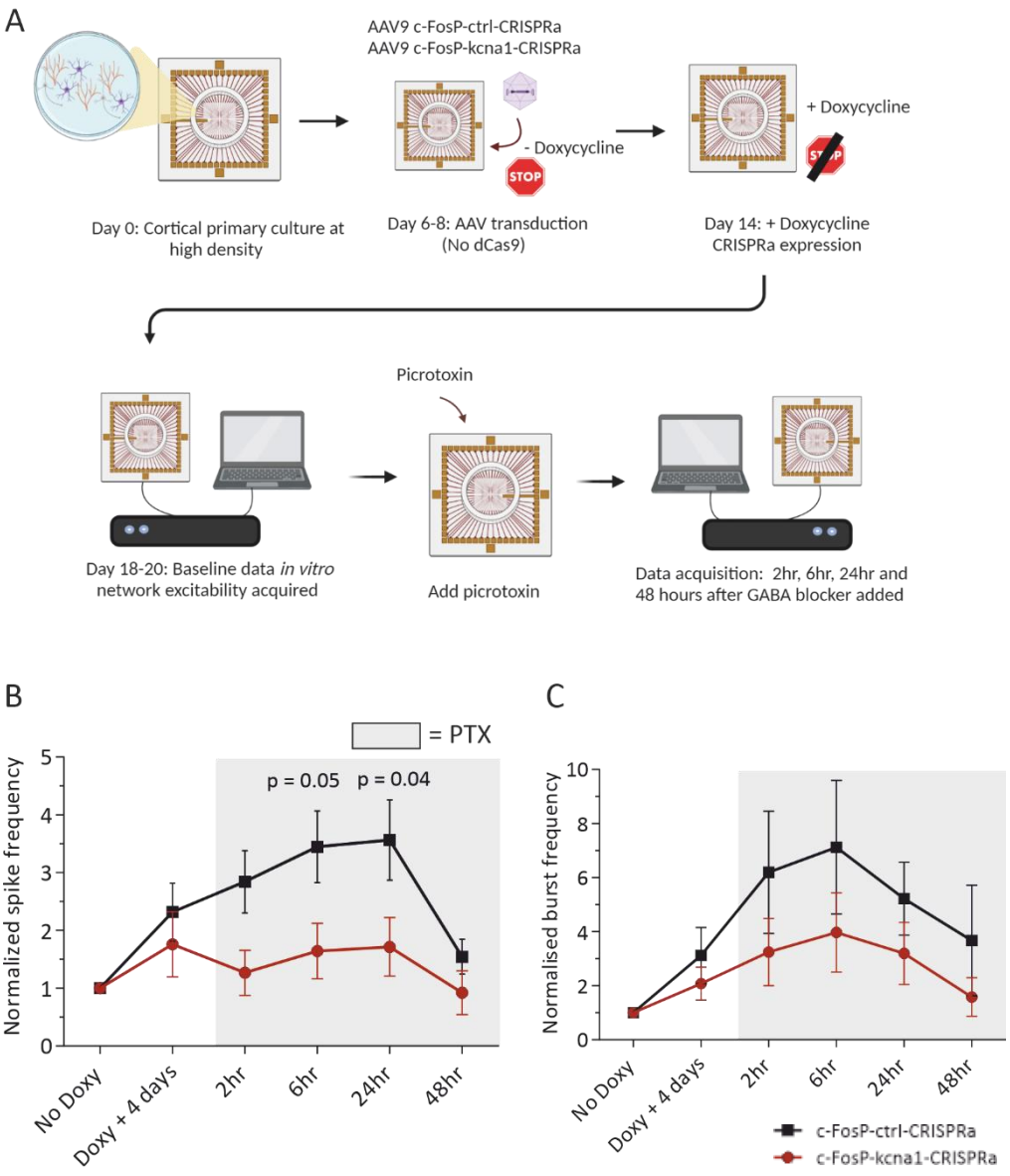

Figure 4.15 MEA recordings of cortical neuronal cultures treated with c-FosP-ctrl-CRISPRa and c-FosP-kcna1-CRISPRa. (A) Experiment outline. 18-20DIV, cultures were incubated with ptx for up to 48 hours. c-FosP-ctrl-CRISPRa n=17; c-FosP-kcna1-CRISPRa n=14. (B,C) Normalized spontaneous activities before and after ptx (30μM) treatments. All datapoints were normalised to corresponding pre-doxycycline conditions.

4.5.2.4. Network excitability measured with alternative IEG promoter-effector combinations

So far, we have demonstrated that c-FosP-KCNA1 reduces network excitability in an activity-dependent manner. The MEA protocol is an efficient method to quantitatively evaluate the network effect of the treatment. Next, we asked the question if alternative inducible promoters with similar properties to c-Fos would recapitulate similar effect on network excitation. The experiments and data acquisition were performed by Dr Nathanael O'Neill.

In addition to cFos-KCNA1 combination, we screened for other promoter-effector gene combinations in MEA assay, with same protocol as described in 4.5.2.1.

We selected mArc, ESARE, Nram, and Egr1 inducible KCNA1 or KCNJ2 transgenes as described in section 4.3. We then applied same protocol as in 4.5.1 and measured the network activities on 18-20DIV. In the sections below, we will discuss and compare them. Due to limited resource and time, we did not successfully produce dsGFP control viruses for all promoters tested, we therefore combined the data from c-FosP-dsGFP and mArc-dsGFP, and used them as control (IEG-dsGFP). All the data are presented are normalised to IEG-dsGFP virus transduced MEAs.

4.5.2.4.1. *KCNA1*

With promising results observed c-FosP-*KCNA1* virus transduced cells, we first investigated other promoter combinations with *KCNA1*. Among the mArc, ESARE, N_{RAM} and Egr1 promoters, only mArc-*KCNA1* showed a significant reduction in burst frequency in comparison to the IEG-dsGFP transduced cells. Other *KCNA1* combinations did not lead to a significant reduction in spike or burst frequency (one sample test vs 1.).

Nevertheless, there was a trend for ESARE-*KCNA1* to reduce spiking, with a mean decrease comparable to that seen with c-FosP, but one data point made the effect non-significant (Figure 4.16). N_{RAM} and Egr1 did not show such a trend. None of the new promoter combinations showed significant change in number of spikes per burst.

4.5.2.4.2. *KCNJ2*

The second effector gene we choose to test was *KCNJ2*, which encodes the Kir2.1 channel. This channel mediates a potassium flux across the membrane near the RMP. It thereby drives the RMP towards the potassium reversal potential(Hibino *et al.*, 2010). Interestingly, Kir2.1 channel expression increases after intrahippocampal kainic acid injection, as a possible adaptive mechanism to counteract hyperexcitability (Young *et al.*, 2009).

We applied the same protocol with IEG promoter-*KCNJ2* viruses on neuronal cultures and measured spontaneous activity. We first investigated the effect of c-FosP-*KCNJ2* virus transduction on network excitability and compared the results to IEG-dsGFP control viruses. Surprisingly, we observed no significant difference from IEG-dsGFP transduced cells with spike frequency or burst frequency (Figure 4.16). This could be lack of functional effect of the KCNJ2 overexpression or issues with Kir2.1 channel expression. Subsequent experiments with mArc, ESARE, N_{RAM} promoters did not show significant decrease in network spiking properties either. Interestingly, the mArc-*KCNJ2* showed significant

shorter burst duration (one sample test vs 1) (Figure4.16). This is similar to what was observed with c-FosP-*KCNA1,* suggesting this could be an interesting candidate for next part of the study *(*Figure 4.13*)*. Unfortunately, we did not successfully produce Egr1-KCNJ2 AAV, so it was not tested here. The virus packaging process failed due to unknown causes.

Overall, *KCNJ2* seems a less promising effector transgene to use with an activity-dependent promoter, and c-FosP, mArc and possibly ESARE seem more effective at achieving a reduction in activity than N_{RAM} or Egr1. In those experiment, we did not check for specific protein expression changes, but we confirmed the expression of virus using fluorescent marker.

In summary, this cohort of MEA studies showed that among the candidate promoter and transgene combinations tested, c-FosP-KCNA1 produced most prominent candidate for modulating network activity, it is chosen as the main focus of the subsequent experiments and *in vivo* characterizations.

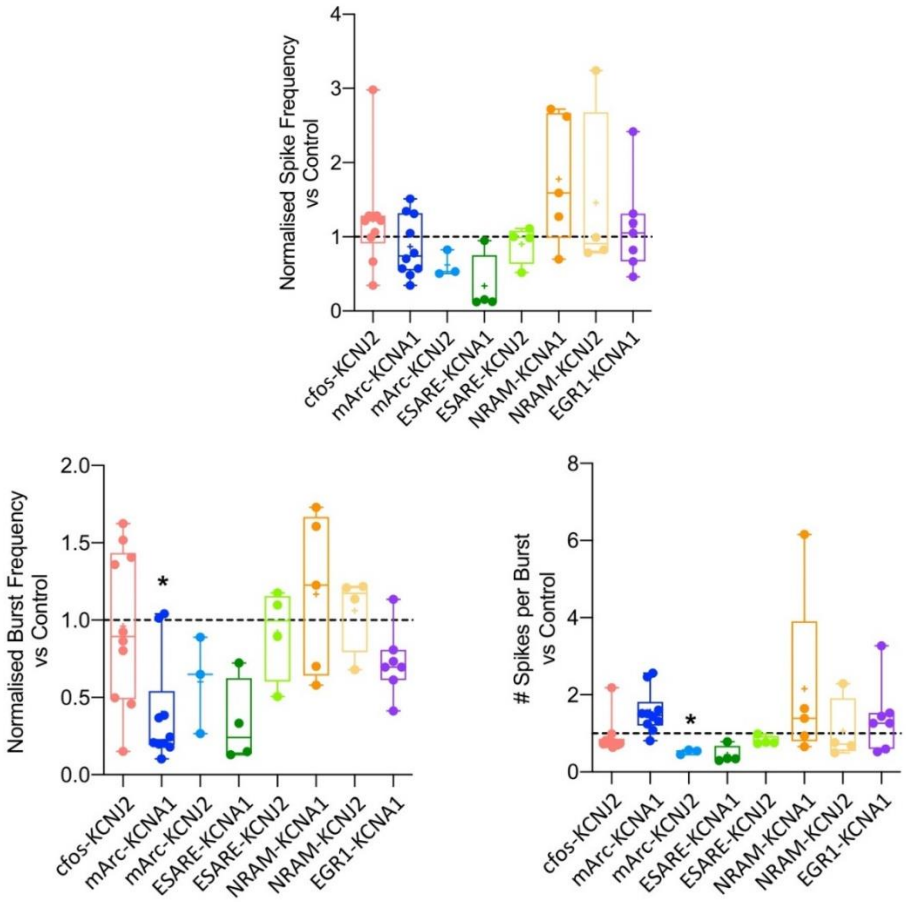

Figure 4.16. Normalised firing frequency parameters of the remaining IEG-effector combinations (A) spike frequency (B) burst frequency (C) Number of spikes per burst of IEG promoter-Effector viruses. All spike frequency was normalised to c-FosP-dsGFP as shown in Figure 4.7. All analysis was conducted with 1 sample test vs 1, corrected for multiple comparisons, $p < 0.006$*

4.6. Acute seizures induce c-FosP activation in rodent visual cortex

We have shown that upregulated expression of *KCNA1* induced by increasing neuronal activity *in vitro* reduces overall network excitability.

We then wanted to investigate whether the c-Fos promoter could be induced by seizures *in vivo*. We compared the AAV c-FosP-dsGFP virus with an AAV CaMKII-dsGFP virus. The CaMKII promoter is constitutively active in excitatory principal cells in vivo, therefore, we used it as positive control. We injected the same dose of either AAV c-FosP-dsGFP or AAV CaMKII-dsGFP (1.5µl, 10^{12} vg/ml) in the mouse primary visual cortex (V1, layer 2/3). We injected two mice with each virus, and allowed two weeks for AAV to express. Of the two mice injected with the same virus at identical coordinates, one was injected with saline, and the one was injected with pilocarpine (3.5M) injection via an implanted cannula to elicit single focal seizure. This cholinergic muscarinic agonist induced a single focal cortical seizure which started within 5 minutes of injection and lasted for 45-60 minutes (Kätzel *et al.*, 2014). We hypothesized that c-FosP would be activated by the seizure. The mice were sacrificed 2 hours after the pilocarpine injection and fixed for imaging (Figure 4.17(A)).

We prepared 50µm PFA-perfused sections across the V1 region, and obtained images for dsGFP expression in saline and pilocarpine injected brains (n = 1). In c-FosP-dsGFP virus injected mice, there was no detectable fluorescence expression following saline, while there was positive expression of dsGFP following pilocarpine(Figure 4.17(E)). As expected, the constitutive promoter CaMKII led to expression in the non-seizure brain infused with only saline, and clearly labelled cells with morphology typical of excitatory neurons (Figure 4.17(D)). It was also interesting that CamKII-dsGFP demonstrated widespread expression across cortical regions, while c-FosP-dsGFP expression was less strong even after pilocarpine (Figure 4.17(B,C)). However the small sample size makes it difficult to draw strong conclusions regarding the relative strengths of the promoters.

These results argue that the c-FosP promoter is activated by a focal seizure in the visual cortex and that it is not activated in physiological conditions. It is more advantageous than constitutive promoter which is constantly overexpressing the downstream gene.

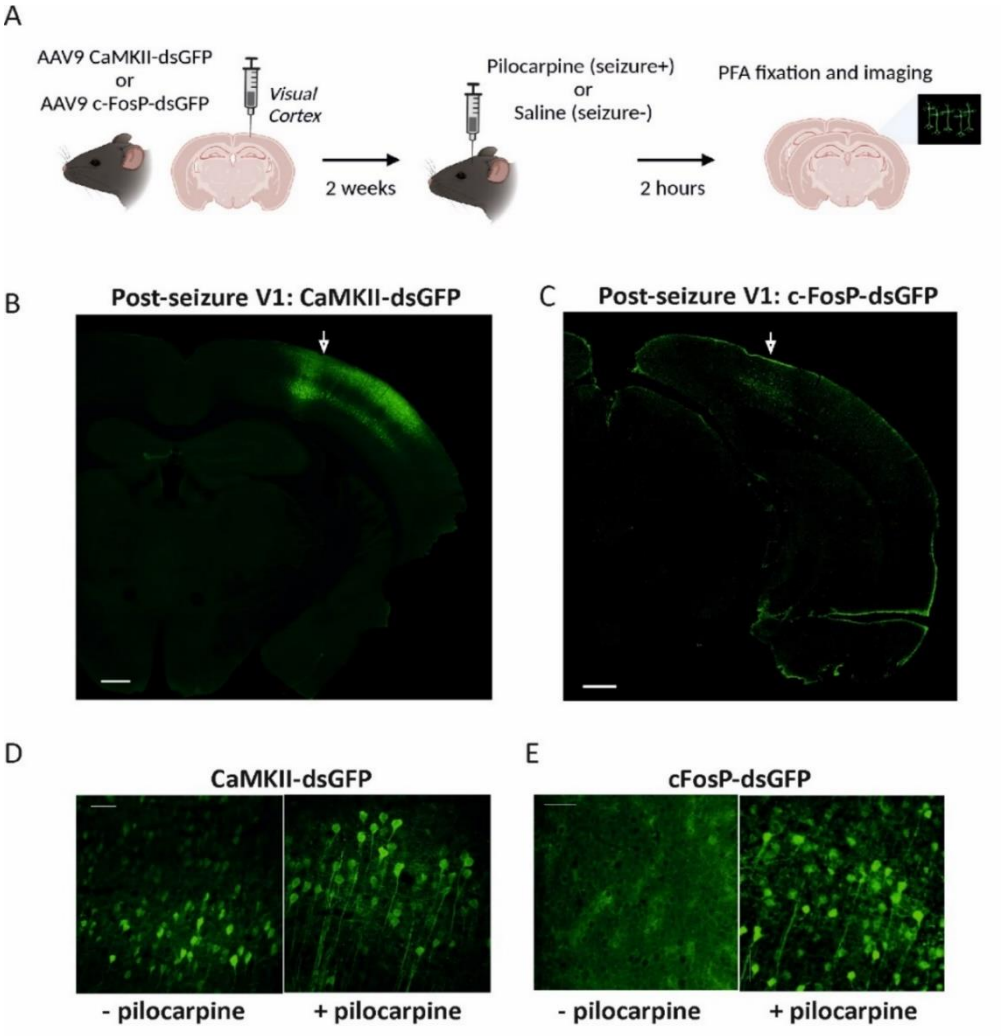

Figure 4.17. CaMKII-dsGFP and c-FosP-dsGFP in acute pilocarpine seizure model (overview Scale bar = 500µm; focused = 50 µm). (A) Experiment design (B)-(C) Immunofluorescence overview of post-seizure brain coronal section. (D)-(E). Zoom in images of injection site non-seizure and seizure.

4.7. Acute *ex vivo* slice electrophysiology immediately post-seizure attack in mice

The comparisons between the constitutive CaMKII promoter and inducible c-FosP activation in control and post-seizure brains argue that, under basal (physiological) conditions, c-FosP is driving KCNA1 overexpression at detectable level. Therefore, we designed a protocol with high-dose pentylenetetrazol (PTZ) injection to induce a single generalized seizure which will activate the IEG promoter and induce downstream effector expression. This part of electrophysiology experiment was carried out in collaboration with Dr Nathanael O'Neill.

We first tested this protocol with c-FosP-*KCNA1* and c-FosP-*KCNJ2* viruses in mouse. Either AAV9 c-FosP-*KCNA1* (3 mice) or AAV9 c-FosP-*KCNJ2* (1 mouse) was injected unilaterally in the ventral hippocampus (AP: 2/3 bregma-lambda, MD: +3, DV: 2.5/3/3.5). The stereotaxic virus injections were followed by a two week recovery period (Figure 4.18(A)). For control virus c-FosP-dsGFP, we injected 3 mice with the same protocol.

After that, mice were administered a single high dose of PTZ (55mg/kg) intraperitoneally to induce a single generalized seizure and, in turn, activate IEG and transgene expression. Mice were then observed for two hours before they were culled. Brains were extracted and prepared as detailed in the methods section for acute patch-clamp electrophysiology recordings (Figure 4.18(A)). Viral injection, PTZ administration and confocal imaging were performed by me; the *ex vivo* electrophysiology was performed by Dr Nathanael O'Neill who has also kindly permitted the use of data in this section.

For patch-clamp recordings, we recorded the input-output relationship of dsGFP-positive CA1 pyramidal cells. Recordings were performed in the current-clamp recording configuration, and the input-output relationship was obtained by injecting square-wave current pulses (25pA steps, 500ms; 0 – 525pA) from a holding membrane potential of -60mV (Figure 4.18(B)). The Input-Output curves were plotted for c-FosP-dsGFP, *KCNA1* and *KCNJ2* overexpressing neurons (Figure 4.18(C)). It was clear that c-FosP-*KCNA1*

transduced pyramidal neurons were less excitable than neurons expressing c-FosP-dsGFP (p = 0.003, 2-way ANOVA with Bonferroni's multiple comparisons test). In particular, all neurons patched in the c-FosP-*KCNA1* viral group only fired a single action potential, demonstrating an almost complete silencing effect (Figure 4.18(D)). This result was in a good agreement with previous patch experiments performed on cultured neurons *in vitro* (Figure 4.11). In contrast, c-FosP-*KCNJ2* showed minimal effect on input-output relationship: neurons fired similar number action potentials in response to the current steps as the c-FosP-dsGFP control virus (p = 0.399, 2-way ANOVA with Bonferroni's multiple comparisons test). In fact, c-FosP-*KCNJ2* showed slightly greater excitability than c-FosP-dsGFP (Figure 4.18(D)).

The resting membrane potential of c-FosP-*KCNA1* was similar to that of c-FosP-dsGFP neurons. In contrast, c-FosP-*KCNJ2* showed a markedly hyperpolarised RMP compared to c-FosP-dsGFP expressing neurons (-74.7±0.685(SEM), 57.5±0.2.79(SEM) respectively) (p = 0.0032, 1-way ANOVA with Bonferroni's multiple comparisons test) (Figure 4.18(E)). This observation is consistent with the inward rectifier role of Kir2.1 channels. Kir2.1 overexpression acts to drive the RMP more negative by increasing the permeability to potassium (Hibino *et al.*, 2010). There was no significant difference in RMP between c-FosP-*KCNA1* and c-FosP-dsGFP expressing neurons (p= 0.321, ordinary 1-way ANOVA with Bonferroni's multiple comparisons test).

The threshold current for c-FosP-*KCNA1* expressing neurons was greater than for c-FosP-dsGFP (p = 0.0078, 1-way ANOVA with Bonferroni's multiple comparisons test). This indicates that it was more difficult to induce APs in c-FosP-*KCNA1* neurons. When the threshold current was added to holding current required to bring neurons to -60mV, the difference between c-FosP-*KCNA1* and c-FosP-dsGFP became non-significant. This was partially due to the fact that more current was required in holding c-FosP-*KCNJ2* neurons near -60mV (Figure 4.18(D,E)).

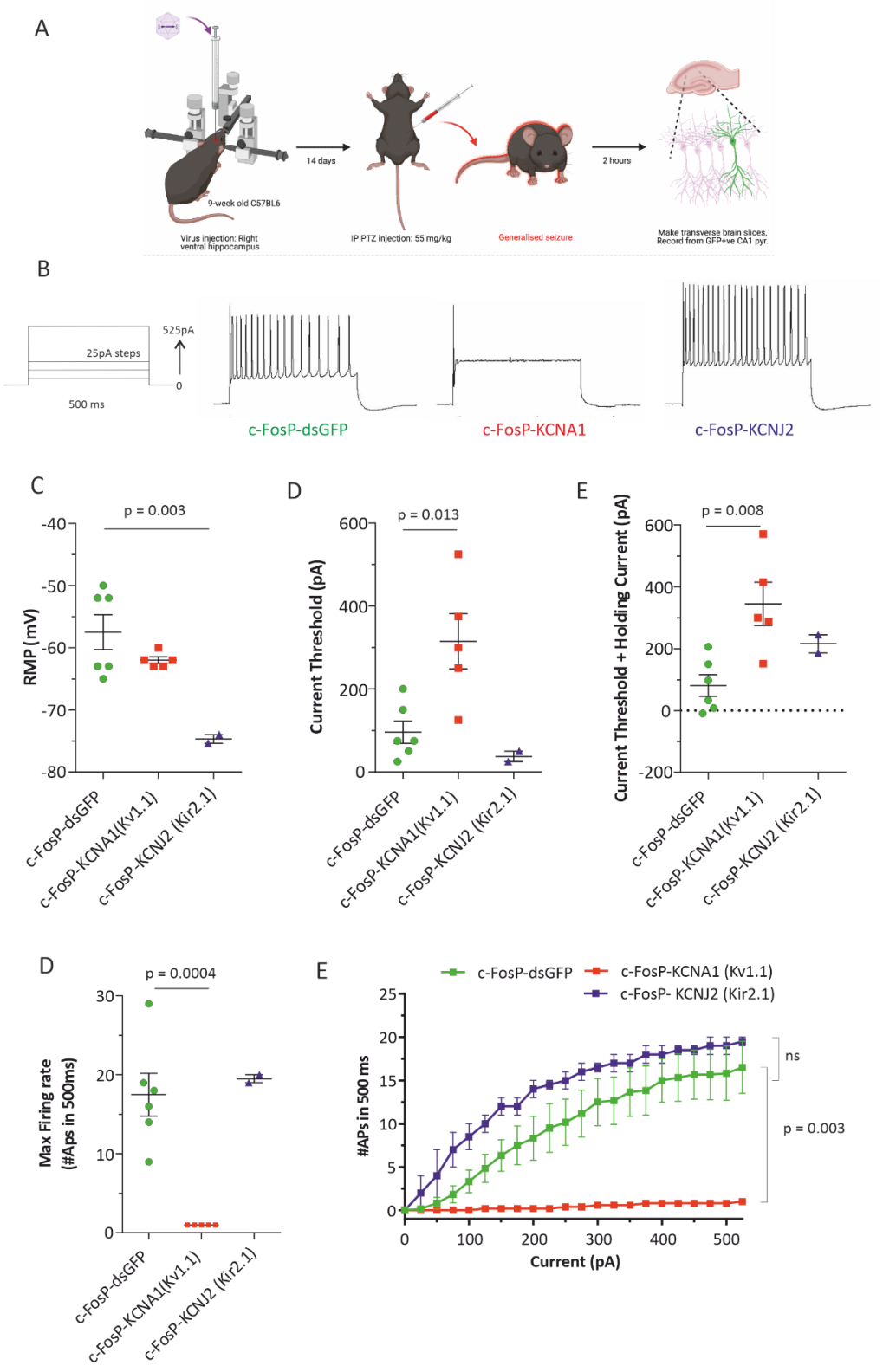

Figure 4.18. Ex vivo electrophysiological characterization of c-fosp-dsgfp, c-fosp-kcna1 and c-fosp-kcnj2 viruses in mice hippocampal ca1 pyramidal neurons. (n=6 c-fosp-dsgfp, n = 5 c-fosp-kcna1, n=2, c-fosp-kcnj2, n represents cell numbers) (a) illustration of the experiment protocol with ptz injection to trigger a single seizure. (b) current step protocol and representative traces recorded from viral expressing neurons. (c)-(d) plots for rmp, current threshold, threshold current with holding current, and maximal firing rate with 525pa step. (e) the input-output curve plotted for viral expressing neurons.

After the patch clamp experiments performed with c-FosP-KCNA1 and c-FosP-KCNJ2 viruses, we decided to explore mArc, ESARE, and Egr1 promoters, each combined with either KCNA1 or KCNJ2 genes. We also prepared an additional control virus: mArc-dsGFP. All *KCNA1* overexpressing neurons were markedly less excitable than neurons expressing the two dsGFP control viruses. mArc-*KCNA1* positive neurons showed a moderate decrease in firing propensity; however, ESARE-*KCNA1*, c-FosP-*KCNA1*, EGR1-*KCNA1* and N_{RAM}-*KCNA1* all showed a near-complete silencing effect, typically firing only one or two action potentials in response to maximal depolarising currents (Figure 4.19(C)). The resting membrane potential (RMP) showed no significant changes when compared to cFos-dsGFP. Different IEG promoters may have differential expression profiles, dynamic range and cell specificity; further investigations of expression profile of each promoter are needed. Nevertheless, the effect of *KCNA1* overexpression was clearly illustrated by this data.

With *KCNJ2* expressing viruses, we selectively patched mArc-*KCNJ2* and ESARE-*KCNJ2* (Figure 4.19(B)). Both showed minimal effects on neuronal excitability. mArc-*KCNJ2* may have a slight effect on reducing firing propensity, but it was not comparable to what was obtained from *KCNA1* overexpressing neurons. The RMP of mArc-*KCNJ2* was similar to what was obtained from mArc-dsGFP neurons. Only ESARE-*KCNJ2* viruses showed even more negative RMP in the neurons.

In conclusion, these experiments showed a clear effect of IEG-driven *KCNA1* overexpression in CA1 pyramidal. *KCNJ2* overexpressing neurons showed a hyperpolarized RMP but had little impact on the I-O relationship obtained from a holding potential of -60 mV. Future electrophysiological experiments should also be performed on mice that were not administered PTZ in order to further verify the activity-dependent properties and evaluate background expression of $N_{RAM,}$ EGR1, ESARE and mArc to evaluate the leakiness of the system in the non-seizure brains.

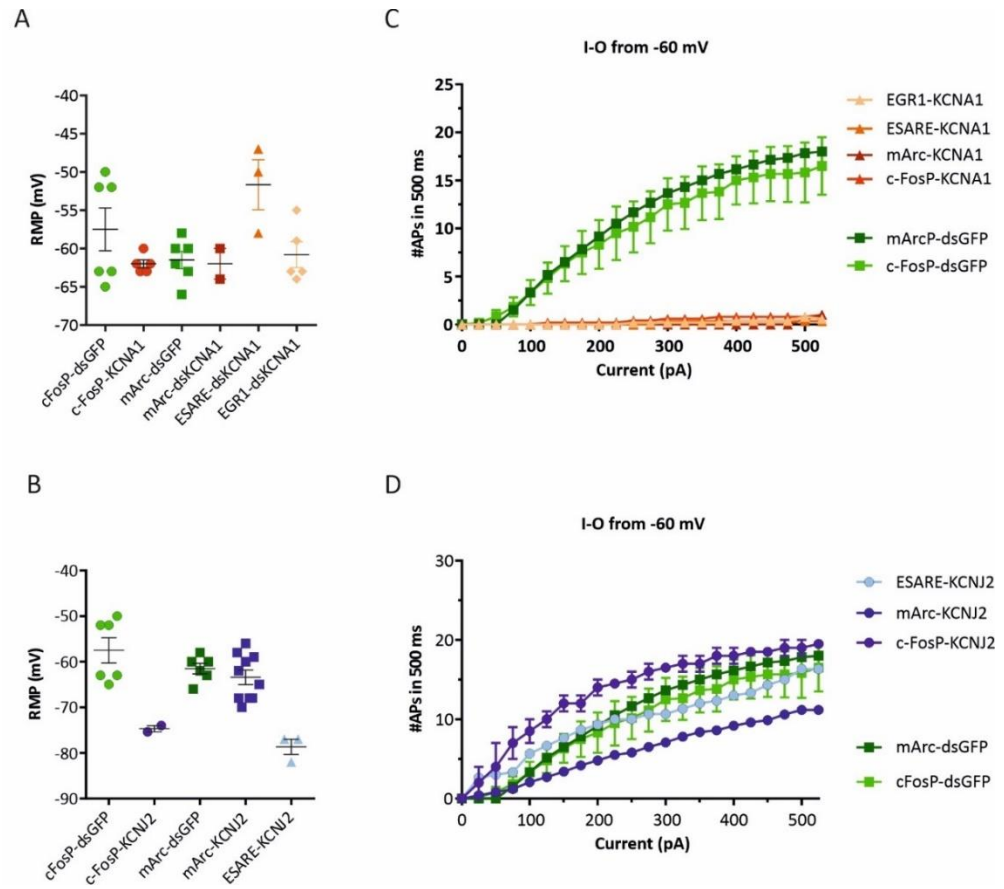

Figure 4.19 Ex vivo electrophysiological characterizations with effector genes driven by mArc, ESARE and Egr1 promoters. (A) RMP for KCNA1 overexpressing pyramidal cells with IEG promoters. (B) RMP KCNJ2 overexpressing pyramidal cells with IEG promoters (C) Input-Output (I/O) recorded for KCNA1 overexpressing neurons, from holding potential of -60mV. promoters (D) Input-Output (I/O) recorded for KCNJ2 overexpressing neurons, from holding potential of -60mV.

4.8. Cell-specific activation of c-FosP induced by seizures

As c-FosP-*KCNA1* does not use a cell-type specific promoter, it was important to understand the cell target specificity of the therapy. Because pyramidal neurons are the main source of synaptic excitation, we asked if activity-dependent gene therapy selectively switched on in these cells (Kandel and Spencer, 1961). However, inhibitory interneuron populations are also implicated in hippocampal seizures. For example, fast spiking PV-positive interneurons mediate feedforward inhibition at least in part via perisomatic synapses on pyramidal cells (Gulyás and Freund, 2015). Indeed, preferential loss of PV-positive interneurons has been observed both in human TLE and in animal models, suggesting a possible role in spontaneous recurrent seizures and therefore may be potential targets of the activity-dependent gene therapy (Drexel *et al.*, 2017). The immunohistochemistry experiments was carried out in collaboration with Benito Maffei.

We injected the c-FosP-dsGFP (N = 3) virus into ventral hippocampus of the mice, and induced a single-seizure with high-dose of PTZ with same protocol as in the *ex vivo* electrophysiology experiments. At 2 hours after the seizure, the mice brain was extracted and fixed, ready for slicing and immunohistochemistry. We first tested the immunohistochemistry protocol with interneuron markers which have been extensively studied in the hippocampus (Whissell *et al.*, 2015). Immunohistochemistry was performed against interneuron markers, GAD67 (Glutamate decarboxylase 67) and PV, in dorsal and ventral hippocampal fixed brain slices as shown in Figure 4.20. The dsGFP signal was amplified by immunoblotting with copGFP (Copepoda GFP) antibody (Li *et al.*, 1998; Shagin *et al.*, 2004).

We observed that GFP positive cells spread across CA1-CA3 and DG regions in both dorsal and ventral hippocampal slices. The viral construct spread was however variable between individual brains. The most intense dsGFP labelling was present in CA3, with moderate expressions in CA1-CA2 pyramidal layers. The PV immunohistochemistry showed PV-positive

cells along the CA1-CA3 and DG regions of both dorsal and ventral hippocampus (Figure 4.20). The images showed dominant expression of dsGFP positive cells in the area of superficial CA1 layer, although further studies are needed to confirm this observation. The differential pattern of dsGFP expression may provide us with insights on mechanisms of c-FosP induced gene therapy.

With immunohistochemistry results, we quantitatively analysed the co-localization between interneuron markers and dsGFP by manually counting the cells. Approximately 3.22±2.11(SEM)% of GFP positive cells were identified as also positive for GAD67 staining (Figure 4.20 (C)). The PV immunohistochemistry showed PV-positive cells along the CA1-CA3 and DG regions of both dorsal and ventral hippocampus (Figure 4.20(B)). The morphology and distribution of the PV positive markers were as expected, and showed a high signal-to-noise ratio. The percentage of PV positive cells that were also GFP positive was as low as 1.69 ± 1.27(SEM)%. Overall, both interneuron markers demonstrated low overlap with GFP positive cells, implying that c-FosP does not target interneuron populations substantially in the post-seizure brain. The GAD67 staining was more difficult to visualize than PV, and the results were less clear from the brain sections. We are yet to investigate the expression of the virus in other cell types, e.g. astrocytes, glia.

Following the first cohort of inhibitory marker staining, we then performed multichannel fluorescent immunostaining with neuronal marker NeuN, GABAergic neuronal marker GABA, and dsGFP. This combination of immunostaining targets allowed identification of inhibitory and excitatory neurons in hippocampus, and then investigated the percentage of overlap between them and $GFP^{+/-}$ cells. Overall, this experiment demonstrated that majority of GFP^{+} neurons from CA1-3 and hilus are excitatory neurons, only very small percentage of them are GABA positive (Figure 4.20(D)). This suggests that majority of the cells expressing the cFos-dsGFP virus was excitatory neurons.

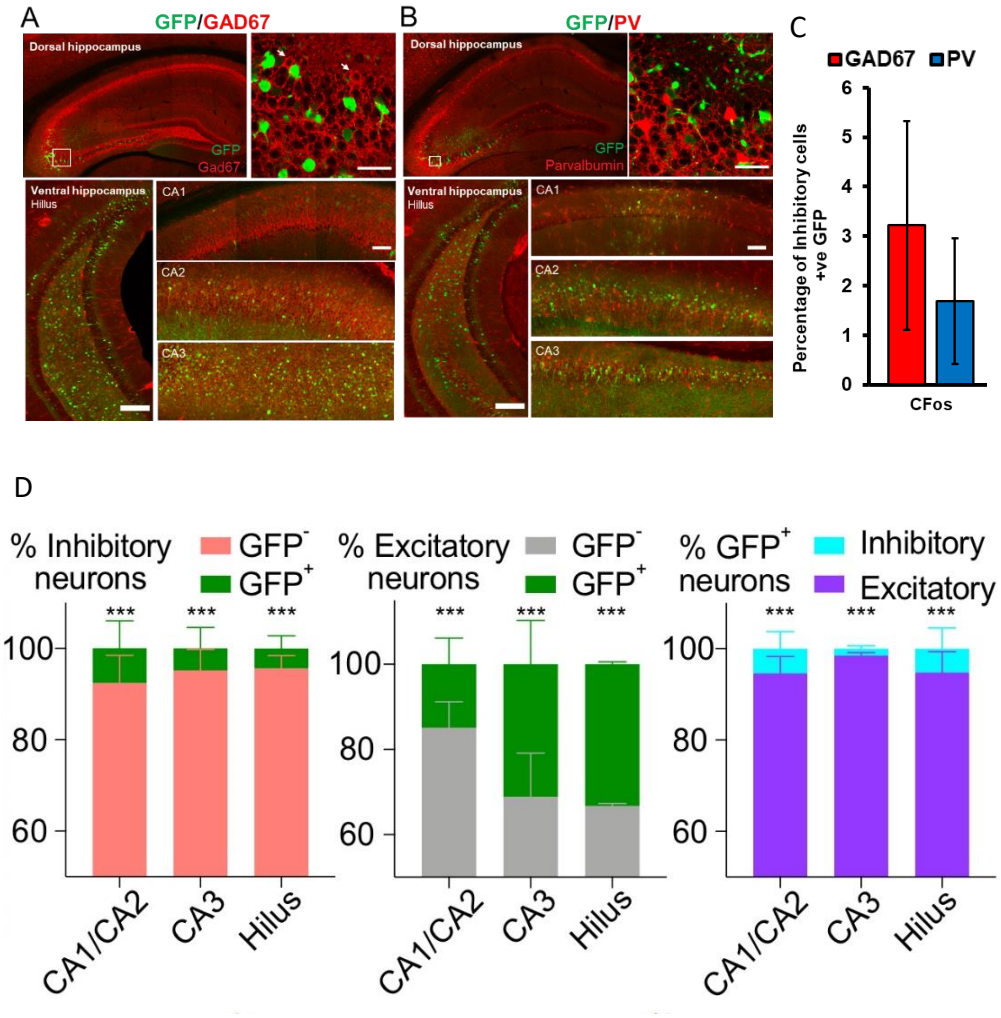

Figure 4.20. Immunohistochemistry for c-FosP expression specificity in hippocampus (A) Representative images from seizure positive brain slices with immunofluorescent staining: PV (red) and dsGFP (green). Images were taken for dorsal and ventral hippocampi, and zoomed in on CA1 and CA3. (B) Same experiment and representative images taken from dual-staining samples: GAD67 (red) and dsGFP (green). (C) Quantitative analysis of GAD67 and PV positive neurons as percentage of GFP^+ cells. (D) Quantitative analysis of (i) Percentage of inhibitory neurons that were GFP positive vs GFP negative; (ii) Percentage excitatory neurons that were GFP positive vs GFP negative; The y-axis represent percentage (%) (iii) Percentage of GFP positive neurons that were inhibitory vs excitatory. (***$p < 0.001$, 2-way ANOVA with Bonferroni multi-comparisons test).

4.9. Activity-dependent gene therapy is transient

4.9.1. Hypothesis and experiment design of PTZ-PTZ repeated challenge

The *in vitro* and *ex vivo* electrophysiological characterisations above argue that IEG promoters can drive functional potassium channel overexpression, which leads to changes in neuronal properties.

Based on the results, we continued to investigate whether this was sufficient to protect from seizures. As we have shown that a single seizure effectively induced potent potassium channel overexpression, we hypothesized that the channels would persist in the membrane and protect the network from future seizures (Fornasiero *et al.*, 2018). However, if seizures remain suppressed for a long time, we also expect that the treatment will eventually switch off and no longer overexpress the potassium channel.

We took advantage of the acute PTZ model, where it was possible to induce a single generalized seizure with each injection at controlled timepoints. We designed an experimental protocol to test our hypothesis with the c-FosP-*KCNA1* virus for proof of principle. The experiment consisted of three repeated PTZ i.p. injections. The first injection was designed to switch on the c-FosP and induce Kv1.1 channel overexpression in the cells recruited by the evoked generalised seizure. After 24 hours, we gave a second dose of PTZ to determine whether c-FosP-*KCNA1* had a protective effect. Then we allowed the mice to recover for two weeks, and then administered a third dose of PTZ. We hypothesized that the treatment was likely to have switched itself off after the two week interval and that the network would again be susceptible to the chemoconvulsant (Figure 4.21(A)).

We injected wild type C57BL/6J mice with either AAV c-FosP-dsGFP or AAV c-FosP-*KCNA1* bilaterally in ventral hippocampi (1.5µl, 10^{13} vg/ml) at least five weeks before the experiments were performed (Colasante *et al.*, 2020). We used the same PTZ dose as described in the previous section (55mg/kg) to induce an acute generalized

seizure. The mice were recorded with video for 30 minutes after injection and their behavioural manifestations were evaluated and scored according to the modified Racine scale (Van Erum, Van Dam and De Deyn, 2019) (Figure 4.21(A)). The revised scale consists of seven stages: sudden behaviour arrest (stage 1), facial jerking (stage 2), neck jerks (stage 3), sitting clonic seizure (stage 4), clonic, tonic-clonic seizure (lying on belly) (stage 5), clonic, tonic-clonic seizure (jumps, lying on side)(stage 6), and respiratory arrest (stage7) (Van Erum, Van Dam and De Deyn, 2019). We also pre-defined a 'convulsive seizure' threshold, as any score higher than stage 3. This is supported by EEG recordings that have shown that, above this stage, continuous SWR (spike-wave ripples) can be detected across the cortex (Van Erum, Van Dam and De Deyn, 2019). The scoring was performed blind to the virus injected. We took seizure severity and latency to the first behavioural convulsion onset as measurements for effectiveness.

4.9.2. PTZ-induced seizure activated c-FosP-*KCNA1* and reduced severity of subsequent seizure

We analysed seizure severity scores of mice treated with c-FosP-dsGFP and c-FosP-*KCNA1* (Figure 4.18(B)). With the first PTZ injection, 7 out of 10 (70%) c-FosP-dsGFP injected mice and 6 out of 9 (66.7%) c-FosP-*KCNA1* injected mice reached at least stage 4 (Figure 4.21(C)). This was not significantly different, suggesting that under basal (physiological) conditions, the c-FosP was unlikely to be activated ($p = 0.999$, 2-way ANOVA followed by Bonferroni multiple comparison tests). After 24 hours, the mice were subjected to the second PTZ injection. 80% of c-FosP-dsGFP injected mice reached convulsive seizure threshold, while only 33% of c-FosP-*KCNA1* treated mice did the same. There was a 33% decrease in the number of mice experiencing convulsive seizures, consistent with c-FosP-*KCNA1* having been activated by the first seizure (Figure 4.21(B)).

The Racine scoring is on an ordinal scale, and so not optimally suited to conventional statistics. Nevertheless, we further explored the severity by treating the scores as continuous. The first injection gave an average score of 4.50±0.522(SEM) and 4.56±0.475 in mice treated with c-FosP-dsGFP and c-FosP-*KCNA1*, respectively. With the second PTZ injection, the mean severity of c-Fos-dsGFP injected mice increased to 5.4±0.542, more severe than the first injection. This was in line with expectations as PTZ may change the brain network and make it more susceptible to future attacks. In contrast, we observed a lower score in c-FosP-*KCNA1* treated mice with the second PTZ injection (3.56±0.0.338). The lower severity is again consistent with the first PTZ-evoked seizure activating c-FosP-*KCNA1* (p = 0.012, 2-way ANOVA followed by Bonferroni multiple comparison tests) (Figure 4.21(B)).

A third PTZ injection was delivered two weeks later, at the same dose of 55mg/kg. We hypothesized that at this timepoint, the c-FosP should be switched off. We observed an increase in severity in both groups: 100% of the c-FosP-dsGFP treated mice and 88% of c-FosP-*KCNA1* treated mice reached the predefined convulsive seizure threshold (Figure 4.21(C)). This was echoed by the severity score data. There was no significant difference between c-Fos-dsGFP and c-FosP-*KCNA1* treated mice (p = 0.999, 2-way ANOVA followed by *Bonferroni multiple comparison tests*).

In addition, we also recorded the latency from injection to first behavioural onset. We recorded the time taken for neck jerks to appear as mice reached seizure score 3 (Figure 4.21(D)). This is a clear behavioural sign that can be confidently distinguished from grooming. We observed a high degree of variability between individuals and therefore compared the latency between the second or third PTZ injection to the latency on the first injection. To our surprise, with the second injection, the c-FosP-*KCNA1* treated mice showed a shorter latency to Racine score 3, even though they were

relatively protected from more severe seizures, while c-FosP-dsGFP showed a longer latency. In the final injection, both groups of mice showed longer latency to score 3. Overall, those mice that showed an increase in latency seemed to be the same as those that showed a more severe seizure score. In particular, the shorter latency after the second PTZ injection could be resulted from small proportion of interneurons expressing cFos-KCNA1, reducing their firing. This unexpected result may provide some insights on the activation profile and potential adverse effect of cFos-KCNA1 expression in neurons other than excitatory neurons, and therefore calls for further investigation.

This set of experiment provided important evidence to support the hypothesis of this project by showing that single-seizure was sufficient to activate c-FosP-*KCNA1* in hippocampus and reduced severity of subsequent attacks. We also found evidence that following an extended seizure-free period, c-FosP-*KCNA1* was likely turned off, as indicated by the lack of protection against a third dose of PTZ.

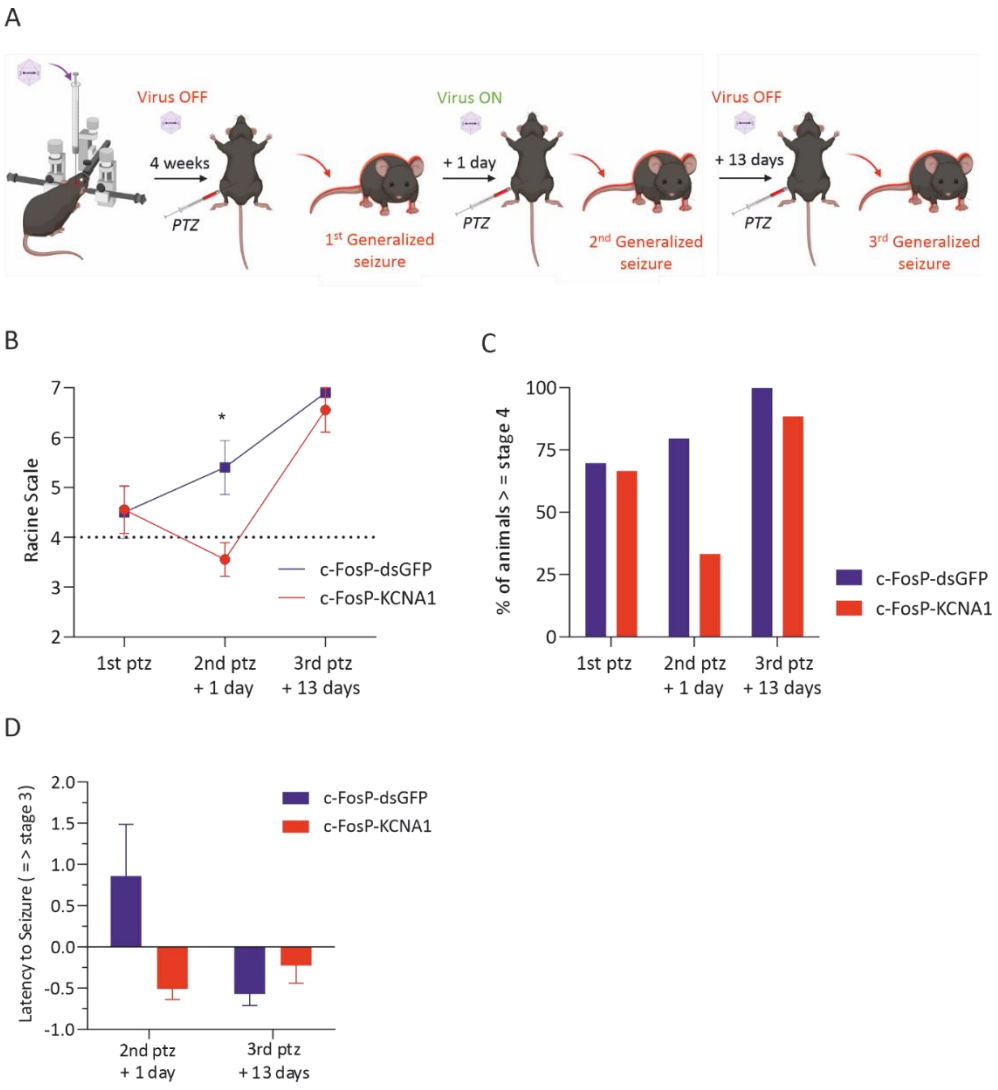

Figure 4.21. Repeated acute ptz-ptz challenge (n=10 c-FosP-dsGFP, n=9 c-FosP-KCNA1). (A) Experimental protocol. (B) Racine scale plotted on 1st, 2nd and 3rd seizures. (C) Percentage of mice score stage 4 or above on Racine scale. (D) Changes in latency to first behaviour onset, normalised to the 1st ptz injection observations.

4.10. Activity-dependent gene therapy decreases seizure frequency in a model of temporal lobe epilepsy

4.10.1. Experiment design and rationale

We have collected promising evidence with acute seizure model for a potential anti-seizure effect of AAV c-FosP-*KCNA1*. We set out to further examine the effectiveness of c-FosP-*KCNA1* in a chronic preclinical animal model to investigate whether it was able to rescue recurrent spontaneous seizures.

We used the intra-amygdala kainic acid mouse epilepsy model, as described in Chapter 3. This model is gives rise to less hippocampal damage than the intrahippocampal kainic acid model(Puttachary *et al.*, 2015). The intra-amygdala KA injection was performed under brief anaesthesia. The status epilepticus (SE) episode was scored for each mouse, and terminated with diazepam administration at 40 minutes post-KA to reduce mortality. Both the duration and severity of SE are parameters that can partially influence the development of spontaneous recurrent seizures, but also mortality and response to the drug treatment (Costa *et al.*, 2020). Only animals that reached convulsive behaviour seizures (stage 3-5) during SE were carried forward for EEG recordings as they were most likely to develop spontaneous seizures (Puttachary *et al.*, 2015).

After two weeks, mice were implanted with ECoG wireless transmitters with electrodes placed above the cortex (MD +3; AP -2/3 Bregma to Lambda) (Colasante *et al.*, 2019) (Figure 4.22). On the side ipsilateral to the kainic acid injection, the recording electrode was fixed at the same location as the cannula for viral delivery directly above the ventral hippocampus. On the contralateral side, an identical cannula was implanted above the same site. The reference electrode was implanted in the posterior cortical area on the contralateral side (Colasante *et al.*, 2020). The baseline recording started 48 hours after the surgery and lasted for two weeks. The ECoG data was screened to identify mice with

spontaneous seizures as a selection criterion. These mice were then randomized to receive either the therapeutic or the control virus in both ventral hippocampi (researcher blinded to the treatments). After allowing two weeks for viral expression, during which the transmitter was switched off, ECoG recording was restarted and continued for another two weeks. At the end of this period, animals were sacrificed for immunohistochemistry.

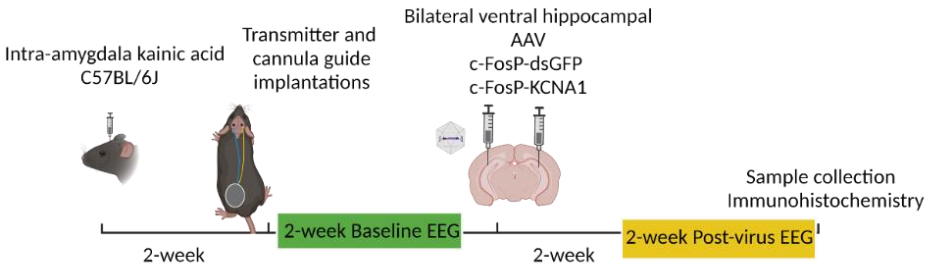

Figure 4.22. Schematic representation of the experimental plan for chronic mouse kainic acid intra-amygdala model.

4.10.2. AAV c-FosP-*KCNA1* decreases seizure frequency in the mouse TLE model

The continuous ECoG data was analysed with a Python analysis suite (PyEcoG) to identify generalized seizures. The PyEcoG program is based on a supervised learning algorithm using >1000 manually annotated generalized seizures in the intra-amygdala kainic acid model, verified along with video recordings for behavioural manifestations (Colasante *et al.*, 2020). The identified seizures were manually checked to remove false positive entries. We also checked the continuous ECoG data collected to identify any false negative not picked up by the algorithm. For each generalized seizure entry, we collected information on seizure duration and time of occurrence.

The seizure frequency per day was plotted for c-Fos-dsGFP and c-FosP-*KCNA1* injected mice groups, and we compared the seizure frequency during the baseline and post-treatment periods.

All seizures identified as described above were plotted against time and date in Raster plots in Figure 4.23(A). In the c-FosP-*KCNA1* group, three out of seven mice were completely seizure-free in post-virus recordings, and two mice had a single seizure in the post-virus period. Five out of six mice treated with c-FosP-dsGFP continued to experience seizures, as shown in Figure 4.23(A). Statistical analysis of seizure frequency showed a significant decrease in mice treated with bilateral AAV c-FosP-*KCNA1* injections, when comparted to baseline recordings of the same individuals ($p=0.0007$, 2-way ANOVA followed by Bonferroni multiple comparison tests) (Figure 4.23(C)). This significant decrease in seizure frequency showed that c-FosP-*KCNA1* was sufficient to reduce seizures *in vivo*.

We also calculated the weighted cumulative frequency which was normalized to the cumulative total seizure recorded in the baseline. The weighted cumulative post-treatment seizure frequency in the c-FosP-*KCNA1* group was significantly smaller than in the c-FosP-dsGFP group ($p = 0.03$, 2-way ANOVA followed by Bonferroni multiple comparison tests) (Figure 4.23(D)).

Therefore, c-FosP-*KCNA1* demonstrated evident anti-seizure effects in chronic preclinical TLE model.

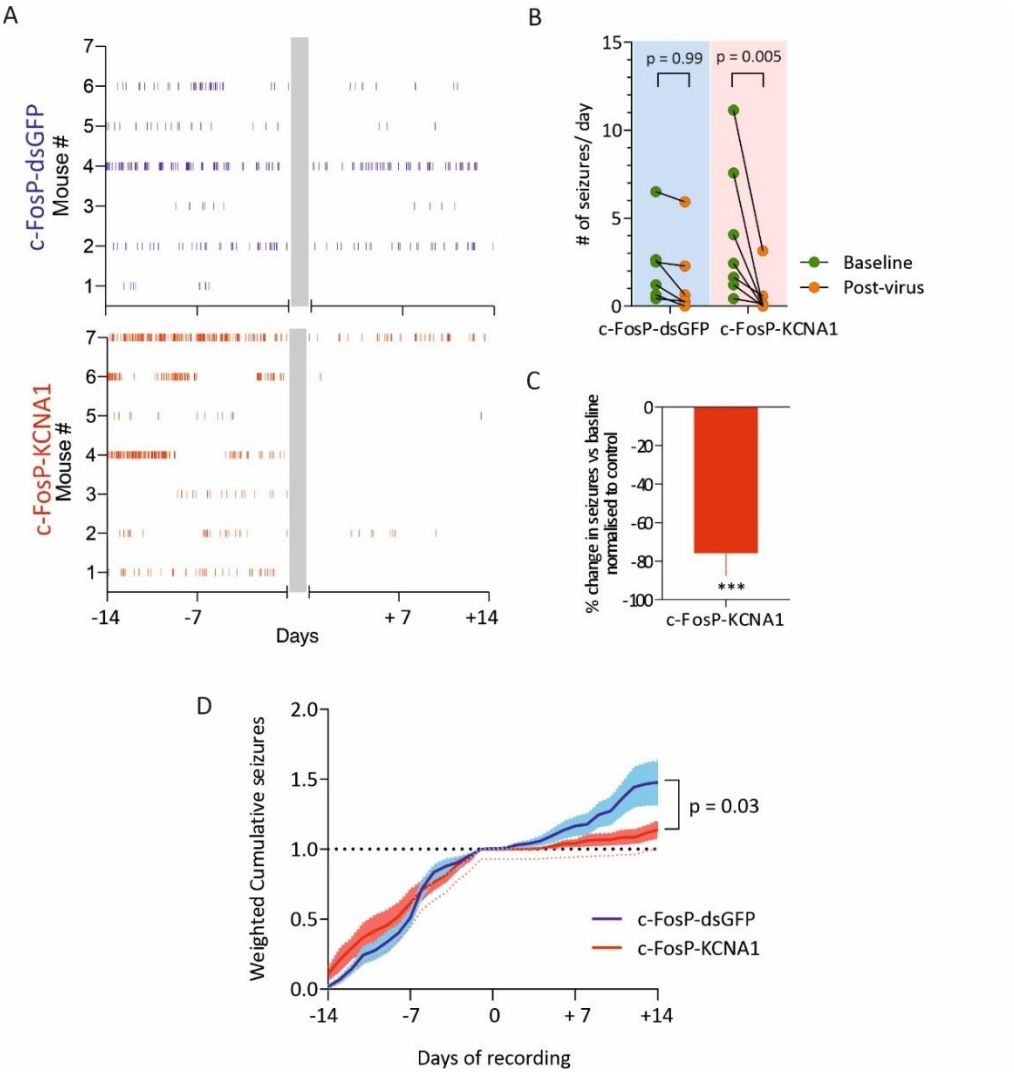

Figure 4.23. c-FosP-KCNA1 bilateral infusion in hippocampi reduced seizure frequency in mice intra-amygdala kainic acid model. (A) Raster plot of seizures against days of recording. (B) Seizures per day before and after virus treatments. (C) Percentage of change in seizure numbers in mice treated with c-FosP-KCNA1, normalised to baseline. (D) Weighted cumulative seizures. Cumulative seizures were normalized to the last day of baseline (y=1, dashed line)

4.10.3. Power spectrum analysis revealed reductions in several frequency bands

In addition to seizure numbers, we also processed the whole ECoG for several parameters. The coastline (cumulative absolute difference between successive data points) in the AAV c-FosP-*KCNA1* group decreased significantly after the treatment (p=0.03, Student's t-test) (Figure 4.24(A)), while the coastline in the c-FosP-dsGFP injected mice did not change significantly. Coastline takes into account all activity, including interictal spikes, and because seizures are relatively infrequent, they do not contribute substantially to the metric. The change in the c-FosP-*KCNA1* group suggests that the overall brain activity has decreased. We also divided the power spectra into different frequency bands between delta and high gamma (1-120Hz), covering the main range of frequencies relevant to biological brain activity. The total power across frequency bands was reduced with c-FosP-*KCNA1* treatment (p = 0.0003, 2-way ANOVA) (Figure 4.24(B)).

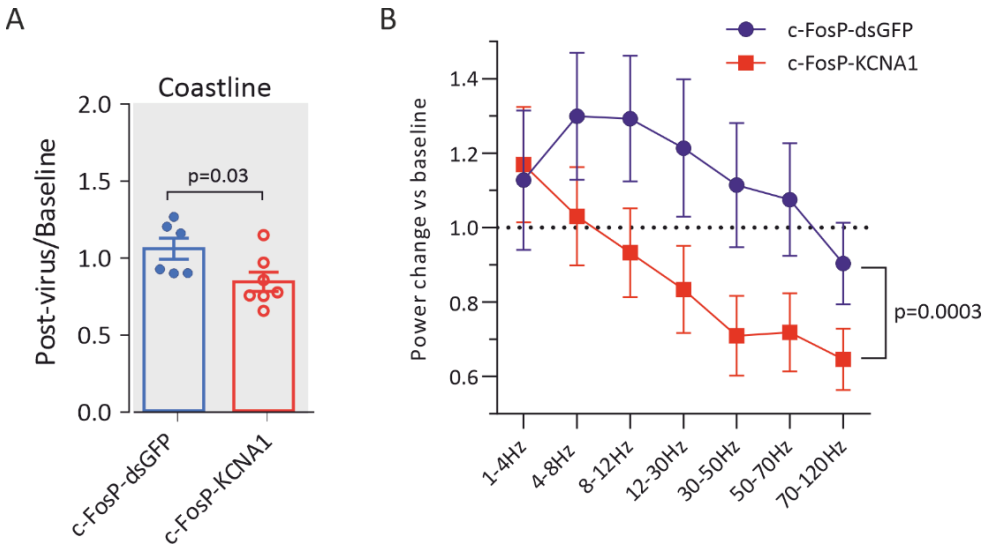

Figure 4.24. Power spectrum analysis of c-Fos-dsGFP and c-FosP-KCNA1 injected mice before and after virus treatments. (A) Coastline analysis normalised to baseline before virus treatments. (B) Power spectrum analysis across frequency bands (1-120Hz) normalized to before virus treatments (y=1, dashed line) (p = 0.0003, 2-way ANOVA, Bonferroni multiple comparison's tests).

4.10.4. Protective effect of c-FosP-Kv1.1 against further seizure attacks

At the end of the chronic epilepsy model recording, we asked the question whether c-FosP-KCNA1 still had protective effect with long-term epileptic conditions. We injected the mice with low-dose PTZ (26mg/kg) to induce a single generalised seizure in the brain. The mice were monitored for behaviour and mortality conditions post-PTZ injection. We observed significant difference in survival rate between c-FosP-dsGFP (n=4) and c-FosP-KCNA1 (n=7) treated mice groups, with that of c-FosP-KCNA1 showing significantly lower mortality than c-FosP-dsGFP injected group (Log-rank (Mantel-Cox) test, p = 0.05) (Figure 4.25). This result indicated that with chronically expressed c-FosP-KCNA1 in hippocampi regions, it protected the brains from further hyperactivity challenge.

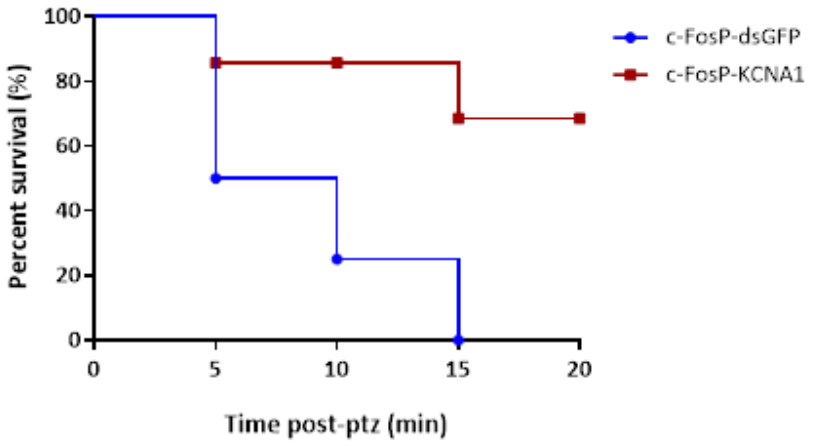

Figure 4.25. Single acute ptz seizure survival plot for c-FosP-dsGFP and c-FosP-KCNA1 treated mice groups (p=0.05, Log-rank Mantel Cox test).

4.10.5. Alternative effector Kir2.1 does not have an anti-seizure effect in the mouse TLE model

The c-FosP-*KCNA1* virus showed consistent effects on reducing neuronal excitability in in vitro and ex vivo electrophysiology characterizations. In the in vivo chronic mice TLE model, c-FosP-*KCNA1* expressed bilaterally resulted in a reduction in seizure frequency and in selected bands of the ECoG power spectrum. The alternative potassium channel candidate, Kir2.1, however, showed less consistent results in the in vitro experiments. Therefore, we asked whether c-FosP-*KCNJ2* has anti-seizure effects *in vivo*.

We performed the same experiment as described in section 4.10.1 using c-FosP-*KCNJ2* expressed bilaterally in ventral hippocampi. These experiments were actually performed in parallel with the c-FosP-dsGFP and c-FosP-*KCNA1* mice. Therefore, the data for these cohorts are replotted from the previous Figure 4.26.

To our surprise, c-FosP-*KCNJ2* did not show any effect on seizure suppression; mice had an outcome more to the c-FosP-dsGFP group, with no clear decrease in seizure frequency (Figure 4.26(B)). In addition, two of the mice from the c-FosP-*KCNJ2* group suffered from seizure-related premature death. The seizure frequency decreases compared to c-fosP-dsGFP were significantly different between c-FosP-*KCNA1*, and c-FosP-*KCNJ2* treated mice ($p=0.03$, 2-way ANOVA followed by Bonferroni multiple comparison tests) (Figure 4.26(B)).

Although Kir2.1 overexpression may acutely hyperpolarize the RMP, prolonged overexpression of Kir2.1 appears to have little or no anti-epileptic effect in the chronic kainic acid model. This phenomenon may be explained by several possible mechanisms, which will be discussed in detail in the next chapter.

In summary, with the same inducible promoter c-FosP, activity-dependent Kv1.1 channel overexpression had a significant seizure-attenuation effect. However, Kir2.1 channel overexpression did not

have any anti-seizure effects. We conclude that AAV c-FosP-*KCNA1* is more promising to be taken into downstream pre-clinical assessment and eventual clinical translation. We therefore used AAV c-FosP-*KCNA1* to perform cognitive assessments described in the following sections.

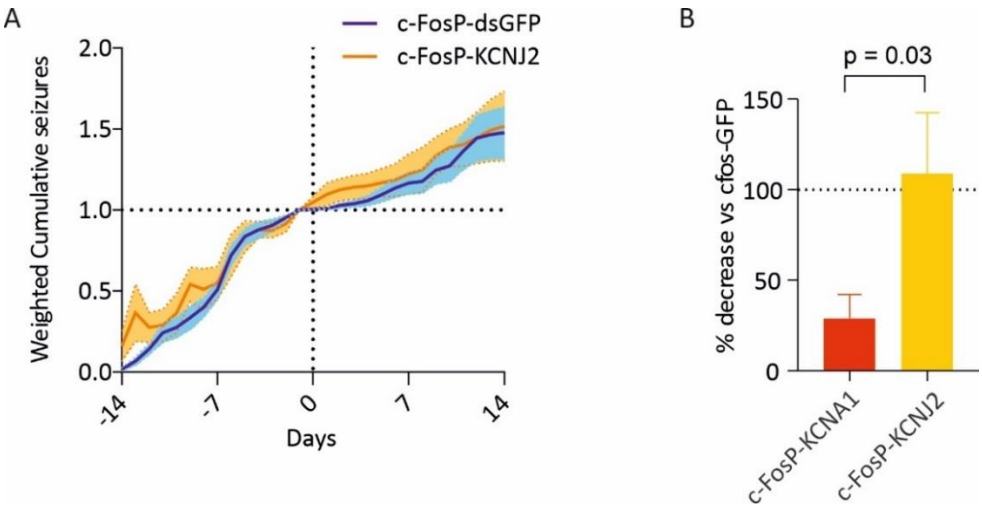

Figure 4.26. AAV c-FosP-KCNJ2 showed no effect on seizures in chronically epileptic mice. (A) Weighted cumulative seizures, values normalized to the last day of baseline (y = 1, dash line). (B) Percentage of changes in seizure frequencies compared between c-FosP-KCNA1 and c-Fos-KCNJ2, normalized to baseline (p = 0.03, unpaired Student's t-test).

4.11. Cognitive assessment of mice treated with AAV c-FosP-*KCNA1*

IEGs are extensively involved in physiological behaviours, especially in learning and memory processes(Josselyn and Tonegawa, 2020). For example, c-Fos has been implicated in memory formation in the non-epileptic brain. We therefore considered it important to determine whether c-FosP-*KCNA1* interferes with normal behaviour in the absence of seizures. We designed and performed a series of assessments to investigate whether c-FosP-KCNA1 therapy under physiological conditions interfere with memory and learning process.

Furthermore, behaviour comorbidity is key part of TLE disease manifestation and diagnosis component. Behaviour alternations in kainic acid TLE models may partially reflected the neurobiological mechanism of the disease. With gene therapy applied, we also asked the question of whether seizure-related behaviour traits in mice models can be reversible and rescued by gene therapy.

4.11.1. Contextual fear conditioning (CFC)

The first experiment was designed based on the crucial role of c-Fos in memory consolidation and memory recall, with reference to the studies published by the Tonegawa laboratory who used the c-Fos promoter to express ChR2 for manipulation of fear memory formation and recall (Ramirez *et al.*, 2015; Roy *et al.*, 2016; Kitamura *et al.*, 2017). Those results implicated c-Fos in memory consolidation and recall. We designed a simplified protocol based on those publications, as explained below. Naive mice were first injected bilaterally in ventral hippocampi with either AAV c-FosP-dsGFP or c-FosP-*KCNA1*. After waiting 3-4 weeks of virus expression, the mice were brought into an experimental chamber designed to deliver mild foot shocks with specified time intervals (‘Context A’). The foot shock constitutes a salient aversive stimulus and elicits behavioural arrest (freezing behaviour). In the conditioning phase, mice received 3 2s-long foot-shocks (0.7mA) at 60s intervals (Condition in Context

A). The mice were returned to their home cage overnight. After 24 hours, the mice were returned to the same box (Context A) for 5 minutes with no food shock, and their behaviour was observed and recorded by an experimenter blinded to the treatment. The total duration of freezing behaviour was taken as a read-out of memory recall. After 1 hour, mice were taken to a different context (Context B) for another 5 minutes, during which their behaviour were again recorded. To create a new environment different from Context A, we replaced the metal floor grid of the foot shock box with a smooth plastic board, the walls were lined with paper to change colour and texture, and we also added a novel olfactory stimulus (almond oil) (Figure 4.27(A)).

We compared freezing behaviour between the conditioning phase and the fear recall phase 24 hours later. Freezing behaviour in the conditioning phase was measured from the habituation period before the first foot shock was delivered. There was a significant increase in freezing time in the fear recall session in both AAV treated cohorts. Freezing behaviour in mice treated with c-FosP-dsGFP increased from 3.6±1.33(SEM)% to 50.2±8.25(SEM)% ($p < 0.0001$, 2-way ANOVA, Bonferroni multiple comparisons test). Freezing behaviour in the c-FosP-*KCNA1* virus transduced mice incresed from 2.36±0.656(SEM)% to 50.5±5.33(SEM)% ($p < 0.0001$, 2-way ANOVA, Bonferroni multiple comparisons test) (Figure 4.27(B)).

After the fear recall phase, we introduced a new context to determine whether the fear memory is contextual. The AAV c-FosP-dsGFP mice showed a significant decrease in freezing time in the new context to 22.6±7.434 (SEM)% ($p = 0.011$, 2-way ANOVA, Bonferroni multiple comparisons test). The mice transduced with AAV c-FosP-*KCNA1* also showed a reduced freezing time in the new context ($p = 0.049$, 2-way ANOVA, Bonferroni multiple comparisons test) (Figure 4.27(B)).

The results show that c-FosP-*KCNA1* has no effect on contextual memory in an experimental design that has previously implicated c-Fos.

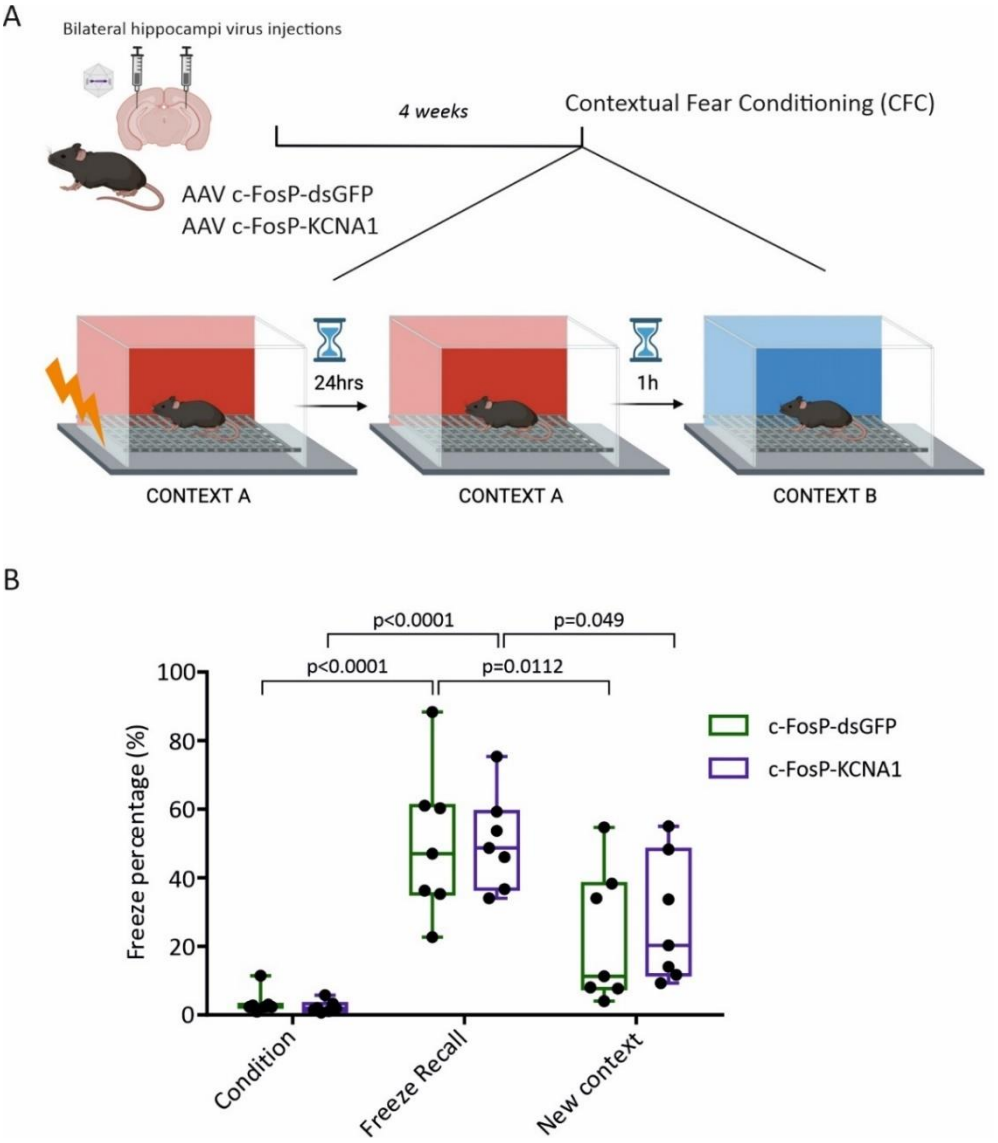

Figure 4.27. Contextual Fear Conditioning (CFC). (A) Experimental protocol. (B) Freeze percentage analysis of freeze recall and novel context (2-way ANOVA, Bonferroni multiple-comparisons test).

4.11.2. Open field novel habituation test

As demonstrated above, driving *KCNA1* expression with the c-Fos promoter did not interfere with fear memory acquisition or recall. We asked if c-FosP-*KCNA1* leads to deficits in other memory and learning tasks where the hippocampus and its connected pathways have been implicated. Since it was first introduced in 1934, the open field test has been used widely in rodents for stress, anxiety, and spontaneous locomotion assessments(Hall, 1934). The pattern of locomotion in this test is sensitive to anxiety and exploratory motivation.

The mice were allowed to explore freely in an open field apparatus (50x50x50 cm) for 30 minutes without prior habituation to the arena. Their behaviour in the arena was recorded by Raspberry pi camera from a bird's eye view. The C57VBL/6J mice were easily distinguished from the floor because of their colour. This enabled us to analyse the video automatically using a script based on the Bonsai video analysis open-source platform (Lopes *et al.*, 2015). The script extracted information on the relative location and movement of the mice in the arena. Anxiety can be evaluated by understanding how much time mice spent close to the perimeter versus in the middle (thigmotaxis) (Figure 4.28(B)). The more fearful or stressed the mice, the higher the thigmotaxis measure should be. In addition, we also extracted the total travelled distance, and the distance travelled in every 5 minute time block to understand habituation to the new arena. With increased in time spent in the arena, mice gradually reduce their explorative behaviour.

We conducted the experiment in two cohorts, one cohort was injected with kainic acid in the amygdala, using a protocol identical to the chronic epilepsy experiment. Those mice were selected with the same criteria, in that they had to reach stage 3 in SE to be included in the study. The other cohort were injected with the same volume of saline at the same coordinates.

In baseline tests, the saline group spent an average of 84±1% of the time in the peripheral region, while epileptic cohort spent 90±1% in the peripheral region. The kainic acid cohort preferred to stay in the peripheral region significantly more than that of saline cohort ($p < 0.0001$, Student's t-test) (Figure 4.28(C)). Furthermore, we also observed a significant increase in motor activity (travelled distance) in the epileptic cohort ($p = 0.012$, Student's t-test) (Figure 4.28(D)). This result suggested that KA injected mice did not have locomotion deficits, and that the outcomes of other movement tests are not affected by this potential confound. The increased total distance could potentially be explained by mice running between corners along walls to avoid the central region. This result is in agreement with published studies in KA rodent models (Pearson, Schutz and Patel, 2014).

After the baseline test, mice were randomised into two groups, each injected bilaterally with either c-Fos-dsGFP or c-FosP-*KCNA1* with the same protocol (coordinates and volume) as in the chronic epilepsy experiment in ventral hippocampi. Mice remained in group-housing after the virus injections and were allowed to recover for four weeks. Post-virus tests were performed using the same set-up and protocol as the baseline test. In the saline cohort, mice injected with c-FosP-dsGFP or c-FosP-*KCNA1* showed no significant differences in thigmotaxis ($p = 0.64$, $p=0.99$ 2-way ANOVA, Bonferroni multiple comparisons test) (Figure 4.28(E)). This implied that the virus injections had no effect on anxiety or locomotion on the mice. Interestingly, both c-FosP-dsGFP and c-FosP-*KCNA1* treated mice groups showed a reduction in the total distance travelled ($p = 0.03$ and $p = 0.01$ respectively, 2-way ANOVA with Bonferroni multiple comparisons test) (Figure 4.28(F)). A possible explanation is that mice retained spatial memory from the previous session and habituated to the arena faster.

The epileptic cohort injected with c-FosP-dsGFP continued to spend most of the time in the periphery. The peripheral exploration occupied from 91±1.3(SEM)% to 92.3±1.3(SEM)% of total time of the experiment. The mice injected with c-FosP-*KCNA1* virus also showed high thigmotaxis at 90.3±1.7(SEM)% (Figure 4.28(E,F)). This suggests that the viral treatment did not significantly affect anxiety or stress levels. The kainic acid intra-amygdala injections unavoidably led to neuronal loss in both amygdalae, the core region for fear and adverse responses, but any consequence of amygdala damage was not detected in the present experiment. This may influence the outcome of the post-virus results (Prut and Belzung, 2003).

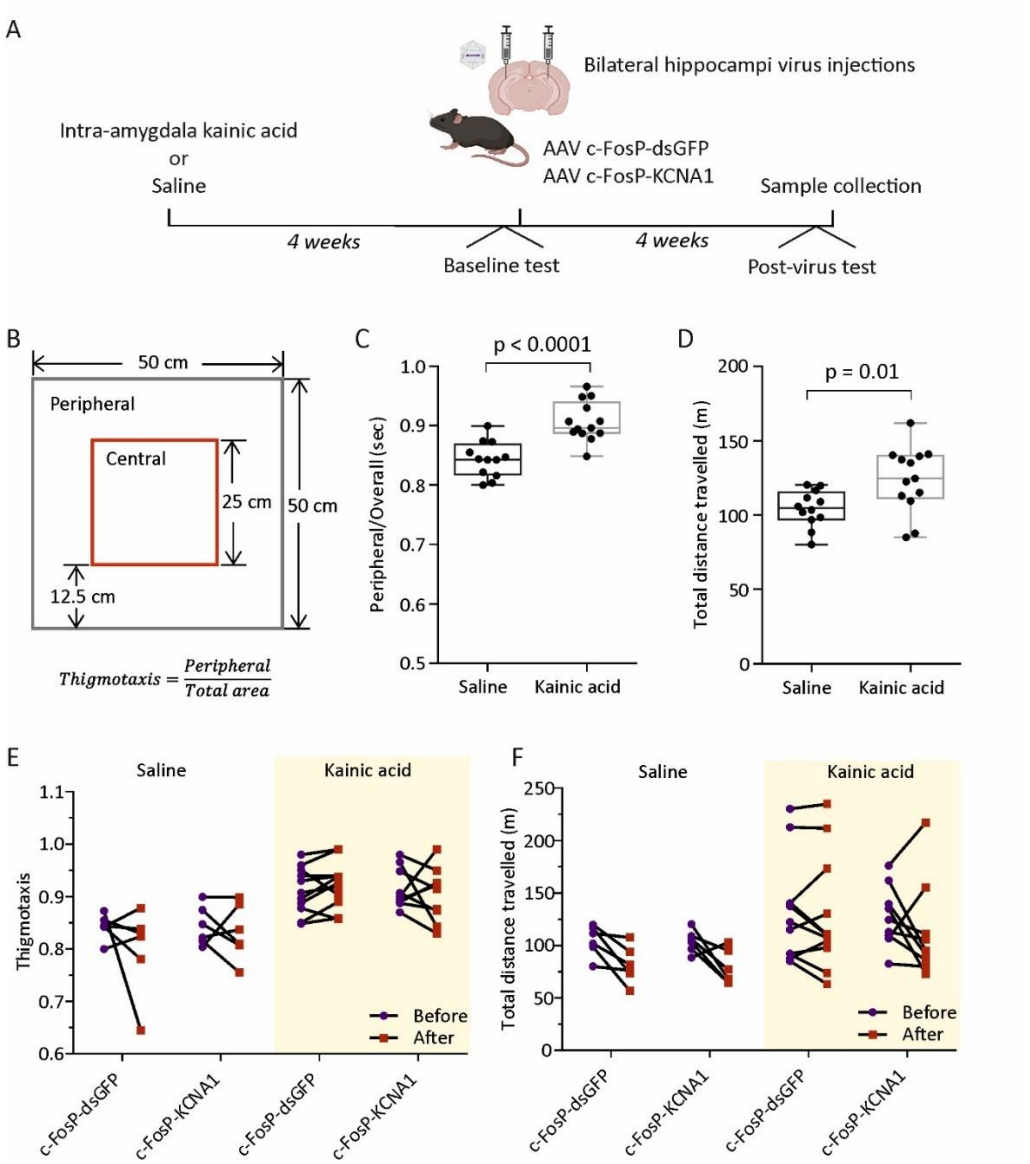

Figure 4.28 Open field exploration experiment. (A) Illustration of experiment protocol. (B) Arena layout and the definitions of peripheral and central areas. (C) The thigmotaxis of saline and kainic acid injected mice, saline and kainic acid (KA)-treated group (Unpaired Student's t-test). (D) Total distance travelled by mice (Unpaired Student's t-test). (E) Thigmotaxis plot of saline and kainic acid epileptic mice before and after c-FosP-dsGFP or c-FosP-KCNA1 treatments.(2-way ANOVA, Bonferroni multiple comparisons test). (F) Total distance travelled (m) plot of saline and kainic acid epileptic mice before and after c-FosP-dsGFP or c-FosP-KCNA1 treatments.

4.11.3. Object location recognition test

In the publication described in Chapter 3, we showed that intra-amygdala kainic acid model leads to compromised spatial memory in the object location test (OLT) (Colasante *et al.*, 2020). The behaviour test design composed of large objects which we noticed that mice were able to climb easily, and they may be too big in proportion to the size of the animal, and conducting the experiment with bright house light could be stressful for the animals. Therefore, we made repeated the evaluation with minor improvements to the design to help eliminate the problems. To help improve the problem of climbing, we changed the objects to two 50ml falcon tube filled with coloured water. The inter-trial interval time remained the same as previous (6hrs) and for each of the recorded exploration session, it was the same for 8 minutes. The object exploration was manually scored by a researcher blinded to the treatments. To compare the innate exploration preference for the novel location, a discrimination index (DI) was calculated as the time spent at the novel location exploration minus the unmoved object as a fraction of the overall exploration time. When DI > 0, it indicates the mice spent more time at the novel location, while if DI < 0, it suggests that they preferred the unmoved object (Leger *et al.*, 2013; Colasante *et al.*, 2020).

The first cohort of mice assigned to the OLT were the same cohort as the open field test assessment. In this cohort, we did not observe significant impairment in epileptic mice compared to non-epileptic cohort. Both epileptic and non-epileptic cohort showed preference towards the moved object. This test showed no clear readout for spatial recognition alternations in the epileptic mice. And we also noticed relatively low exploration time during the test session. This observation may be explained by several facts, for example, that the mice had previously been exposed to the same arena in the open field test, resulting in reduced exploration motivation.

In the following cohort, we changed the test to a new arena of different dimension with same 50ml Falcon tubes. In this repeated test, we found that the epileptic and non-epileptic mice showed again clear differentiation between moved and un-moved objects with no detectable difference in DI. This could be related to the size of the arena, a smaller arena may be less demanding for spatial memory.

We may continue to search for alternative objects, arena or protocol design with different inter-section interval. In the meanwhile, we are conducting several parallel behaviour assessments to evaluate seizure-related cognitive deficits. Alternatively, we have turned to other memory tests to evaluate the behaviour traits of epileptic mice.

4.11.4. Spontaneous T-maze alternations

To further evaluate learning and memory, we chose the T-maze spontaneous alternation task. Rodents have an innate exploratory tendency to alternate between arms of the T-maze (Dember and Fowler, 1958; Lalonde, 2002). When they are placed in a T-shaped apparatus, rats and mice show a strong tendency to enter alternate arms on successive trials, which is known as spontaneous alternation. The schematic illustration of experiment outline is shown in Figure 4.29(A). T-maze tests were performed at least 24 hours after the open field tests. Five trials was considered the minimum number to detect a pattern of alternation above chance. We therefore recorded ten consecutive trials to minimise individual variability (Deacon and Rawlins, 2006). With higher cognitive demands from more repetitive trials, there could be potentially higher chance to detect minor hippocampal abnormality (Deacon and Rawlins, 2006).

Mice were placed in the start area for free exploration of both left and right arms with the central partition inserted; once they have

entered one arm, the guillotine door was closed and the mice were left in the chosen arm for 30 seconds of free exploration. Immediately after, the mice were placed back to the start area and allowed to run into one of the arms with the central partition and guillotine doors all lifted. Both choices were recorded; if the second was different from the immediately preceding one, it was recorded as a correct alternation, and *vice versa* (Figure 4.29(B)). The trials were conducted with no intervals. If a mouse failed to run from the start position within 90s, it was returned to the home cage for 5-10 minutes before another trial. If it required more than two such breaks, the mice was returned to the home cage and a new test was performed on the next day. If the mouse failed again, it was removed from the study.

We first performed the protocol on non-epileptic mice, which showed alternation above chance (50%) (Figure 4.29(E)). In the post-virus trials, mice again exhibited alternation above chance in both virus treated groups with 0.78±0.031(SEM) and 0.77±0.042(SEM) for c-FosP-dsGFP and c-FosP-*KCNA1* viruses respectively. All mice showed slightly higher rates of correct alternation in post-virus sessions, possibly as a result of a decrease in stress level (Figure 4.29(C)). These results argue that expressing AAV c-FosP-*KCNA1* in non-epileptic mice does not interfere with episodic memory and decision making processes.

We then asked whether this protocol was sufficient to detect cognitive deficits in epileptic mice. It has been reported that rodents with hippocampal lesions perform worse in the T-maze spontaneous alternation test than sham controls (Lalonde, 2002). We therefore hypothesized that kainic acid epileptic mice might show compromised performance in the T-maze alternation (Lalonde, 2002). The comparison between baseline tests of non-epileptic and epileptic (kainic-acid treated) mice showed a significant differences in performance ($p = 0.033$, Student's t-test). The correct alternation

rate was 71±0.067(SEM)% in non-epileptic mice and only 61±0.014(SEM)% with epileptic mice cohort. Among the epileptic mice cohort, 5 out of 15 mice showed correction rate fell to chance (50%). The correct rate therefore could be used as one of phenotypic readouts for compromised working memory in kainic acid induced epileptic mice.

We then investigated the effect of virus transduction in the epileptic mice on spontaneous alternation. The epileptic cohort was the same as used in open field analysis. The post-virus test showed a slight decrease in the correct altrnation rate in both groups, which could have resulted from an increase in stress level with recurrent seizures. With c-FosP-dsGFP virus treatment, the correct alternation rate dropped by 14% and with c-FosP-*KCNA1* virus, the correct alternation rate dropped 8% (Figure 4.29(D)). The difference in correct alternation rate was not significantly different between viral groups. This decrease in working memory could be caused by continuously worsening hippocampal sclerosis and increasing anxiety levels. This result suggests that although the c-FosP-*KCNA1* virus treatment did not reverse the cognitive deficits in epileptic mice, it did not show significant worsening when compared with control c-FosP-dsGFP injected epileptic mice.

In addition, for the spontaneous alternation to be effective, the mice must have equal possibilities of choosing left or right arm. With unilateral kainic acid injection, the right hand side of hippocampi may obtain more damage. We therefore also evaluated the directional preference potentially caused by the injection damage. In the baseline test of kainic acid mice cohort, the right/left comparison however showed no preference for directions ($p=0.5$, unpaired Student's t-test) (Figure 4.29(F)).

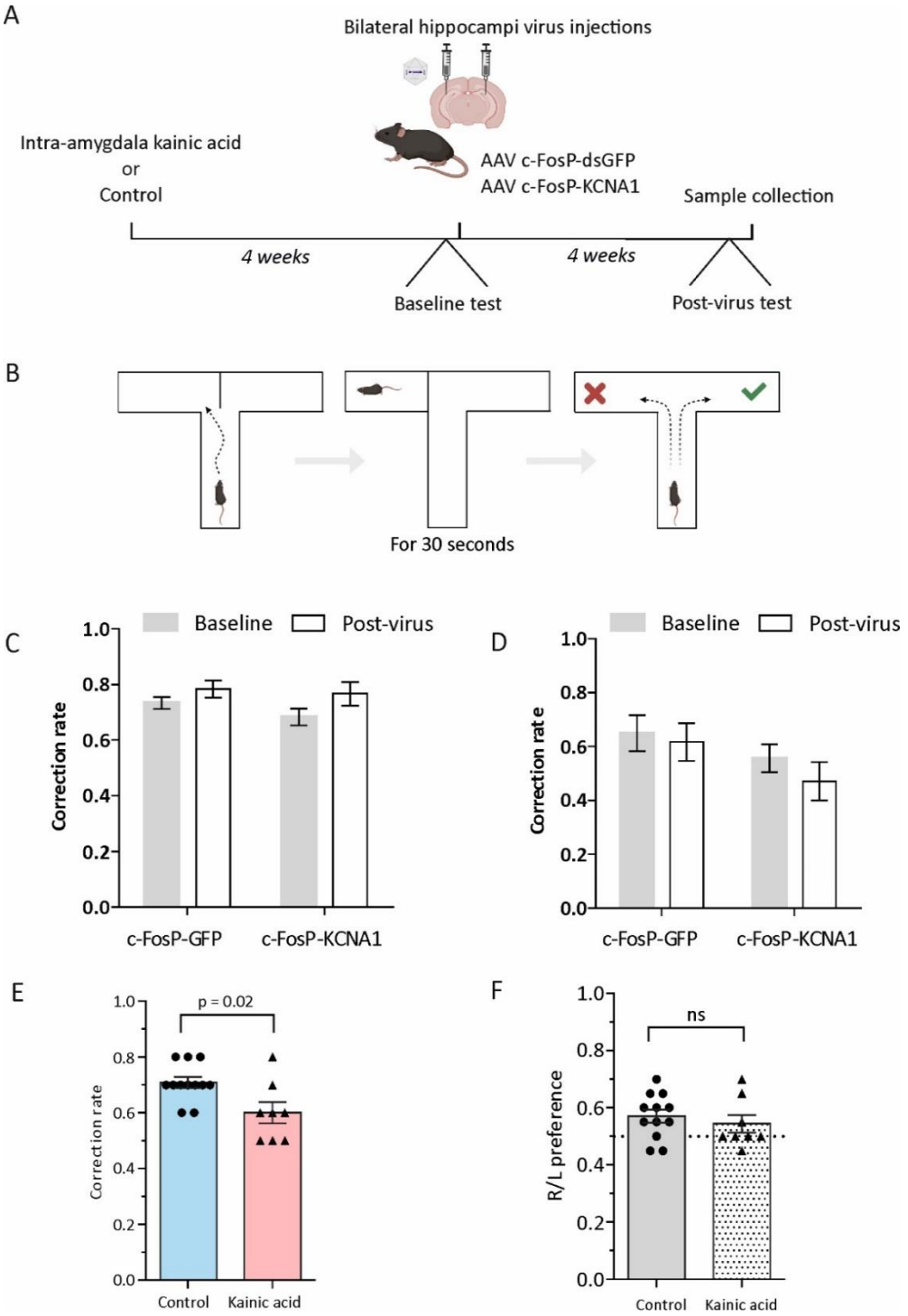

Figure 4.29 .Spontaneous T-maze alternation experiment (A) Schematic representation of experiment plan. (B) Illustration of the T-maze apparatus and spontaneous alternation protocol. (C). Correction rate in control cohort mice before and after virus treatment. (D) Correction rate in kainic acid cohort mice before and after virus treatment. (E) Alternation correct rate. Kainic acid group showed significant decrease in alternation correction rate than control group (p=0.02, Unpaired t-test). (F) Right/left preference in control and kainic acid mice groups. Dashed line represent 50% balanced right/left choices (unpaired Student's t-test).

4.11.5. Olfactory discrimination test

In addition to the learning and memory processes, we asked whether viral transduction in hippocampal area has any effect on structures outside the limbic system. We chose a test which does not primarily involve hippocampus, the olfactory discrimination test (Gottfried, 2010; Arbuckle *et al.*, 2015).

Mice were subjected to 3 consecutive trials of the same novel scent which they were not previously exposed to, and their exploration time was taken and compared between trials and between scents. In this experiment, mice were exposed to water, peppermint and almond in sequence. When a new scent was introduced, the exploration time went up as mice were innately attracted to novelty (Figure 4.30(A)). This change in exploration time indicated that mice were capable of discriminating different olfactory stimuli. With repeated exposure to the same scent, the mice spent gradual less time exploring, implying olfactory habituation. The same saline and kainic acid mice from open field analysis were subjected to the olfactory discrimination test here.

We first experimented with the protocol on mice injected with saline in the amygdala. We observed a clear difference in exploration time between different scents and an attenuation with repeated presentation. The mice were then randomized and injected with either AAV c-FosP-dsGFP or c-FosP-*KCNA1* bilaterally, they were allowed to rest for 4 weeks before subjecting to the post-virus tests. The mice used for olfactory discrimination was the same cohort as in open field analysis. Olfactory discrimination was performed at least 48 hours after the open field novelty exploration test with completely different apparatus to minimise cross-effects between tests.

In the post-virus conditions, the same protocol was performed. We observed a general decrease in exploration time, possibly due to residual memory from the previous baseline test. The c-FosP-dsGFP

transduced mice showed a difference in exploration time between water, peppermint and almonds (3-way ANOVA, Bonferroni multiple comparison test). The c-FosP-*KCNA1* showed less apparent discrimination between water, peppermint and almond, and showed shorter exploration time as well (Figure 4.30(C)).

We then asked whether the mice retained the ability to distinguish a new scent, different from previously exposed ones. After 24hrs, the same mice were returned to the test chamber, and we performed a modified protocol with water, peppermint and a nove scent, raspberry. The AAV c-FosP-dsGFP and AAV c-FosP-*KCNA1* transduced mice both showed ability to distinguish between peppermint and raspberry and repeated exposure reduced their exploration time.

We then performed the test in the kainic acid injected cohort. The baseline test was carried out 4 weeks after kainic acid injection. We observed a significant decrease in exploration time with epileptic mice (Unpaired student's test) (Figure 4.30(B)). This decrease could be a reflection of stress in epileptic mice. The mice were then randomized and injected bilaterally with either c-FosP-dsGFP or c-FosP-*KCNA1* AAV virus (as described previously). In the post-virus test, c-FosP-dsGFP transduced mice showed less clear discrimination between water and peppermint, but they were able to show moderate discrimination between peppermint and almond. The other cohort transduced with the c-FosP-*KCNA1* virus showed similarly low exploration time; however, they still demonstrated moderate discrimination between scents (3-way ANOVA, Bonferroni multiple comparison test) (Figure 4.30(D)). With the novel scent task, mice treated with control and therapeutic viruses showed similar discrimination and habituation to raspberry. This suggests that the capability of epileptic mice to learn novel scents was retained, as was habituation with repeated exposures.

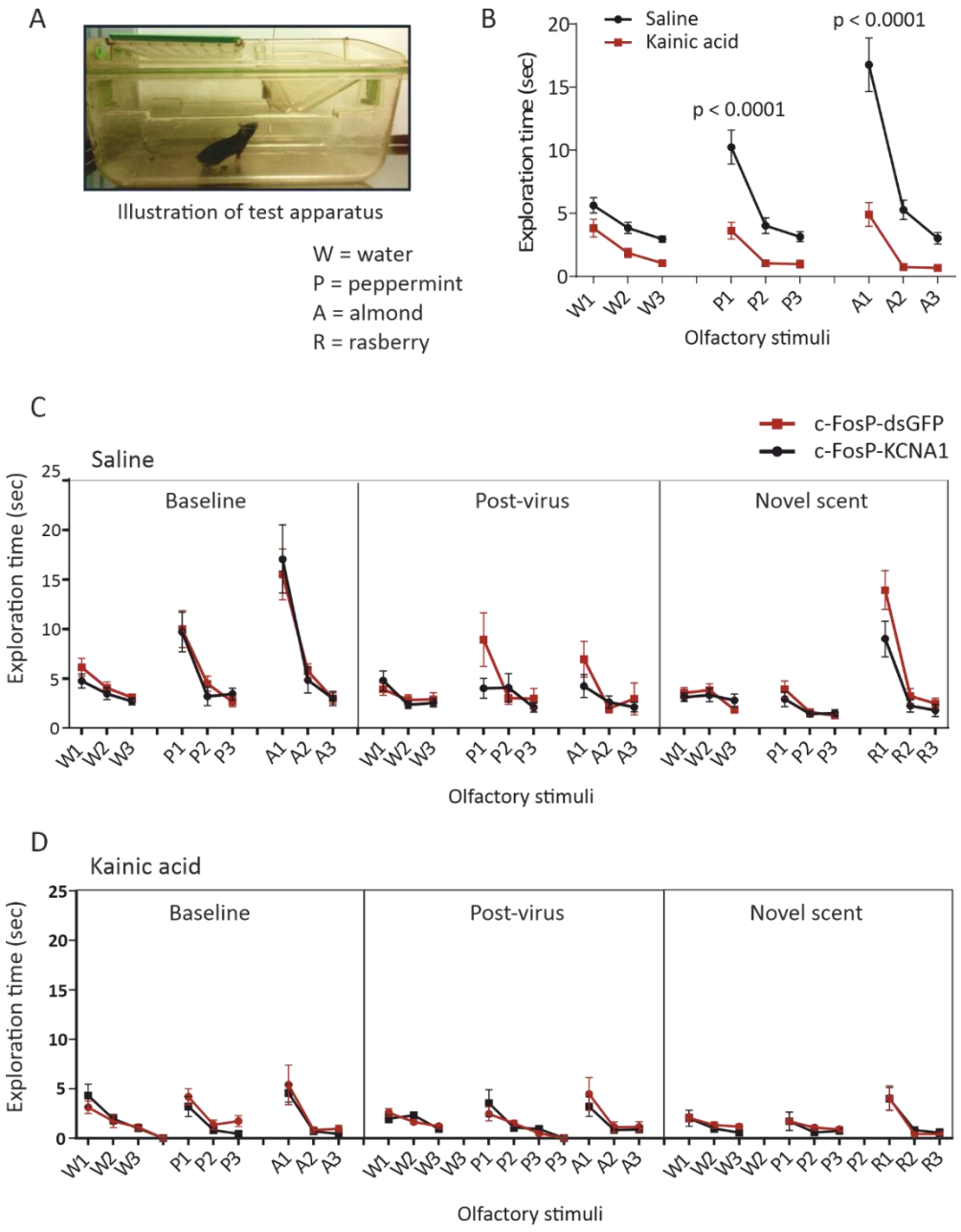

Figure 4.30. Olfactory Discrimination. (A) Illustration of behaviour chamber (with permission from Dr. Amanda Almacellas Barbanoj). (B) Exploration time comparison between saline injected and kainic acid injected mice for water, peppermint and almond. (Unpaired Student's t-test). (C) Saline mice discrimination test results (3-way ANOVA, Bonferroni multiple comparison test). (D) Kainic acid mice discrimination test results (3-way ANOVA, Bonferroni multiple comparison test).

Chapter 5
Discussion

5.1. Summary

Gene therapy brings precision and specificity at both molecular and cellular levels to treat refractory focal epilepsy. The gene therapy can be targeted to the seizure onset zone or to regions implicated in seizure propagation, sparing healthy parts of the brain. This thesis describes two new strategies: constitutive upregulation of endogenous ion channels and closed-loop expression of an ion channel in response to pathological hyperactivity.

Previous anti-epileptic gene therapy studies have focused on exogenous transgenes delivered by viral vectors into the CNS (Kullmann *et al.*, 2014; Simonato, 2014). The therapeutic transgenes include peptides and transmembrane proteins, aiming to alter the excitation/inhibition balance of the neural circuit (Simonato, 2014). However, exogenous transgene delivery is limited by the packaging capacity of viral vectors (Wu, Yang and Colosi, 2010). Some ion channels, such as sodium or calcium channels exceed the packaging limits of viral vectors. Manipulation of endogenous gene expression bypasses the limit on cDNA length, allowing large proteins or proteins consisting of multiple subunits to be used as effectors. Here we showed, using inducible gene overexpression of the endogenous *Kcna1* gene in mice, that it was possible to upregulate mRNA and Kv1.1 protein expression, which ultimately led to anti-seizure effects in the animal epilepsy model. Transmembrane proteins often assemble as multimeric complexes. Although not tested here, the dCas9 system can, in principle, be multiplexed by using more than one sgRNA, leading to simultaneous changes in the expression of genes from multiple genomic loci (Cheng *et al.*, 2013; Wu *et al.*, 2014; Konermann *et al.*, 2015). Importantly, by combining a nuclease-defective Cas9 with transcriptional

activators, it is possible to manipulate endogenous gene expression without editing genomic sequences (Konermann *et al.*, 2015).

The second gene therapy strategy applied in this thesis aims to tackle a different limitation of conventional gene therapy for epilepsy. The constitutive promoters normally used to drive exogenous genes do not distinguish between pathological and normal neurons in the treated region of the brain. This could potentially lead to adverse effects, for instance, by silencing neurons that do not participate in seizure generation or propagation but which are intermingled with pathologically hyperexcitable neurons. Furthermore, the effect on neuronal excitability may persist after seizures remit. We designed a series of new activity-induced promoters based on IEG gene promoters to specifically target hyperactive neurons. Using the expression of the Kv1.1 channel as a proof of principle, we demonstrated strong anti-seizure effects. This closed-loop strategy aims to restore the physiological state of the network by returning the electrical properties of hyperactive neurons to their 'ground state'. Because the treatment switches itself off if seizures remit, it has specificity both in space (selecting between neurons that are or are not involved in episodes) and in time.

We validated these gene therapies in mouse models of TLE, which recapitulate symptoms, morphological changes and electrophysiological characteristics of TLE in human patients.

5.2. Using AAV to deliver gene therapies to the CNS

AAV is a popular choice for gene therapy carriers in the CNS because of its ability to transduce post-mitotic cells and low immunogenicity (Lisowski, Tay and Alexander, 2015). High-efficiency CNS transduction *in vivo* by AAV has been demonstrated in a wide range of mammalian species (Deverman *et al.*, 2018). Its low propensity for genomic integration is a further theoretical advantage over lentivirus and other retroviruses. The risks of insertional mutagenesis are low in post-mitotic cells such as neurons in the CNS (Choudhury *et al.*, 2017; Deverman *et al.*, 2018). The local spread

and pattern of infection of cells in the targeted area are critical determinants for successful AAV-based gene therapy (Deverman *et al.*, 2018). Intracranial or intraparenchymal delivery as we used in this project relies on clear identification of epileptic foci, which can be locally treated by direct application of the AAV virus. Eventual clinical trials could benefit from extensive and detailed mapping of epileptogenic zones, an essential component of epilepsy surgery programmes.

In the projects described here, we demonstrated high neuronal transduction efficiency with intraparenchymal injection of serotype AAV9. Alternative routes of delivery such as systemic, intra-arterial or intracerebroventricular injection may not be the best option to treat focal epilepsy, as widespread manipulation of neuronal excitability may lead to functional deficits by affecting brain regions remote from the epileptogenic zone. This limitation is, however, potentially less important for the activity-dependent gene therapy design because of its intrinsic ability to distinguish between normal and pathological activity. Indeed, global expression in the CNS could represent a new strategy that could be deployed where the seizure focus is diffuse or where multiple candidate zones occur. Indeed, in the management of patients with refractory epilepsy, a substantial number of patients are turned down for epilepsy surgery for these reasons.

Another consideration that may influence the efficacy and safety of systemic (intravascular) AAV treatment is the role of neutralising antibodies. These can either be pre-existing, found in a substantial proportion of the healthy population (Mathiesen *et al.*, 2020; Ronzitti, Gross and Mingozzi, 2020), or secondary to previous AAV administration. New engineered AAV capsids have been developed to overcome the low levels of CNS transfection following systemic delivery. AAV-PHP.B and AAV-PHP.eB have been shown to transduce CNS neurons following IV administration in mice (Deverman *et al.*, 2016). Intravenous AAV-PHP.B injection, for instance, has been shown to induce neutralising antibodies, which reduce transduction efficacy with repeated systemic injections

(Shinohara *et al.*, 2019). Whether neutralising antibodies have any effect on transduction efficacy following direct intraparenchymal injection is less clear, because immunoglobulin levels in the CSF are generally lower by at least two orders of magnitude than in the plasma. Even less is known about T-cell immunity in AAV-based CNS treatment.

Some insights into the efficacy and safety of systemically administered AAVs in humans are available from clinical trials. Historically, several adverse cases were reported from several clinical trials using viral vectors, including death as worst outcome. Zolgensma, the first intravenous AAV9 infusion gene therapy approved, treats spinal muscular atrophy (SMA) in infants (Novartis, 2019; European Medicine Agency, 2020). There are some reported adverse events, especially at very high total doses, including hepatotoxicity, kidney damage, thrombotic microangiopathy (TMA), and neuronal loss (Kuzmin *et al.*, 2021). In addition to potential safety issues from the virus itself, some concerns may also be related to dosage estimation. As human brains are drastically different from animal brains, it is extremely difficult to calculate appropriate delivery dose.

This clinical trial also emphasized the importance of long-term follow-up observations after gene therapy delivery, which is now also officially published as part of FDA guidance.

Other capsids have been developed to achieve CNS expression in non-human primates and reduce hepatic expression, which has been implicated in the toxicity of some high-dose intravenous AAV treatments. For example, AAV-PHP.B and AAV-PHP.eB viruses were engineered for high-efficiency syhstemic delivery (Deverman *et al.*, 2016). Although the AAV-PHP.B strain was developed in mice, it offered little expression in the marmoset brain when administrated intravenously, implying that the efficacy of CNS transduction depends on the host species (Matsuzaki *et al.*, 2018). Further modifications to the capsids have, however, overcome this barrier (Goertsen *et al.*, 2022).

In summary, AAV was chosen in this project because it is currently the best available option for gene therapy, with high-efficiency transduction of

neurons in the region of interest. Potential improvements in AAV capsid design may broaden the range of delivery routes of treatment.

5.3. CRISPRa-*Kcna1* gene therapy for refractory epilepsy

5.3.1. Use of CRISPRa-*kcna1* to treat refractory epilepsy

This project focused on the modulation of endogenous gene expression to alter neural circuit activity and reduce the propensity for seizures. The CRISPRa tool increased expression of the *Kcna1* gene, upregulating functional Kv1.1 channels in the membrane. This provided proof of principle that the nuclease-defective Cas9 protein is able to interact with high specificity with the target sgRNA sequence and to recruit transcriptional activators to specific loci in the genome. Targeting the region immediately upstream of the promoter region of endogenous *Kcna1* gene led to at least a 2-fold increase in functional channel expression, increasing the firing threshold of transduced excitatory neurons (Colasante *et al.*, 2020). The change in channel expression also resulted in a substantial reduction in seizure frequency, as assessed by comparing mice treated with the CRISPRa-*Kcna1* virus with mice treated with the CRISPRa-ctrl virus (Colasante *et al.*, 2020).

There are several advantages of using CRISPR to achieve specific and efficient modulation of gene expression. Other genome-targeting systems developed before the discovery of CRISPR, such as zinc-finger nucleases (ZFNs) and Transcription activator-like effector nucleases (TALENs), are less versatile with respect to the target sequences upon which they can act, restricting the pool of potential functional targets. sgRNAs working with Cas9 and related nucleases can interact with a broader range of genomic sequences for functional editing (Heidenreich and Zhang, 2016).

The Kv1.1 channel was chosen as a proof principle because it has an important role in setting the threshold for action potential generation but is also implicated in limiting the duration of action potentials in

presynaptic boutons, and thereby calcium influx and neurotransmitter release (D'Adamo *et al.*, 2013). However, the ease of reprogramming the CRISPR epigenetic editing tool allows the target gene to be swapped by changing only the sgRNA sequence. Indeed, In a parallel study, a similar strategy was used to target *Scn1a* in a mouse model of Dravet syndrome (Colasante *et al.*, 2019)..

5.3.2. Off-target genomic binding of sgRNA and potential adverse effects

Although bioinformatic tools are available to design sgRNAs, the ability to influence transcription is affected by the dynamic topology of promoter and enhancer regions and, therefore, the accessibility of the dCas9-sgRNA complex to target loci. Interestingly, even with silenced genes preferentially located in compact chromatins, the CRISPR-Cas9 complex can still activate the transcription initiation process (Perez-Pinera *et al.*, 2013; Polstein *et al.*, 2015).

We looked for off-target effects and possible consequences for clinical safety. The CRISPR platform used to generate potential sgRNA sites returned with a total of 250 off-target predictions for sg19. Among them, only six were mapped to close proximity of promoters of other genes. They were evaluated and showed no significant off-site gene modifications (Colasante *et al.*, 2020). No considerate changes in expression other than Kv1.1 channels were observed with sgRNA-dCas9 treatment in transcriptomics (Colasante *et al.*, 2020).

The inability of dCas9 to act as a nuclease means that a deleterious outcome from off-target site binding is unlikely. Moreover, CRISPRa and its complementary inhibitory CRISPRi tool are both highly sensitive to mismatches in sgRNA sequence (Kuscu *et al.*, 2014; Wu *et al.*, 2014). This property was also reported in human cells, minimising undesirable off-target effects (Duan *et al.*, 2014).

5.3.3. The immunogenicity of CRISPRa in mammalian brain

The clinical translational potential of the CRISPRa/i strategy also depends on the stable long-term expression of the components of the CRISPR system, dCas9 protein and sgRNA. Antibodies targeting CRISPR-Cas9 have been reported in some recent studies (Charlesworth *et al.*, 2019; Wagner *et al.*, 2019). Multiple reports have revealed pre-existing immunity in the human population against Cas9 orthologues, raising concerns of immune response to gene therapy based on CRISPR (Crudele and Chamberlain, 2018; Charlesworth *et al.*, 2019; Wagner *et al.*, 2019). However, when used therapeutically, dCas9 is expected to be expressed intracellularly and therefore inaccessible to extracellular antibodies. Furthermore, as pointed out above, antibody levels are generally much lower in the CSF than in the plasma. Whether T-cell immunity is likely to have an effect on the efficacy and safety of CSRPR in the brain remains to be determined (Charlesworth *et al.*, 2019).

5.3.4. Alternative transcriptional components for finely tuned modulation

This project examined the combination of the CamKII-promoter-driven deactivated spCas9 system coupled with VP64/VP160 to achieve effective endogenous *Kcna1* gene overexpression. Recently, several new molecular tools have been developed to achieve selective modulation of transcription. One important advance would be to reduce the size of the machinery that needs to be delivered. We had to split the gene therapy into two separate AAV viruses in this project, partly due to the large gene size of spCas9 (4.2kb) (Cheng *et al.*, 2013). More compact orthologue saCas9 from *Staphylococcus aureus* with shorter cDNA (3.1kb) may enable all the relevant components to be packaged into the same vector (Ran *et al.*, 2015; Gao *et al.*, 2016). The mutated sadCas9 can also be fused with transcriptional regulators (activator or repressor) for high-efficiency regulation of endogenous gene expression using an AAV vector (Lau

et al., 2019). We also used two synthetic activators, VP160 and VP64, fused with the dCas9 protein, to drive transcriptional initiation (Beerli *et al.*, 1998; Maeder *et al.*, 2013; Colasante *et al.*, 2020). Second-generation transcriptional activators have recently been reported; these include VPR (virus protein R), SAM (Synergistic Activation Mediator) and Suntag (Chavez *et al.*, 2016). They have generally shown more potent transcriptional upregulation, and have been validated for several genes and in several species and cell lines (Chavez *et al.*, 2016). Interestingly. there seems to be a negative relationship between basal expression levels and induced upregulation, suggesting that choosing target genes that are less expressed under normal conditions, we may be able to achieve more robust upregulation with CRISPRa (Chavez *et al.*, 2016).

In addition, the promoter itself can be potentially engineered for a smaller gene size without losing specificity. Currently, we use the CamKII promoter for preferential expression in pyramidal neurons; with bioinformatic studies, new promoters with shorter lengths may be possible in the future (Mich *et al.*, 2021).

5.3.5. Clinical translation of CRISPRa- *Kcna1* gene therapy

In addition to immunogenicity, off-target effects and dual-viral delivery, several points related to clinical use of dCas9-based therapy should also be addressed. For example, to increase clinical safety, it would also be useful to introduce an off switch to terminate the gene therapy when the therapeutic outcome has been achieved.

5.4. Activity-dependent gene therapy for refractory epilepsy

We have reported a potent seizure suppression effect with activity-dependent *KCNA1* overexpression in the ventral hippocampus in a chronic rodent model. This therapy was designed based on the hypothesis that pathological hyperexcitable neurons can be distinguished from normal healthy ones by the activity of an IEG

promoter. This leads to expression of the therapeutic transgene, reducing further spiking and increasing the threshold for seizure initiation or propagation. Because this inducible gene therapy is selectively activated in hyperactive neurons and not in healthy ones, it automatically biases the reduction in excitability to cells that participate in seizures.

5.4.1. Network recruitment of neurons to seizure initiation and propagation

This project was based on the assumption that in the epileptic network, cells responsible for seizure initiation or propagation are hyperactive and hyper-synchronized. Whether the same propagation pathway is involved in recurrent seizures remains unresolved. In cortical focal PTX or 4AP models, a recent study using two-photon (2P) microscopy and local field potential (LFP) recordings reported a stereotypical pattern of recruitment of neurons across the cortical layers over multiple seizures (Wenzel, Jordan P. Hamm, *et al.*, 2017). The temporal recruitment profile, however, varied between seizures and largely depended on local GABAergic interneuron function (Wenzel, Jordan P Hamm, *et al.*, 2017). This observation supports the hypothesis that selectively targeting and treating neurons directly participating in seizure initiation and propagation in an activity-dependent manner is sufficient to reduce firing propensity and prevent future seizures. Alternative single-neuron dynamic data in human focal epilepsy suggests a high level of heterogeneity in seizure propagation and neuron recruitment, which proceeds in a stochastic fashion (Truccolo *et al.*, 2011). The data showed that, although the spiking patterns were reproducible between consecutive seizures, different populations of active neurons were involved between seizures. In addition, neurons outside the initiation zone also exhibit significant changes in excitability (Truccolo *et al.*, 2011). It argues for using activity-dependent gene therapy to self-identify and self-target

neurons to activate c-FosP-*KCNA1* therapy as they become abnormal. The dynamic profile of neurons change over time, suggesting that not all neurons in the epileptic foci need to be treated in the same way.

5.4.2. Activity-inducible cFosP-*KCNA1* to treat seizure clusters in epilepsy

The activation of c-FosP-*KCNA1* depends on pre-existing hyperactivity in target neurons, and it is likely to self-terminate if the activity level falls below a pathological threshold. Many patients with focal epilepsy experience seizures that are not randomly distributed in time but are instead clustered, with multiple seizures occurring with relatively short intervals, interspersed with prolonged seizure-free periods (Haut *et al.*, 2005; Haut, 2015; Karoly *et al.*, 2021). For example, clinical studies have shown higher seizure incidence around sleep-wake transitions, with some correlation with circadian rhythms or hormonal cycles (Karoly *et al.*, 2018, 2021). Clustered seizures are often observed to occur in a cycle; the cycle then repeats itself over a longer timescale (Baud *et al.*, 2018; Lim *et al.*, 2018; Karoly *et al.*, 2021). This phenomenon has also been reported in animal epilepsy models, showing clusters of seizures separated by seizure-free periods over days or weeks (Debski *et al.*, 2020; Bernard, 2021; Rusina, Bernard and Williamson, 2021).

Activity-inducible c-FosP-*KCNA1* treatment could, in principle, be especially effective in aborting seizure clusters. This hypothesis calls for seizure clustering analysis. We were unable to test this with a sufficient sample size because most mice had entirely stopped having seizures after the treatment. It remains to be determined whether this reflects a long-term 're-set' of the epileptic focus or continued expression of the therapeutic transgene, for instance because of basal activity of the c-Fos promoter or because it is activated by neuronal activity that fell below the detection threshold.

In this project, we took ECoG recordings from the surface of the visual cortex using a machine learning tool that captures generalised

seizures. However, such recordings do not necessarily detect focal epileptiform activity inside limbic regions where seizures are thought to initiate in the intra-amygdala kainic acid model. This limitation means that 'seizure-free' only referred to the absence of generalised seizures. Continuous EcoG recording includes information for the 'seizure-free' period where a phenomenon known as 'interictal spikes' could be investigated further. Interictal spikes are a frequent biomarker of epileptogenic tissue and consist of brief high-amplitude electrographic discharges (Alarcon *et al.*, 1997). They may be sufficient to activate c-FosP-*KCNA1* therapy locally and suppress the propagation of pathological activity beyond limbic structures. This hypothesis requires further investigation. A further limitation is that we only recorded the ECoG in the preclinical animal studies up to 8 weeks after kainic acid induction. This recording time was mainly restricted by technical constraints, in particular the battery life of the wireless transmitter. If we could record for longer period beyond the initial 8 weeks, it may be possible to address the question of whether the effect of c-FosP-KCNA1 persists or there's a recurrence of seizures.

5.4.3. The effects of variable IEG promoters as potential gene therapy for epilepsy

In this project, we investigated a range of IEG promoters in addition to the original version of the c-Fos promoter. We observed a wide disparity of transgene expression among them. We included natural IEGs promoters with essential roles in synaptic plasticity and synthetic promoters designed for high sensitivity to activity dynamics. As expected, the high-potency synthetic promoter ESARE showed a strong silencing effect (Kawashima *et al.*, 2013). The synthetic ESARE promoter sequence has a low threshold for activation. Therefore, it may be possible that ESARE-*KCNA1* was activated during basal activity, explaining why it was less effective. A substantial increase in

Kcna1 expression occurred with the natural promoters of Arc and Egr1, and these were also associated with a decrease in neuronal excitability in the electrophysiology experiments. The mini-Arc promoter, composed of core transcriptional elements, did not significantly affect neuronal firing. Why this failed is unclear. In addition to their dynamic ranges, promotors may differ in their time-course of activation. potentially further contributing to the different functional outputs.

In addition, with fluorescence imaging of different promoters, the active zones within the hippocampus were not uniform. For example, c-Fos and EGR1 were consistently turned on in DG, CA2 and CA3 post-seizures, while others had a less clear pattern. The molecular mechanisms underlying the different expression profiles require further investigation. Whether different promoters would be suited to distinct epilepsy syndromes also deserves investigation. In addition, we have not yet investigated the leakiness of the IEG promoter-effector system in the absence of seizures. It could be for future investigations using electrophysiology and possibly immunohistochemistry.

Furthermore, as introduced earlier, the process of epileptogenesis prior to first spontaneous seizures occur with selected changes in gene expressions (Pitkänen *et al.*, 2015). This process introduced epileptic changes to the network, including early activation of IEGs in response to the overwhelmingly elevated activities from status epilepticus. The network dynamics continue to change during the course of the disease with various mechanisms in place, possibly as the brain attempted to restore its physiological state. Study showed that immediately after the status epilepticus, significant increase in IEG expression was observed, however, it progressively dropped over days after the status epilepticus, possibly as a result of homeostatic compensation mechanisms (Calais *et al.*, 2013). A recent study showed some evidence that there might be the relative level of IEG

expressions decreased in rat hippocampus with repetitive seizures (Kalinina *et al.*, 2022). However, the evidence for this is relatively unclear, so it remained unknown whether this may have an effect on activity-dependent gene therapy. Our data demonstrated a clear anti-seizure effect of the Kv1.1 overexpression up to 8 weeks after the kainic acid induction.

5.4.4. The anti-seizure effects of Kv1.1 channel overexpression

The fast-acting voltage-gated potassium channel Kv1.1 has an essential role in modulating action potentials. Overexpressing Kv1.1 channels led to a significant increase in the firing threshold of transduced neurons in *ex vivo* patch-clamp experiments. Kv1.1 normally co-assembles with other members of the Kv1 family and is principally expressed in axons and presynaptic boutons (Kim *et al.*, 1995; Rhodes *et al.*, 1997; Köhling and Wolfart, 2016). Presynaptic Kv1.1 channels help to terminate action potentials at boutons, thereby limiting calcium influx (Begum *et al.*, 2016). Overexpressing Kv1.1 channels in autaptic cultures reduced neurotransmitter and neurotransmitter release probability. The anti-epileptic effect of Kv1.1 overexpression may therefore be due to both a reduction in intrinsic excitability and a reduction in transmitter release from transduced neurons.

5.4.5. Cognitive deficits and elevated anxiety in the TLE model

In this work, we have shown that chronic epileptic mice generated with intra-amygdala kainic acid injection displayed memory and other behavioural deficits. We asked if these deficits could be mitigated by activity-dependent gene therapy, but we could not show significant rescue. This stands in contrast with CRISPRa treatment, which improved performance in an object location test. We have not performed detailed investigations to dissect the roles of innate responses in the tests of memory and learning. However, it is likely

that anxiety and stress are major confounds in the cognitive tests performed. Indeed, relatively few mice completed the tasks successfully.

Because c-Fos and other IEGs are extensively involved in memory formation and consolidation, it remained unclear what potential effects the activity-dependent gene therapy could have on those mechanisms or pathways.

Hippocampal theta oscillations have been related to memory consolidation and spatial recognition (Chauvière *et al.*, 2009). Loss of theta oscillations is observed in the TLE brain and is related to cognitive and memory deficits (Chauvière, 2020). An extension of the work presented here could include an assessment of theta rhythms in hippocampal circuits to determine whether they go hand-in-hand with behavioural deficits and their rescue.

5.4.6. Alternative therapeutic transgenes

Despite *in vitro* and *ex vivo* electrophysiological evidence that Kir2.1 channel overexpression hyperpolarised neurons, there was no convincing anti-epileptic effect when the *KCNJ2* transgene was used instead of *KCNA1*. Several possible explanations can be proposed. First, it is not known to what extent the membrane expression of Kir2.1 increased following spontaneous seizures when placed under the cFos promoter. Indeed, there is evidence that Kir2.1 surface expression is tightly regulated by neurons (Okada, Kano and Matsuda, 2013). This study reported that intrinsic degradation mechanisms might be activated to retrieve membrane-bound Kir2.1 channels to reduce toxicity (Okada, Kano and Matsuda, 2013). Second, because Kir2.1 is active when neurons are at their resting membrane potential, there may be unexpected homeostatic compensatory mechanisms, for instance, increasing the strength of excitatory synapses innervating transduced neurons. Third, the two channels have different expression and activity profiles. Kv1.1 channels and Kir2.1

channels are found at different sub-cellular locations (Hibino *et al.*, 2010; Kuba *et al.*, 2015), and while the Kv1.1 channel is a fast-acting voltage-sensitive ion channel, Kir2.1 is active at rest. While Kir2.1 tends to bring the resting potential close to E_k, the channel has little influence on excitability once neurons have been depolarized. Moreover, Kir2.1 is not generally thought to be expressed in axon terminals and so is unlikely to have a major influence on neurotransmitter release.

5.4.7. Future experiments and further investigations

In this project, we have investigated critical aspects of activity-dependent gene therapy and explored alternative promoter and transgene candidates to fine-tune the treatment's effectiveness. However, there are still some questions that remain unanswered. The first is related to the time course of exogenous Kv1.1 channel expression relative to endogenous Kv1.1. The transgene used in activity-dependent gene therapy here was codon optimised for human expression and contained a single-site mutation to skip a post-transcriptional editing step (Snowball *et al.*, 2019). This is based on the assumption that protein synthesis limitation is due to the use of rare codons, which seems to be poorly supported in mammalian expression systems (Mauro, 2018). Codon optimization may potentially induce abnormal protein expression levels and interfere with synthesis of other proteins. The overexpression of Kv1.1 channel may saturate membrane insertion sites for the channel, possibly as a result of ceiling effect. However, so far, there is no clear evidence to demonstrate the existence of such effect on protein synthesis in neurons. If this were to be investigated to understand the trafficking and turnover the of the Kv1.1 channel, It may be possible to attach a non-interfering epitope tag, or to use a fluorescent marker that forms a fusion protein with the channel for precise evaluation of protein turnover and membrane expression. Alternatively, a western blot

experiment to investigate whether the protein expression has increased shall be included as part of future experiments. There's also the possibilities of transcriptomics to understand fold change on a transcription level as a result of gene therapy activation.

In addition, the probability of ectopic expression of genes as a result of using viral vector deliveries in neurons may also be taken into consideration.

Moreover, we hypothesised that c-FosP-*KCNA1* gene therapy alters network excitability, reducing seizure occurrence. This was explored at the level of neurons in primary cultures using MEAs, showing reduced population firing. However, it would be important to investigate this at high resolution in different brain structures *in vivo*, for example, with Neuropixels probes which can collect high-resolution data simultaneously across the cortical and hippocampal network, in order to understand how c-FosP-*KCNA1* acts to stop generalised seizures (Jun *et al.*, 2017).

5.4.8. Potential clinical translation of cFosP-*KCNA1*

This gene therapy approach was designed with clinical translation in mind. Because the Kv1.1 channel is endogenously and abundantly expressed by neurons, it is likely to be well tolerated. AAV vectors have been chosen for several human clinical trials of neurological disorders (Hudry and Vandenberghe, 2019) and approved for some indications. Focal delivery of the gene therapy should restrict expression to the region of interest, lowering safety concerns. The activity-dependent nature of the treatment, restricted to hyperactive cells, further improves safety, and reduces the possibility of adverse effects. It will, nevertheless, be important to assess transgene expression levels in neurons with different viral titres and delivery volumes for effective therapy without negative consequences in clinical trials. A recent study of SMN (survival motor neuron) protein overexpression for treating neuromuscular disease revealed that

elevated protein synthesis could lead to aggregation and cytoplasmic toxicity in neurons (Finkel and Fischbeck, 2021). This suggests that exogenous gene delivery safety should also account for protein expression levels in neurons.

Several clinical trials of AAV9 delivered via the intrathecal or intracerebroventricular route are under way, although we are not aware of active trials of intraparenchymal delivery with AAV9 serotype. In active clinical trials with intraparenchymal delivery, serotype AAV2 and AAVrh.10 are the most favoured choices (Hudry and Vandenberghe, 2019). Therefore, the choice of AAV serotype for clinical application will also be crucial for successfully treating epilepsy.

In this study, we primarily chose intracranial administration for high biodistribution in the epileptogenic zone. Direct infusion of AAV into the brain is beneficial because it requires less viral particles and direct infusion to the target site with less immune response concerns (Hudry and Vandenberghe, 2019). Although, the procedure itself intraparenchymal delivery is not free of risks. it may be accompanied with adverse events such as nausea, injection site reactions and headaches (Kuzmin *et al.*, 2021). Alternative delivery routes may lead to less effective therapeutic outcomes; the administration route needs to be carefully evaluated before bringing it into a human study.

Interestingly, abnormally hyperexcitable network activity also occurs in other neurological diseases, including schizophrenia and Alzheimer's disease (Lam *et al.*, 2017; Chai, Ma and Jin, 2019; Nomoto *et al.*, 2021). The hyperexcitability detected in those disorders may also be potentially treatable by activity-dependent gene therapy to return network function to physiological levels. Activity-dependent gene therapy thus has potential applications to treat a range of neurological disorders beyond epilepsy.

Reference

Abbott, L. F. and Nelson, S. B. (2000) 'Synaptic plasticity: taming the beast', *Nature Neuroscience*, 3(S11), pp. 1178–1183. doi: 10.1038/81453.

Abremski, K. and Hoess, R. (1984) 'Bacteriophage P1 site-specific recombination. Purification and properties of the Cre recombinase protein', *Journal of Biological Chemistry*, 259(3), pp. 1509–1514. doi: 10.1016/s0021-9258(17)43437-5.

Abremski, K., Hoess, R. and Sternberg, N. (1983) 'Studies on the properties of P1 site-specific recombination: Evidence for topologically unlinked products following recombination', *Cell*, 32(4), pp. 1301–1311. doi: 10.1016/0092-8674(83)90311-2.

Abudayyeh, O. O. *et al.* (2016) 'C2c2 is a single-component programmable RNA-guided RNA-targeting CRISPR effector', *Science*, 353(6299). doi: 10.1126/science.aaf5573.

Agostinho, A. S. *et al.* (2019) 'Dynorphin-based "release on demand" gene therapy for drug-resistant temporal lobe epilepsy', *EMBO Molecular Medicine*, 11(10), pp. 1–16. doi: 10.15252/emmm.201809963.

Ahn, S. *et al.* (1998) ' A Dominant-Negative Inhibitor of CREB Reveals that It Is a General Mediator of Stimulus-Dependent Transcription of c- fos ', *Molecular and Cellular Biology*, 18(2), pp. 967–977. doi: 10.1128/mcb.18.2.967.

Akli, S. *et al.* (1993) 'Transfer of a foreign gene into the brain using adenovirus vectors', *Nature Genetics*, 3(3), pp. 224–228. doi: 10.1038/ng0393-224.

Alarcon, G. *et al.* (1997) 'Origin and propagation of interictal discharges in the acute electrocorticogram. Implications for pathophysiology and surgical treatment of temporal lobe epilepsy', *Brain*, 120(12), pp. 2259–2282. doi: 10.1093/brain/120.12.2259.

Ambrosini, E. *et al.* (2014) 'Genetically induced dysfunctions of Kir2.1 channels: Implications for short QT3 syndrome and autism-epilepsy phenotype', *Human Molecular Genetics*, 23(18), pp. 4875–4886. doi: 10.1093/hmg/ddu201.

Arbuckle, E. P. *et al.* (2015) 'Testing for odor discrimination and habituation in mice', *Journal of Visualized Experiments*, 2015(99), pp. 1–7. doi: 10.3791/52615.

Armstrong, C. *et al.* (2013) 'Closed-loop optogenetic intervention in mice', *Nature Protocols*, 8(8), pp. 1475–1493. doi: 10.1038/nprot.2013.080.

Artusi, S. *et al.* (2018) 'Herpes Simplex Virus Vectors for Gene Transfer to the Central Nervous System', *Diseases*, 6(3), p. 74. doi: 10.3390/diseases6030074.

Aschauer, D. F., Kreuz, S. and Rumpel, S. (2013) 'Analysis of Transduction Efficiency, Tropism and Axonal Transport of AAV Serotypes 1, 2, 5, 6, 8 and 9

in the Mouse Brain', *PLoS ONE*, 8(9), pp. 1–16. doi: 10.1371/journal.pone.0076310.

Atchison, R. W., Casto, B. C. and Hammon, W. M. D. (1965) 'Adenovirus-associated defective virus particles', *Science*, 149(3685), pp. 754–756. doi: 10.1126/science.149.3685.754.

Augustin, K. *et al.* (2018) 'Mechanisms of action for the medium-chain triglyceride ketogenic diet in neurological and metabolic disorders', *The Lancet Neurology*, 17(1), pp. 84–93. doi: 10.1016/S1474-4422(17)30408-8.

Avoli, M. (2010) *Herbert H. Jasper and the basic mechanisms of the epilepsies*, *Epilepsia*. doi: 10.1111/j.1528-1167.2010.02793.x.

Bading, H., Ginty, D. D. and Greenberg, M. E. (1993) 'Regulation of gene expression in hippocampal neurons by distinct calcium signaling pathways', *Science*, 260(5105), pp. 181–186. doi: 10.1126/science.8097060.

Baird, M. (2020) 'Progress and Challenges in Clinical AAV Gene Therapy for Neurological and Neuromuscular Disorders', *Current Trends in Clinical & Medical Sciences*, 2(2). doi: 10.33552/ctcms.2020.02.000535.

Balestrini, S. *et al.* (2021) 'The aetiologies of epilepsy', *Epileptic Disorders*, 23(1), pp. 1–16. doi: 10.1684/epd.2021.1255.

Barrangou, R. *et al.* (2007) 'CRISPR Provides Acquired Resistance Against Viruses in Prokaryotes', *Science*, 315(5819), pp. 1709–1712. doi: 10.1126/science.1138140.

Bartos, M., Vida, I. and Jonas, P. (2007) 'Synaptic mechanisms of synchronized gamma oscillations in inhibitory interneuron networks', *Nature Reviews Neuroscience*, 8(1), pp. 45–56. doi: 10.1038/nrn2044.

Bateup, H. S. *et al.* (2013) 'Temporal dynamics of a homeostatic pathway controlling neural network activity', *Frontiers in Molecular Neuroscience*, 6(SEP). doi: 10.3389/fnmol.2013.00028.

Baud, M. O. *et al.* (2018) 'Multi-day rhythms modulate seizure risk in epilepsy', *Nature Communications*, 9(1), pp. 1–10. doi: 10.1038/s41467-017-02577-y.

Bean, B. P. (2007) 'The action potential in mammalian central neurons', *Nature Reviews Neuroscience*, 8(6), pp. 451–465. doi: 10.1038/nrn2148.

Beerli, R. R. *et al.* (1998) 'Toward controlling gene expression at will: Specific regulation of the erbB-2/HER-2 promoter by using polydactyl zinc finger proteins constructed from modular building blocks', *Proceedings of the National Academy of Sciences of the United States of America*, 95(25), pp. 14628–14633. doi: 10.1073/pnas.95.25.14628.

Beghi, E. *et al.* (2019) 'Global, regional, and national burden of epilepsy, 1990–2016: a systematic analysis for the Global Burden of Disease Study 2016', *The Lancet Neurology*, 18(4), pp. 357–375. doi: 10.1016/S1474-4422(18)30454-X.

Beghi, E. (2020) 'The Epidemiology of Epilepsy', *Neuroepidemiology*, 54(2), pp. 185–191. doi: 10.1159/000503831.

Beghi, E., Giussani, G. and Sander, J. W. (2015) 'The natural history and prognosis of epilepsy', *Epileptic Disorders*, 17(3), pp. 243–253. doi: 10.1684/epd.2015.0751.

Begum, R. *et al.* (2016) 'Action potential broadening in a presynaptic channelopathy', *Nature Communications*, 7(May). doi: 10.1038/ncomms12102.

Béïque, J. C. *et al.* (2011) 'Arc-dependent synapse-specific homeostatic plasticity', *Proceedings of the National Academy of Sciences of the United States of America*, 108(2), pp. 816–821. doi: 10.1073/pnas.1017914108.

Ben-Ari, Y. *et al.* (1978) 'Diazepam pretreatment reduces distant hippocampal damage induced by intra-amygdaloid injections of kainic acid', *European Journal of Pharmacology*, 52(3–4), pp. 419–420. doi: 10.1016/0014-2999(78)90302-3.

Ben-Ari, Y. (1985) 'Limbic seizure and brain damage produced by kainic acid: Mechanisms and relevance to human temporal lobe epilepsy', *Neuroscience*, 14(2), pp. 375–403. doi: 10.1016/0306-4522(85)90299-4.

Ben-Ari, Y. (2010) 'Kainate and temporal lobe epilepsies: Three decades of progress', *Epilepsia*, 51, p. 40. doi: 10.1111/j.1528-1167.2010.02826.x.

Bendahhou, S. *et al.* (2003) 'Defective Potassium Channel Kir2.1 Trafficking Underlies Andersen-Tawil Syndrome', *Journal of Biological Chemistry*, 278(51), pp. 51779–51785. doi: 10.1074/jbc.M310278200.

Beneski, D. A. and Catterall, W. A. (1980) 'Covalent labeling of the Na+ channel with a photoactivable derivative of scorpion toxin', *Journal of Supramolecular and Cellular Biochemistry*, 12(SUPPL. 4), pp. 639–643.

Benito, E. and Barco, A. (2015) 'The Neuronal Activity-Driven Transcriptome', *Molecular Neurobiology*, 51(3), pp. 1071–1088. doi: 10.1007/s12035-014-8772-z.

Berens, C. and Hillen, W. (2003) 'Gene regulation by tetracyclines: Constraints of resistance regulation in bacteria shape TetR for application in eukaryotes', *European Journal of Biochemistry*, 270(15), pp. 3109–3121. doi: 10.1046/j.1432-1033.2003.03694.x.

Berg, A. T. *et al.* (2010) 'Revised terminology and concepts for organization of seizures and epilepsies: Report of the ILAE Commission on Classification and Terminology, 2005-2009', *Epilepsia*, 51(4), pp. 676–685. doi: 10.1111/j.1528-1167.2010.02522.x.

Berkowitz, L. A., Riabowol, K. T. and Gilman, M. Z. (1989) 'Multiple sequence elements of a single functional class are required for cyclic AMP responsiveness of the mouse c-fos promoter', *Molecular and Cellular Biology*, 9(10), pp. 4272–4281. doi: 10.1128/mcb.9.10.4272-4281.1989.

Bernard, C. (2021) ‘Circadian/multidien Molecular Oscillations and Rhythmicity of Epilepsy (MORE)’, *Epilepsia*, 62(S1), pp. S49–S68. doi: 10.1111/epi.16716.

Berndt, A. *et al.* (2014) ‘Light-Activated Chloride Channel’, 23(April), pp. 1509–1511. doi: 10.5061/dryad.9r0p6.

Bhalla, T. *et al.* (2004) ‘Control of human potassium channel inactivation by editing of a small mRNA hairpin’, *Nature Structural and Molecular Biology*, 11(10), pp. 950–956. doi: 10.1038/nsmb825.

Biervert, C. *et al.* (1998) ‘A potassium channel mutation in neonatal human epilepsy’, *Science*, 279(5349), pp. 403–406. doi: 10.1126/science.279.5349.403.

Bischofberger, J. *et al.* (2006) ‘Patch-clamp recording from mossy fiber terminals in hippocampal slices’, *Nature Protocols*, 1(4), pp. 2075–2081. doi: 10.1038/nprot.2006.312.

Bito, H., Deisseroth, K. and Tsien, R. W. (1996) ‘CREB phosphorylation and dephosphorylation: A Ca2+- and stimulus duration-dependent switch for hippocampal gene expression’, *Cell*, 87(7), pp. 1203–1214. doi: 10.1016/S0092-8674(00)81816-4.

Black, D. C. (1897) *The treatment of epilepsy*, *British Medical Journal*. doi: 10.1136/bmj.1.1888.625.

Blauwblomme, T., Jiruska, P. and Huberfeld, G. (2014) *Mechanisms of ictogenesis*. 1st edn, *International Review of Neurobiology*. 1st edn. Elsevier Inc. doi: 10.1016/B978-0-12-418693-4.00007-8.

Blömer, U. *et al.* (1996) ‘Applications of gene therapy to the CNS’, *Human Molecular Genetics*, 5(REVIEW), pp. 1397–1404. doi: 10.1093/hmg/5.supplement_1.1397.

Bloodgood, B. L. *et al.* (2013) ‘The activity-dependent transcription factor NPAS4 regulates domain-specific inhibition’, *Nature*, 503(7474), pp. 121–125. doi: 10.1038/nature12743.

Blumcke, I. *et al.* (2017) ‘Histopathological Findings in Brain Tissue Obtained during Epilepsy Surgery’, *New England Journal of Medicine*, 377(17), pp. 1648–1656. doi: 10.1056/nejmoa1703784.

De Boer, T. P. *et al.* (2010) ‘The mammalian KIR2.x inward rectifier ion channel family: Expression pattern and pathophysiology’, *Acta Physiologica*, 199(3), pp. 243–256. doi: 10.1111/j.1748-1716.2010.02108.x.

Boison, D. (2006) ‘Adenosine kinase, epilepsy and stroke: mechanisms and therapies’, *Trends in Pharmacological Sciences*, 27(12), pp. 652–658. doi: 10.1016/j.tips.2006.10.008.

Bologna, L. L. *et al.* (2010) ‘Investigating neuronal activity by SPYCODE multi-channel data analyzer’, *Neural Networks*, 23(6), pp. 685–697. doi:

10.1016/j.neunet.2010.05.002.

Booker, S. A., Song, J. and Vida, I. (2014) 'Whole-cell Patch-clamp Recordings from Morphologically- and Neurochemically-identified Hippocampal Interneurons', *Journal of Visualized Experiments*, (91), p. e51706. doi: 10.3791/51706.

Botterill, J. J. *et al.* (2019) 'An Excitatory and Epileptogenic Effect of Dentate Gyrus Mossy Cells in a Mouse Model of Epilepsy', *Cell Reports*, 29(9), pp. 2875-2889.e6. doi: 10.1016/j.celrep.2019.10.100.

Bouilleret, V. *et al.* (1999) 'Recurrent seizures and hippocampal sclerosis following intrahippocampal kainate injection in adult mice: Electroencephalography, histopathology and synaptic reorganization similar to mesial temporal lobe epilepsy', *Neuroscience*, 89(3), pp. 717–729. doi: 10.1016/S0306-4522(98)00401-1.

Bout, A. (1996) 'Prospects for human gene therapy', *European Journal of Drug Metabolism and Pharmacokinetics*, 21(2), pp. 175–179. doi: 10.1007/BF03190267.

Boyden, E. S. *et al.* (2005) 'Millisecond-timescale, genetically targeted optical control of neural activity', *Nature Neuroscience*, 8(9), pp. 1263–1268. doi: 10.1038/nn1525.

Bramham, C. R. and Wells, D. G. (2007) 'Dendritic mRNA: Transport, translation and function', *Nature Reviews Neuroscience*, 8(10), pp. 776–789. doi: 10.1038/nrn2150.

van Breemen, M. S., Wilms, E. B. and Vecht, C. J. (2007) 'Epilepsy in patients with brain tumours: epidemiology, mechanisms, and management', *The Lancet Neurology*, 6(5), pp. 421–430. doi: 10.1016/S1474-4422(07)70103-5.

Brew, H. M., Hallows, J. L. and Tempel, B. L. (2003) 'Hyperexcitability reduced low threshold potassium currents auditory neurons of mice lacking the channel subunit Kv1.1', *Journal of Physiology*, 548(1), pp. 1–20. doi: 10.1113/jphysiol.2002.035568.

Brodtkorb, E. and Sjaastad, O. (2008) 'Epilepsy prevalence by individual interview in a Norwegian community', *Seizure*, 17(7), pp. 646–650. doi: 10.1016/j.seizure.2008.03.005.

Brown, D. A. and Passmore, G. M. (2009) 'Neural KCNQ (Kv7) channels', *British Journal of Pharmacology*, 156(8), pp. 1185–1195. doi: 10.1111/j.1476-5381.2009.00111.x.

Bryant, L. M. *et al.* (2013) 'Lessons learned from the clinical development and market authorization of Glybera.', *Human gene therapy. Clinical development*, 24(2), pp. 55–64. doi: 10.1089/humc.2013.087.

Buckmaster, P. S. (2012) 'Mossy Fiber Sprouting in the Dentate Gyrus.', in Noebels, J. L. et al. (eds). Bethesda (MD).

Büeler, H. (1999) ‘Adeno-associated viral vectors for gene transfer and gene therapy’, *Biological Chemistry*, 380(6), pp. 613–622. doi: 10.1515/BC.1999.078.

Buzsáki, G. (2015) ‘Hippocampal sharp wave-ripple: A cognitive biomarker for episodic memory and planning’, *Hippocampus*, 25(10), pp. 1073–1188. doi: 10.1002/hipo.22488.

Buzsáki, G., Anastassiou, C. A. and Koch, C. (2012) ‘The origin of extracellular fields and currents-EEG, ECoG, LFP and spikes’, *Nature Reviews Neuroscience*, 13(6), pp. 407–420. doi: 10.1038/nrn3241.

Calais, J. B. *et al.* (2013) ‘Long-term decrease in immediate early gene expression after electroconvulsive seizures’, *Journal of Neural Transmission*, 120(2), pp. 259–266. doi: 10.1007/s00702-012-0861-4.

Cascino, G. D. and Sirven, J. I. (2011) ‘Adult Epilepsy’, *Adult Epilepsy*, pp. 1087–1100. doi: 10.1002/9780470975039.

Catterall, W. A. (2012) ‘Voltage-gated sodium channels at 60: Structure, function and pathophysiology’, *Journal of Physiology*, 590(11), pp. 2577–2589. doi: 10.1113/jphysiol.2011.224204.

Catterall, W. A., Kalume, F. and Oakley, J. C. (2010) ‘NaV1.1 channels and epilepsy’, *Journal of Physiology*, 588(11), pp. 1849–1859. doi: 10.1113/jphysiol.2010.187484.

Cavarsan, C. F. *et al.* (2018) ‘Is mossy fiber sprouting a potential therapeutic target for epilepsy?’, *Frontiers in Neurology*, 9(NOV), pp. 1–13. doi: 10.3389/fneur.2018.01023.

Cavazzana-Calvo, M. *et al.* (2000) ‘Gene therapy of human severe combined immunodeficiency (SCID)-X1 disease’, *Science*, 288(5466), pp. 669–672. doi: 10.1126/science.288.5466.669.

Cela, E. *et al.* (2019) ‘An Optogenetic Kindling Model of Neocortical Epilepsy’, *Scientific Reports*, 9(1), pp. 1–12. doi: 10.1038/s41598-019-41533-2.

Chai, Z., Ma, C. and Jin, X. (2019) ‘Homeostatic activity regulation as a mechanism underlying the effect of brain stimulation’, *Bioelectronic Medicine*, 5(1), pp. 1–9. doi: 10.1186/s42234-019-0032-0.

Challis, R. C. *et al.* (2019) ‘Systemic AAV vectors for widespread and targeted gene delivery in rodents’, *Nature Protocols*, 14(2), pp. 379–414. doi: 10.1038/s41596-018-0097-3.

Chan, K. Y. *et al.* (2017) ‘Engineered AAVs for efficient noninvasive gene delivery to the central and peripheral nervous systems’, *Nature Neuroscience*, 20(8), pp. 1172-+. doi: 10.1038/nn.4593.

Chang, B. S. and Lowenstein, D. H. (2003) ‘Epilepsy’, *New England Journal of Medicine*, 349(13), pp. 1257–1266. doi: 10.1056/NEJMra022308.

Charlesworth, C. T. *et al.* (2019) ‘Identification of preexisting adaptive

immunity to Cas9 proteins in humans', *Nature Medicine*, 25(2), pp. 249–254. doi: 10.1038/s41591-018-0326-x.

Chauvière, L. *et al.* (2009) 'Early deficits in spatial memory and theta rhythm in experimental temporal lobe epilepsy', *Journal of Neuroscience*, 29(17), pp. 5402–5410. doi: 10.1523/JNEUROSCI.4699-08.2009.

Chauvière, L. (2020) 'Potential causes of cognitive alterations in temporal lobe epilepsy', *Behavioural Brain Research*, 378(October 2019), p. 112310. doi: 10.1016/j.bbr.2019.112310.

Chavez, A. *et al.* (2016) 'Comparison of Cas9 activators in multiple species', *Nature Methods*, 13(7), pp. 563–567. doi: 10.1038/nmeth.3871.

Cheah, C. S. *et al.* (2012) 'Specific deletion of NaV1.1 sodium channels in inhibitory interneurons causes seizures and premature death in a mouse model of Dravet syndrome', *Proceedings of the National Academy of Sciences of the United States of America*, 109(36), pp. 14646–14651. doi: 10.1073/pnas.1211591109.

Chen, X. R. *et al.* (2010) 'Structure of the full-length Shaker potassium channel Kv1.2 by normal-mode-based X-ray crystallographic refinement', *Proceedings of the National Academy of Sciences of the United States of America*, 107(25), pp. 11352–11357. doi: 10.1073/pnas.1000142107.

Cheng, A. W. *et al.* (2013) 'Multiplexed activation of endogenous genes by CRISPR-on, an RNA-guided transcriptional activator system', *Cell Research*, 23(10), pp. 1163–1171. doi: 10.1038/cr.2013.122.

Chiappalone, M. *et al.* (2006) 'Dissociated cortical networks show spontaneously correlated activity patterns during in vitro development', *Brain Research*, 1093(1), pp. 41–53. doi: 10.1016/j.brainres.2006.03.049.

Chirmule, N. *et al.* (1999) 'Immune responses to adenovirus and adeno-associated virus in humans', *Gene Therapy*, 6(9), pp. 1574–1583. doi: 10.1038/sj.gt.3300994.

Chiu, R. *et al.* (1988) 'The c-fos protein interacts with c-Jun AP-1 to stimulate transcription of AP-1 responsive genes', *Cell*, 54(4), pp. 541–552. doi: 10.1016/0092-8674(88)90076-1.

Chiu, R., Angel, P. and Karin, M. (1989) 'Jun-B differs in its biological properties from, and is a negative regulator of, c-Jun', *Cell*, 59(6), pp. 979–986. doi: 10.1016/0092-8674(89)90754-X.

Choudhury, S. R. *et al.* (2017) 'Viral vectors for therapy of neurologic diseases', *Neuropharmacology*, 120, pp. 63–80. doi: 10.1016/j.neuropharm.2016.02.013.

Chowdhury, S. *et al.* (2006) 'Arc/Arg3.1 Interacts with the Endocytic Machinery to Regulate AMPA Receptor Trafficking', *Neuron*, 52(3), pp. 445–459. doi: 10.1016/j.neuron.2006.08.033.

Christian-Hinman, C. A. (2021) ‘Is On-Demand Dynorphin Destined to Be in Demand to Decrease Seizures?’, *Epilepsy Currents*, 21(1), pp. 48–50. doi: 10.1177/1535759720951791.

Christiansen, M. G., Senko, A. W. and Anikeeva, P. (2019) ‘Magnetic Strategies for Nervous System Control’, *Annual Review of Neuroscience*, 42, pp. 271–293. doi: 10.1146/annurev-neuro-070918-050241.

Chu, D. *et al.* (2003) ‘Direct comparison of efficiency and stability of gene transfer into the mammalian heart using adeno-associated virus versus adenovirus vectors’, *Journal of Thoracic and Cardiovascular Surgery*, 126(3), pp. 671–679. doi: 10.1016/S0022-5223(03)00082-5.

Chung, L. (2015) ‘A Brief Introduction to the Transduction of Neural Activity into Fos Signal’, *Development & Reproduction*, 19(2), pp. 61–67. doi: 10.12717/dr.2015.19.2.061.

Cobb, S. R. *et al.* (1995) ‘Synchronization of neuronal activity in hippocampus by individual GABAergic interneurons’, *Nature*, 378(6552), pp. 75–78. doi: 10.1038/378075a0.

Colasante, G. *et al.* (2019) ‘dCas9-Based Scn1a Gene Activation Restores Inhibitory Interneuron Excitability and Attenuates Seizures in Dravet Syndrome Mice’, *Molecular Therapy*, 28(1), pp. 235–253. doi: 10.1016/j.ymthe.2019.08.018.

Colasante, G. *et al.* (2020) ‘In vivo CRISPRa decreases seizures and rescues cognitive deficits in a rodent model of epilepsy’, *Brain*, 143(3), pp. 891–905. doi: 10.1093/brain/awaa045.

Colombi, I. *et al.* (2013) ‘Effects of antiepileptic drugs on hippocampal neurons coupled to micro-electrode arrays’, *Frontiers in Neuroengineering*, 6(NOV), pp. 1–11. doi: 10.3389/fneng.2013.00010.

Cong, L. *et al.* (2013) ‘Multiplex Genome Engineering Using CRISPR/Cas Systems’, *Science*, 339(6121), pp. 819–823. doi: 10.1126/science.1231143.

Conte, G. *et al.* (2020) ‘High concordance between hippocampal transcriptome of the mouse intra-amygdala kainic acid model and human temporal lobe epilepsy’, *Epilepsia*, 61(12), pp. 2795–2810. doi: 10.1111/epi.16714.

Costa, A. M. *et al.* (2020) ‘Status epilepticus dynamics predicts latency to spontaneous seizures in the kainic acid model’, *Cellular Physiology and Biochemistry*, 54(3), pp. 493–507. doi: 10.33594/000000232.

Cotterill, E. *et al.* (2016) ‘Characterization of early cortical neural network development in multiwell microelectrode array plates’, *Journal of Biomolecular Screening*, 21(5), pp. 510–519. doi: 10.1177/1087057116640520.

CRAWFORD, I. L. and CONNOR, J. D. (1973) ‘Localization and Release of Glutamic Acid in Relation to the Hippocampal Mossy Fibre Pathway’, *Nature*,

244(5416), pp. 442–443. doi: 10.1038/244442a0.

Crudele, J. M. and Chamberlain, J. S. (2018) 'Cas9 immunity creates challenges for CRISPR gene editing therapies', *Nature Communications*, 9(1), pp. 9–11. doi: 10.1038/s41467-018-05843-9.

Cully, D. F. *et al.* (1994) 'Cloning of an avermectin-sensitive glutamate-gated chloride channel from Caenorhabditis elegans', *Nature*, 371(6499), pp. 707–711. doi: 10.1038/371707a0.

Curran, T. and Teich, N. M. (1982) 'Identification of a 39,000-dalton protein in cells transformed by the FBJ murine osteosarcoma virus', *Virology*, 116(1), pp. 221–235. doi: https://doi.org/10.1016/0042-6822(82)90415-9.

de Curtis, M. and Avanzini, G. (2001) 'Interictal spikes in focal epileptogenesis', *Progress in Neurobiology*, 63(5), pp. 541–567. doi: 10.1016/S0301-0082(00)00026-5.

de Curtis, M. and Avoli, M. (2015) 'Initiation, propagation, and termination of partial (Focal) seizures', *Cold Spring Harbor Perspectives in Medicine*, 5(7), pp. 1–15. doi: 10.1101/cshperspect.a022368.

de Curtis, M., Librizzi, L. and Avanzini, G. (2015) *Mechanisms of Focal Epileptogenesis*, *Epilepsy and Brain Tumors*. Elsevier Inc. doi: 10.1016/B978-0-12-417043-8.00006-7.

D'adamo, M. C. *et al.* (2020) 'Kv1.1 channelopathies: Pathophysiological mechanisms and therapeutic approaches', *International Journal of Molecular Sciences*, 21(8), pp. 1–21. doi: 10.3390/ijms21082935.

D'Adamo, M. C. *et al.* (1999) ' Mutations in the KCNA1 gene associated with episodic ataxia type-1 syndrome impair heteromeric voltage-gated K + channel function ', *The FASEB Journal*, 13(11), pp. 1335–1345. doi: 10.1096/fasebj.13.11.1335.

D'Adamo, M. C. *et al.* (2013) 'K+ channelepsy: Progress in the neurobiology of potassium channels and epilepsy', *Frontiers in Cellular Neuroscience*, 7(SEP), pp. 1–21. doi: 10.3389/fncel.2013.00134.

Deacon, R. M. J. and Rawlins, J. N. P. (2006) 'T-maze alternation in the rodent', *Nature Protocols*, 1(1), pp. 7–12. doi: 10.1038/nprot.2006.2.

Debski, K. J. *et al.* (2020) 'The circadian dynamics of the hippocampal transcriptome and proteome is altered in experimental temporal lobe epilepsy', *Science Advances*, 6(41), pp. 1–16. doi: 10.1126/sciadv.aat5979.

Decher, N. *et al.* (2010) 'RNA editing modulates the binding of drugs and highly unsaturated fatty acids to the open pore of Kv potassium channels', *EMBO Journal*, 29(13), pp. 2101–2113. doi: 10.1038/emboj.2010.88.

Dember, W. N. and Fowler, H. (1958) 'Spontaneous alternation behavior.', *Psychological Bulletin*. US: American Psychological Association, pp. 412–428. doi: 10.1037/h0045446.

Deverman, B. E. *et al.* (2016) 'Cre-dependent selection yields AAV variants for widespread gene transfer to the adult brain', *Nature Biotechnology*, 34(2), pp. 204–209. doi: 10.1038/nbt.3440.

Deverman, B. E. *et al.* (2018) 'Gene therapy for neurological disorders: Progress and prospects', *Nature Reviews Drug Discovery*, 17(9), pp. 641–659. doi: 10.1038/nrd.2018.110.

Devinsky, O. *et al.* (2018) 'Epilepsy', *Nature Reviews Disease Primers*, 4(May). doi: 10.1038/nrdp.2018.24.

De Deyn, P. P. *et al.* (1992) 'Chemical models of epilepsy with some reference to their applicability in the development of anticonvulsants', *Epilepsy Research*, 12(2), pp. 87–110. doi: 10.1016/0920-1211(92)90030-W.

Dimidschstein, J. *et al.* (2016) 'A viral strategy for targeting and manipulating interneurons across vertebrate species', *Nature Neuroscience*, 19(12), pp. 1743–1749. doi: 10.1038/nn.4430.

Doyle, D. A. *et al.* (1998) 'The structure of the potassium channel: Molecular basis of K+ conduction and selectivity', *Science*, 280(5360), pp. 69–77. doi: DOI 10.1126/science.280.5360.69.

Drexel, M. *et al.* (2017) 'Selective silencing of hippocampal parvalbumin interneurons induces development of recurrent spontaneous limbic seizures in mice', *Journal of Neuroscience*, 37(34), pp. 8166–8179. doi: 10.1523/jneurosci.3456-16.2017.

Duan, J. *et al.* (2014) 'Genome-wide identification of CRISPR/Cas9 off-targets in human genome', *Cell Research*, 24(8), pp. 1009–1012. doi: 10.1038/cr.2014.87.

Duclot, F. and Kabbaj, M. (2017) 'The role of early growth response 1 (EGR1) in brain plasticity and neuropsychiatric disorders', *Frontiers in Behavioral Neuroscience*, 11(March), pp. 1–20. doi: 10.3389/fnbeh.2017.00035.

During, M. J. and Spencer, D. D. (1993) 'Extracellular hippocampal glutamate and spontaneous seizure in the conscious human brain', *The Lancet*, 341(8861), pp. 1607–1610. doi: 10.1016/0140-6736(93)90754-5.

Van Dyke, D. H. *et al.* (1975) 'Hereditary myokymia and periodic ataxia', *Journal of the Neurological Sciences*, 25(1), pp. 109–118. doi: 10.1016/0022-510X(75)90191-4.

Ebert, D. H. and Greenberg, M. E. (2013) 'Activity-dependent neuronal signalling and autism spectrum disorder', *Nature*, 493(7432), pp. 327–337. doi: 10.1038/nature11860.

Eferl, R. and Wagner, E. F. (2003) 'AP-1: A double-edged sword in tumorigenesis', *Nature Reviews Cancer*, 3(11), pp. 859–868. doi: 10.1038/nrc1209.

Ellis, C. A., Petrovski, S. and Berkovic, S. F. (2020) 'Epilepsy genetics: clinical

impacts and biological insights', *The Lancet Neurology*, 19(1), pp. 93–100. doi: 10.1016/S1474-4422(19)30269-8.

Engel J., J. (1998) 'Etiology as a risk factor for medically refractory epilepsy: A case for early surgical intervention', *Neurology*, 51(5), pp. 1243–1244. doi: 10.1212/wnl.51.5.1243.

Engel J., J. (2001) 'Mesial temporal lobe epilepsy: What have we learned?', *Neuroscientist*, 7(4), pp. 340–352. doi: 10.1177/107385840100700410.

Erles, K., Sebökovà, P. and Schlehofer, J. R. (1999) 'Update on the prevalence of serum antibodies (IgG and IgM) to adeno- associated virus (AAV)', *Journal of Medical Virology*, 59(3), pp. 406–411. doi: 10.1002/(SICI)1096-9071(199911)59:3<406::AID-JMV22>3.0.CO;2-N.

Van Erum, J., Van Dam, D. and De Deyn, P. P. (2019) 'PTZ-induced seizures in mice require a revised Racine scale', *Epilepsy and Behavior*, 95, pp. 51–55. doi: 10.1016/j.yebeh.2019.02.029.

European Medicine Agency (2020) *Zolgensma*. Available at: https://www.ema.europa.eu/en/medicines/human/EPAR/zolgensma#assessment-history-section.

Eytan, D. and Marom, S. (2006) 'Dynamics and effective topology underlying synchronization in networks of cortical neurons', *Journal of Neuroscience*, 26(33), pp. 8465–8476. doi: 10.1523/JNEUROSCI.1627-06.2006.

FDA/CBER (2020) 'Long Term Follow-Up After Administration of Human Gene Therapy Products Draft Guidance for Industry', *Fda*, (January), pp. 1–37. Available at: https://www.fda.gov/BiologicsBloodVaccines/GuidanceComplianceRegulatoryInformation/Guid.

Fendt, M. and Fanselow, M. S. (1999) 'The neuroanatomical and neurochemical basis of conditioned fear', *Neuroscience and Biobehavioral Reviews*, 23(5), pp. 743–760. doi: 10.1016/S0149-7634(99)00016-0.

Fiest, K. M. *et al.* (2017) 'Prevalence and incidence of epilepsy', *Neurology*, 88(3), pp. 296–303. doi: 10.1212/WNL.0000000000003509.

Finkel, R. S. and Fischbeck, K. H. (2021) 'Maybe too much of a good thing in gene therapy', *Nature Neuroscience*, (May), pp. 8–9. doi: 10.1038/s41593-021-00882-w.

Fisher, R. S. *et al.* (2014) 'ILAE Official Report: A practical clinical definition of epilepsy', *Epilepsia*, 55(4), pp. 475–482. doi: 10.1111/epi.12550.

Flavell, S. W. and Greenberg, M. E. (2008) 'Signaling mechanisms linking neuronal activity to gene expression and plasticity of the nervous system', *Annual Review of Neuroscience*, 31, pp. 563–590. doi: 10.1146/annurev.neuro.31.060407.125631.

Flood, W. D. *et al.* (2004) 'Nxf and Fbxo33: Novel seizure-responsive genes in

mice', *European Journal of Neuroscience*, 20(7), pp. 1819–1826. doi: 10.1111/j.1460-9568.2004.03646.x.

Fornasiero, E. F. *et al.* (2018) 'Precisely measured protein lifetimes in the mouse brain reveal differences across tissues and subcellular fractions', *Nature Communications*, 9(1). doi: 10.1038/s41467-018-06519-0.

Foulkes, N. S. and Sassone-Corsi, P. (1992) 'More is better: Activators and repressors from the same gene', *Cell*, 68(3), pp. 411–414. doi: 10.1016/0092-8674(92)90178-F.

Friedmann, T. and Roblin, R. (1972) 'Gene Therapy for Human', *Science*, 175(4025), pp. 949–955.

Fukata, Y. (2006) 'Epilepsy-Related Ligand/Receptor Complex LGI1 and ADAM22 Regulate Synaptic Transmission', *Science*, 313(5794), pp. 1792–1795. doi: 10.1126/science.1129947.

Fukata, Y. *et al.* (2021) 'LGI1–ADAM22–MAGUK configures transsynaptic nanoalignment for synaptic transmission and epilepsy prevention', *Proceedings of the National Academy of Sciences*, 118(3), p. e2022580118. doi: 10.1073/pnas.2022580118.

Furshpan, E. J. and Potter, D. D. (1989) 'Seizure-like activity and cellular damage in rat hippocampal neurons in cell culture', *Neuron*, 3(2), pp. 199–207. doi: 10.1016/0896-6273(89)90033-0.

Furtinger, S. *et al.* (2001) 'Plasticity of Y1 and Y2 receptors and neuropeptide Y fibers in patients with temporal lobe epilepsy', *Journal of Neuroscience*, 21(15), pp. 5804–5812. doi: 10.1523/jneurosci.21-15-05804.2001.

Gaitatzis, A., Sisodiya, S. M. and Sander, J. W. (2012) 'The somatic comorbidity of epilepsy: A weighty but often unrecognized burden', *Epilepsia*, 53(8), pp. 1282–1293. doi: 10.1111/j.1528-1167.2012.03528.x.

Gallo, F. T. *et al.* (2018) 'Immediate early genes, memory and psychiatric disorders: Focus on c-Fos, Egr1 and Arc', *Frontiers in Behavioral Neuroscience*, 12(April), pp. 1–16. doi: 10.3389/fnbeh.2018.00079.

Gao, Y. *et al.* (2016) 'Complex transcriptional modulation with orthogonal and inducible dCas9 regulators', *Nature Methods*, 13(12), pp. 1043–1049. doi: 10.1038/nmeth.4042.

Gau, D. *et al.* (2002) 'Phosphorylation of CREB Ser142 Regulates Light-Induced Phase Shifts of the Circadian Clock being the day-night cycle. Indeed, light pulses applied during early or late subjective night result in phase de-lays or advances, respectively, while light pulses ', *Neuron*, 34, pp. 245–253. Available at: https://ac.els-cdn.com/S0896627302006566/1-s2.0-S0896627302006566-main.pdf?_tid=5529a694-b679-4c40-a25f-c65dd17cea02&acdnat=1541367489_e2d740db0827dc705494f4a81cd87985.

Geis, C. *et al.* (2019) 'Autoimmune seizures and epilepsy', *Journal of Clinical Investigation*, 129(3), pp. 926–940. doi: 10.1172/JCI125178.

Ghosh, A. and Greenberg, M. (1995) 'Calcium signaling in neurons: molecular mechanisms and cellular consequences', *Science*, 268(5208), pp. 239–247. doi: 10.1126/science.7716515.

Gibson, A. P. and Patel, N. C. (2008) 'Mechanisms of action of antiepileptic drugs', *Antiepileptic Drugs to Treat Psychiatric Disorders*, pp. 1–15. doi: 10.3109/9780849382666-4.

Gilbert, L. A. *et al.* (2013) 'CRISPR-Mediated Modular RNA-Guided Regulation of Transcription in Eukaryotes', *Cell*, 154(2), pp. 442–451. doi: 10.1016/j.cell.2013.06.044.

Gilbert, L. A. *et al.* (2014) 'Genome-Scale CRISPR-Mediated Control of Gene Repression and Activation', *Cell*, 159(3), pp. 647–661. doi: 10.1016/j.cell.2014.09.029.

Goddard, G. V (1983) 'The Kindling Model of Epilepsy', *Trends in Neurosciences*, 6(7), pp. 275–279. doi: Doi 10.1016/0166-2236(83)90118-2.

Goertsen, D. *et al.* (2022) 'AAV capsid variants with brain-wide transgene expression and decreased liver targeting after intravenous delivery in mouse and marmoset', *Nature Neuroscience*, 25(1), pp. 106–115. doi: 10.1038/s41593-021-00969-4.

Gomez, J. L. *et al.* (2017) 'Chemogenetics revealed: DREADD occupancy and activation via converted clozapine', *Science*, 357(6350), pp. 503–507. doi: 10.1126/science.aan2475.

Gootenberg, J. S. *et al.* (2017) 'Nucleic acid detection with CRISPR-Cas13a/C2c2', *Science*, 356(6336), pp. 438–442. doi: 10.1126/science.aam9321.

Gossen, M. *et al.* (1995) 'Transcriptional activation by tetracyclines in mammalian cells', *Science*, 268(5218), pp. 1766–1769. doi: 10.1126/science.7792603.

Gossen, M. and Bujard, H. (1992) 'Tight Control of Gene-Expression in Mammalian-Cells by Tetracycline-Responsive Promoters', *Proceedings of the National Academy of Sciences of the United States of America*, 89(12), pp. 5547–5551. doi: DOI 10.1073/pnas.89.12.5547.

Gottfried, J. A. (2010) 'Central mechanisms of odour object perception', *Nature Reviews Neuroscience*, 11(9), pp. 628–641. doi: 10.1038/nrn2883.

Gourmaud, S. *et al.* (2020) 'Alzheimer-like amyloid and tau alterations associated with cognitive deficit in temporal lobe epilepsy', *Brain*, 143(1), pp. 191–209. doi: 10.1093/brain/awz381.

Graves, T. D. *et al.* (2014) 'Episodic ataxia type 1: Clinical characterization, quality of life and genotype-phenotype correlation', *Brain*, 137(4), pp. 1009–1018. doi: 10.1093/brain/awu012.

Graybuck, L. T. *et al.* (2021) 'Enhancer viruses for combinatorial cell-subclass-

specific labeling', *Neuron*, 109(9), pp. 1449-1464.e13. doi: 10.1016/j.neuron.2021.03.011.

Greenberg, M. E., Thompson, M. A. and Sheng, M. (1992) 'Calcium regulation of immediate early gene transcription', *Journal of Physiology - Paris*, 86(1–3), pp. 99–108. doi: 10.1016/S0928-4257(05)80013-0.

Greenberg, M. E. and Ziff, E. B. (1984) 'Stimulation of 3T3 cells induces transcription of the c-fos proto-oncogene', *Nature*, 311(5985), pp. 433–438. doi: 10.1038/311433a0.

Greenberg, M. E., Ziff, E. B. and Greene, L. A. (1986) 'Stimulation of neuronal acetylcholine receptors induces rapid gene transcription', *Science*, 234(4772), pp. 80–83. doi: 10.1126/science.3749894.

Greer, P. L. and Greenberg, M. E. (2008) 'From Synapse to Nucleus: Calcium-Dependent Gene Transcription in the Control of Synapse Development and Function', *Neuron*, 59(6), pp. 846–860. doi: 10.1016/j.neuron.2008.09.002.

Grieger, J. C., Choi, V. W. and Samulski, R. J. (2006) 'Production and characterization of adeno-associated viral vectors', *Nature Protocols*, 1(3), pp. 1412–1428. doi: 10.1038/nprot.2006.207.

Grieger, J. C. and Samulski, R. J. (2005) 'Packaging Capacity of Adeno-Associated Virus Serotypes: Impact of Larger Genomes on Infectivity and Postentry Steps', *Journal of Virology*, 79(15), pp. 9933–9944. doi: 10.1128/jvi.79.15.9933-9944.2005.

Guerrini, R. and Dobyns, W. B. (2014) 'Malformations of cortical development: Clinical features and genetic causes', *The Lancet Neurology*, 13(7), pp. 710–726. doi: 10.1016/S1474-4422(14)70040-7.

Gulyás, A. I. and Freund, T. T. (2015) 'Generation of physiological and pathological high frequency oscillations: The role of perisomatic inhibition in sharp-wave ripple and interictal spike generation', *Current Opinion in Neurobiology*, 31, pp. 26–32. doi: 10.1016/j.conb.2014.07.020.

Guzowski, J. F. *et al.* (1999) 'Environment-specific expression of the immediate-early gene Arc in hippocampal neuronal ensembles', *Nature Neuroscience*, 2(12), pp. 1120–1124. doi: 10.1038/16046.

Guzowski, J. F. *et al.* (2005) 'Mapping behaviorally relevant neural circuits with immediate-early gene expression', *Current Opinion in Neurobiology*, 15(5), pp. 599–606. doi: 10.1016/j.conb.2005.08.018.

Habener, J. F. (1990) 'Cyclic AMP response element binding proteins: A cornucopia of transcription factors', *Molecular Endocrinology*, 4(8), pp. 1087–1094. doi: 10.1210/mend-4-8-1087.

Hacein-Bey-Abina, S. *et al.* (2003) 'A Serious Adverse Event after Successful Gene Therapy for X-Linked Severe Combined Immunodeficiency', *New England Journal of Medicine*, 348(3), pp. 255–256. doi: 10.1056/nejm200301163480314.

Hacein-Bey-Abina, S. *et al.* (2008) 'Insertional oncogenesis in 4 patients after retrovirus-mediated gene therapy of SCID-X1', *Journal of Clinical Investigation*, 118(9), pp. 3132–3142. doi: 10.1172/JCI35700.

Hadley, J. K. *et al.* (2003) 'Stoichiometry of expressed KCNQ2/KCNQ3 potassium channels and subunit composition of native ganglionic M channels deduced from block by tetraethylammonium', *Journal of Neuroscience*, 23(12), pp. 5012–5019. doi: 10.1523/jneurosci.23-12-05012.2003.

Hagiwara, S. and Takahashi, K. (1974) 'The anomalous rectification and cation selectivity of the membrane of a starfish egg cell', *The Journal of Membrane Biology*, 18(1), pp. 61–80. doi: 10.1007/BF01870103.

Hales, C. M., Rolston, J. D. and Potter, S. M. (2010) 'How to culture, record and stimulate neuronal networks on micro-electrode arrays (MEAs)', *Journal of Visualized Experiments*, (39), pp. 1–7. doi: 10.3791/2056.

Hall, C. S. (1934) 'Emotional behavior in the rat. I. Defecation and urination as measures of individual differences in emotionality.', *Journal of Comparative Psychology*, 18(3), pp. 385–403. doi: 10.1037/h0071444.

Han, Z. *et al.* (2020) 'Antisense oligonucleotides increase Scn1a expression and reduce seizures and SUDEP incidence in a mouse model of Dravet syndrome', *Science Translational Medicine*, 12(558). doi: 10.1126/SCITRANSLMED.AAZ6100.

Hardingham, G. E. *et al.* (1997) 'Distinct functions of nuclear and cytoplasmic calcium in the control of gene expression', *Nature*, 385(6613), pp. 260–265. doi: 10.1038/385260a0.

Harrill, J. A. *et al.* (2015) 'Ontogeny of biochemical, morphological and functional parameters of synaptogenesis in primary cultures of rat hippocampal and cortical neurons', *Molecular Brain*, 8(1), pp. 1–15. doi: 10.1186/s13041-015-0099-9.

Haut, S. R. *et al.* (2005) 'Identifying seizure clusters in patients with epilepsy', *Neurology*, 65(8), pp. 1313–1315. doi: 10.1212/01.wnl.0000180685.84547.7f.

Haut, S. R. (2015) 'Seizure clusters: Characteristics and treatment', *Current Opinion in Neurology*, 28(2), pp. 143–150. doi: 10.1097/WCO.0000000000000177.

He, H. and Ping, F. (2009) 'The SIE, SRE, CRE, and FAP-1 four intracellular signal pathways between stimulus and the expression of c-fos promoter', *Journal of Cellular Biochemistry*, 106(5), pp. 764–768. doi: 10.1002/jcb.22058.

Heidenreich, M. and Zhang, F. (2016) 'Applications of CRISPR-Cas systems in neuroscience', *Nature Reviews Neuroscience*, 17(1), pp. 36–44. doi: 10.1038/nrn.2015.2.

Helmstaedter, C. and Witt, J. A. (2017) 'Epilepsy and cognition – A bidirectional relationship?', *Seizure*, 49, pp. 83–89. doi: 10.1016/j.seizure.2017.02.017.

Herdegen, T. and Leah, J. D. (1998) 'Inducible and constitutive transcription factors in the mammalian nervous system: Control of gene expression by Jun, Fos and Krox, and CREB/ATF proteins', *Brain Research Reviews*, 28(3), pp. 370–490. doi: 10.1016/S0165-0173(98)00018-6.

Hermann, B. P. *et al.* (2021) 'Neurobehavioural comorbidities of epilepsy: towards a network-based precision taxonomy', *Nature Reviews Neurology*, 17(12), pp. 731–746. doi: 10.1038/s41582-021-00555-z.

HERRERA, D. and ROBERTSON, H. (1996) 'Activation of c-fos in the brain', *Progress in Neurobiology*, 50(2–3), pp. 83–107. doi: 10.1016/S0301-0082(96)00021-4.

Hesdorffer, D. C. *et al.* (1996) 'Dementia and adult-onset unprovoked seizures', *Neurology*, 46(3), pp. 727 LP – 730. doi: 10.1212/WNL.46.3.727.

Hibino, H. *et al.* (2010) 'Inwardly rectifying potassium channels: Their structure, function, and physiological roles', *Physiological Reviews*, 90(1), pp. 291–366. doi: 10.1152/physrev.00021.2009.

High, K. A. and Aubourg, P. (2012) 'rAAV Human Trial Experience', in Snyder, R. O. and Moullier, P. (eds). Totowa, NJ: Humana Press, pp. 429–457. doi: 10.1007/978-1-61779-370-7_18.

Hitoshi, N., Ken-ichi, Y. and Jun-ichi, M. (1991) 'Efficient selection for high-expression transfectants with a novel eukaryotic vector', *Gene*, 108(2), pp. 193–199. doi: 10.1016/0378-1119(91)90434-D.

Hodgkin, A. L. and Huxley, A. F. (1952) 'A quantitative description of membrane current and its application to conduction and excitation in nerve', *The Journal of Physiology*, 117(4), pp. 500–544. doi: 10.1113/jphysiol.1952.sp004764.

Hoopengardner, B. *et al.* (2003) 'Nervous system targets of RNA editing identified by comparative genomics', *Science*, 301(5634), pp. 832–836. doi: 10.1126/science.1086763.

Hoshino, C. *et al.* (2021) 'GABAergic neuron-specific whole-brain transduction by AAV-PHP.B incorporated with a new GAD65 promoter', *Molecular Brain*, 14(1), pp. 1–18. doi: 10.1186/s13041-021-00746-1.

Houser, C. R. *et al.* (1990) 'Altered patterns of dynorphin immunoreactivity suggest mossy fiber reorganization in human hippocampal epilepsy', *Journal of Neuroscience*, 10(1), pp. 267–282. doi: 10.1523/jneurosci.10-01-00267.1990.

Howard, D. B. *et al.* (2008) 'Tropism and toxicity of adeno-associated viral vector serotypes 1, 2, 5, 6, 7, 8, and 9 in rat neurons and glia in vitro', *Virology*, 372(1), pp. 24–34. doi: 10.1016/j.virol.2007.10.007.

Hrvatin, S. *et al.* (2017) 'Transcriptomic States in the Mouse Visual Cortex', *Nature Neuroscience*, 21(January), pp. 1–19. doi: 10.1038/s41593-017-0029-5.

Hrvatin, S. *et al.* (2019) 'A scalable platform for the development of cell-type-specific viral drivers', *eLife*, 8, pp. 1–23. doi: 10.7554/eLife.48089.

Hubel, D. H. and Wiesel, T. N. (1970) 'The period of susceptibility to the physiological effects of unilateral eye closure in kittens', *The Journal of Physiology*, 206(2), pp. 419–436. doi: 10.1113/jphysiol.1970.sp009022.

Hudry, E. and Vandenberghe, L. H. (2019) 'Therapeutic AAV Gene Transfer to the Nervous System: A Clinical Reality', *Neuron*, 101(5), pp. 839–862. doi: 10.1016/j.neuron.2019.02.017.

Hussein, A. S. and Shafran, S. D. (2000) 'Acute Bacterial Meningitis in Adults: A 12-Year Review', *Medicine*, 79(6), pp. 360–368. doi: 10.1097/00005792-200011000-00002.

Ingusci, S. *et al.* (2019) 'Gene Therapy Tools for Brain Diseases', *Frontiers in Pharmacology*, 10(July), pp. 1–19. doi: 10.3389/fphar.2019.00724.

Inoue, M. *et al.* (2010) 'Synaptic Activity Responsive Element (SARE)', *Communicative & Integrative Biology*, 3(5), pp. 443–446. doi: 10.4161/cib.3.5.12287.

International, T. *et al.* (2018) 'Genome-wide mega-analysis identifies 16 loci and highlights diverse biological mechanisms in the common epilepsies', *Nature communications*, 9(1), p. 5269. doi: 10.1038/s41467-018-07524-z.

Ip, J. P. K., Mellios, N. and Sur, M. (2018) 'Rett syndrome: Insights into genetic, molecular and circuit mechanisms', *Nature Reviews Neuroscience*, 19(6), pp. 368–382. doi: 10.1038/s41583-018-0006-3.

Ito, D. *et al.* (2010) 'Minimum neuron density for synchronized bursts in a rat cortical culture on multi-electrode arrays', *Neuroscience*, 171(1), pp. 50–61. doi: 10.1016/j.neuroscience.2010.08.038.

Jain, P., Sharma, S. and Tripathi, M. (2013) 'Diagnosis and Management of Epileptic Encephalopathies in Children', *Epilepsy Research and Treatment*, 2013, pp. 1–9. doi: 10.1155/2013/501981.

Janz, P. *et al.* (2018) 'Position- and time-dependent arc expression links neuronal activity to synaptic plasticity during epileptogenesis', *Frontiers in Cellular Neuroscience*, 12(August), pp. 1–18. doi: 10.3389/fncel.2018.00244.

Jenkins, P. M. *et al.* (2011) 'Subunit-dependent axonal trafficking of distinct α heteromeric potassium channel complexes', *Journal of Neuroscience*, 31(37), pp. 13224–13235. doi: 10.1523/JNEUROSCI.0976-11.2011.

Jett, D. A. (2012) 'Chemical toxins that cause seizures', *NeuroToxicology*, 33(6), pp. 1473–1475. doi: 10.1016/j.neuro.2012.10.005.

Jinek, M. *et al.* (2012) 'A programmable dual-RNA-guided DNA endonuclease in adaptive bacterial immunity', *Science*, 337(6096), pp. 816–821. doi: 10.1126/science.1225829.

Jinek, M. *et al.* (2013) 'RNA-programmed genome editing in human cells',

eLife, 2013(2), pp. 1–9. doi: 10.7554/eLife.00471.

Johnson, C. M. *et al.* (1997) 'Calcium controls gene expression via three distinct pathways that can function independently of the Ras/mitogen-activated protein kinases (ERKs) signaling cascade', *Journal of Neuroscience*, 17(16), pp. 6189–6202. doi: 10.1523/jneurosci.17-16-06189.1997.

Johnson, R. S., Spiegelman, B. M. and Papaioannou, V. (1992) 'Pleiotropic effects of a null mutation in the c-fos proto-oncogene', *Cell*, 71(4), pp. 577–586. doi: 10.1016/0092-8674(92)90592-Z.

Joo, J. Y. *et al.* (2015) 'Stimulus-specific combinatorial functionality of neuronal c-fos enhancers', *Nature Neuroscience*, 19(1), pp. 75–83. doi: 10.1038/nn.4170.

Josselyn, S. A. and Tonegawa, S. (2020) 'Memory engrams: Recalling the past and imagining the future', *Science*, 367(6473). doi: 10.1126/science.aaw4325.

Jun-ichi, M. *et al.* (1989) 'Expression vector system based on the chicken β-actin promoter directs efficient production of interleukin-5', *Gene*, 79(2), pp. 269–277. doi: 10.1016/0378-1119(89)90209-6.

Jun, J. J. *et al.* (2017) 'Fully integrated silicon probes for high-density recording of neural activity', *Nature*, 551(7679), pp. 232–236. doi: 10.1038/nature24636.

Kaczmarek, L. and Chaudhuri, A. (1997) 'Sensory regulation of immediate-early gene expression in mammalian visual cortex: Implications for functional mapping and neural plasticity', *Brain Research Reviews*, 23(3), pp. 237–256. doi: 10.1016/S0165-0173(97)00005-2.

Kaczmarek, L., Zangenehpour, S. and Chaudhuri, A. (1999) 'Sensory regulation of immediate-early genes c-fos and zif268 in monkey visual cortex at birth and throughout the critical period', *Cerebral Cortex*, 9(2), pp. 179–187. doi: 10.1093/cercor/9.2.179.

Kalinina, A. *et al.* (2022) 'Effect of repeated seizures on spatial exploration and immediate early gene expression in the hippocampus and dentate gyrus', *IBRO Neuroscience Reports*, 12(September 2021), pp. 73–80. doi: 10.1016/j.ibneur.2021.12.008.

Kandel, E. R. and Spencer, W. A. (1961) 'Excitation and inhibition of single pyramidal cells during hippocampal seizure', *Experimental Neurology*, 4(2), pp. 162–179. doi: 10.1016/0014-4886(61)90038-3.

Kanter-Schlifke, I. *et al.* (2007) 'Seizure suppression by GDNF gene therapy in animal models of epilepsy', *Molecular Therapy*, 15(6), pp. 1106–1113. doi: 10.1038/sj.mt.6300148.

Kariyawasam, Di. *et al.* (2020) 'Great expectations: Virus-mediated gene therapy in neurological disorders', *Journal of Neurology, Neurosurgery and Psychiatry*, 91(8), pp. 849–860. doi: 10.1136/jnnp-2019-322327.

Karoly, P. J. *et al.* (2018) 'Circadian and circaseptan rhythms in human epilepsy: a retrospective cohort study', *The Lancet Neurology*, 17(11), pp. 977–985. doi: 10.1016/S1474-4422(18)30274-6.

Karoly, P. J. *et al.* (2021) 'Cycles in epilepsy', *Nature Reviews Neurology*, 17(5), pp. 267–284. doi: 10.1038/s41582-021-00464-1.

Kasof, G. M. *et al.* (1995) 'Kainic acid-induced neuronal death is associated with DNA damage and a unique immediate-early gene response in c-fos-lacZ transgenic rats', *Journal of Neuroscience*, 15(6), pp. 4238–4249. doi: 10.1523/jneurosci.15-06-04238.1995.

Kätzel, D. *et al.* (2014) 'Chemical-genetic attenuation of focal neocortical seizures', *Nature Communications*, 5(May). doi: 10.1038/ncomms4847.

Kawashima, T. *et al.* (2009) 'Synaptic activity-responsive element in the Arc/Arg3.1 promoter essential for synapse-to-nucleus signaling in activated neurons', *Proceedings of the National Academy of Sciences*, 106(1), pp. 316–321. doi: 10.1073/pnas.0806518106.

Kawashima, T. *et al.* (2013) 'Functional labeling of neurons and their projections using the synthetic activity-dependent promoter E-SARE', *Nature Methods*, 10(9), pp. 889–895. doi: 10.1038/nmeth.2559.

Kawashima, T., Okuno, H. and Bito, H. (2014) 'A new era for functional labeling of neurons: Activity-dependent promoters have come of age', *Frontiers in Neural Circuits*, 8(APR), pp. 1–9. doi: 10.3389/fncir.2014.00037.

Keezer, M. R., Sisodiya, S. M. and Sander, J. W. (2016) 'Comorbidities of epilepsy: Current concepts and future perspectives', *The Lancet Neurology*, 15(1), pp. 106–115. doi: 10.1016/S1474-4422(15)00225-2.

Kenet, T. *et al.* (2003) 'Spontaneously emerging cortical representations of visual attributes', *Nature*, 425(6961), pp. 954–956. doi: 10.1038/nature02078.

Kim, D.-W. *et al.* (1998) ' TFII-I Enhances Activation of the c- fos Promoter through Interactions with Upstream Elements ', *Molecular and Cellular Biology*, 18(6), pp. 3310–3320. doi: 10.1128/mcb.18.6.3310.

Kim, D. M. and Nimigean, C. M. (2016) 'Voltage-gated potassium channels: A structural examination of selectivity and gating', *Cold Spring Harbor Perspectives in Biology*, 8(5), pp. 1–20. doi: 10.1101/cshperspect.a029231.

Kim, E. *et al.* (1995) 'Clustering of Shaker-type K+ channels by interaction with a family of membrane-associated guanylate kinases', *Nature*, 378(6552), pp. 85–88. doi: 10.1038/378085a0.

Kim, E. H. and Ko, T. S. (2016) 'Cognitive impairment in childhood onset epilepsy: Up-to-date information about its causes', *Korean Journal of Pediatrics*, 59(4), pp. 155–164. doi: 10.3345/kjp.2016.59.4.155.

Kim, J. H. *et al.* (2011) 'High Cleavage Efficiency of a 2A Peptide Derived from Porcine Teschovirus-1 in Human Cell Lines, Zebrafish and Mice', *Plos One*,

6(4). doi: ARTN e1855610.1371/journal.pone.0018556.

Kim, Y. *et al.* (2016) 'Whole-brain mapping of neuronal activity in the learned helplessness model of depression', *Frontiers in Neural Circuits*, 10(FEB), pp. 1–11. doi: 10.3389/fncir.2016.00003.

Kitamura, T. *et al.* (2017) 'Engrams and circuits crucial for systems consolidation of a memory', *Science*, 356(6333), pp. 73–78. doi: 10.1126/science.aam6808.

Kleinstiver, B. P. *et al.* (2015) 'Broadening the targeting range of Staphylococcus aureus CRISPR-Cas9 by modifying PAM recognition', *Nature Biotechnology*, 33(12), pp. 1293–1298. doi: 10.1038/nbt.3404.

Köhling, R. (2002) 'GABA becomes exciting', *Science*, pp. 1350–1351. doi: 10.1126/science.1079446.

Köhling, R. and Wolfart, J. (2016) 'Potassium channels in epilepsy', *Cold Spring Harbor Perspectives in Medicine*, 6(5), p. 24. doi: 10.1101/cshperspect.a022871.

Konermann, S. *et al.* (2015) 'Genome-scale transcriptional activation by an engineered CRISPR-Cas9 complex', *Nature*, 517(7536), pp. 583–588. doi: 10.1038/nature14136.

Korb, E. and Finkbeiner, S. (2011) 'Arc in synaptic plasticity: From gene to behavior', *Trends in Neurosciences*, 34(11), pp. 591–598. doi: 10.1016/j.tins.2011.08.007.

Kornhauser, J. M. *et al.* (2002) 'CREB transcriptional activity in neurons is regulated by multiple, calcium-specific phosphorylation events', *Neuron*, 34(2), pp. 221–233. doi: 10.1016/S0896-6273(02)00655-4.

Kovács, K. J. (1998) 'c-Fos as a transcription factor: A stressful (re)view from a functional map', *Neurochemistry International*, 33(4), pp. 287–297. doi: 10.1016/S0197-0186(98)00023-0.

Krook-Magnuson, E. *et al.* (2013) 'On-demand optogenetic control of spontaneous seizures in temporal lobe epilepsy', *Nature Communications*, 4, pp. 1–8. doi: 10.1038/ncomms2376.

Kuang, Q., Purhonen, P. and Hebert, H. (2015) 'Structure of potassium channels', *Cellular and Molecular Life Sciences*, 72(19), pp. 3677–3693. doi: 10.1007/s00018-015-1948-5.

Kuba, H. *et al.* (2015) 'Redistribution of Kv1 and Kv7 enhances neuronal excitability during structural axon initial segment plasticity', *Nature Communications*, 6(May), pp. 1–12. doi: 10.1038/ncomms9815.

Kubo, Y. *et al.* (1993) 'Primary structure and functional expression of a mouse inward rectifier potassium channel', *Nature*, 362(6416), pp. 127–133. doi: 10.1038/362127a0.

Kubo, Y. *et al.* (2005) 'International union of pharmacology. LIV. Nomenclature

and molecular relationships of inwardly rectifying potassium channels', *Pharmacological Reviews*, 57(4), pp. 509–526. doi: 10.1124/pr.57.4.11.

Kügler, S., Kilic, E. and Bähr, M. (2003) 'Human synapsin 1 gene promoter confers highly neuron-specific long-term transgene expression from an adenoviral vector in the adult rat brain depending on the transduced area', *Gene Therapy*, 10(4), pp. 337–347. doi: 10.1038/sj.gt.3301905.

Kullmann, D. M. (2002) 'Genetics of epilepsy', *Journal of Neurology, Neurosurgery & Psychiatry*, 73(90002), pp. 32ii – 35. doi: 10.1136/jnnp.73.suppl_2.ii32.

Kullmann, D. M. *et al.* (2014) 'Gene therapy in epilepsy-is it time for clinical trials?', *Nature Reviews Neurology*, 10(5), pp. 300–304. doi: 10.1038/nrneurol.2014.43.

Kullmann, D. M. and Hanna, M. G. (2002) 'Neurological disorders caused by inherited ion-channel mutations', *Lancet Neurology*, 1(3), pp. 157–166. doi: 10.1016/S1474-4422(02)00071-6.

Kuscu, C. *et al.* (2014) 'Genome-wide analysis reveals characteristics of off-target sites bound by the Cas9 endonuclease', *Nature Biotechnology*, 32(7), pp. 677–683. doi: 10.1038/nbt.2916.

Kuzmin, D. A. *et al.* (2021) 'The clinical landscape for AAV gene therapies', *Nature reviews. Drug discovery*, 20(3), pp. 173–174. doi: 10.1038/d41573-021-00017-7.

Kwan, P. *et al.* (2010) 'Definition of drug resistant epilepsy: Consensus proposal by the ad hoc Task Force of the ILAE Commission on Therapeutic Strategies', *Epilepsia*, 51(6), pp. 1069–1077. doi: 10.1111/j.1528-1167.2009.02397.x.

Kwon, I. and Schaffer, D. V. (2008) 'Designer gene delivery vectors: Molecular engineering and evolution of adeno-associated viral vectors for enhanced gene transfer', *Pharmaceutical Research*, 25(3), pp. 489–499. doi: 10.1007/s11095-007-9431-0.

Lalonde, R. (2002) 'The neurobiological basis of spontaneous alternation', *Neuroscience and Biobehavioral Reviews*, 26(1), pp. 91–104. doi: 10.1016/S0149-7634(01)00041-0.

Lam, A. D. *et al.* (2017) 'Silent hippocampal seizures and spikes identified by foramen ovale electrodes in Alzheimer's disease', *Nature Medicine*, 23(6), pp. 678–680. doi: 10.1038/nm.4330.

De Lanerolle, N. C. *et al.* (1997) 'Dynorphin and the kappa 1 ligand [3H]U69,593 binding in the human epileptogenic hippocampus', *Epilepsy Research*, 28(3), pp. 189–205. doi: 10.1016/S0920-1211(97)00044-2.

Lang, J. *et al.* (2014) 'Comprehensive treatment of squamous cell cancer of head and neck: Chinese expert consensus 2013', *Future Oncology*, 10(9), pp. 1635–1648. doi: 10.2217/fon.14.44.

Lau, C. H. *et al.* (2019) 'Targeted Transgene Activation in the Brain Tissue by Systemic Delivery of Engineered AAV1 Expressing CRISPRa', *Molecular Therapy - Nucleic Acids*, 16(June), pp. 637–649. doi: 10.1016/j.omtn.2019.04.015.

Ledri, M. *et al.* (2015) 'Differential effect of neuropeptides on excitatory synaptic transmission in human epileptic hippocampus', *Journal of Neuroscience*, 35(26), pp. 9622–9631. doi: 10.1523/JNEUROSCI.3973-14.2015.

Lee, A. T. *et al.* (2014) 'A class of GABAergic neurons in the prefrontal cortex sends long-range projections to the nucleus accumbens and elicits acute avoidance behavior', *Journal of Neuroscience*, 34(35), pp. 11519–11525. doi: 10.1523/JNEUROSCI.1157-14.2014.

Lee, C. M. *et al.* (2020) 'Single-cell RNA-seq analysis revealed long-lasting adverse effects of tamoxifen on neurogenesis in prenatal and adult brains', *Proceedings of the National Academy of Sciences of the United States of America*, 117(32), pp. 19578–19589. doi: 10.1073/pnas.1918883117.

Lee, Y. *et al.* (2008) 'GFAP promoter elements required for region-specific and astrocyte-specific expression', *Glia*, 56(5), pp. 481–493. doi: 10.1002/glia.20622.

Leger, M. *et al.* (2013) 'Object recognition test in mice', *Nature Protocols*, 8(12), pp. 2531–2537. doi: 10.1038/nprot.2013.155.

Leonoudakis, D. *et al.* (2004) 'A Multiprotein Trafficking Complex Composed of SAP97, CASK, Veli, and Mint1 Is Associated with Inward Rectifier Kir2 Potassium Channels', *Journal of Biological Chemistry*, 279(18), pp. 19051–19063. doi: 10.1074/jbc.M400284200.

Leppert, M. *et al.* (1989) 'Benign familial neonatal convulsions linked to genetic markers on chromosome 20', *Nature*, 337(6208), pp. 647–648. doi: 10.1038/337647a0.

Lévesque, M. and Avoli, M. (2013) 'The kainic acid model of temporal lobe epilepsy', *Neuroscience and Biobehavioral Reviews*, 37(10), pp. 2887–2899. doi: 10.1016/j.neubiorev.2013.10.011.

Levira, F. *et al.* (2017) 'Premature mortality of epilepsy in low- and middle-income countries: A systematic review from the Mortality Task Force of the International League Against Epilepsy', *Epilepsia*, 58(1), pp. 6–16. doi: 10.1111/epi.13603.

Li, X. Q. *et al.* (1998) 'Generation of destabilized green fluorescent protein transcription reporter', *Journal of Biological Chemistry*, 273(52), pp. 34970–34975. doi: DOI 10.1074/jbc.273.52.34970.

Lieb, A. *et al.* (2018) 'Biochemical autoregulatory gene therapy for focal epilepsy', *Nature Medicine*, 24(9), pp. 1324-+. doi: 10.1038/s41591-018-0103-x.

Lignani, G., Baldelli, P. and Marra, V. (2020) 'Homeostatic Plasticity in

Epilepsy', *Frontiers in Cellular Neuroscience*, 14(June), pp. 1–9. doi: 10.3389/fncel.2020.00197.

Lillis, K. P. *et al.* (2015) 'Evolution of network synchronization during early epileptogenesis parallels synaptic circuit alterations', *Journal of Neuroscience*, 35(27), pp. 9920–9934. doi: 10.1523/JNEUROSCI.4007-14.2015.

Lim, J. A. *et al.* (2018) 'Clustering of spontaneous recurrent seizures separated by long seizure-free periods: An extended video-EEG monitoring study of a pilocarpine mouse model', *Plos One*, 13(3). doi: ARTN e019455210.1371/journal.pone.0194552.

Lin, E. J. D. *et al.* (2003) 'Recombinant AAV-mediated expression of galanin in rat hippocampus suppresses seizure development', *European Journal of Neuroscience*, 18(7), pp. 2087–2092. doi: 10.1046/j.1460-9568.2003.02926.x.

Lin, Y. *et al.* (2008) 'Activity-dependent regulation of inhibitory synapse development by Npas4', *Nature*, 455(7217), pp. 1198–1204. doi: 10.1038/nature07319.

Linehan, C. *et al.* (2010) 'Examining the prevalence of epilepsy and delivery of epilepsy care in Ireland', *Epilepsia*, 51(5), pp. 845–852. doi: 10.1111/j.1528-1167.2009.02417.x.

Link, W. *et al.* (1995) 'Somatodendritic expression of an immediate early gene is regulated by synaptic activity', *Proceedings of the National Academy of Sciences of the United States of America*, 92(12), pp. 5734–5738. doi: 10.1073/pnas.92.12.5734.

Lisowski, L., Tay, S. S. and Alexander, I. E. (2015) 'Adeno-associated virus serotypes for gene therapeutics', *Current Opinion in Pharmacology*, 24, pp. 59–67. doi: 10.1016/j.coph.2015.07.006.

Liu, R. *et al.* (2020) 'Role of NKCC1 and KCC2 in Epilepsy: From Expression to Function', *Frontiers in Neurology*, 10(January), pp. 10–12. doi: 10.3389/fneur.2019.01407.

Liu, X. *et al.* (2012) 'Optogenetic stimulation of a hippocampal engram activates fear memory recall', *Nature*, 484(7394), pp. 381–385. doi: 10.1038/nature11028.

Loacker, S. *et al.* (2007) 'Endogenous dynorphin in epileptogenesis and epilepsy: Anticonvulsant net effect via kappa opioid receptors', *Brain*, 130(4), pp. 1017–1028. doi: 10.1093/brain/awl384.

Loew, R. *et al.* (2010) 'Improved Tet-responsive promoters with minimized background expression', *BMC Biotechnology*, 10, pp. 1–13. doi: 10.1186/1472-6750-10-81.

Lombardo, A. *et al.* (2007) 'Gene editing in human stem cells using zinc finger nucleases and integrase-defective lentiviral vector delivery', *Nature Biotechnology*, 25(11), pp. 1298–1306. doi: 10.1038/nbt1353.

Longueville, S. *et al.* (2021) 'Long-lasting tagging of neurons activated by seizures or cocaine administration in Egr1-CreERT2 transgenic mice', *European Journal of Neuroscience*, 53(5), pp. 1450–1472. doi: 10.1111/ejn.15060.

Van Loo, K. M. J. *et al.* (2019) 'Calcium channel subunit α2σ4 is regulated by early growth response 1 and facilitates epileptogenesis', *Journal of Neuroscience*, 39(17), pp. 3175–3187. doi: 10.1523/JNEUROSCI.1731-18.2019.

Lopes, G. *et al.* (2015) 'Bonsai: An event-based framework for processing and controlling data streams', *Frontiers in Neuroinformatics*, 9(APR), pp. 1–14. doi: 10.3389/fninf.2015.00007.

López-López, D. *et al.* (2017) 'Overexpression of the immediate-early genes Egr1, Egr2, and Egr3 in two strains of rodents susceptible to audiogenic seizures', *Epilepsy and Behavior*, 71, pp. 226–237. doi: 10.1016/j.yebeh.2015.12.020.

Lowenstein, D. H., Bleck, T. and Macdonald, R. L. (1999) 'It's time to revise the definition of status epilepticus', *Epilepsia*, 40(1), pp. 120–122. doi: 10.1111/j.1528-1157.1999.tb02000.x.

Lugarà, E. *et al.* (2020) 'LGI1 downregulation increases neuronal circuit excitability', *Epilepsia*, 61(12), pp. 2836–2846. doi: 10.1111/epi.16736.

Lyford, G. L. *et al.* (1995) 'Arc, a growth factor and activity-regulated gene, encodes a novel cytoskeleton-associated protein that is enriched in neuronal dendrites', *Neuron*, 14(2), pp. 433–445. doi: 10.1016/0896-6273(95)90299-6.

Maeder, M. L. *et al.* (2013) 'CRISPR RNA-guided activation of endogenous human genes', *Nature Methods*, 10(10), pp. 977–979. doi: 10.1038/nmeth.2598.

Magloire, V. *et al.* (2019) 'KCC2 overexpression prevents the paradoxical seizure-promoting action of somatic inhibition', *Nature Communications*, 10(1), pp. 1–13. doi: 10.1038/s41467-019-08933-4.

Magloire, V. and Lignani, G. (2021) 'DBS for refractory epilepsy: is closed-loop stimulation of the medial septum the way forward?', *Brain*, 144(3), pp. 702–705. doi: 10.1093/brain/awab051.

Mainardi, M. *et al.* (2012) 'Tetanus neurotoxin-induced epilepsy in mouse visual cortex', *Epilepsia*, 53(7), pp. 132–136. doi: 10.1111/j.1528-1167.2012.03510.x.

Mali, P. *et al.* (2013) 'RNA-guided human genome engineering via Cas9', *Science*, 339(6121), pp. 823–826. doi: 10.1126/science.1232033.

Mardinly, A. R. *et al.* (2016) 'Sensory experience regulates cortical inhibition by inducing IGF1 in VIP neurons', *Nature*, 531(7594), pp. 371–375. doi: 10.1038/nature17187.

Mariga, A. *et al.* (2015) 'Definition of a Bidirectional Activity-Dependent Pathway Involving BDNF and Narp', *Cell Reports*, 13(9), pp. 1747–1756. doi:

10.1016/j.celrep.2015.10.064.

Mathiesen, S. N. *et al.* (2020) 'CNS Transduction Benefits of AAV-PHP.eB over AAV9 Are Dependent on Administration Route and Mouse Strain', *Molecular Therapy - Methods and Clinical Development*, 19(December), pp. 447–458. doi: 10.1016/j.omtm.2020.10.011.

Matsumoto, H. and Marsan, C. A. (1964) 'Cortical cellular phenomena in experimental epilepsy: Ictal manifestations', *Experimental Neurology*, 9(4), pp. 305–326. doi: 10.1016/0014-4886(64)90026-3.

Matsuzaki, Y. *et al.* (2018) 'Intravenous administration of the adeno-associated virus-PHP.B capsid fails to upregulate transduction efficiency in the marmoset brain', *Neuroscience Letters*, 665(November 2017), pp. 182–188. doi: 10.1016/j.neulet.2017.11.049.

Mauro, V. P. (2018) 'Codon Optimization in the Production of Recombinant Biotherapeutics: Potential Risks and Considerations', *BioDrugs*, 32(1), pp. 69–81. doi: 10.1007/s40259-018-0261-x.

Mazarati, A. M. *et al.* (1998) 'Galanin modulation of seizures and seizure modulation of hippocampal galanin in animal models of status epilepticus', *Journal of Neuroscience*, 18(23), pp. 10070–10077. doi: 10.1523/jneurosci.18-23-10070.1998.

McCown, T. J. (2006) 'Adeno-associated Virus-Mediated Expression and Constitutive Secretion of Galanin Suppresses Limbic Seizure Activity in Vivo', *Molecular Therapy*, 14(1), pp. 63–68. doi: 10.1016/j.ymthe.2006.04.004.

Meeren, H. *et al.* (2005) 'Evolving concepts on the pathophysiology of absence seizures: The cortical focus theory', *Archives of Neurology*, 62(3), pp. 371–376. doi: 10.1001/archneur.62.3.371.

Meinardi, H. *et al.* (2001) 'The treatment gap in epilepsy: The current situation and ways forward', *Epilepsia*, 42(1), pp. 136–149. doi: 10.1046/j.1528-1157.2001.32800.x.

Meinke, G. *et al.* (2016) 'Cre Recombinase and Other Tyrosine Recombinases', *Chemical Reviews*, 116(20), pp. 12785–12820. doi: 10.1021/acs.chemrev.6b00077.

Mello, L. E. A. M. *et al.* (1993) 'Circuit Mechanisms of Seizures in the Pilocarpine Model of Chronic Epilepsy: Cell Loss and Mossy Fiber Sprouting', *Epilepsia*, 34(6), pp. 985–995. doi: 10.1111/j.1528-1157.1993.tb02123.x.

Metzger, D. *et al.* (1995) 'Conditional site-specific recombination in mammalian cells using a ligand- dependent chimeric Cre recombinase', *Proceedings of the National Academy of Sciences of the United States of America*, 92(15), pp. 6991–6995. doi: 10.1073/pnas.92.15.6991.

Metzger, D. and Chambon, P. (2001) 'Site- and time-specific gene targeting in the mouse', *Methods*, 24(1), pp. 71–80. doi: 10.1006/meth.2001.1159.

Mich, J. K. *et al.* (2021) 'Functional enhancer elements drive subclass-selective expression from mouse to primate neocortex', *Cell Reports*, 34(13), p. 108754. doi: 10.1016/j.celrep.2021.108754.

Mickle, A. D. *et al.* (2019) 'A wireless closed-loop system for optogenetic peripheral neuromodulation', *Nature*, 565(7739), pp. 361–365. doi: 10.1038/s41586-018-0823-6.

Mihalick, S. M. *et al.* (2000) 'An Olfactory Discrimination Procedure for Mice', *Journal of the Experimental Analysis of Behavior*, 73(3), pp. 305–318. doi: 10.1901/jeab.2000.73-305.

Mikuni, N. *et al.* (1999) 'Time course of transient expression of GDNF protein in rat granule cells of the bilateral dentate gyri after unilateral intrahippocampal kainic acid injection', *Neuroscience Letters*, 262(3), pp. 215–218. doi: 10.1016/S0304-3940(99)00074-9.

Miller, A. D. (1992) 'Human gene therapy comes of age', *Nature*, 357(6378), pp. 455–460. doi: 10.1038/357455a0.

Morgan, J I *et al.* (1987) 'Mapping Patterns of C-Fos Expression in the Central-Nervous-System after Seizure', *Science*, 237(4811), pp. 192–197. doi: DOI 10.1126/science.3037702.

Morgan, James I. *et al.* (1987) 'Mapping patterns of c-fos expression in the central nervous system after seizure', *Science*, 237(4811), pp. 192–197. doi: 10.1126/science.3037702.

Müller, Christine J. *et al.* (2009) 'Behavioral and cognitive alterations, spontaneous seizures, and neuropathology developing after a pilocarpine-induced status epilepticus in C57BL/6 mice', *Experimental Neurology*, 219(1), pp. 284–297. doi: 10.1016/j.expneurol.2009.05.035.

Müller, Christine J *et al.* (2009) 'Pilocarpine vs . lithium – pilocarpine for induction of status epilepticus in mice : Development of spontaneous seizures , behavioral alterations and neuronal damage', *European Journal of Pharmacology*, 619(1–3), pp. 15–24. doi: 10.1016/j.ejphar.2009.07.020.

Murakami, S., Takemoto, T. and Shimizu, Z. (1953) 'Studies on the Effective Principles of *Digenea simplex* Aq. I', *YAKUGAKU ZASSHI*, 73(9), pp. 1026–1028. doi: 10.1248/yakushi1947.73.9_1026.

Murphy, T. H., Worley, P. F. and Baraban, J. M. (1991) 'L-type voltage-sensitive calcium channels mediate synaptic activation of immediate early genes', *Neuron*, 7(4), pp. 625–635. doi: 10.1016/0896-6273(91)90375-A.

Nathanson, J. L. *et al.* (2009) 'Preferential labeling of inhibitory and excitatory cortical neurons by endogenous tropism of adeno-associated virus and lentivirus vectors', *Neuroscience*, 161(2), pp. 441–450. doi: 10.1016/j.neuroscience.2009.03.032.

Navidhamidi, M., Ghasemi, M. and Mehranfard, N. (2017) 'Epilepsy-associated alterations in hippocampal excitability', *Reviews in the Neurosciences*, 28(3),

pp. 307–334. doi: 10.1515/revneuro-2016-0059.

Naylor, D. E. *et al.* (2013) 'Rapid surface accumulation of NMDA receptors increases glutamatergic excitation during status epilepticus', *Neurobiology of Disease*, 54, pp. 225–238. doi: 10.1016/j.nbd.2012.12.015.

Negri, J., Menon, V. and Young-Pearse, T. L. (2020) 'Assessment of spontaneous neuronal activity In vitro using multi-well multi-electrode arrays: Implications for assay development', *eNeuro*, 7(1), pp. 1–27. doi: 10.1523/ENEURO.0080-19.2019.

Negrini, M. *et al.* (2020) 'AAV Production Everywhere: A Simple, Fast, and Reliable Protocol for In-house AAV Vector Production Based on Chloroform Extraction', *Current Protocols in Neuroscience*, 93(1), pp. 1–10. doi: 10.1002/cpns.103.

Nehlig, A. (1998) 'Mapping of neuronal networks underlying generalized seizures induced by increasing doses of pentylenetetrazol in the immature and adult rat: A c-Fos immunohistochemical study', *European Journal of Neuroscience*, 10(6), pp. 2094–2106. doi: 10.1046/j.1460-9568.1998.00223.x.

Neumann, A. R. *et al.* (2017) 'Involvement of fast-spiking cells in ictal sequences during spontaneous seizures in rats with chronic temporal lobe epilepsy', *Brain*, 140(9), pp. 2355–2369. doi: 10.1093/brain/awx179.

Ngugi, A. K. *et al.* (2010) 'Estimation of the burden of active and life-time epilepsy: A meta-analytic approach', *Epilepsia*, 51(5), pp. 883–890. doi: 10.1111/j.1528-1167.2009.02481.x.

Nilsen, K. E., Walker, M. C. and Cock, H. R. (2005) 'Characterization of the tetanus toxin model of refractory focal neocortical epilepsy in the rat', *Epilepsia*, 46(2), pp. 179–187. doi: 10.1111/j.0013-9580.2005.26004.x.

Noe, F. *et al.* (2010) 'Anticonvulsant effects and behavioural outcomes of rAAV serotype 1 vector-mediated neuropeptide y overexpression in rat hippocampus', *Gene Therapy*, 17(5), pp. 643–652. doi: 10.1038/gt.2010.23.

Noè, F. *et al.* (2008) 'Neuropeptide Y gene therapy decreases chronic spontaneous seizures in a rat model of temporal lobe epilepsy', *Brain*, 131(6), pp. 1506–1515. doi: 10.1093/brain/awn079.

Noé, F. M. *et al.* (2016) 'Kainic acid-induced albumin leak across the blood-brain barrier facilitates epileptiform hyperexcitability in limbic regions', *Epilepsia*, 57(6), pp. 967–976. doi: 10.1111/epi.13394.

Nomoto, M. *et al.* (2021) 'Clinical evidence that a dysregulated master neural network modulator may aid in diagnosing schizophrenia', *Proceedings of the National Academy of Sciences of the United States of America*, 118(31), pp. 1–7. doi: 10.1073/pnas.2100032118.

Novartis (2019) 'MEDIA RELEASE • COMMUNIQUE AUX MEDIAS • MEDIENMITTEILUNG AveXis receives FDA approval for Zolgensma ® , the first and only gene therapy for pediatric patients with spinal muscular atrophy

(SMA)', *May 24, 2019*, pp. 1–6. Available at: http://www.novartis.com.

O'Donovan, K. J. *et al.* (1999) 'The EGR family of transcription-regulatory factors: Progress at the interface of molecular and systems neuroscience', *Trends in Neurosciences*, 22(4), pp. 167–173. doi: 10.1016/S0166-2236(98)01343-5.

Okada, M., Kano, M. and Matsuda, H. (2013) 'The degradation of the inwardly rectifying potassium channel, Kir2.1, depends on the expression level: Examination with fluorescent proteins', *Brain Research*, 1528, pp. 8–19. doi: 10.1016/j.brainres.2013.07.008.

Olafsson, E. *et al.* (2005) 'Incidence of unprovoked seizures and epilepsy in Iceland and assessment of the epilepsy syndrome classification: A prospective study', *Lancet Neurology*, 4(10), pp. 627–634. doi: 10.1016/S1474-4422(05)70172-1.

Olson, C. A. *et al.* (2018) 'The Gut Microbiota Mediates the Anti-Seizure Effects of the Ketogenic Diet', *Cell*, 173(7), pp. 1728-1741.e13. doi: 10.1016/j.cell.2018.04.027.

Ooe, N. *et al.* (2004) 'Identification of a Novel Basic Helix-Loop-Helix-PAS Factor, NXF, Reveals a Sim2 Competitive, Positive Regulatory Role in Dendritic-Cytoskeleton Modulator Drebrin Gene Expression', *Molecular and Cellular Biology*, 24(2), pp. 608–616. doi: 10.1128/mcb.24.2.608-616.2004.

Ovsepian, S. V. *et al.* (2016) 'Distinctive role of KV1.1 subunit in the biology and functions of low threshold K+ channels with implications for neurological disease', *Pharmacology and Therapeutics*, 159, pp. 93–101. doi: 10.1016/j.pharmthera.2016.01.005.

Pan, Z. *et al.* (2006) 'A common ankyrin-G-based mechanism retains KCNQ and Na V channels at electrically active domains of the axon', *Journal of Neuroscience*, 26(10), pp. 2599–2613. doi: 10.1523/JNEUROSCI.4314-05.2006.

Paolone, G. *et al.* (2019) 'Long-term, targeted delivery of GDNF from encapsulated cells is neuroprotective and reduces seizures in the pilocarpine model of epilepsy', *Journal of Neuroscience*, 39(11), pp. 2144–2156. doi: 10.1523/JNEUROSCI.0435-18.2018.

Papazian, D. M. *et al.* (1987) 'Cloning of genomic and complementary DNA from Shaker, a putative potassium channel gene from Drosophila', *Science*, 237(4816), pp. 749–753. doi: 10.1126/science.2441470.

Pasquale, V., Martinoia, S. and Chiappalone, M. (2010) 'A self-adapting approach for the detection of bursts and network bursts in neuronal cultures', *Journal of Computational Neuroscience*, 29(1–2), pp. 213–229. doi: 10.1007/s10827-009-0175-1.

Patel, L. R., Curran, T. and Kerppola, T. K. (1994) 'Energy transfer analysis of fos-jun dimerization and DNA binding', *Proceedings of the National Academy of Sciences of the United States of America*, 91(15), pp. 7360–7364. doi:

10.1073/pnas.91.15.7360.

Paz, J. T. *et al.* (2013) 'Closed-loop optogenetic control of thalamus as a tool for interrupting seizures after cortical injury', *Nature Neuroscience*, 16(1), pp. 64–70. doi: 10.1038/nn.3269.

Paz, J. T. and Huguenard, J. R. (2014) 'Optogenetics and epilepsy: Past, present and future', *Epilepsy Currents*, 15(1), pp. 34–38. doi: 10.5698/1535-7597-15.1.34.

Pearson, J. N., Schutz, K. M. and Patel, M. (2014) 'Specific alterations in the performance of learning and memory tasks in models of chemoconvulsant-induced status epilepticus', *Epilepsy Research*, 108(6), pp. 1032–1040. doi: 10.1016/j.eplepsyres.2014.04.003.

Pearson, S., Jia, H. and Kandachi, K. (2004) 'China approves first gene therapy.', *Nature biotechnology*, 22(1), pp. 3–4. doi: 10.1038/nbt0104-3.

Pecoraro-Bisogni, F. *et al.* (2018) 'REST-Dependent Presynaptic Homeostasis Induced by Chronic Neuronal Hyperactivity', *Molecular Neurobiology*, 55(6), pp. 4959–4972. doi: 10.1007/s12035-017-0698-9.

Penfield, W. and Jasper, H. (1954) *Epilepsy and the functional anatomy of the human brain.*, *Epilepsy and the functional anatomy of the human brain.* Oxford, England: Little, Brown & Co.

Peng, Z. C. and Houser, C. R. (2005) 'Temporal patterns of fos expression in the dentate gyrus after spontaneous seizures in a mouse model of temporal lobe epilepsy', *Journal of Neuroscience*, 25(31), pp. 7210–7220. doi: 10.1523/Jneurosci.0838-05.2005.

Perez-Pinera, P. *et al.* (2013) 'RNA-guided gene activation by CRISPR-Cas9-based transcription factors', *Nature Methods*, 10(10), pp. 973–976. doi: 10.1038/nmeth.2600.

Phelan, K. D. *et al.* (2015) 'Pilocarpine-induced status epilepticus in mice: A comparison of spectral analysis of electroencephalogram and behavioral grading using the Racine scale', *Epilepsy Research*, 117, pp. 90–96. doi: 10.1016/j.eplepsyres.2015.09.008.

Pitkänen, A. *et al.* (2015) 'Epileptogenesis', *Cold Spring Harbor Perspectives in Medicine*, 5(10), p. a022822. doi: 10.1101/cshperspect.a022822.

Pitkänen, A. and Sutula, T. P. (2002) 'Is epilepsy a progressive disorder? Prospects for new therapeutic approaches in temporal-lobe epilepsy', *Lancet Neurology*, 1(3), pp. 173–181. doi: 10.1016/S1474-4422(02)00073-X.

Polstein, L. R. *et al.* (2015) 'Genome-wide specificity of DNA binding, gene regulation, and chromatin remodeling by TALE- and CRISPR/Cas9-based transcriptional activators', *Genome Research*, 25(8), pp. 1158–1169. doi: 10.1101/gr.179044.114.

Pozzi, D. *et al.* (2013) 'REST/NRSF-mediated intrinsic homeostasis protects

neuronal networks from hyperexcitability', *Embo Journal*, 32(22), pp. 2994–3007. doi: 10.1038/emboj.2013.231.

Prince, D. A. (1978) 'Neurophysiology of Epilepsy', *Annual Review of Neuroscience*, 1(1), pp. 395–415. doi: 10.1146/annurev.ne.01.030178.002143.

Prut, L. and Belzung, C. (2003) 'The open field as a paradigm to measure the effects of drugs on anxiety-like behaviors: A review', *European Journal of Pharmacology*, pp. 3–33. doi: 10.1016/S0014-2999(03)01272-X.

Puttachary, S. *et al.* (2015) 'Immediate Epileptogenesis after Kainate-Induced Status Epilepticus in C57BL/6J Mice: Evidence from Long Term Continuous Video-EEG Telemetry', *Plos One*, 10(7). doi: ARTN e013170510.1371/journal.pone.0131705.

Qi, L. S. *et al.* (2013) 'Repurposing CRISPR as an RNA-guided platform for sequence-specific control of gene expression', *Cell*, 152(5), pp. 1173–1183. doi: 10.1016/j.cell.2013.02.022.

Qian, J., Colmers, W. F. and Saggau, P. (1997) 'Inhibition of synaptic transmission by neuropeptide Y in rat hippocampal area CA1: Modulation of presynaptic Ca2+ entry', *Journal of Neuroscience*, 17(21), pp. 8169–8177. doi: 10.1523/jneurosci.17-21-08169.1997.

Qin, J. Y. *et al.* (2010) 'Systematic comparison of constitutive promoters and the doxycycline-inducible promoter', *PLoS ONE*, 5(5), pp. 3–6. doi: 10.1371/journal.pone.0010611.

Quian Quiroga, R. and Panzeri, S. (2009) 'Extracting information from neuronal populations: Information theory and decoding approaches', *Nature Reviews Neuroscience*, 10(3), pp. 173–185. doi: 10.1038/nrn2578.

Rakhade, S. N. *et al.* (2007) 'Activity-dependent gene expression correlates with interictal spiking in human neocortical epilepsy', *Epilepsia*, 48(SUPPL. 5), pp. 86–95. doi: 10.1111/j.1528-1167.2007.01294.x.

Ramamoorthi, K. *et al.* (2011) 'Npas4 Regulates a Transcriptional Program in CA3 Required for Contextual Memory Formation', *Science*, 334(6063), pp. 1669–1675. doi: 10.1126/science.1208049.

Ramirez, S. *et al.* (2013) 'Creating a False Memory in the Hippocampus', *Science*, 341(6144), pp. 387–391. doi: 10.1126/science.1239073.

Ramirez, S. *et al.* (2015) 'Activating positive memory engrams suppresses depression-like behaviour', *Nature*, 522(7556), pp. 335–339. doi: 10.1038/nature14514.

Ran, F. A. *et al.* (2015) 'In vivo genome editing using Staphylococcus aureus Cas9', *Nature*, 520(7546), pp. 186–191. doi: 10.1038/nature14299.

Reijmers, L. G. *et al.* (2007) 'Localization of a stable neural correlate of associative memory', *Science*, 317(5842), pp. 1230–1233. doi: 10.1126/science.1143839.

Represa, A., Tremblay, E. and Ben-Ari, Y. (1987) 'Kainate binding sites in the hippocampal mossy fibers: Localization and plasticity', *Neuroscience*, 20(3), pp. 739–748. doi: 10.1016/0306-4522(87)90237-5.

Rho, J. M. *et al.* (1999) 'Developmental Seizure Susceptibility of Kv1.1 Potassium Channel Knockout Mice', *Developmental Neuroscience*, 21(3–5), pp. 320–327. doi: 10.1159/000017381.

Rhodes, K. J. *et al.* (1997) 'Association and colocalization of the Kvβ1 and Kvβ2 β-subunits with Kv1 α-subunits in mammalian brain K+ channel complexes', *Journal of Neuroscience*, 17(21), pp. 8246–8258. doi: 10.1523/jneurosci.17-21-08246.1997.

Robertson, L. M. *et al.* (1995) 'Regulation of c-fos expression in transgenic mice requires multiple interdependent transcription control elements', *Neuron*, 14(2), pp. 241–252. doi: 10.1016/0896-6273(95)90282-1.

Ronzitti, G., Gross, D. A. and Mingozzi, F. (2020) 'Human Immune Responses to Adeno-Associated Virus (AAV) Vectors', *Frontiers in Immunology*, 11(April), pp. 1–13. doi: 10.3389/fimmu.2020.00670.

Roth, B. L. (2016) 'DREADDs for Neuroscientists', *Neuron*, 89(4), pp. 683–694. doi: 10.1016/j.neuron.2016.01.040.

Roy, D. S. *et al.* (2016) 'Memory retrieval by activating engram cells in mouse models of early Alzheimer's disease', *Nature*, 531(7595), pp. 508–512. doi: 10.1038/nature17172.

Roy, D. S. *et al.* (2022) 'Brain-wide mapping reveals that engrams for a single memory are distributed across multiple brain regions', *Nature Communications*, 13(1), p. 1799. doi: 10.1038/s41467-022-29384-4.

Rusina, E., Bernard, C. and Williamson, A. (2021) 'The Kainic Acid Models of Temporal Lobe Epilepsy', *eneuro*, 8(2), p. ENEURO.0337-20.2021. doi: 10.1523/ENEURO.0337-20.2021.

Saffen, D. W. *et al.* (1988) 'Convulsant-induced increase in transcription factor messenger RNAs in rat brain', *Proceedings of the National Academy of Sciences of the United States of America*, 85(20), pp. 7795–7799. doi: 10.1073/pnas.85.20.7795.

Saha, R. N. *et al.* (2011) 'Rapid activity-induced transcription of Arc and other IEGs relies on poised RNA polymerase II', *Nature Neuroscience*, 14(7), pp. 848–856. doi: 10.1038/nn.2839.

Samulski, R. J., Chang, L. S. and Shenk, T. (1989) 'Helper-free stocks of recombinant adeno-associated viruses: normal integration does not require viral gene expression', *Journal of Virology*, 63(9), pp. 3822–3828. doi: 10.1128/jvi.63.9.3822-3828.1989.

Sander, J. W. A. S. (1993) 'Some Aspects of Prognosis in the Epilepsies: A Review', *Epilepsia*, 34(6), pp. 1007–1016. doi: 10.1111/j.1528-1157.1993.tb02126.x.

Santoro, S. W. and Schultz, P. G. (2002) 'Directed evolution of the site specificity of Cre recombinase', *Proceedings of the National Academy of Sciences of the United States of America*, 99(7), pp. 4185–4190. doi: 10.1073/pnas.022039799.

Savell, K. E. *et al.* (2019) 'A Neuron-Optimized CRISPR/dCas9 Activation System for Robust and Specific Gene Regulation', *Eneuro*, 6(1). doi: Unsp Eneuro.0495-18.201910.1523/Eneuro.0495-18.2019.

Schagen, F. H. E. *et al.* (2000) 'Ammonium sulphate precipitation of recombinant adenovirus from culture medium: An easy method to increase the total virus yield', *Gene Therapy*, 7(18), pp. 1570–1574. doi: 10.1038/sj.gt.3301285.

Scheffer, I. E. *et al.* (2017) 'ILAE classification of the epilepsies: Position paper of the ILAE Commission for Classification and Terminology', *Epilepsia*, 58(4), pp. 512–521. doi: 10.1111/epi.13709.

Schiavo, G. G. *et al.* (1992) 'Tetanus and botulinum-B neurotoxins block neurotransmitter release by proteolytic cleavage of synaptobrevin', *Nature*, 359(6398), pp. 832–835. doi: 10.1038/359832a0.

Schilling, K. *et al.* (1991) 'Regulation of a fos-lacZ fusion gene: A paradigm for quantitative analysis of stimulus-transcription coupling', *Proceedings of the National Academy of Sciences of the United States of America*, 88(13), pp. 5665–5669. doi: 10.1073/pnas.88.13.5665.

Schmeiser, B. *et al.* (2017) 'Different mossy fiber sprouting patterns in ILAE hippocampal sclerosis types', *Epilepsy Research*, 136(March), pp. 115–122. doi: 10.1016/j.eplepsyres.2017.08.002.

Schmidt-Kastner, R. *et al.* (1994) 'Glial cell-line derived neurotrophic factor (GDNF) mRNA upregulation in striatum and cortical areas after pilocarpine-induced status epilepticus in rats', *Molecular Brain Research*, 26(1–2), pp. 325–330. doi: 10.1016/0169-328X(94)90106-6.

Schuele, S. U. and Lüders, H. O. (2008) 'Intractable epilepsy: management and therapeutic alternatives', *The Lancet Neurology*, 7(6), pp. 514–524. doi: 10.1016/S1474-4422(08)70108-X.

Schuman, E. M., Dynes, J. L. and Steward, O. (2006) 'Synaptic regulation of translation of dendritic mRNAs.', *The Journal of neuroscience : the official journal of the Society for Neuroscience*, 26(27), pp. 7143–7146. doi: 10.1523/JNEUROSCI.1796-06.2006.

Schwartz, R. A. *et al.* (2007) 'The Mre11/Rad50/Nbs1 Complex Limits Adeno-Associated Virus Transduction and Replication', *Journal of Virology*, 81(23), pp. 12936–12945. doi: 10.1128/jvi.01523-07.

Scorza, F. A. *et al.* (2009) 'The pilocarpine model of epilepsy: What have we learned?', *Anais da Academia Brasileira de Ciencias*, 81(3), pp. 345–365. doi: 10.1590/S0001-37652009000300003.

Seagar, M. *et al.* (2017) 'LGI1 tunes intrinsic excitability by regulating the density of axonal Kv1 channels', *Proceedings of the National Academy of Sciences of the United States of America*, 114(29), pp. 7719–7724. doi: 10.1073/pnas.1618656114.

Selinger, J. V. *et al.* (2007) 'Methods for characterizing interspike intervals and identifying bursts in neuronal activity', *Journal of Neuroscience Methods*, 162(1–2), pp. 64–71. doi: 10.1016/j.jneumeth.2006.12.003.

Senior, M. (2017) 'After Glybera's withdrawal, what's next for gene therapy?', *Nature biotechnology*, 35(6), pp. 491–492. doi: 10.1038/nbt0617-491.

Shagin, D. A. *et al.* (2004) 'GFP-like Proteins as Ubiquitous Metazoan Superfamily: Evolution of Functional Features and Structural Complexity', *Molecular Biology and Evolution*, 21(5), pp. 841–850. doi: 10.1093/molbev/msh079.

Shan, W. *et al.* (2018) 'Neuronal PAS domain protein 4 (Npas4) controls neuronal homeostasis in pentylenetetrazole-induced epilepsy through the induction of Homer1a', *Journal of Neurochemistry*, 145(1), pp. 19–33. doi: 10.1111/jnc.14274.

Sharma, A. K. *et al.* (2007) 'Mesial temporal lobe epilepsy: Pathogenesis, induced rodent models and lesions', *Toxicologic Pathology*, 35(7), pp. 984–999. doi: 10.1080/01926230701748305.

Sheng, M. and Greenberg, M. E. (1990) 'The regulation and function of c-fos and other immediate early genes in the nervous system', *Neuron*, 4(4), pp. 477–485. doi: 10.1016/0896-6273(90)90106-P.

Sheng, M., Thompson, M. A. and Greenberg, M. E. (1991) 'CREB: A Ca2+-regulated transcription factor phosphorylated by calmodulin-dependent kinases', *Science*, 252(5011), pp. 1427–1430. doi: 10.1126/science.1646483.

Shepherd, J. D. and Bear, M. F. (2011) 'New views of Arc, a master regulator of synaptic plasticity', *Nature Neuroscience*, 14(3), pp. 279–284. doi: 10.1038/nn.2708.

Shinohara, Y. *et al.* (2019) 'Effects of Neutralizing Antibody Production on AAV-PHP.B-Mediated Transduction of the Mouse Central Nervous System', *Molecular Neurobiology*, 56(6), pp. 4203–4214. doi: 10.1007/s12035-018-1366-4.

Simonato, M. (2014) 'Gene therapy for epilepsy', *Epilepsy and Behavior*, 38, pp. 125–130. doi: 10.1016/j.yebeh.2013.09.013.

Singh, N. A. *et al.* (1998) 'A novel potassium channel gene, KCNQ2, is mutated in an inherited epilepsy of newborns', *Nature Genetics*, 18(1), pp. 25–29. doi: 10.1038/ng0198-25.

Singh, N. A. *et al.* (2003) 'KCNQ2 and KCNQ3 potassium channel genes in benign familial neonatal convulsions: Expansion of the functional and mutation spectrum', *Brain*, 126(12), pp. 2726–2737. doi:

10.1093/brain/awg286.

Singh, N. A. *et al.* (2008) 'Mouse models of human KCNQ2 and KCNQ3 mutations for benign familial neonatal convulsions show seizures and neuronal plasticity without synaptic reorganization', *Journal of Physiology*, 586(14), pp. 3405–3423. doi: 10.1113/jphysiol.2008.154971.

Sirven, J. I. (2015) 'Epilepsy: A Spectrum Disorder', *Cold Spring Harbor perspectives in medicine*, 5(9), p. a022848. doi: 10.1101/cshperspect.a022848.

Smart, S. L. *et al.* (1998) 'Deletion of the KV1.1 Potassium Channel Causes Epilepsy in Mice', *Neuron*, 20(4), pp. 809–819. doi: https://doi.org/10.1016/S0896-6273(00)81018-1.

Smeyne, R. J. *et al.* (1992) 'Fos-lacZ transgenic mice: Mapping sites of gene induction in the central nervous system', *Neuron*, 8(1), pp. 13–23. doi: https://doi.org/10.1016/0896-6273(92)90105-M.

Smith, D., Defalla, B. A. and Chadwick, D. W. (1999) 'The misdiagnosis of epilepsy and the management of refractory epilepsy in a specialist clinic', *QJM - Monthly Journal of the Association of Physicians*, 92(1), pp. 15–23. doi: 10.1093/qjmed/92.1.15.

Snowball, A. *et al.* (2019) 'Epilepsy gene therapy using an engineered potassium channel', *Journal of Neuroscience*, 39(16), pp. 3159–3169. doi: 10.1523/JNEUROSCI.1143-18.2019.

Somia, N. and Verma, I. M. (2000) 'Gene therapy: trials and tribulations', 1(November), pp. 1–9.

Sørensen, A. T. *et al.* (2016) 'A robust activity marking system for exploring active neuronal ensembles', *eLife*, 5(September), pp. 1–28. doi: 10.7554/eLife.13918.

Sperling, M. R. *et al.* (2008) 'Prognosis after late relapse following epilepsy surgery', *Epilepsy Research*, 78(1), pp. 77–81. doi: 10.1016/j.eplepsyres.2007.10.011.

Spiegel, I. *et al.* (2014) 'Npas4 regulates excitatory-inhibitory balance within neural circuits through cell-type-specific gene programs', *Cell*, 157(5), pp. 1216–1229. doi: 10.1016/j.cell.2014.03.058.

Spira, M. E. and Hai, A. (2013) 'Multi-electrode array technologies for neuroscience and cardiology', *Nature Nanotechnology*, 8(2), pp. 83–94. doi: 10.1038/nnano.2012.265.

Srivastava, A., Lusby, E. W. and Berns, K. I. (1983) 'Nucleotide sequence and organization of the adeno-associated virus 2 genome', *Journal of Virology*, 45(2), pp. 555–564. doi: 10.1128/jvi.45.2.555-564.1983.

Stafstrom, C. E. and Carmant, L. (2015) 'Seizures and epilepsy: an overview for neuroscientists', *Cold Spring Harbor perspectives in medicine*, 5(6), p. a022426. doi: 10.1101/cshperspect.a022426.

Staley, K. (2015) 'Molecular mechanisms of epilepsy', *Nature Neuroscience*, 18(3), pp. 367–372. doi: 10.1038/nn.3947.

Stephens, M. L. *et al.* (2014) 'Tonic glutamate in CA1 of aging rats correlates with phasic glutamate dysregulation during seizure', *Epilepsia*, 55(11), pp. 1817–1825. doi: 10.1111/epi.12797.

Steward, O. *et al.* (1998) 'Synaptic activation causes the mRNA for the leg Arc to localize selectively near activated postsynaptic sites on dendrites', *Neuron*, 21(4), pp. 741–751. doi: 10.1016/S0896-6273(00)80591-7.

Streit, A. K. *et al.* (2011) 'RNA editing of Kv1.1 channels may account for reduced ictogenic potential of 4-aminopyridine in chronic epileptic rats', *Epilepsia*, 52(3), pp. 645–648. doi: 10.1111/j.1528-1167.2011.02986.x.

Strekalova, T. *et al.* (2003) 'Memory retrieval after contextual fear conditioning induces c-Fos and JunB expression in CA1 hippocampus', *Genes, Brain and Behavior*, 2(1), pp. 3–10. doi: 10.1034/j.1601-183X.2003.00001.x.

Sun, X. *et al.* (2020) 'Functionally Distinct Neuronal Ensembles within the Memory Engram In Brief Two functionally distinct neuronal ensembles within a single memory engram undergo different learning-induced synaptic modifications and drive memory-guided behaviors in opposite d', *Cell*, 181, pp. 1–14. doi: 10.1016/j.cell.2020.02.055.

Suzuki, K. *et al.* (2016) 'In vivo genome editing via CRISPR/Cas9 mediated homology-independent targeted integration', *Nature*, 540(7631), pp. 144–149. doi: 10.1038/nature20565.

Suzuki, K. and Izpisua Belmonte, J. C. (2018) 'In vivo genome editing via the HITI method as a tool for gene therapy', *Journal of Human Genetics*, 63(2), pp. 157–164. doi: 10.1038/s10038-017-0352-4.

Swiech, L. *et al.* (2015) 'In vivo interrogation of gene function in the mammalian brain using CRISPR-Cas9', *Nature Biotechnology*, 33(1), pp. 102–106. doi: 10.1038/nbt.3055.

Szczygieł, J. A. *et al.* (2020) 'Gene Therapy Vector Encoding Neuropeptide Y and Its Receptor Y2 for Future Treatment of Epilepsy: Preclinical Data in Rats', *Frontiers in Molecular Neuroscience*, 13(December), pp. 1–13. doi: 10.3389/fnmol.2020.603409.

Szyndler, J. *et al.* (2013) 'Changes in the Egr1 and Arc expression in brain structures of pentylenetetrazole-kindled rats', *Pharmacological Reports*, 65(2), pp. 368–378. doi: 10.1016/S1734-1140(13)71012-0.

T. Das, A., Tenenbaum, L. and Berkhout, B. (2016) 'Tet-On Systems For Doxycycline-inducible Gene Expression', *Current Gene Therapy*, 16(3), pp. 156–167. doi: 10.2174/1566523216666160524144041.

Tallent, M. K. and Qiu, C. (2008) 'Somatostatin: An endogenous antiepileptic', *Molecular and Cellular Endocrinology*, 286(1–2), pp. 96–103. doi: 10.1016/j.mce.2007.12.004.

Thijs, R. D. *et al.* (2019) 'Epilepsy in adults', *The Lancet*, 393(10172), pp. 689–701. doi: 10.1016/S0140-6736(18)32596-0.

Thompson, A. *et al.* (2017) 'Activity-dependent development of visual receptive fields', *Current Opinion in Neurobiology*, 42(3), pp. 136–143. doi: 10.1016/j.conb.2016.12.007.

Thurman, D. J. *et al.* (2017) 'The burden of premature mortality of epilepsy in high-income countries: A systematic review from the Mortality Task Force of the International League Against Epilepsy', *Epilepsia*, 58(1), pp. 17–26. doi: 10.1111/epi.13604.

Timpe, L. C. *et al.* (1988) 'Expression of functional potassium channels from Shaker cDNA in Xenopus oocytes', *Nature*, 331(6152), pp. 143–145. doi: 10.1038/331143a0.

Tiscornia, G., Singer, O. and Verma, I. M. (2006) 'Production and purification of lentiviral vectors', *Nature Protocols*, 1(1), pp. 241–245. doi: 10.1038/nprot.2006.37.

Tonegawa, S. *et al.* (2015) 'Memory engram storage and retrieval', *Current Opinion in Neurobiology*, 35, pp. 101–109. doi: 10.1016/j.conb.2015.07.009.

Tonegawa, S., Morrissey, M. D. and Kitamura, T. (2018) 'The role of engram cells in the systems consolidation of memory', *Nature Reviews Neuroscience*, 19(August). doi: 10.1038/s41583-018-0031-2.

Tønnesen, J. *et al.* (2009) 'Optogenetic control of epileptiform activity', *Proceedings of the National Academy of Sciences of the United States of America*, 106(29), pp. 12162–12167. doi: 10.1073/pnas.0901915106.

Traub, R. D. *et al.* (2004) 'Gap junctions, fast oscillations and the initiation of seizures', *Advances in Experimental Medicine and Biology*, 548, pp. 110–122. doi: 10.1007/978-1-4757-6376-8_9.

Treisman, R. (1985) 'Transient accumulation of c-fos RNA following serum stimulation requires a conserved 5' element and c-fos 3' sequences', *Cell*, 42(3), pp. 889–902. doi: 10.1016/0092-8674(85)90285-5.

Trimmer, J. S. (2015) 'Subcellular localization of K+ channels in mammalian brain neurons: Remarkable precision in the midst of extraordinary complexity', *Neuron*, 85(2), pp. 238–256. doi: 10.1016/j.neuron.2014.12.042.

Truccolo, W. *et al.* (2011) 'Single-neuron dynamics in human focal epilepsy', *Nature Neuroscience*, 14(5), pp. 635-U130. doi: 10.1038/nn.2782.

Tsai-Morris, C.-H., Cao, X. and Sukhatme, V. P. (1988) '5' flanking sequence and genomic structure of Egr-1, a murine mitogen inducible zinc finger encoding gene', *Nucleic Acids Research*, 16(18), pp. 8835–8846. doi: 10.1093/nar/16.18.8835.

Tsai, J. C. *et al.* (2000) 'The egr-1 promoter contains information for constitutive and inducible expression in transgenic mice', *The FASEB Journal*,

14(13), pp. 1870–1872. doi: 10.1096/fj.99-1072fje.

Tse, K. *et al.* (2014) 'Advantages of repeated low dose against single high dose of kainate in C57BL/6J mouse model of status epilepticus: Behavioral and electroencephalographic studies', *PLoS ONE*. Edited by S. L. Sensi, 9(5), p. e96622. doi: 10.1371/journal.pone.0096622.

Turrigiano, G. (2012) 'Homeostatic synaptic plasticity: Local and global mechanisms for stabilizing neuronal function', *Cold Spring Harbor Perspectives in Biology*, 4(1), pp. 1–18. doi: 10.1101/cshperspect.a005736.

Turrigiano, G. G. (1999) 'Homeostatic plasticity in neuronal networks: The more things change, the more they stay the same', *Trends in Neurosciences*, 22(5), pp. 221–227. doi: 10.1016/S0166-2236(98)01341-1.

Turski, W. A. *et al.* (1983) 'Limbic seizures produced by pilocarpine in rats: Behavioural, electroencephalographic and neuropathological study', *Behavioural Brain Research*, 9(3), pp. 315–335. doi: 10.1016/0166-4328(83)90136-5.

Tye, K. M. *et al.* (2011) 'Amygdala circuitry mediating reversible and bidirectional control of anxiety', *Nature*, 471(7338), pp. 358–362. doi: 10.1038/nature09820.

Vandekerckhove, B. *et al.* (2021) 'Technological challenges in the development of optogenetic closed-loop therapy approaches in epilepsy and related network disorders of the brain', *Micromachines*, 12(1), pp. 1–30. doi: 10.3390/mi12010038.

Varma, S. and Voldman, J. (2015) 'A cell-based sensor of fluid shear stress for microfluidics', *Lab on a Chip*, 15(6), pp. 1563–1573. doi: 10.1039/c4lc01369g.

Verlengia, G. *et al.* (2017) 'Engineered HSV vector achieves safe long-term transgene expression in the central nervous system', *Scientific Reports*, 7(1), pp. 1–11. doi: 10.1038/s41598-017-01635-1.

Victor Nadler, J. (1981) 'Kainic acid as a tool for the study of temporal lobe epilepsy', *Life Sciences*, 29(20), pp. 2031–2042. doi: 10.1016/0024-3205(81)90659-7.

Vivekananda, U. *et al.* (2017) 'Kv1.1 channelopathy abolishes presynaptic spike width modulation by subthreshold somatic depolarization', *Proceedings of the National Academy of Sciences of the United States of America*, 114(9), pp. 2395–2400. doi: 10.1073/pnas.1608763114.

Vol, N. *et al.* (1973) 'Cycloheximide affects Memory within Minutes after the Onset of Training Encephalitis , in Hot Spring Effluents , Thermal Soils and Self-heated Coal Waste Piles', 242, pp. 201–202.

Wagenaar, D. A. *et al.* (2005) 'Controlling bursting in cortical cultures with closed-loop multi-electrode stimulation', *Journal of Neuroscience*, 25(3), pp. 680–688. doi: 10.1523/JNEUROSCI.4209-04.2005.

Wagner, D. L. *et al.* (2019) 'High prevalence of Streptococcus pyogenes Cas9-reactive T cells within the adult human population', *Nature Medicine*, 25(2), pp. 242–248. doi: 10.1038/s41591-018-0204-6.

Walker, M. C. *et al.* (2013) 'Gene therapy in status epilepticus', *Epilepsia*, 54(SUPPL. 6), pp. 43–45. doi: 10.1111/epi.12275.

Walker, M. C. and Kullmann, D. M. (2019) 'Optogenetic and chemogenetic therapies for epilepsy', *Neuropharmacology*, 168(September 2019), p. 107751. doi: 10.1016/j.neuropharm.2019.107751.

Wang, D., Wang, K. and Cai, Y. (2020) 'An overview of development in gene therapeutics in China', *Gene Therapy*, 27(7–8), pp. 338–348. doi: 10.1038/s41434-020-0163-7.

Wang, G. *et al.* (2021) 'Egr1-EGFP transgenic mouse allows in vivo recording of Egr1 expression and neural activity', *Journal of Neuroscience Methods*, 363(September), p. 109350. doi: 10.1016/j.jneumeth.2021.109350.

Wang, H. *et al.* (1994) 'Localization of Kv1.1 and Kv1.2, two K channel proteins, to synaptic terminals, somata, and dendrites in the mouse brain', *Journal of Neuroscience*, 14(8), pp. 4588–4599. doi: 10.1523/jneurosci.14-08-04588.1994.

Wang, H. S. *et al.* (1998) 'KCNQ2 and KCNQ3 potassium channel subunits: Molecular correlates of the M-channel', *Science*, 282(5395), pp. 1890–1893. doi: DOI 10.1126/science.282.5395.1890.

Wang, K. H. *et al.* (2006) 'In Vivo Two-Photon Imaging Reveals a Role of Arc in Enhancing Orientation Specificity in Visual Cortex', *Cell*, 126(2), pp. 389–402. doi: 10.1016/j.cell.2006.06.038.

Watakabe, A. *et al.* (2015) 'Comparative analyses of adeno-associated viral vector serotypes 1, 2, 5, 8 and 9 in marmoset, mouse and macaque cerebral cortex', *Neuroscience Research*, 93, pp. 144–157. doi: 10.1016/j.neures.2014.09.002.

Webling, K. *et al.* (2016) 'Pharmacological stimulation of GAL1R but not GAL2R attenuates kainic acid-induced neuronal cell death in the rat hippocampus', *Neuropeptides*, 58, pp. 83–92. doi: 10.1016/j.npep.2015.12.009.

Weitzman, M. D. and Linden, R. M. (2011) 'Adeno-associated virus biology', *Methods in Molecular Biology*, 807, pp. 1–23. doi: 10.1007/978-1-61779-370-7_1.

Welzel, L. *et al.* (2020) 'A face-to-face comparison of the intra-amygdala and intrahippocampal kainate mouse models of mesial temporal lobe epilepsy and their utility for testing novel therapies', *Epilepsia*, 61(1), pp. 157–170. doi: 10.1111/epi.16406.

Wenzel, M., Hamm, Jordan P, *et al.* (2017) 'Reliable and Elastic Propagation of Cortical Seizures In Vivo', *Cell Reports*, 19(13), pp. 2681–2693. doi: https://doi.org/10.1016/j.celrep.2017.05.090.

Wenzel, M., Hamm, Jordan P., *et al.* (2017) 'Reliable and Elastic Propagation of Cortical Seizures In Vivo', *Cell Reports*, 19(13), pp. 2681–2693. doi: 10.1016/j.celrep.2017.05.090.

Wenzel, M. *et al.* (2019) 'Acute Focal Seizures Start As Local Synchronizations of Neuronal Ensembles', *The Journal of Neuroscience*, 39(43), pp. 8562–8575. doi: 10.1523/jneurosci.3176-18.2019.

West, A. E. *et al.* (2001) 'Calcium regulation of neuronal gene expression', *Proceedings of the National Academy of Sciences of the United States of America*, 98(20), pp. 11024–11031. doi: 10.1073/pnas.191352298.

West, P. J. *et al.* (2021) 'Spontaneous recurrent seizures in an intra-amygdala kainate microinjection model of temporal lobe epilepsy are differentially sensitive to antiseizure drugs', *Experimental Neurology*, 349(June 2021), p. 113954. doi: 10.1016/j.expneurol.2021.113954.

Westenbroek, R. E., Ahlijanian, M. K. and Catterall, W. A. (1990) 'Clustering of L-type Ca + channels', pp. 281–284.

Weston, M. *et al.* (2019) 'Olanzapine: A potent agonist at the hM4D(Gi) DREADD amenable to clinical translation of chemogenetics', *Science Advances*, 5(4), pp. 1–7. doi: 10.1126/sciadv.aaw1567.

Whissell, P. D. *et al.* (2015) 'Comparative density of CCK- and PV-GABA cells within the cortex and hippocampus', *Frontiers in Neuroanatomy*, 9(September), pp. 1–16. doi: 10.3389/fnana.2015.00124.

Wietek, J. *et al.* (2014) 'Conversion of channelrhodopsin into a light-gated chloride channel', *Science*, 344(6182), pp. 409–412. doi: 10.1126/science.1249375.

Williams, P. A. *et al.* (2009) 'Development of Spontaneous Recurrent Seizures after Kainate-Induced Status Epilepticus', *The Journal of Neuroscience*, 29(7), pp. 2103–2112. doi: 10.1523/jneurosci.0980-08.2009.

Williamson, R. *et al.* (2009) 'Generalized-onset seizures with secondary focal evolution', *Epilepsia*, 50(7), pp. 1827–1832. doi: 10.1111/j.1528-1167.2009.02045.x.

Woldbye, D. P. D. *et al.* (1997) 'Powerful inhibition of kainic acid seizures by neuropeptide Y via Y5-like receptors', *Nature Medicine*, 3(7), pp. 761–764. doi: Doi 10.1038/Nm0797-761.

Woldbye, D. P. D. D. *et al.* (2010) 'Adeno-associated viral vector-induced overexpression of neuropeptide y Y2 receptors in the hippocampus suppresses seizures', *Brain*, 133(9), pp. 2778–2788. doi: 10.1093/brain/awq219.

Wu, X. *et al.* (2014) 'Genome-wide binding of the CRISPR endonuclease Cas9 in mammalian cells', *Nature Biotechnology*, 32(7), pp. 670–676. doi: 10.1038/nbt.2889.

Wu, Z., Yang, H. and Colosi, P. (2010) 'Effect of genome size on AAV vector packaging', *Molecular Therapy*, 18(1), pp. 80–86. doi: 10.1038/mt.2009.255.

Wykes, R. C. *et al.* (2012) 'Optogenetic and Potassium Channel Gene Therapy in a Rodent Model of Focal Neocortical Epilepsy', *Science Translational Medicine*, 4(161). doi: ARTN 161ra15210.1126/scitranslmed.3004190.

Wykes, R. C. *et al.* (2016) 'Optogenetic approaches to treat epilepsy', *Journal of Neuroscience Methods*, 260, pp. 215–220. doi: 10.1016/j.jneumeth.2015.06.004.

Wykes, R. C. and Lignani, G. (2018) 'Gene therapy and editing: Novel potential treatments for neuronal channelopathies', *Neuropharmacology*, 132, pp. 108–117. doi: 10.1016/j.neuropharm.2017.05.029.

Xia, W. *et al.* (2006) 'High levels of protein expression using different mammalian CMV promoters in several cell lines', *Protein Expression and Purification*, 45(1), pp. 115–124. doi: 10.1016/j.pep.2005.07.008.

Xu, J. *et al.* (2018) 'Genetic identification of leptin neural circuits in energy and glucose homeostases', *Nature*, 556(7702), pp. 505–509. doi: 10.1038/s41586-018-0049-7.

Yamada, Y. *et al.* (1999) 'Differential expression of immediate-early genes, c-fos and zif268, in the visual cortex of young rats: Effects of a noradrenergic neurotoxin on their expression', *Neuroscience*, 92(2), pp. 473–484. doi: 10.1016/S0306-4522(99)00003-2.

Yang, J. *et al.* (2010) 'An Epilepsy/Dyskinesia-Associated Mutation Enhances BK Channel Activation by Potentiating Ca2+ Sensing', *Neuron*, 66(6), pp. 871–883. doi: 10.1016/j.neuron.2010.05.009.

Yap, E. L. and Greenberg, M. E. (2018) 'Activity-Regulated Transcription: Bridging the Gap between Neural Activity and Behavior', *Neuron*, 100(2), pp. 330–348. doi: 10.1016/j.neuron.2018.10.013.

Yasuda, M. *et al.* (2021) 'An activity-dependent determinant of synapse elimination in the mammalian brain', *Neuron*, 109(8), pp. 1333-1349.e6. doi: 10.1016/j.neuron.2021.03.006.

Yazaki, K. *et al.* (2022) 'Child Neurology: Pathologically Confirmed Thrombotic Microangiopathy Caused by Onasemnogene Abeparvovec Treatment for Spinal Muscular Atrophy', *Neurology*, p. 10.1212/WNL.0000000000200676. doi: 10.1212/WNL.0000000000200676.

Yizhar, O. *et al.* (2011) 'Neocortical excitation/inhibition balance in information processing and social dysfunction', *Nature*, 477(7363), pp. 171–178. doi: 10.1038/nature10360.

Young, C. C. *et al.* (2009) 'Upregulation of inward rectifier K+ (Kir2) channels in dentate gyrus granule cells in temporal lobe epilepsy', *Journal of Physiology*, 587(17), pp. 4213–4233. doi: 10.1113/jphysiol.2009.170746.

Zeidler, Z. *et al.* (2018) 'Targeting the mouse ventral hippocampus in the intrahippocampal kainic acid model of temporal lobe epilepsy', *eNeuro*, 5(4). doi: 10.1523/ENEURO.0158-18.2018.

Zetsche, B. *et al.* (2015) 'Cpf1 Is a Single RNA-Guided Endonuclease of a Class 2 CRISPR-Cas System', *Cell*, 163(3), pp. 759–771. doi: 10.1016/j.cell.2015.09.038.

Zhang, F., Aravanis, A. M. and Adamantidis, A. (2007) 'Neural Signals and Systems', *Nature*, 8(August), pp. 577–581. Available at: http://www.nature.com/nrn/journal/vaop/ncurrent/full/nrn2192.html.

Zhang, J. *et al.* (2002) 'C-Fos Regulates Neuronal Excitability and Survival', *Nature Genetics*, 30(4), pp. 416–420. doi: 10.1038/ng859.

Zhang, Z. J. *et al.* (2012) 'Transition to seizure: Ictal discharge is preceded by exhausted presynaptic GABA release in the hippocampal CA3 region', *Journal of Neuroscience*, 32(7), pp. 2499–2512. doi: 10.1523/JNEUROSCI.4247-11.2012.

Zhou, X. *et al.* (2006) 'Optimization of the Tet-On system for regulated gene expression through viral evolution', *Gene Therapy*, 13(19), pp. 1382–1390. doi: 10.1038/sj.gt.3302780.

Zolotukhin, S. *et al.* (1999) 'Recombinant adeno-associated virus purification using novel methods improves infectious titer and yield', *Gene Therapy*, 6(6), pp. 973–985. doi: 10.1038/sj.gt.3300938.

Zuberi, S. M. *et al.* (1999) 'A novel mutation in the human voltage-gated potassium channel gene (Kv1.1) associates with episodic ataxia type 1 and sometimes with partial epilepsy', *Brain*, 122(5), pp. 817–825. doi: 10.1093/brain/122.5.817.

Appendix. I

doi:10.1093/brain/awaa045 BRAIN 2020: 143; 891–905 | 891

BRAIN
A JOURNAL OF NEUROLOGY

In vivo CRISPRa decreases seizures and rescues cognitive deficits in a rodent model of epilepsy

Gaia Colasante,[1,*] Yichen Qiu,[2,*] Luca Massimino,[1] Claudia Di Berardino,[1] Jonathan H. Cornford,[2] Albert Snowball,[2] Mikail Weston,[2] Steffan P. Jones,[2] Serena Giannelli,[1] Andreas Lieb,[2,#] Stephanie Schorge,[2,3] Dimitri M. Kullmann,[2] Vania Broccoli[1,4] and Gabriele Lignani[2]

*These authors contributed equally to this work.

Epilepsy is a major health burden, calling for new mechanistic insights and therapies. CRISPR-mediated gene editing shows promise to cure genetic pathologies, although hitherto it has mostly been applied *ex vivo*. Its translational potential for treating non-genetic pathologies is still unexplored. Furthermore, neurological diseases represent an important challenge for the application of CRISPR, because of the need in many cases to manipulate gene function of neurons *in situ*. A variant of CRISPR, CRISPRa, offers the possibility to modulate the expression of endogenous genes by directly targeting their promoters. We asked if this strategy can effectively treat acquired focal epilepsy, focusing on ion channels because their manipulation is known be effective in changing network hyperactivity and hypersynchronization. We applied a doxycycline-inducible CRISPRa technology to increase the expression of the potassium channel gene *Kcna1* (encoding $K_v1.1$) in mouse hippocampal excitatory neurons. CRISPRa-mediated $K_v1.1$ upregulation led to a substantial decrease in neuronal excitability. Continuous video-EEG telemetry showed that AAV9-mediated delivery of CRISPRa, upon doxycycline administration, decreased spontaneous generalized tonic-clonic seizures in a model of temporal lobe epilepsy, and rescued cognitive impairment and transcriptomic alterations associated with chronic epilepsy. The focal treatment minimizes concerns about off-target effects in other organs and brain areas. This study provides the proof-of-principle for a translational CRISPR-based approach to treat neurological diseases characterized by abnormal circuit excitability.

1 San Raffaele Scientific Institute, Via Olgettina 58, 20132, Milan, Italy
2 Department of Clinical and Experimental Epilepsy, UCL Institute of Neurology, University College London, London, UK
3 Department of Pharmacology, UCL School of Pharmacy, University College London, London, UK
4 CNR Institute of Neuroscience, Via Vanvitelli 32, 20129, Milan, Italy

#Present address: Department of Pharmacology, Medical University of Innsbruck, Peter Mayr Strasse 1A, 6020 Innsbruck, Austria

Correspondence to: Gabriele Lignani
Department of Clinical and Experimental Epilepsy, UCL Institute of Neurology
University College London, London, UK
E-mail: g.lignani@ucl.ac.uk

Correspondence may also be addressed to: Vania Broccoli
San Raffaele Scientific Institute, Via Olgettina 58, 20132, Milan, Italy
E-mail: v.broccoli@hsr.it

Received August 23, 2019. Revised December 31, 2019. Accepted January 14, 2020. Advance access publication March 4, 2020

https://academic.oup.com/brain/article/143/3/891/5780426

Appendix. II

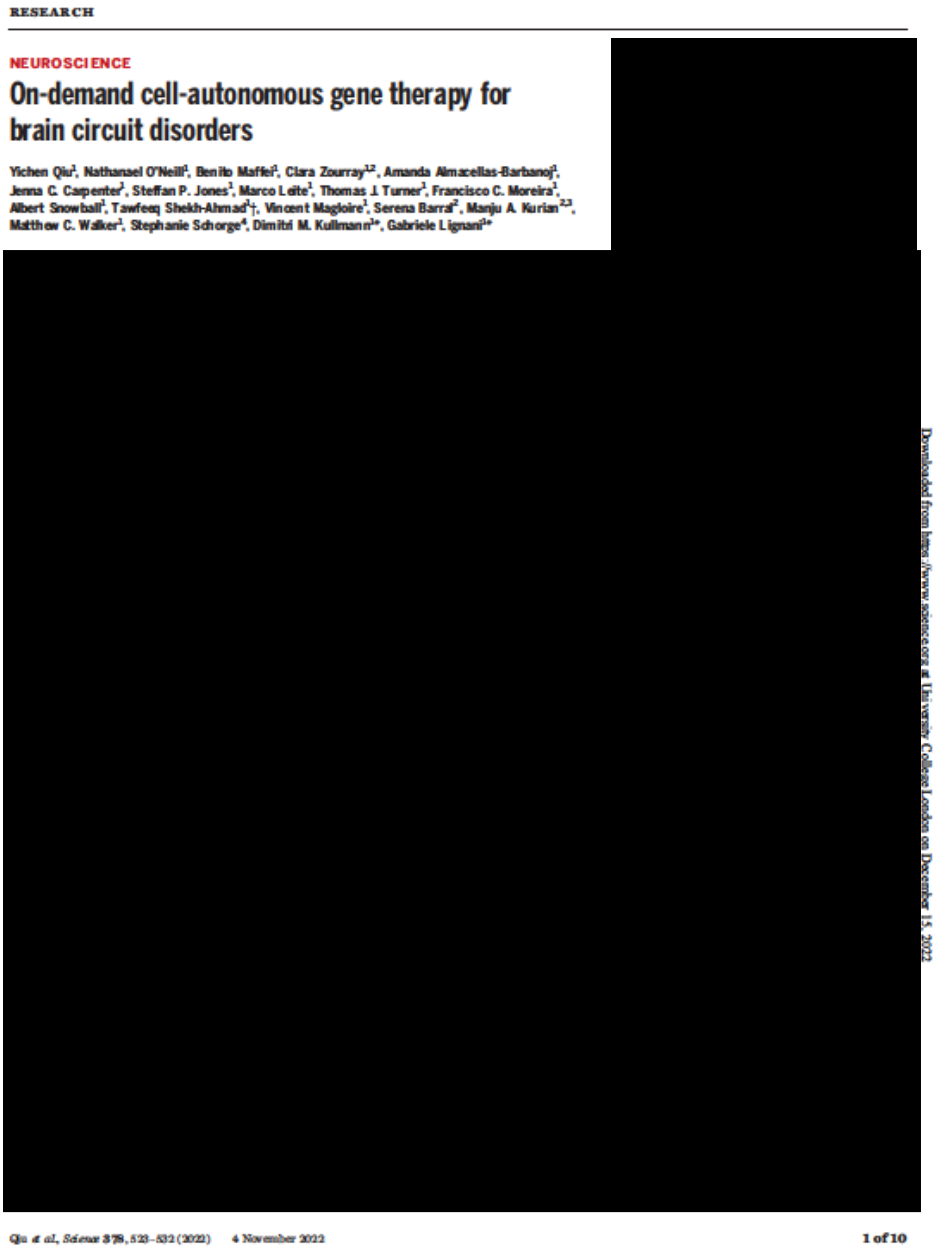

RESEARCH

NEUROSCIENCE

On-demand cell-autonomous gene therapy for brain circuit disorders

Yichen Qiu[1], Nathanael O'Neill[1], Benito Maffei[1], Clara Zourray[1,2], Amanda Almacellas-Barbanoj[1], Jenna C. Carpenter[1], Steffan P. Jones[1], Marco Leite[1], Thomas J. Turner[1], Francisco C. Moreira[1], Albert Snowball[1], Tawfeeq Shekh-Ahmad[1]†, Vincent Magloire[1], Serena Barral[2], Manju A. Kurian[2,3], Matthew C. Walker[1], Stephanie Schorge[4], Dimitri M. Kullmann[1]*, Gabriele Lignani[1]*

https://www.science.org/doi/10.1126/science.abq6656